



THÈSE

PRÉSENTÉE A

L'UNIVERSITÉ BORDEAUX 1

ÉCOLE DOCTORALE DES SCIENCES CHIMIQUES

Par Daniela Melanie DELANNOY LOPEZ

POUR OBTENIR LE GRADE DE

DOCTEUR

SPÉCIALITÉ : **CHIMIE ORGANIQUE**

Synthèse de dérivés de polyphénols bioactifs pour l'étude de leurs interactions avec des protéines

Directeur de recherche : Pr. Stéphane Quideau

Soutenue le : 02 Juillet 2012

Après avis de :

Mme RENARD, C.

M. MONTI J.

Devant la commission d'examen formée de :

Mme RENARD, C.

M. MONTI J.

M. GENOT E.

M. Di Primo C.

M. DEFFIEUX, D.

M. QUIDEAU, S.

Directrice de Recherche, INRA-Avignon

Professeur Université de Bordeaux 2

Directrice de Recherche, INRA-Avignon

Professeur Université de Bordeaux 2

Group leader, IECB Université Bordeaux 2

Chargé de recherche, Université Bordeaux

Maître de conférence, Université Bordeaux 1

Professeur, Université Bordeaux 1

Rapporteur

Rapporteur

Rapporteur

Rapporteur

Présidente

Examineur

Co-directeur de thèse

Directeur de thèse

Table of Contents

Acknowledgements	5
Résumé en français	8
List of communications	12
Introduction	13
Chapter I. Polyphenol-Protein Interactions	16
Ia. Polyphenols	17
Ia.1 Physico-chemical properties of polyphenols	24
Ia.2 Antioxidant/Pro-oxidant Activity.....	25
Ia.3 Tanning Action.....	26
Ib. Polyphenols and Proteins Interactions	27
Ib.1 Brief generalities about proteins	27
Ib.2 Polyphenols-Protein Complex Precipitation.....	28
Ib.3 Polyphenols-Proteins and Specific Interactions.....	31
Ib.3.1 F0F1-ATPase/ATP synthase protein- resveratrol	31
Ib.3.2 Anthocyanidin synthase-flavonoids	33
Ib.3.3 β -Amyloid peptide-flavonoids	35
Ib.3.4 Topoisomerase II-ellagitannins	37
Ib.3.5 Squalene epoxidase and proteasome activity vs. catechin	38
Ib.3.6 Herpes simplex virus-ellagitannins	39
Ib.3.7 Actin-ellagitannins	39
Ic. Techniques used to Study Polyphenol-Protein Interaction	40
Ic.1 Commonly used techniques to measure protein-ligand interaction	40
Ic.2 SPR as an alternative technique in the study of polyphenol-protein interaction	41
Ic.3 Classical SPR experiment vs. reverse SPR experiment	42
Id. Polyphenol-fluorescent adducts and their use in cellulo studies.....	45
Chapter II. Polyphenol Derivatization for Surface Plasmon Resonance Studies	50
IIa. Design of Polyphenol-Biotin Conjugates.....	51

IIb.	Hemisynthesis of Vescalagin- and Vescalin-Biotin Conjugates.....	52
IIc.	Hemisynthesis of Catechin- and Epicatechin- Biotin Conjugates.	56
IIc.1	C-Ring derivatization of catechin (1a) and epicatechin (1b)	57
IIc.1.1	Approach without the use of protecting groups on the catechin skeleton.....	58
IIc.1.2	Approach using protecting groups on the catechin skeleton.....	60
IIc.2	A-Ring derivatization of catechin (1a) and epicatechin (1b).....	69
IId.	Hemisynthesis of B-Type Procyanidins Biotin Conjugates	72
IId.1	F-Ring derivatization of B-type procyanidin.....	72
IId.1.1	Hemisynthesis of per-O-TBDMS B-type procyanidin derivatives.....	72
IId.2	A-Ring derivatization of B-type procyanidin	78
IIE.	Conclusion	80
Chapter III. Polyphenol-Protein Interaction Studies by Surface Plasmon Resonance ...		81
IIIa.	Generalities about the analysis of intermolecular interactions by SPR.....	82
IIIc.	Polyphenol-Protein Interaction Studies	84
IIIc.1	Topoisomerase II α (TopII α) vs. Vescalagin/ Vescalin/Catechin	84
IIIc.2.	Other proteins vs. Vescalin/Vescalagin/Catechin	91
IIIc.3	Actin vs. Vescalagin.....	95
IIIc.4.	ANS vs. Catechin	99
Chapter IV. Fluorescent Labeling of Vescalagin and Bioassays		106
IVa.	Design of Vescalagin-Fluorescent Conjugate	107
IVa.1	At which position of the vescalagin skeleton should we anchor the fluorescent tag?	107
IVa.2	What kind of fluorescent tag should we use?.....	108
IVa.3	What kind of linker should we use?	109
IVb.	Hemisynthesis of Vescalagin-Fluorescein Conjugate.....	111
IVb.1	Hemisynthesis of vescalagin-Fluorescein Conjugate I	112
IVb.2	Hemisynthesis of vescalagin-Fluorescein Conjugate II.....	114
IVb.3	Hemisynthesis of vescalagin-Fluorescein Conjugate III	117

IVc. Hemisynthesis of vescalin-Fluorescein Conjugate	121
IVd. Actin-vescalagin interaction studies: application of vescalagin-fluorescein derivative	122
IVd.1 In vitro assays.....	122
IVd.2 In cellulo assays	123
IVe. Conclusions	125
General Conclusion	125
 Chapter V. Experimental Section	127
Va. Materials and methods	128
Vb. Purification and analysis	128
Vc. Synthetic procedures	130
Vd. Surface plasmon resonance procedures.....	206
Appendix	210
Generalities about SPR detection system for intermolecular interaction studies.....	211
Sensorgrams: proteins injected on to the reference streptavidin surface	216
ANS activity assays.....	217
References	221

Acknowledgements

This work was possible thanks to the funding of **La Fundacion Gran Mariscal Fundayacucho-Convenio Alianza Francesa, Caracas-Venezuela**. I would like to thank this organization for giving me the opportunity to learn in such an interdisciplinary and multicultural environment through the financing of the 3 year doctorate. But also, for the supplementary 6 months granted, which allowed me to finish my formation and to obtain satisfactory results that will allow us to write a publication concerning the last two years and a half of work.

This work was carried out under the direction of **Stéphane Quideau** in the Synthèse et Activite des Substances Naturelles team, at l'Institut Europeen de Chimie et de Biologie de Bordeaux. I would like to express my gratitude to Stéphane Quideau for giving me the opportunity to put myself to the test when I had no experience in organic synthesis or surface plasmon resonance. During this 3 years and a half you have taught me much, of chemistry, responsibility, efficiency in the lab, self-esteem and even of wine! Thank you for all the advice, for the help unblocking the difficult steps in synthesis and for helping me transform this manuscript into a properly written one. I would also like to thank you for allowing me to participate in the different congresses, specially at the ICP 2012, it means a lot to me. Gracias totales!

This work was carried out under the supervision of **Denis Deffieux**, to whom I am very grateful for all the advice concerning the form of this manuscript. I really appreciate all the time you dedicated to this document, to my presentation and the time spent in the lab in this last year and a half, at the hood, trying to help me solve some of the mysteries involving alcohol formation due to the influence of Hard-Rock catalysis. I also appreciate the discussions concerning the protein-polyphenol interactions, specially close to the end, when I had more doubts than certainties; I was a lot more confident thanks to those talks, merci beaucoup !

During the first two years, this work was supervised by **Celine Douat-Cassasus**, to whom I also have a lot to thank for. Having no experience in organic synthesis I really needed someone at the hood to show me the ropes, to launch reactions under inert atmosphere, handling stinky easily oxidizable thiols, using efficiently the search engines, initiating me to the SPR project and so much more! This person was Celine Douat-Cassasus, je te remercie d'avoir pris le temps! I realize the first year wasn't easy for you either with my lacking in French. You were there, when and where I needed you the most, for this I am very grateful.

This interdisciplinary work was possible thanks to the participation of **Carmelo Di Primo** our collaborator in the SPR part of this project and the person who taught me all I know about SPR. I thank you for your participation as an examiner of this thesis, for teaching me how to use the BIAcore apparatus, and how to interpret correctly the sensorgrams, that can be so easily miss-read. Thank you for making everything seem so easy and logical, for your patience and your scientific rigor that I value and admire. It has been a great pleasure for me to work with you, muchisimas gracias por todo.

I would also like to thank **Elisabeth Génot**, our collaborator in the actin-vescalagin project, for allowing me to participate in this rewarding interdisciplinary experience, and for your participation as an examiner-president of the jury of this thesis. I really appreciated being able to talk to you at any time about this project and sharing a bench for some experiences. The knowledge I acquired during the evolution of this project and specially during our meetings is very valuable to me.

I express my gratitude to the rapporteurs **Catherine Renard** and **Jean-Pierre Monti** for their careful and detailed evaluation of this work, their interesting questions and their kind words of encouragement for the future.

The interdisciplinary nature of this project gave me the opportunity to work with people who's knowledge and experience in biology, physics, etc... filled the gaps of mine. Many problems encountered during this thesis were solved thanks to the participation of these people. I would like to start with **Frederic Satel**, all the assays concerning the fluorescent vescalagin-actin system were carried out by this person, who also taught me how to polymerize globular actin and sat with me next to the BIAcore waiting anxiously for the actin-vescalagin results. In the same laboratory, there are **Isabel Egaña** and **Thomas Daubon**, who latter on imaged the fluorescent actin fibers for me, your help was very valuable in figuring out a reproducible protocol for the actin-vescalagin SPR experiences.

In the first floor of the IECB there is **Sabrina Rousseau** and **Thierry Dakhli**, they are responsible for the production and purification of the anthocyanidin synthase (ANS) protein used in this work. The handling of this very sensitive protein was an important factor for the detection of the interaction of the ANS-flavanol systems. I could not have done it without your hard work and determination.

From our team, **Hélène Carrie** performed the activity tests for the ANS protein, to determine its stability in the different buffers tested, but also during the last assays to confirm the activity of the protein before injection in the BIAcore apparatus. These tests took a lot of your time, and in some cases demanded a personal sacrifice from your behalf. These test were

crutial to figure out why things were not working like expected! I thank you for all your work and in a more personal note for the good humor and the all the laughs!

During my thesis I was very lucky to have people like **Axelle Gerald**, **Cecile Courreges** and **Yannick Chollet** to help me with NMR related questions, **Katell Bathany**, **Emmanuel Geneste** and **Claire Mouche** for all the high resolution mass spectrometry and **Bernard Desbat** for the infrared spectroscopy using directly the solid compounds.

From the team I have to thank everybody, **Laurent Poysegu** for the words of encouragment and the talks in spanish!, **Rémi Jaquet** for the purification of vescalagin and all the help with the HPLCs, my wounderful lab parteners **Marion Tarbe**, **Anna Natangelo**, **Emmanuela (Manu) Berni** and **Emilie Petit**, for being so nice and supportive during the hard times, sharing good laughs and cheers of excitement during the great ones! **Céline Chalumeau** for passing on the important details for the handling of the ANS protein, **Cyril Bosset** and **Romin Coffinier**, for taking care of the buying of chemicals, **Mourrad El Assal** and **Dong Tien Tran**, as well as all of the above for their kind and good humored nature! And of course, the interns **Sarah**, **Sebastien** and **Cynthia** who help with some of the large scale reactions. A mis queridos compatriotas, **Ysbelia Obregon**, **Ismer Bracho** y **Johanna Hernandez** que en estos ultimos meses me han dado bastante apoyo moral y calor venezolano!! gracias chicos el destino me los mando cuando mas falta me hacian de pana!!

From rez-de-chaussee, **Clément Arnarez**, **Melanie Defrance (RDC extension)**, **Judith Elkaim**, **Chayan Achayra** and **Pramod Akula**, you guys have been great, you know I would not have gotten this far without your support and words of encouragement when things got rough. But what I treasure the most are the good times we spent together either at lunch, the lucifer, Corcega and so on!!!, I had a blast with you guys!

Special thanks to **Jean-Michel Arbona**, you know this project written and experimental by heart, thanks for showing so much interest in my work, for helping me during all its stages and being that someone I can always rely on.

Résumé en Français

Un nouvel outil d'analyse impliquant la résonance plasmonique de surface (SPR, technologie BIAcore) a été développé pour discriminer les interactions spécifiques protéines-polyphénols des non-spécifiques. Lors d'une expérience classique SPR, la protéine d'intérêt (récepteur) est généralement immobilisée à la surface d'une couche métallique et son ligand est mis en circulation au contact de cette surface. La variation de l'indice de réfraction au voisinage de l'interface quand le ligand se fixe aux récepteurs permet de mesurer l'intensité de l'interaction entre les deux partenaires en temps réel. Dans le cas d'un ligand polyphénolique, celui-ci a tendance à se lier massivement à la surface de la protéine de manière non spécifique (Figure A). Ce phénomène ne permet pas de détecter d'éventuelles interactions spécifiques de la molécule polyphénolique avec la protéine. L'équipe du Pr. Stéphane Quideau a développé une technique SPR "inverse" dans laquelle des polyphénols sont immobilisés sur une surface SPR et les protéines sont mises en circulation (Figure B). Ce type d'expérience limite les interactions non-spécifiques entre les protéines et la surface de polyphénols.⁶¹ Le développement de ce dispositif original, étendu à différentes protéines et polyphénols, a fait l'objet de cette thèse.

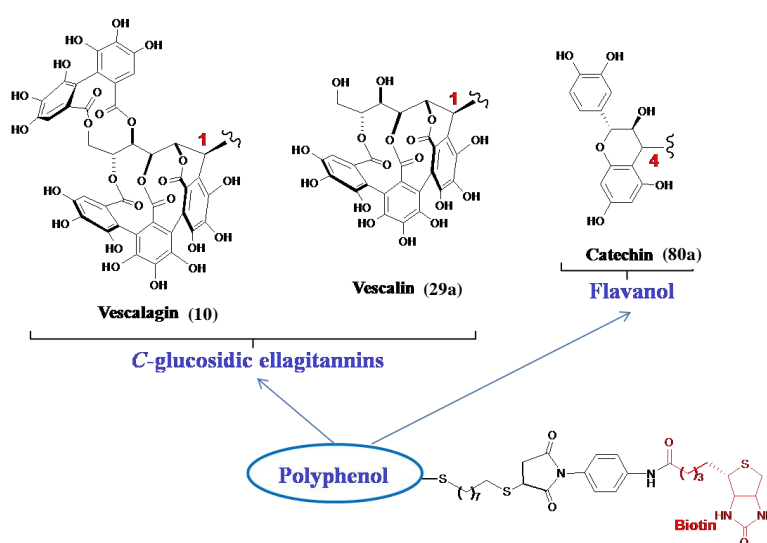
A) Interactions non-spécifique protéine-polyphénol



B) L'immobilisation du polyphénol permet de limiter l'observation des interactions non-spécifiques



Dans un premier temps, cette nouvelle méthodologie d'analyse SPR^{61,46} a été validée à l'aide de trois polyphénols (la vescaline, la vescalagine et la catéchine) associés à la topoisomérase II α humaine (TopII α), une protéine ciblée dans les traitements anticancéreux.^{40,121} Le greffage de ces différents polyphénols sur une surface SPR revêtue de streptavidine a nécessité l'introduction d'un espaceur biotinylé sur chacun des polyphénols. La synthèse des adduits vescalagine-et vescaline-biotine (**60**, **61**) a été réalisée en deux étapes: les ellagitannins C-glucosidiques ont tout d'abord été transformés en leurs dérivés sulfhydryle deoxythioéther correspondants, puis couplés à un



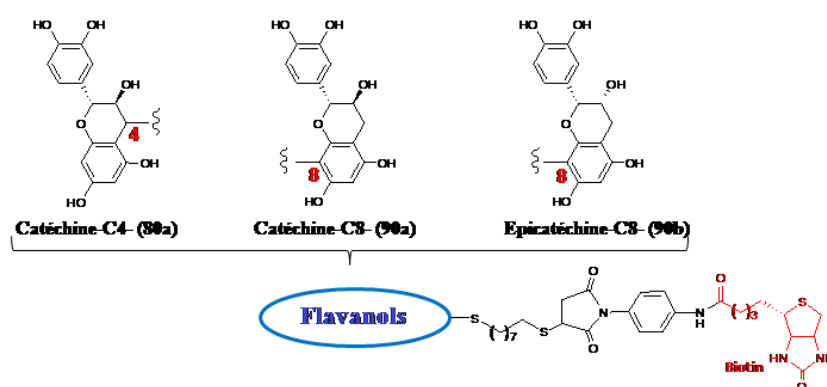
dérivé biotine-maléimide par addition de Michael. La synthèse de l'adduit catéchine-biotine (**80a**) a été réalisée en cinq étapes. La (+)-catéchine a été transformée en un dérivé C-4-(1-thioéthéroctane-8-thiol), par une synthèse en quatre étapes à l'aide d'un groupe protecteur silylé, suivie d'une addition de Michael sur un dérivé biotine-maléimide. Les différents adduits polyphénols-biotine (**60**, **61** et **80a**) obtenus ont été respectivement liés en quantités équimolaires à une surface SPR revêtue de streptavidine. Ce couplage avec la surface SPR a été réalisé par injection d'une solution de **60**, **61** et **80a** à une concentration de 25 nM sur la surface SPR. Après lavage de la surface pour éliminer les molécules non immobilisées, des solutions de TopII α à des concentrations de 6.25, 12.5 et 25 nM ont été injectées par ordre croissant de concentration. Chaque injection ayant lieu toutes les 500 secondes pour laisser au système le temps de se dissocier. L'interaction de la protéine avec les composés vescaline-, vescalagine-, et catéchine-biotine a été suivie en temps réel. La réponse SPR a augmenté de manière dose-dépendante au cours des trois injections successives de TopII α (6.25, 12.5, 25 nM), suggérant une interaction spécifique entre la protéine et les polyphénols étudiés. Il a été observé que la réponse SPR est plus importante pour le système vescalagine-TopII α que pour les systèmes vescaline et catéchine, indiquant une préférence d'affinité de la TopII α pour la vescalagine. Ces résultats sont en accord avec des travaux précédents de l'équipe qui ont montré que l'ellagitannin vescalagine est un inhibiteur de la topoisomérase II α plus puissant que la vescaline.^{40,121} Ce type d'analyse par SPR montre que la protéine TopII α est capable de discriminer des polyphénols de familles différentes (la vescaline, un ellagitannin C-glucosidique vs catéchine, un flavanol) mais aussi au sein d'une même famille de polyphénols (vescaline vs vescalagine, deux ellagitannins C-glucosidiques).

A ce stade, on peut argumenter que la réponse SPR décroissante dans l'ordre vescalagine>vescaline>catéchine est liée à la diminution du nombre de cycles aromatiques hydroxylés présents dans ces composés. Chaque cycle peut en effet être impliqué dans des interactions hydrophiles et hydrophobes avec la protéine. Cela signifierait dans ce cas que l'interaction observée est de nature non spécifique. Si tel était le cas, nous devrions observer la même tendance de réponse SPR pour des protéines de taille et de structure tertiaire différentes. Pour infirmer cette hypothèse, nous avons répété l'expérience avec une série de protéines de tailles et de structures variées : la BSA (globulaire, de 66 kDa), la myoglobine (globulaire, 17 kDa), la streptavidine (tétramérique, 54 kDa), et le collagène de type I (fibrillaire, env. 300 kDa). Aucune variation n'a été observée dans la réponse SPR lors de l'injection des solutions de ces protéines à 6.25, 12.5 et 25 nM, ce qui suggère que celles-ci n'interagissent pas avec la vescalagine, la vescaline ou la catéchine. Par contre, la TopII α

injectée dans les mêmes conditions induit une réponse SPR positive pour les trois surfaces polyphénoliques. Ces résultats montrent que dans les mêmes conditions expérimentales, les protéines testées interagissent différemment avec les polyphénols et démontrent que la tendance observée au niveau de l'interaction entre la TopII α et les polyphénols vescalagine, vescaline et catéchine n'est pas liée aux nombres de fonctions phénoliques, mais plutôt à une complémentarité entre les structures tridimensionnelles des polyphénols et de la protéine. De façon plus général, ces résultats prouvent l'utilité de cet outil SPR pour étudier le type d'interactions entre protéines et polyphénols. Cependant, l'injection de certaines de ces protéines comme la streptavidine ou le collagène type I à des concentrations plus élevées (> 125 nM) a montré que ces protéines peuvent se lier aux polyphénols. Il est donc important de travailler à des concentrations faibles de protéines pour détecter principalement des interactions de type spécifiques.

Pour compléter notre étude, nous avons voulu étudier un système dont l'interaction spécifique polyphénol-protéine est établie. L'ANS est une protéine qui a été particulièrement étudiée ces dernières années compte tenu de son rôle important dans la voie de biosynthèse des anthocyanes (voir chapitre I). Parmi ces différentes études, il a été montré que cette protéine a la capacité de transformer la catéchine³² en un dimère flavanol mais pas l'épicatéchine et la co-cristallisation de cette enzyme avec le flavanol dihydroquercétine a de plus permis d'identifier le site d'interaction de la protéine.³¹ Le système catéchine-ANS constitue donc un exemple type d'interaction spécifique polyphénol-protéine. Des études précédentes de notre équipe ont montré que la position choisie pour l'installation de l'espaceur sur le squelette de la catéchine a des conséquences importantes sur l'affinité de l'ANS pour ce substrat.³⁴ Des adduits de catéchine et

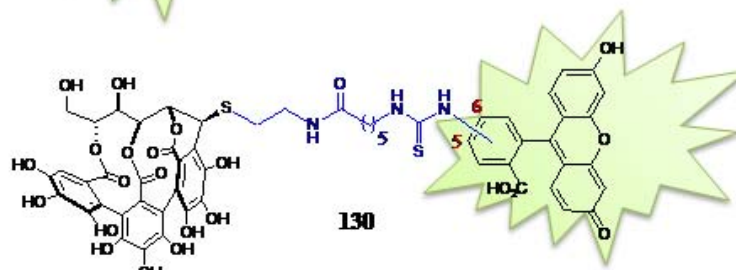
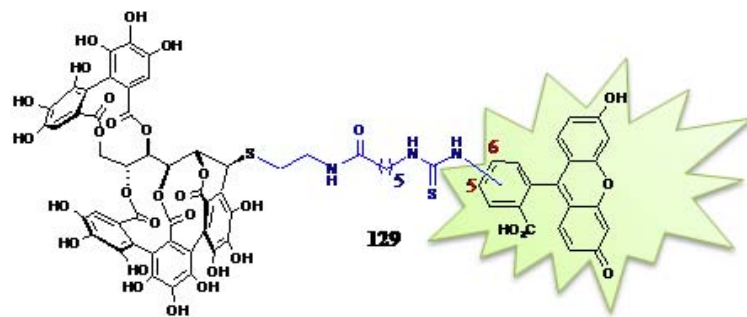
d'épicatéchine modifié en position C-8 ont donc été synthétisés et leurs interactions avec l'ANS évaluées et comparées avec celles de l'adduit catéchine modifié en C-4 (80a) précédemment



obtenu. La nucléophilie de la position C-8 de la (+)-catéchine a été exploitée pour l'installation d'un espaceur portant une biotine via une stratégie de synthèse en sept étapes. Les fonctions hydroxyles de la (+)-catéchine ont été protégées par des groupes benzyles, suivi d'une formylation sélective de la position C-8. Le formyle résultant a été engagé dans une

réaction de Horner–Wadsworth–Emmons pour obtenir un dérivé de la catéchine comportant un espaceur possédant un groupement acide carboxylique masqué terminal. Après déprotection de l'ensemble des groupes benzyles, la fonction acide carboxylique libérée a été couplée à la cystéamine dont la fonction thiol a par la suite été couplée au dérivé biotine-maleimide. Les adduits catéchine-C8- et épicatechine-C8-biotine (**90a**, **90b**) ont ainsi été obtenus avec des rendements globaux satisfaisants. L'analyse des systèmes **80a**, **90a**, **90b** par SPR a montré que L'ANS conserve une affinité sélective pour la catéchine et l'épicatechine modifiées en position C-8, ce qui est en accord avec les études précédentes.³⁴ Cette affinité est de plus comparable à celle observée pour la catéchine modifiée en position C-4 (**80a**). Ces différentes expériences nous ont permis de valider l'utilisation de notre outil SPR pour la détection des interactions spécifiques polyphénol-protéine.

Par ailleurs, dans le cadre d'un projet en collaboration avec l'équipe d'Elizabeth Génot à l'Institut Européen de Chimie Biologie (IECB), nous avons étudié l'interaction d'ellagitannins C-glucosidique liés à une surface SPR avec l'actine globulaire (G-actine, 42 kDa) et l'actine fibrillaire (F-actine, polymère de la G-actine).⁴⁶ Lors de cette étude, nous avons pu montrer que la vescalagine et la vescaline interagissent uniquement avec l'actine fibrillaire, ce qui a fourni un élément de preuve complémentaire concernant l'action destructurante de ces ellagitannins C-glucosidique au niveau de l'actine fibrillaire. L'approche synthétique utilisée pour l'obtention des adduits polyphénol-biotine a également été appliquée dans le cadre de ce projet pour obtenir des adduits fluorescents de vescalagine (**129**) et de vescaline (**130**). La synthèse de trois sondes fluorescentes de la vescalagine a été réalisée en faisant varier la nature de l'espaceur et du dérivé fluorescent. Parmi ces sondes, seul la sonde **129** a la solubilité nécessaire pour permettre son utilisation en milieu physiologique. Le dérivé fluorescent de la vescalagine (**129**) a permis de visualiser in vitro l'interactions de ce polyphénol avec l'actine mais aussi d'évaluer la biodisponibilité de la vescalagine au niveau de l'actine in cellulo. La synthèse du dérivé fluorescent de la vescaline (**130**) a été réalisée en suivant la même approche de synthèse que celle utilisée pour l'obtention du composé **129**. Des études de biodisponibilité complémentaires sont actuellement en cours.



List of communications

PUBLICATIONS:

“Binding of Filamentous Actin and Winding into Fibrillar Aggregates by the Polyphenolic C-Glucosidic Ellagitannin Vescalagin”

Stéphane Quideau, Céline Douat-Casassus, Daniela Melanie Delannoy Lopez, Carmelo Di Primo, Stefan Chassaing, Rémi Jacquet, Frederic Saltel, and Elisabeth Génot. Angew. Chem. Int. Ed. 2011, 50, 5099-5104.

COMMUNICATIONS ORALES:

XVI Jornadas Hispano-Francesas de Química Orgánica (Burgos, Spain, Juin 2011)

“Polyphenol-Protein Interactions Study by Surface Plasmon Resonance”

International Conference on Polyphenols (Florence, Italy, Juillet 2012)

“Study in Real Time of Polyphenol-Protein Interactions by Surface Plasmon Resonance”

POSTERS :

International Conference on Polyphenols (Montpellier, France, Aout 2010)

“Study in Real Time of Polyphenol-Protein Interactions by Surface Plasmon Resonance”

Symposium International d'œnologie (Bordeaux, France, Juin 2011)

“Chemical-Biology study of Vitis Vinifera's leucoanthocyanidin dioxygenase”

BREVET:

C-Glucosidic Ellagitannin Compounds for Use for Altering the Supramolecular Arrangement of Actin.

European Patent N° EP11305186.6.

Quideau, S.; Génot, E.; Saltel, F.; Douat-Casassus, C.; Delannoy López D. M.

Introduction

The alteration of protein function or structure may have catastrophic or benefic effects over the organism. These alterations can be regulated by the use of certain natural products from plants, thanks to the complementarity between the structure of the protein and the structure of the natural product. Among these natural products are polyphenols, which is a group of secondary metabolites that are defined as follows: *The term “polyphenol” should be used to define plant secondary metabolites derived exclusively from the shikimate derived phenylpropanoid and/or the polyketide pathway(s), featuring more than one phenolic ring and being devoid of any nitrogen-based functional group in their most basic structural expression.*² The presence of phenolic rings in their structure, confers polyphenols with physico-chemical properties that makes them appropriate to interact with proteins, by hydrophobic interactions due to the presence of aromatic cycles, and by hydrogen bonding due to the presence of hydroxyl groups. Historically, polyphenol-protein interactions have been studied in the process of tanning, which consists in the transformation of animal skin into leather, as a consequence of the precipitation of the skin's collagen by polyphenolic plant extracts. Polyphenol-protein interactions have also been studied concerning the astringency sensation perceived when consuming drinks like tea, wine or coffee, for example, which is associated to the precipitation of salivary proteins by polyphenols contained in the aforementioned drinks. This capacity of polyphenols to precipitate proteins has long been studied by several research teams^{2a} among which, is noted Haslam's team. In 1985, Haslam²⁵ proposed a model to explain the precipitation of the complex formed between a polyphenol and a protein. In this model, the surface of a protein molecule is surrounded by several polyphenol molecules when in presence of an excess of polyphenol, and at higher concentrations of protein the polyphenol-protein complex crosslinks, agglomerates and precipitates. This plastering of the proteins surface by an excess of polyphenolic molecules is driven by hydrophobic and hydrophilic interactions between the polyphenol and specific residues of the protein that have appropriate characteristics to favor these interactions. However, the plastering of the proteins surface by polyphenols is considered as non-specific and has a negative connotation regarding the pharmaceutical industry, which is more interested in specific interactions.

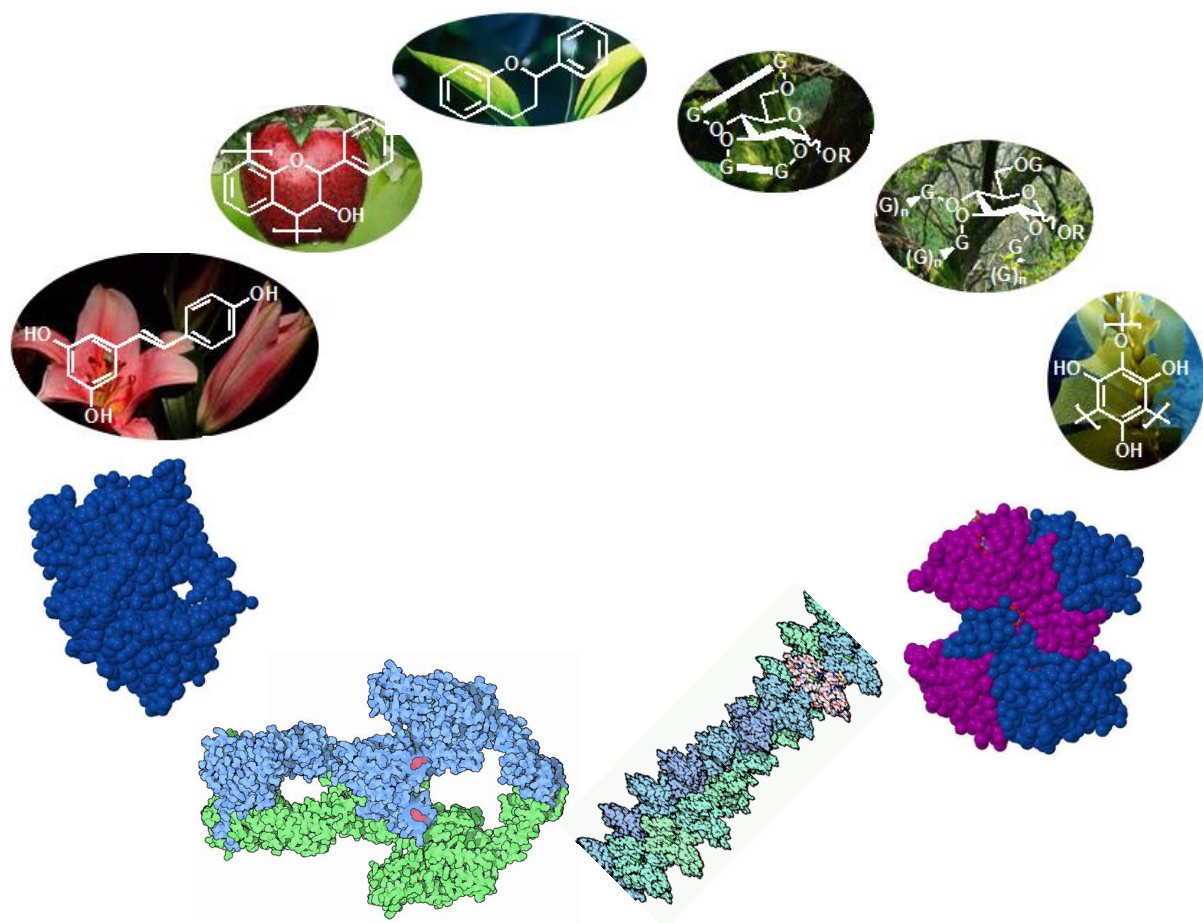
In this work, we are interested in studying specific polyphenol-protein interactions, which we define as a polyphenol that is capable of interacting with a specific site of a protein and that may affect the proteins function. In order to illustrate specific polyphenol-protein interactions, some examples found in the literature are listed in Chapter I. Most of the examples that are given concern polyphenols and proteins used in our study, to give a brief background of what

is known about the polyphenol-protein systems used. In general, polyphenol-protein interactions are studied by a variety of analytical techniques, among which X-ray and NMR are the preferred and lead techniques, because they show directly the interaction site between the protein and the polyphenol. The attempts to obtain crystals of some of the polyphenol-protein systems we desired to study were unsuccessful. The obtention of crystals of polyphenol-protein complex is necessary for X-ray analysis, which is one of the limitations of this technique, because it is not always possible even when possessing pure samples of protein and polyphenol. The large size and in some cases low stability of the proteins we desired to study deprived us from using NMR analysis, which is one of the limitations of this lead technique. Even though X-ray and NMR are nowadays the ideal techniques available, the aforementioned limitations in some cases prevent their use. A few of the other techniques available for polyphenol-proteins interaction study are briefly listed in Chapter I. Among these techniques, emphasis is made on the Surface Plasmon Resonance (SPR) technique because it was the one chosen by our team. For this technique, one of the partners is immobilized over the SPR surface (the ligand) and the interaction with the other partner (the analyte) is detected in solution as an increasing SPR response and has the particularity of following the evolution of the system in real time. In a proof of concept study, our team showed that this technique has the advantage of limiting the observation of non-specific interactions when the polyphenol is immobilized on to the SPR surface and the protein is injected in solution. However, some difficulties were observed in this study concerning the stability of the polyphenol-bound SPR surface.

In this thesis our efforts were aimed to improving the stability of the polyphenol-bound SPR surface in order to extend its use to the study of different polyphenol-protein systems. The use of the tool developed was validated by testing its performance with different polyphenol-protein systems reported in the literature as systems having a specific interaction according to our definition. The advantages and limitations of the use of this technique in the detection of specific polyphenol-protein interactions are discussed in chapter III. Polyphenol-biotin conjugates were synthesized for their immobilization on to the SPR surface and the synthetic approach used for the obtention the biotinylated derivatives was also applied to obtain fluorescent conjugates of vescalagin and vescalin, which were useful in the polyphenol-protein interactions study of using other techniques (in vitro and in cellulo).

Chapter I

Polyphenol-Protein Interactions



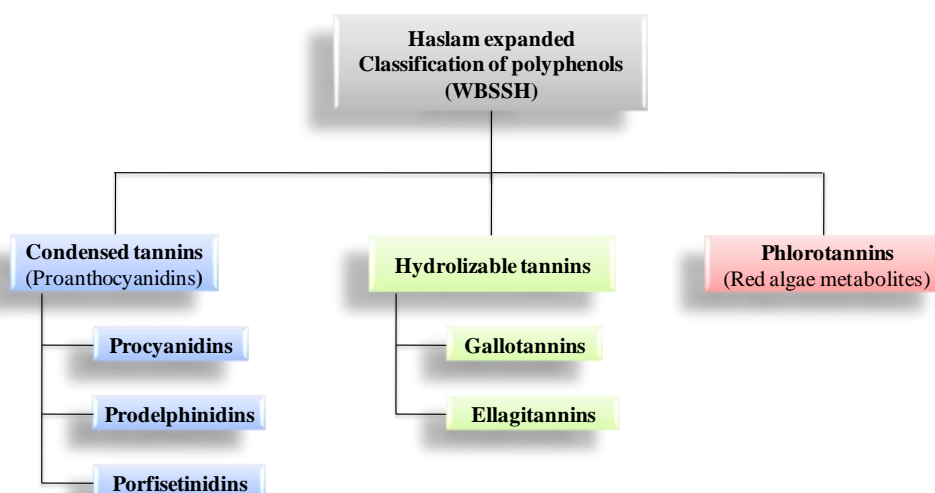
The general interest in natural products such as alkaloids, terpenoids and polyphenols comes from their presence in ancient herbal remedies. Different scientific studies have confirmed the effects of certain traditional remedies by isolating and identifying a compound or a group of compounds (synergistic activity) that show the effect observed for the herbal remedy. One well known example is that of salicin (precursor of acetylsalicylic acid) that owes its name to the preferred natural source Salicaceae. In ancient Egypt, herbal remedies were prepared from the myrtle bark, which was prescribed for rheumatism and back pain. Hippocrates of Kos also prescribed the extract of willow bark (*Salix alba*) for pain and fever. These plants had in common Salicin as a secondary metabolite. Salicin was isolated latter on by Johann Andreas Buchner in 1828 and organic synthesis allowed to transform salicin to acetylsalicylic acid, the Aspirin® that we know today. Other popular examples are morphine and derivatives, isolated from the latex of opium (*Papaver somniferum*). Opium was described in the egyptian ancient medicinal text Ebers papyrus (more than 3500 years ago) as a tonic for colicky children.¹ Polyphenols are also secondary metabolites that are mostly well known for their antioxidant activity. For thousands of years, the use of plant extracts rich in polyphenolic compounds has been commonly used in the oriental traditional medicine. In Asian countries, these polyphenol-rich herbal remedies are still used nowadays. Furthermore, researchers mainly from these countries have reported polyphenols to be the active principles in these herbal remedies. However, this family of natural products has been underestimated by the pharmaceutical companies, most probably due to the generalization that polyphenols are non-specific protein precipitating agents.² This Chapter will be dedicated to introducing the diversity of chemical structures that constitute the polyphenol family, the implication of some polyphenols in the precipitation of polyphenol-protein complexes and finally representative studies that show certain polyphenols to have a specific interaction with target proteins.

Ia. Polyphenols

Through time the growing interest in plant phenolic compounds has given birth to an evolving definition of what a polyphenol is. Edwin Haslam, expanded the Bate-Smith and Tony Swain definition³ to: ***water soluble plant phenolic compounds having molecular masses ranging from 500 to 3000-4000 Da and possessing 12 to 16 phenolic hydroxyl groups on five to seven aromatic rings per 1000 Da of relative molecular mass.*** According to the White, Bate-Smith, Swain, Haslam (WBSSH) definition, polyphenols should also give the usual diagnostic reactions (formation of intense blue-black complexes when treated with iron (III) salts and oxidation with permanganate); have the ability to precipitate some alkaloids, gelatin and other proteins from solution. This definition of polyphenol is given from the point of

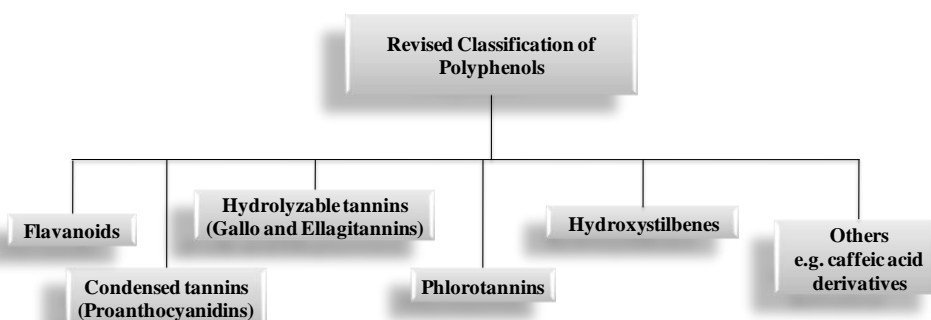
view of their capacity to complex with other molecules from biological origin. From this WBSSH definition the classification of polyphenols derivatives is shown in the following figure.

Figure 1. White, Bate-Smith, Swain, Haslam (WBSSH) definition of polyphenols

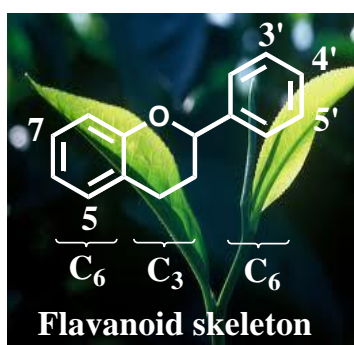


More recently, the concept of polyphenol has been revised from the point of view of chemical structure by Quideau.² In this revised concept, the presence of at least two phenolic moieties is necessary for a natural compound to be called a polyphenol, independently of the number of hydroxyl substituents on each aromatic ring. An additional restriction is taken into account in order to exclude many compounds from natural origin that may include one or more phenol moieties due to their biosynthetic pathways of origin. Thus, the term polyphenol is restricted to compounds derived from the shikimate and/or polyketide pathway. The revised definition thus stated by Quideau is as follows: *The term “polyphenol” should be used to define plant secondary metabolites derived exclusively from the shikimate-derived phenylpropanoid and/or the polyketide pathway(s), featuring more than one phenolic ring and being devoid of any nitrogen-based functional group in their most basic structural expression.* This description allows to include in the classification, the flavonoid and hydroxystilbenes families of secondary metabolites (Figure 2).

Figure 2. Quideau’s classification of polyphenols according to their structural characteristics²



In the following we describe a few aspects of each family comprising this vast variety of natural products.

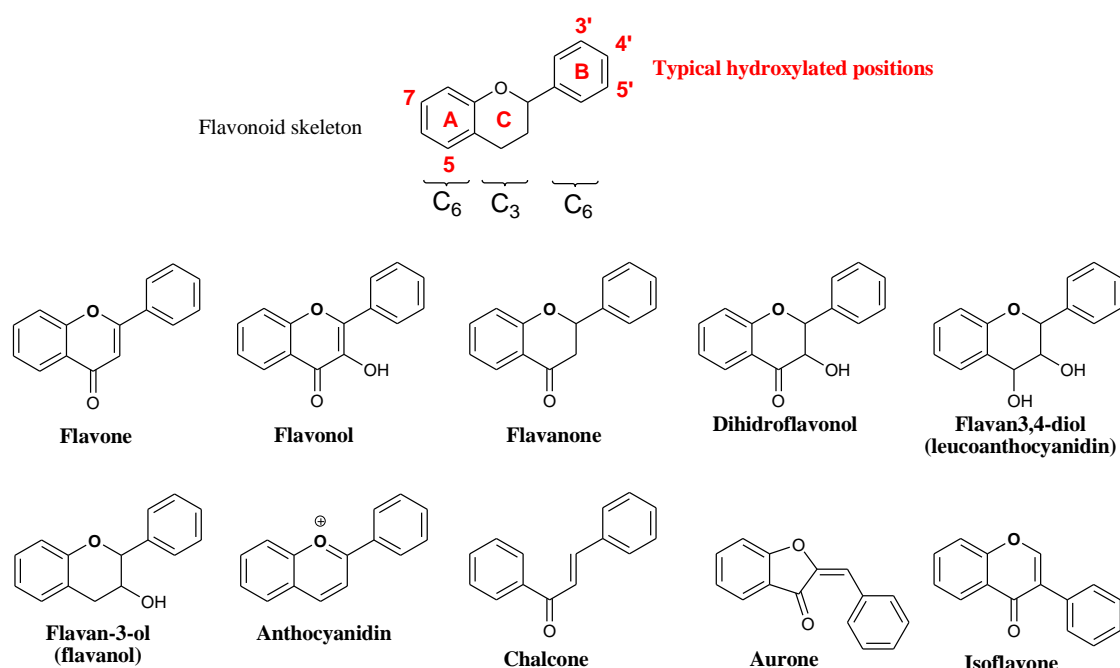


Camellia sinensis

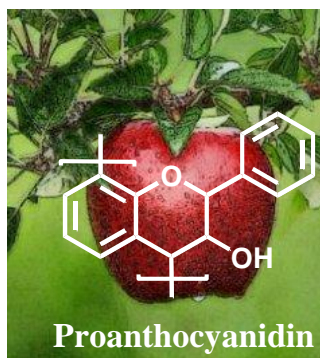
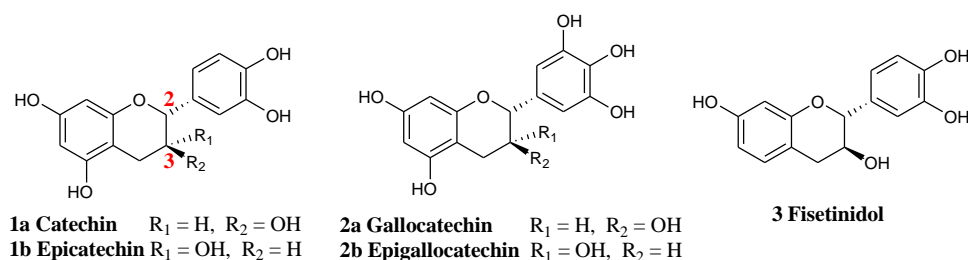
Flavonoids are widely distributed throughout the plant kingdom, with the exception of algae. They are most concentrated in the epidermis of leaves and the skin of fruits and as a consequence are present in everyday foodstuffs as cocoa derived products, tea, wine, among others.⁴ Within the plant, the function of these secondary metabolites are diverse. They are radical scavengers, antimicrobial agents and photoreceptors; they protect the

plant from ultraviolet light (UV) and work as visual attractors for insects.⁵ Flavonoids have a C₆-C₃-C₆ central unit: the flavanoid skeleton. They feature either a central heterocyclic ring (most abundant) or a central open chain (chalcones). Hydroxylation of the aromatic rings is very frequent at positions C7, C4', frequent at C5 and C3', less frequent at C5' and C8 and scarce at C6 and C2' (Figure 3). The subclasses of flavonoids are presented in the following figure.

Figure 3. Typical hydroxylated aromatic positions and structures of subclasses of flavonoids



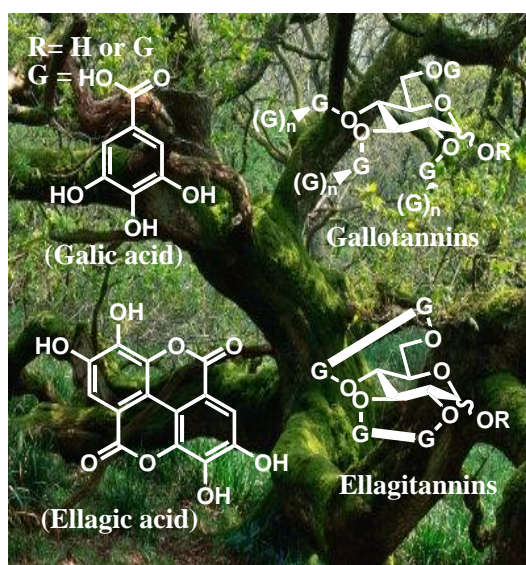
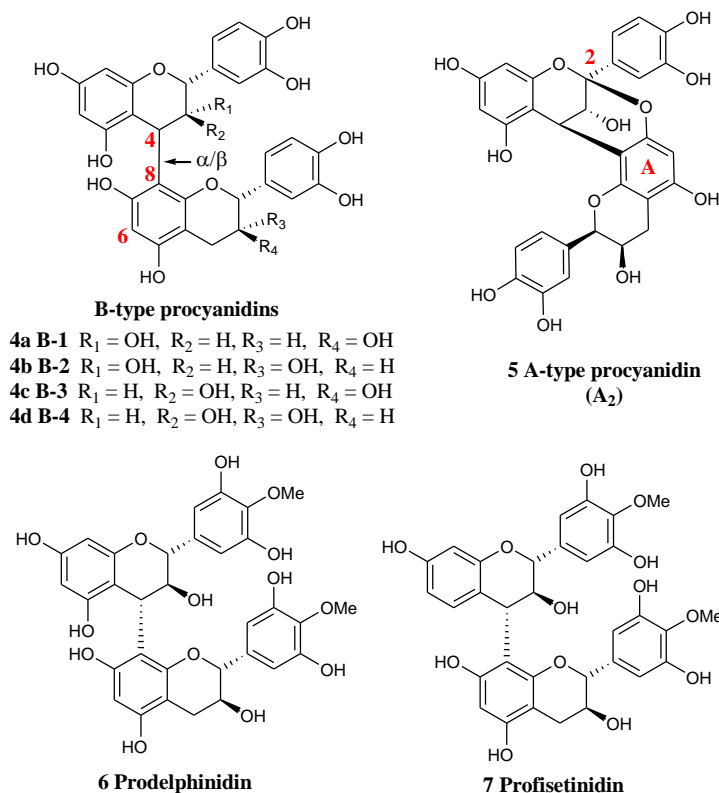
The flavan-3-ols (flavanols) possess two chiral centers at C-2 and C-3 (Figure 4). (+)-Catechin (**1a**) and its epimer at C-3 (–)-epicatechin (**1b**) are polyphenols of this subclass that are widespread in nature.⁴ These flavanols, along with (epi)gallocatechin (**2a,2b**) and fisetinidol (**3**) are the monomeric units that form condensed tannins also called proanthocyanidins.

Figure 4. Structures of (epi)catechin, (epi)gallocatechin and fisetinidol

Red delicious (apple)

Proanthocyanidins have been isolated from fruits, seeds, barks and heart wood of a widespread of plants. They are prominently found in apples, cocoa beans, grape seed and grape skin.⁶⁻⁸ Even though their function within the plants is not clear, it is thought that they are used as a defense mechanism against fungus and parasites, because they are abundant on young tissue and in wounds caused to the stem.⁵

Proanthocyanidins are formed by condensation of two or more flavanol units and according to the types of flavanols that form them they are divided in three major subclasses: procyanidins, prodelphinidins, and profisetinidins.⁹ Of the three subclasses, procyanidins, which are condensates of (epi)catechin units (**1b**, **1a**) represent the most naturally abundant proanthocyanidins in plants. The most common type are B-type procyanidins, where the (epi)catechin units (**1b,a**) are bound between C-4 and C-6 or C-8. Naturally abundant dimers are the procyanidins B1 (**4a**), B2 (**4b**), B-3 (**4c**) and B-4 (**4d**), though they can occur as polymers made of up to 50 units and forming helicoidal structures.^{4,10} A-type procyanidins (**5**) possess an additional ether linkage between an A-ring hydroxyl group and C-2. Less abundant prodelphinidins (**6**) are condensates of (epi)gallocatechin units (**2a**, **2b**)¹¹ while profisetinidins (**7**) are dimers and oligomers of fisetinidol (**3**) and other flavanols.¹²

Figure 5. Examples of dimeric structures of proanthocyanidins or condensed tannins

Quercus robur (oak).

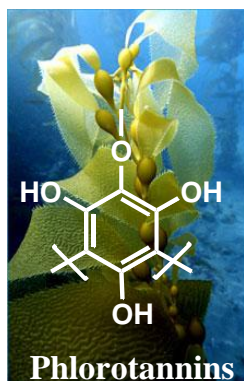
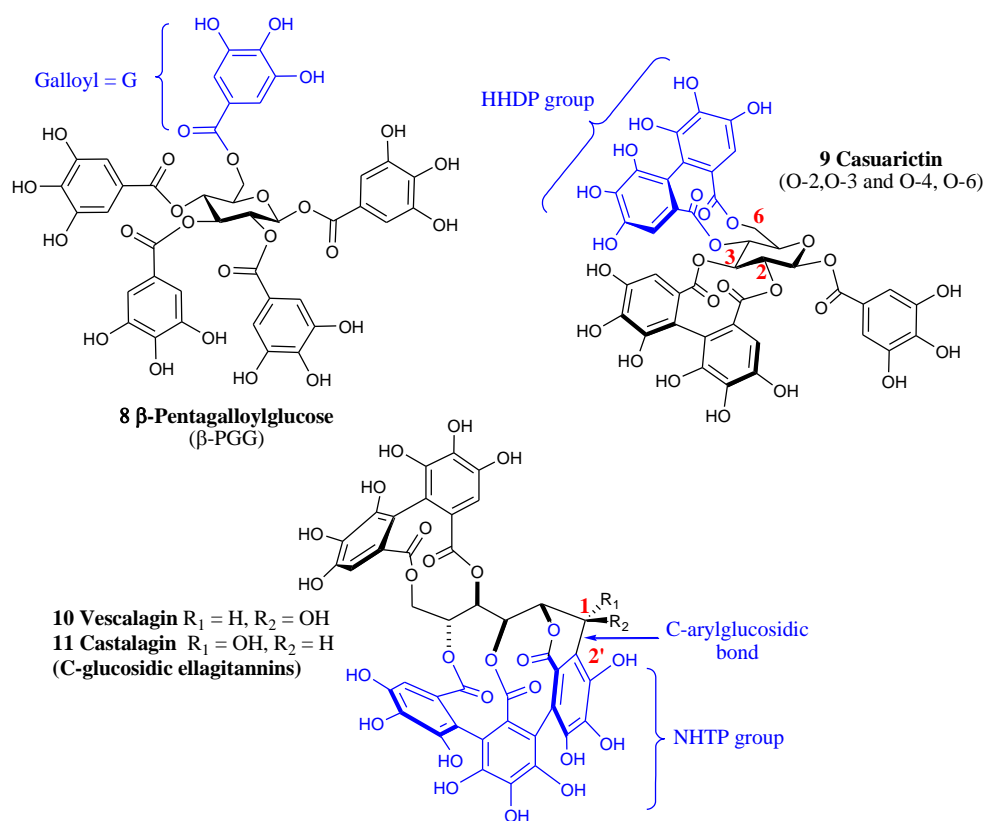
Hydrolysable tannins are subdivided in two subclasses: gallotannins and ellagitannins. They owe their name to the products of their acid hydrolysis; gallotannins furnish a glucoside and gallic acid (left figure, 3,4,5-trihydroxybenzoic acid), while ellagitannins furnish a glucoside and ellagic acid (left figure, or its derivatives).⁵

Gallotannins are commonly extracted from the galls of Chinese gall (*Rhus semialata*) or Turkish gall (*Quercus infectoria*).¹³ These galls are abnormal outgrowths formed on the bark of the tree due to bacterial infection or attack by

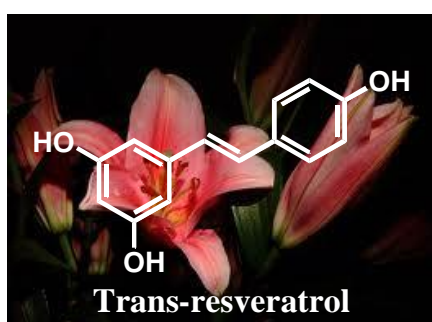
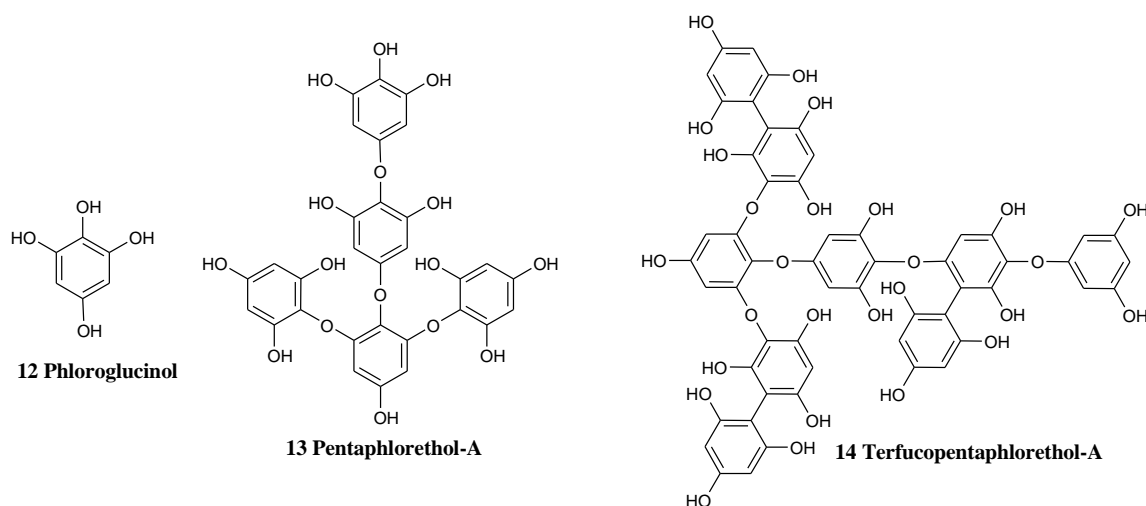
parasites. Gallotannins are formed from two simple entities: D-glucopyranose and gallic acid to furnish structures like β -penta-O-galloyl-D-glucopyranose (β -PGG, **8**). Further coupling reactions with additional gallic acids furnish a vast variety of gallotannins.^{14,15} **Ellagitannins** are present in the dicotyledon group of the angiospermes (flowering plants), more abundantly in the Hamamelidae, Dilleniidae et Rosidae subclasses.³ Ellagitannins are derived from biosynthetic stepwise oxidation of gallotannins as a consequence of oxidative biaryllic coupling of the gallic acid moieties on the polyol core. These couplings give birth to the

characteristic HHDP (**H**exa**H**ydroxy**D**i**P**henoyl, Figure 6).¹³ For the most abundant types of ellagitannins the HHDP group is anchored by the positions O-2, O-3 and/or O-4, O-6 of the glucose (e.g. **9**, figure below), which allows the sugar core to adopt the more stable 4C_1 conformation (all groups in equatorial position). A special type of ellagitannins is composed of the C-glucosidic ellagitannins; they possess the particularity of having an open sugar core and a C-C bond between the C-1 carbon of the open sugar core and C-2' of a HHDP unit or, in some other cases, of a **N**ona**H**ydroxy**T**ri**P**henoyl (NHTP) unit, as exemplified by vescalagin (**10**) and castalagin (**11**) in Figure 6.

Figure 6. Examples of gallotannin and ellagitannin structures

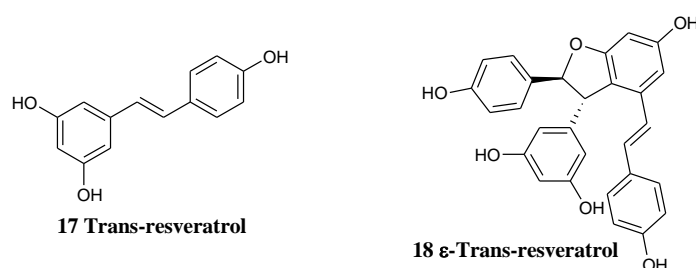


Phlorotannins are secondary metabolites isolated from brown algae (Phaeophyceae). These polyphenols are derivatives of phloroglucinol (**12**, 1,3,5-trihydroxybenzene) and are known to possess an antibiotic activity. Phloroglucinol units are bonded by diaryl ether bonds or biaryl bonds to form polyphloroglucinol derivatives (Figure 7). They are further classified according to the type of bond joining the phloroglucinol units and to the presence of additional hydroxyl groups. Among these classes are fucols (biphenyl bonded units) and fucophlorethols (mixture of diaryl ether and diaryl bonded units).^{16,17}

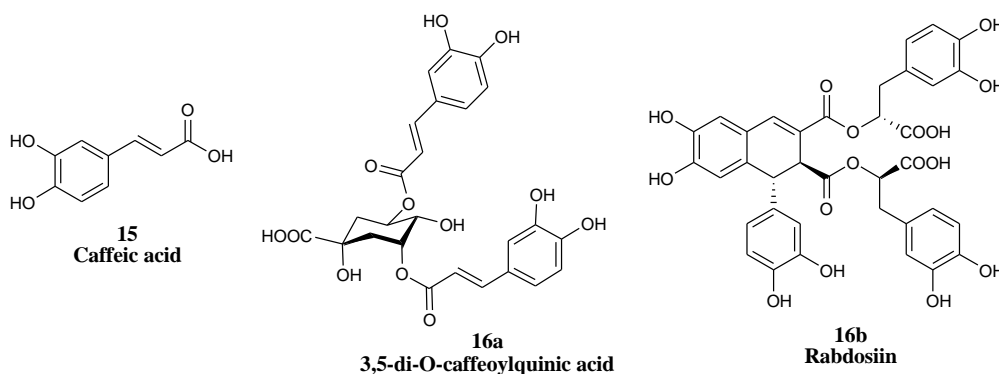
Figure 7. Examples of phlorotannin structures**Trans-resveratrol**
Liliaceae (*Lilium orientalis*)

Hydroxystilbenes are amply distributed in plants and are most frequently found within the Liliaceae, Moraceae, Saxifragaceae, Leguminosae and Polygalaceae families.⁵ Hydroxystilbenes show a repeating C₆-C₂-C₆ motif and are formed by two hydroxyphenol moieties joined by a conjugated double bond. This structural characteristic makes them prone to form oligomeric and polymeric

derivatives by oxidative coupling reactions.² The most popular of these secondary metabolites is the trans-resveratrol (**17**, 3,5,4'-trihydroxy-trans-stilbene); the popularity of which is a consequence of its biological evaluation as a cancer preventing agent and its presence in wine.

Figure 8. Examples of hydroxylstilbene structures

Other polyphenols included in Quideau's classification of polyphenols are exemplified by the derivatives of caffeic acid (3,4-dihydroxycinnamic acid, Figure 9).

Figure 9. Examples of caffeic acid derivatives

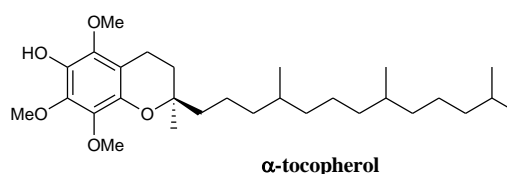
As observed above, the term polyphenols comprises a large family rich in structural diversity that share in common an array of phenolic units; therefore, it is normal that they share certain physico-chemical properties. It is important to take these properties into account for they may shed a light in the role of polyphenols as health beneficial agents.

Ia.1 Physico-chemical properties of polyphenols

UV-radiation absorption. According to the number of hydroxyl groups present on the aromatic ring (as well as, other common substituent's), the secondary ($\pi \rightarrow \pi^*$) absorption maxima ranges from 270 nm-320 nm. This property makes these natural polyphenols good agents to absorb UV-radiation (10 nm-400 nm), which is one of the functions that polyphenols have in plants, protecting them against DNA damage by UV-radiation.¹⁸ This property has been exploited by the cosmetic industry, introducing polyphenol rich extracts in skin products advertised to protect the skin from solar radiation and aging.²

Solubility and reactivity. The planar aromatic rings give these compounds a degree of hydrophobicity while the hydroxyl groups give them hydrophilic properties, making these compounds amphiphilic. The phenolic moiety possesses moderate acidity exploitable in biological systems ($\text{pK}_a = 8\text{-}12$). From the point of view of reactivity, these polyphenols can act as carbon nucleophiles (at ortho- and para- positions), but also as oxygen nucleophiles: weak when in the phenolic form and harder when in phenolate form (PhO^-). These properties make them reactive towards electrophilic species.

The phenolic O-H bond has a bond dissociation energy (BDE) ranging from 87-90 Kcal/mol (in gas phase). This value decreases when in the aromatic ring are also present alkyl and/or alkoxy

Figure 11

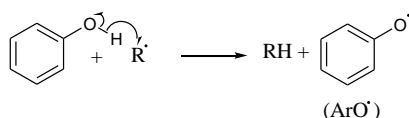
groups (ortho-, para- substituents) making the group more reactive to oxidation by hydrogen extraction (generation of PhO^\bullet).² An example of a phenol in this situation is the reference anti-oxidant, α -tocopherol (Figure 11, a component of vitamin E) which has a BDE of 77-79 Kcal/mol. This capacity of homolytical release of a hydrogen atom is one of the properties that give foundation to the popular anti-oxidant activity of polyphenols.

Metal chelating agents. When at least two hydroxyl groups are positioned next to one another in the same aromatic ring (catechol motif) these groups can act as chelating agents for metals, such as, iron, magnesium, calcium, copper, etc.³ This property can also explain their antioxidant activity by chelation of iron (II and III) and copper (I and II), involved in the production of the aggressive HO^\bullet radicals.

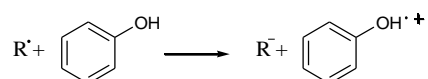
Ia.2 Antioxidant/Pro-oxidant Activity

Reactive oxygen species (ROS) are implicated in various human diseases, though it is not yet clear that they are the causing agents.³ Among these diseases are: cancer, Alzheimer disease, Parkinson disease, atherosclerosis, arthritis, inflammation to mention a few. Numerous scientific studies, both experimental and in silico, show evidence of polyphenols acting as scavengers of reactive oxygen species (ROS).^{2,4} Two mechanisms have been proposed to explain this antioxidant activity; the **Hydrogen Atom Transfer (HAT) mechanism** in which the polyphenol transfers a hydrogen atom (H^\bullet) to a radical species (R^\bullet) and forms a polyphenolic radical (ArO^\bullet), stabilized by resonance and inductive effect depending on the substituent's and their position in the phenolic ring. For this mechanism the BDE of the O-H bond of the polyphenols and the stability of the newly formed polyphenolic radical are determinant for its efficacy.

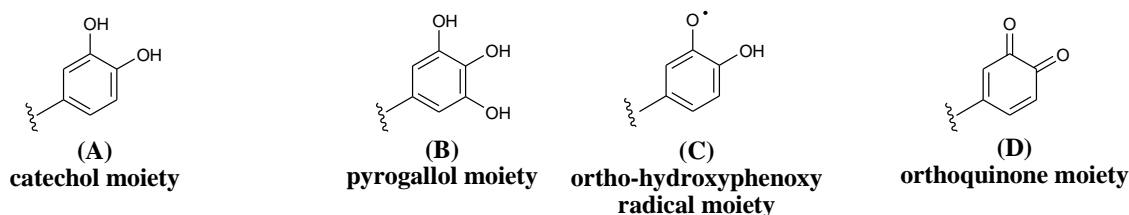
Scheme 1. Hydrogen Atom Transfer (HAT) mechanism



The second proposed mechanism is **the Single Electron Transfer (SET) mechanism**. In this mechanism a single electron is transferred from the polyphenol (ArOH) to the free radical (R^\bullet) to form an anion (R^-) and a stable radical polyphenolic cation ($\text{ArOH}^{+\bullet}$). In this case the ionization potential of the polyphenol and the stability of the radical polyphenolic cation ($\text{ArOH}^{+\bullet}$) are the determinant properties for the efficacy.

Scheme 2. Single Electron Transfer (SET) mechanism

Nowadays, more careful observation is given to the antioxidant effect of polyphenols, particularly in the case of catechol (**A**) and pyrogallol (**B**) polyphenol containing units, since they may form reactive and toxic quinones under certain conditions. For example, oxidation by pro-oxidant species (hydrogen peroxide, nitrite, lipid oxidation products, among others) or by iron (III) or copper (II) ions, could furnish ortho-hydroxyphenoxy radical (**C**). This radical **C** affords an orthoquinone (**D**), which is capable of either covalently binding DNA (modifying it), or it reacts with $^3\text{O}_2$ to produce $\text{O}_2^{\cdot-}$, which can indirectly induce DNA damage. Therefore, polyphenols have a dual antioxidant/pro-oxidant behavior, depending on the environment to which they are submitted.²

Figure 10. Catechol (**A**), pyrogallol (**B**), ortho-hydroxyphenoxy radical (**C**) and orthoquinone (**D**) moieties

Ia.3 Tanning Action

Historically, polyphenols are associated with tanning action and consequently, the names of some of the polyphenol families mentioned above bear the word tannin as part of their name (ellagitannin, gallotannins and phlorotannin). The word tannin is derived from the ancient keltic lexical root “tan” than means oak,² because powdered oak extracts were traditionally used in the transformation of animal skin into leather. This process known as tanning is based on the treatment of the leather collagen matrix of the animal skin with polyphenols.^{3,19} This tannin action is also associated to the astringency sensation felt when ingesting drinks like wine and tea. In this case, the sensation is attributed to the precipitation of salivary proteins by the “tannins” contained in the mentioned drinks. The tannin definition is often associated to the term polyphenol, and has the negative effect of associating compounds with defined structure, to complex oligomeric mixtures of compounds with undefined structure. Though this is true for oligomeric proanthocyanidins, the same is not necessarily true for other polyphenols, which is the subject of the following section.

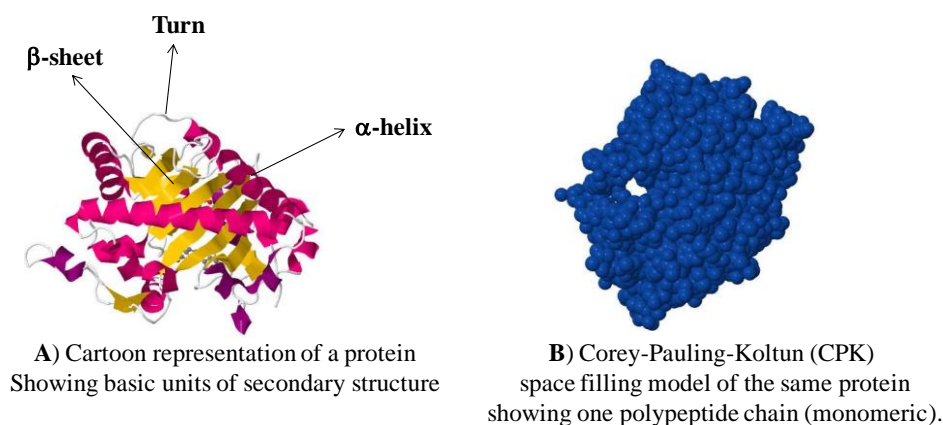
Ib. Polyphenols and Proteins Interactions

Given the vast structural variety of polyphenols, their capacity to interact with proteins in a specific or non-specific manner will depend upon their structural characteristics, as well as their physicochemical properties, which can make them good candidates for interaction with proteins in a target-like manner. In this section, we will present some of the classical studies concerning the formation of polyphenol-protein complexes and the models proposed for the non-specific interaction manner, followed by some examples of polyphenols that show to interact with certain target proteins in a specific manner. Before, we start by giving a brief definition of what a protein is and their classification according to their structure and function.

Ib.1 Brief generalities about proteins²⁰

Proteins are biological macromolecules formed by linear arrangement of amino acids (residues) covalently linked by peptidic bonds. This linear arrangement is called the primary structure of the protein and is constituted by a sequence of twenty natural amino acids; which is determined by the genetic code. In one of the latter steps in the proteins biosynthesis called posttranslational modification, the residues are chemically modified in order to extend the range of functions of the protein. According to the sequence of residues constituting the primary structure, the “linear arrangement” may form three basic units of the secondary structure of a protein: α -helices, β -strands and turns. These basic units may arrange further by covalent disulfide bonds (between distant cysteine residues), charged interactions, hydrogen bonding or hydrophobic interactions to give the tertiary structure of a protein. Finally the interaction between two or more polypeptide chains affords proteins with quaternary structure. Protein models are generally presented as cartoon models (Figure 11A) or by the Corey-Pauling-Koltum model (Figure 11B).

Figure 11. Basic units of the secondary structure (cartoon model) and Corey-Pauling-Koltun CPK model of a protein

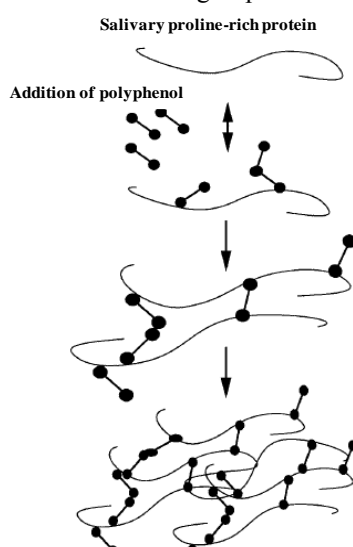


Individually or forming complexes, proteins are essential parts of every living organism since they are involved in almost every process within the cell. Many proteins are enzymes, which catalyze biochemical reactions in the metabolism; others have structural or mechanistic functions. Some examples of proteins that are enzymes are: trypsin, ligases and DNA polymerases; examples of proteins with structural function are: tropocollagen, keratin; and examples of proteins that have mechanistic functions are: actin and myosin in muscle, hemoglobin and myoglobin responsible for oxygen transport in blood and muscle. However, historically, proteins have been divided into globular proteins (compact proteins) and fibrous proteins (elongated rod-like proteins); though nowadays proteins are preferentially treated as belonging to families with structural or sequential homology. Inhibition of specific proteins involved in the development of disease is of interest from a pharmaceutical point of view. Certain small organic molecules have been found to play important roles as inhibitors throughout history.

Ib.2 Polyphenols-Protein Complex Precipitation

The early studies concerning the interaction between polyphenols and proteins were performed in pursue of understanding the precipitation of proteins by polyphenols. These studies showed that certain features within the structure of certain polyphenols would favor or disfavor the formation of the polyphenol-protein complexes. In this section we will show some examples of these studies.

Figure 12. PRP-polyphenol interaction model proposed by Haslam's group²²

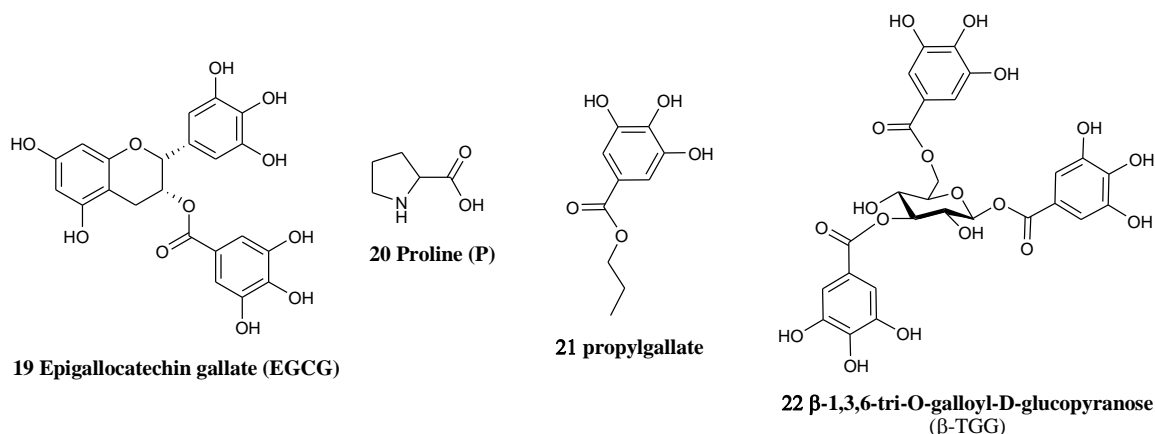


Edwin Haslam,²¹ measured the formation of the complex of a series of gallotannins and condensed tannins with the protein from sweet almonds β -glucosidase (enzyme that breaks β -1 \rightarrow 4 bonds of glucose-glucose derivatives or glucose substituted molecules). Quantification of the precipitated protein was achieved by measuring the amount of enzyme that remained in solution after centrifugation of the protein-polyphenol complex (by measuring the enzymatic activity in the supernatant). It was reported that of the series of polyphenols tested, the β -PGG (**8**, Figure 6) had the optimal shape for the binding with the protein. The ratio for the enzyme/ β -PGG complex was reported to be of 1:20. The

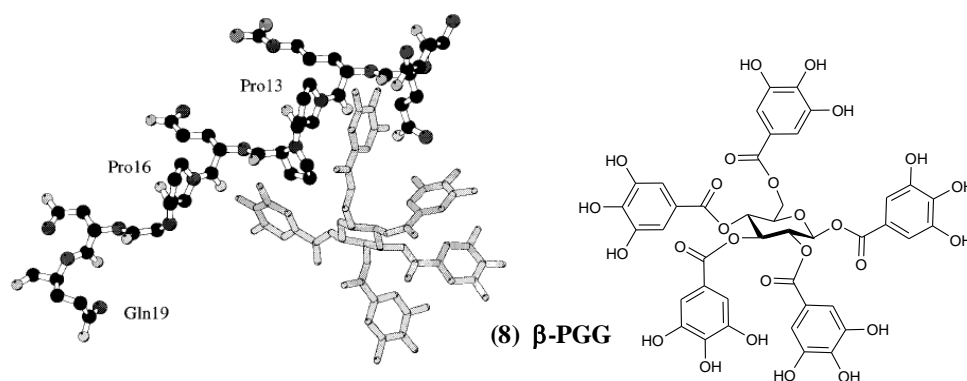
author suggests that “the polyphenol-protein complex formation which results in precipitation is caused by cross linking of separate protein molecules by the phenol”.

Proteins with a high content of the proline aminoacid (P, **20**), known as proline rich proteins (PRP's) have been used to study the formation of polyphenol-protein complexes, within the context of studying the astringency phenomena (precipitation of salivary proteins). In 2002 Haslam's group,²² reported the interaction between the flavonoid epigallocatechin gallate (**19**, EGCG) and extended or random coiled peptides modeling PRPs. Different methods used to study the complex formation showed that approximately 7.5 EGCG (**19**) molecules interacted with one peptide chain bearing 8 proline residues (19 residue long peptide). In comparison approximately 2 molecules of β -PGG (**8**), were involved in binding with the same peptide. For a smaller peptide (7 residue long peptide) the affinity was approximately 50 times smaller. They proposed that several polyphenolic molecules bind simultaneously to the peptide, and that the number of molecules bound is dependant of the type of polyphenol and the length of the peptide; the model of precipitation of the complex is presented in Figure 13.

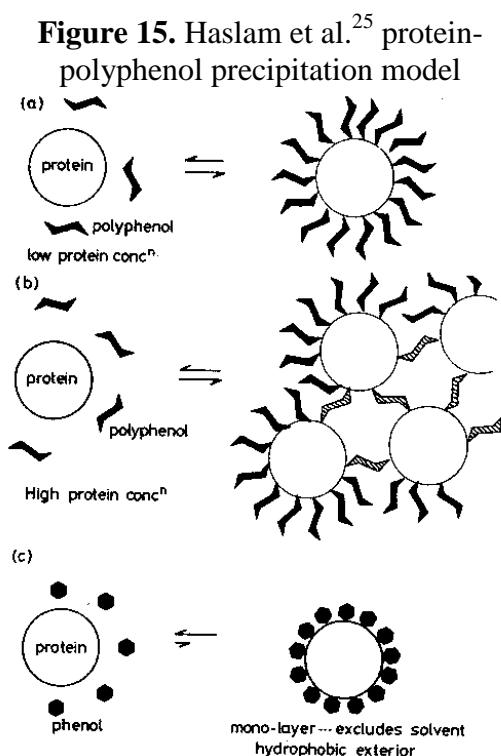
Figure 13 . Structures of EGCG, proline (P), propylgallate and β -TGG



Using a similar system, Baxter *et al.*²³ showed by NMR experiments the interaction between mouse salivary proline rich peptide (GPQQRPPQPGNQQGPPPQGPGPQ, fragment of the MP5 protein) and the following polyphenols: propyl gallate (**21**), β -TGG (**22**), β -PGG (**8**), (–)-epicatechin (**1b**), and procyanidin B-2 (**4b**). The assays showed preferential binding of the polyphenol to proline residues and to its neighboring amino acids. They reported the interaction occurs primarily between the aromatic rings of the polyphenol and the proline ring in a face-to-face manner (σ – π type attraction). They conclude that larger more hydrophobic polyphenols bind more strongly to PRPs in the following order: B-2 > PGG > TGG > (–)-epicatechin \approx propylgallate which is in agreement with previous reports.^{3,24}

Figure 14. Stacking interaction between β -PGG (**8**) and PRP proposed by Baxter *et al.*²³

The structural characteristics of both the polyphenols and the proteins are important factors in defining their capacity of interaction. Among these structural characteristics are size, and conformational flexibility. The work of Haslam's group²⁵ illustrates with a series of polyphenols and the bovine serum albumin (BSA, globular protein) how these factors influence protein polyphenol interaction. Their assays with a galloyl D-glucose series showed the efficacy of binding to BSA to increase with the number of galloyl units, and therefore molecular size (tri-GG < tetra-GG < penta-GG). However, the higher molecular weight polyphenols (hepta-GG) didn't show significant increase in protein binding capacity. They

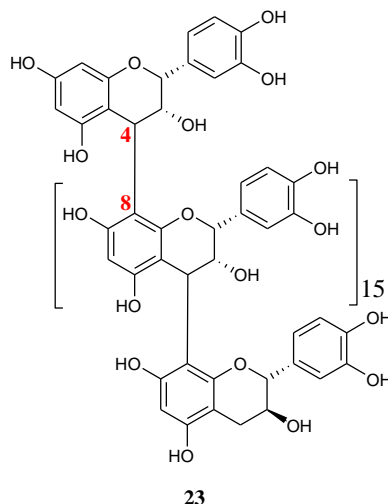


also compared β -PGG (**8**) and their more structurally rigid “analogues” ellagitannins vescalagin (**10**) and castalagin (**11**). These less flexible ellagitannins showed to bind 30 times less to BSA than the β -PGG (**8**). The model for precipitation proposed by the authors based on their findings is shown the figure to the right. Similar results were observed in the study conducted by Tang and co-workers,¹⁹ between collagen (fibrous protein) and 24 different gallotannins and ellagitannins; among which were vescalagin (**10**) and castalagin (**11**). Furthermore, Hagerman *et al.*²⁶ compared the precipitation of BSA by gallotannin β -PGG (**8**)

and the B-type procyanidin epicatechin₁₆ (4→8) catechin (**23**, EC₁₆-C). This study showed that the elongated high molecular weight EC₁₆-C (**23**) precipitated the roughly spherically shaped BSA, and that the ratio for the complex BSA/EC₁₆-C (**23**) was significantly lower (1:2.5) compared to that with **8** (1:25). Concerning the type of interaction, the BSA/EC₁₆-C

complex seemed to interact through hydrogen bonding forces, while the β -PGG (8) complexes showed predominantly hydrophobic type interactions.

Figure 16. Structure of procyanidin epicatechin₁₆ (4→8) catechin (EC₁₆-C)^{26,27}



The multiple-interaction-site models presented in this section implicate a non-specific association manner, which is not necessarily true for all kinds of polyphenol-protein systems. Complex formation is dependent of the polyphenol-protein system under study, and the precipitation of the polyphenol-protein complex occurs in the presence of a large excess of polyphenol, which masks the detection of any specific interaction, if there is one. This plastering of the protein by polyphenol compounds is defined as **non-specific polyphenol-protein interaction**. On the other hand, the enzymes that are involved in the biosynthetic pathway of polyphenols are examples of **specific polyphenol-protein interaction**, because a certain type of polyphenol binds to a specific site of its corresponding enzyme, which transforms its polyphenolic substrate. Recent studies show that polyphenols bind to specific sites of proteins in a 1:1 ratio affecting their functions, which also implies specific polyphenol-protein interactions. Some examples concerning polyphenols involved in specific interactions with proteins or peptides are presented in the following section.

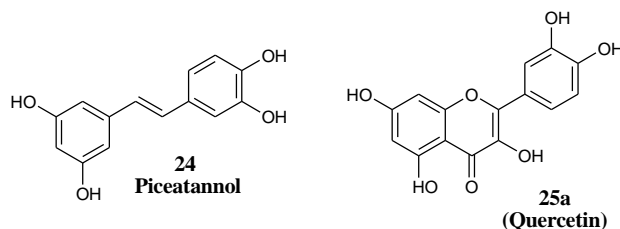
Ib.3 Polyphenols-Proteins and Specific Interactions

Ib.3.1 F₀F₁-ATPase/ATP synthase protein- resveratrol

One example of a polyphenol interacting in a specific manner with a protein is found within the works of Zheng *et al.*²⁸ and Glendhill *et al.*,²⁹ in which the hydroxylstilbene resveratrol (17) binds in a 1:1 ratio and with strong affinity to the rat brain and liver F₀F₁-ATPase/ATP synthase protein. ATP synthase is an enzyme that is present in the inner membrane of eukaryotic mitochondria; the F₁-ATPase is the region (F₁) of the protein that synthesizes

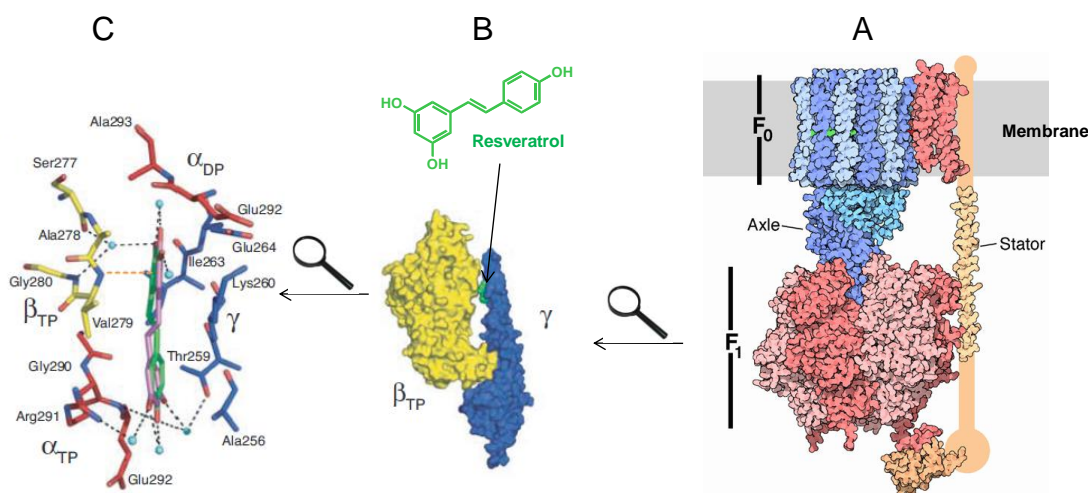
ATP and the F₀ domain is the axle that connects it to several membrane proteins (Figure 18A). This protein is a molecular motor that can also work in the reverse sense, hydrolyzing ATP under certain conditions (ATPase activity).^{28,30} Resveratrol (**17**) showed to inhibit both activities of the enzyme (ATPase/ATP synthase activity) with IC₅₀ values between 12-28 μM.

Figure 17. Structures of other polyphenols that interact with F₀F₁-ATPase/ATP synthase



On the contrary, other polyphenols tested such as catechin (**1a**), epicatechin (**1b**) and epigallocatechin (**2b**, EGC) showed to have little anti-ATPase activity. Furthermore, resveratrol (**17**) showed little activity when tested with other ATPases (Na⁺/K⁺-ATPase from porcine cerebral cortex).²⁸ Concerning the mechanism of action of resveratrol (**17**) with this enzyme, Glendhill *et al.*²⁹ reported co-crystals of this polyphenol with F₁-ATPase from bovine heart mitochondria. The authors report localization of resveratrol (**17**) within the F₁-ATPase domain (Figure 18A) by binding in a pocket located between the γ- and β_{TP}-subunits (Figure 18B). Figure 18C, shows the interactions observed between the enzyme residues and resveratrol (**17**) in the binding pocket. Resveratrol (**17**) showed to be within 4 Å from the enzymes residues and is bound by hydrophobic interactions or via hydrogen bonds via water molecules. They also reported co-crystal structures with piceatannol (**24**) and quercetin (**25**) showing similar localization of the polyphenols within the enzyme.

Figure 18. F₀F₁-ATPase/ATP synthase CPK model³⁰ and site of binding of resveratrol in bovine F₁-ATPase co-crystals²⁹

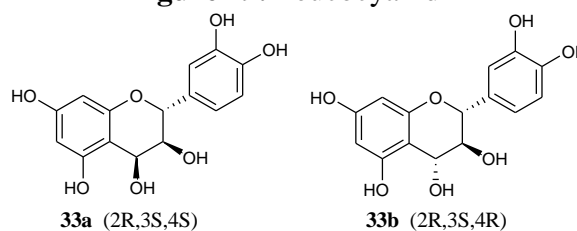


Ib.3.2 Anthocyanidin synthase-flavonoids

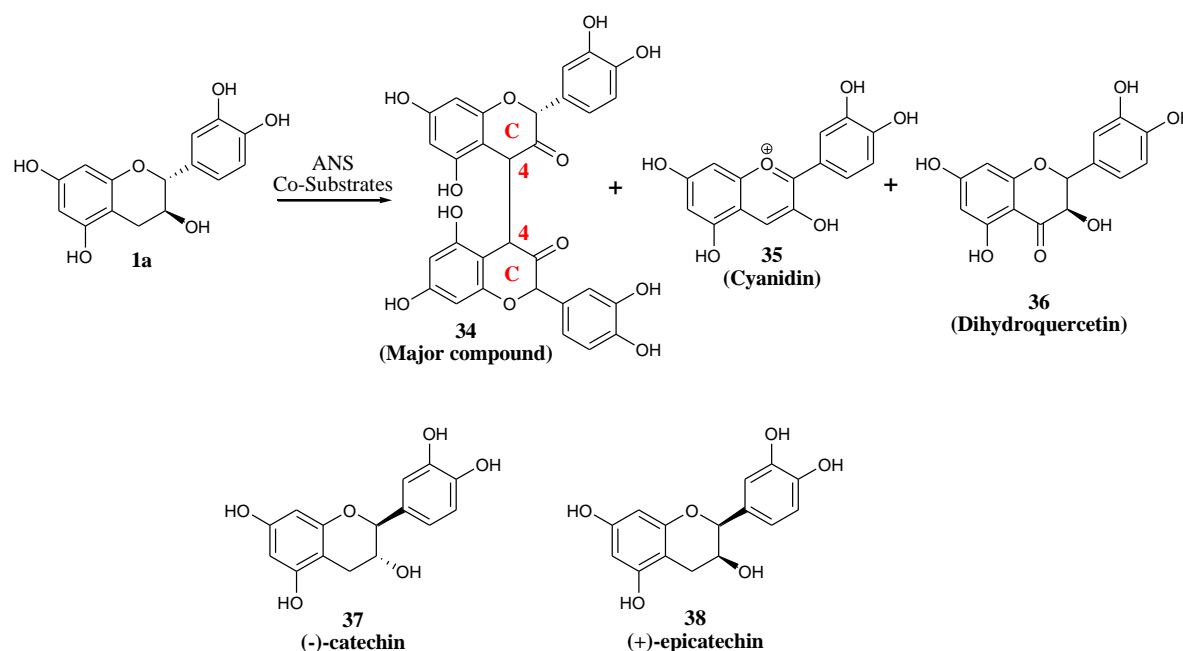
The anthocyanidin synthase-flavanol system (ANS, also known as LDOX **Leucocyanidin dioxygenase**) is an example of a specific interaction between a polyphenol and a protein in nature. More specifically, it's a 2-oxoglutarate, iron

dependent oxygenase enzyme that catalyses the penultimate step in the biosynthesis of the anthocyanin flavonoids.³¹ Previous studies show this enzyme recognizes and transforms leucocyanidin (**33a**) and (+)-catechin (**1a**) but not (-)-catechin (**37**) or (+)-epicatechin (**38**). Incubation of ANS with (2R,3S,4S)-cis-leucocyanidin or (2R,3S,4R)-trans-leucocyanidin furnishes quercetin (**25a**) or dihydroquercetin (**36**) and cyanidin (**35**); while (+)-catechin (**1a**) gives cyanidin (**35**), dihydroquercetin (**36**), and an unusual catechin C4→C4 dimer (**34**) as the major product.³²

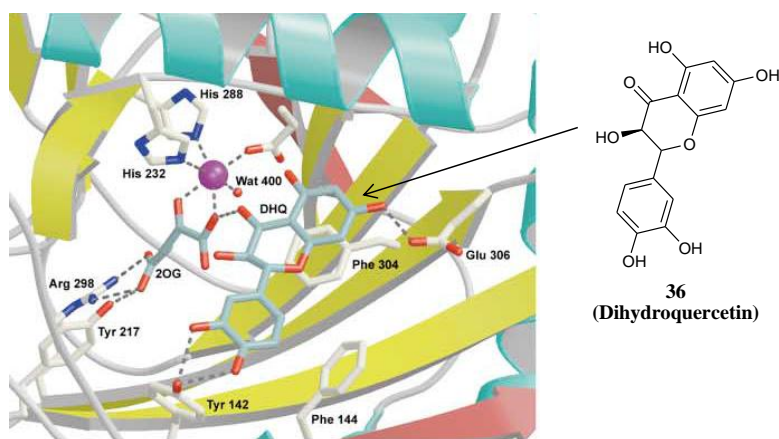
Figure 19. Leucocyanidin



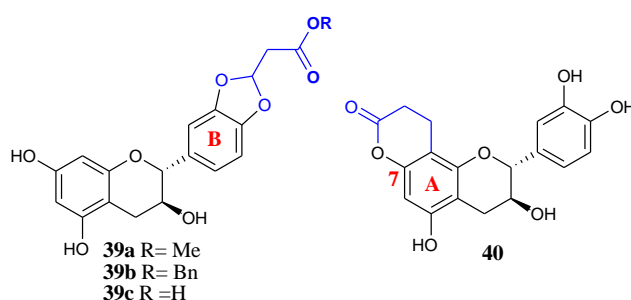
Scheme 3. (+)-Catechin transformation upon reaction with ANS; (-)-catechin and (+)-epicatechin structures.



ANS from *Arabidopsis thaliana* was co-crystallized with dihydroquercetin (DHQ, **36**) in presence of ferrous ions (Fe^{+2}), 2-oxoglutarate (necessary for the transformation) and acid ascorbate (catalyst of the reaction, scheme 3).^{31,33} A Michaelis constant (K_m) value of 175 μM was estimated for interaction of the catechin-ANS (*Gerbera*) system.³²

Figure 20. ANS (*Arabidopsis thaliana*) co-crystallized with dihydroquercetin (**36**)³¹

Quideau and co-workers have also studied the ANS-flavanol interaction.³⁴ These studies concern the development of affinity-based tools for grape derived protein extracts aimed at isolating proteins involved in the biosynthetic pathway of flavonoids. The catechin-ANS interaction was used as a model to validate the utility of the affinity tools, which consisted of resin-bound flavan-3-ol. For this, the flavan-3-ols were modified to bear a spacer before attachment to the resin. When a spacer was introduced through the B-ring of the catechin substrate (**39a-c**), it was found that no transformation of the substrate took place. These results were rationalized by taking into account the aforementioned co-crystal structure of ANS from *Arabidopsis thaliana* with DHQ (**36**), in which the B-ring hydroxyl groups form hydrogen bonds with the Tyr142 residue within the active site of the enzyme (Figure 20). It was also observed that when the C-7 hydroxyl group was involved in an intramolecular covalent bond (**40**), no transformation of the substrates takes place upon reaction with the ANS enzyme.

Figure 21. Catechin derivatives showing no transformation upon reaction with ANS

However, when the spacer was anchored through the A-ring at the C-8 position and ended by an ethylester group (**41**), its reaction in presence of ANS furnished a C4→C4 dimer (**42**) analogous to **34** as the major product. The affinity tools thus developed, consisting of both

supported catechin and epicatechin, showed satisfactory results in binding the ANS enzyme from a partially purified ANS extract (*Vitis vinifera*). The resin-bound catechin (**43**) does not retain the ANS enzyme, but the catechin and epicatechin bound to the resin through their A-ring as in **44a** and **44b** bind the ANS enzyme. These results indicated that there is recognition and thus affinity of the ANS enzyme for catechin and, to a lesser extent, for epicatechin and confirmed activity only for the catechin derivative.

Figure 22. Catechin derivative transformed by ANS

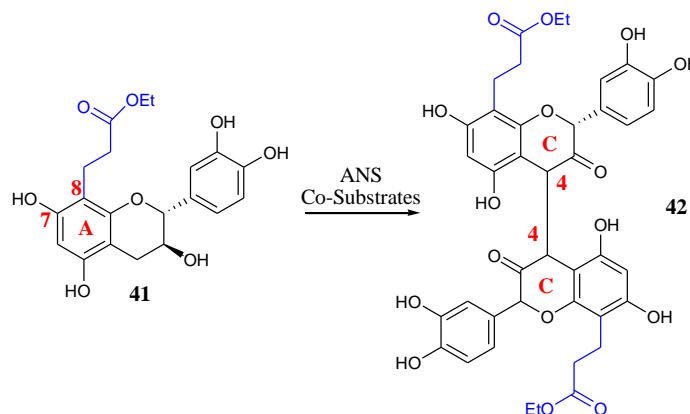
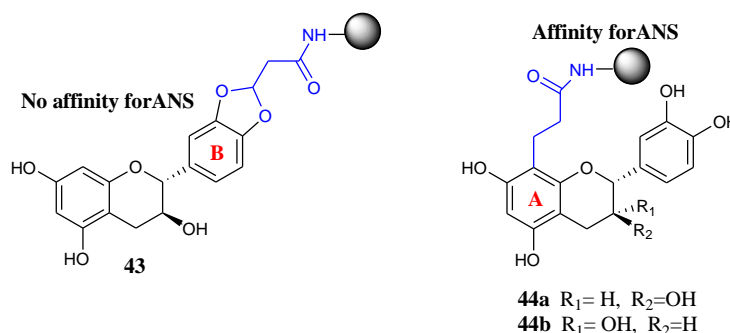


Figure 23. (Epi)catechin immobilized affinity resins



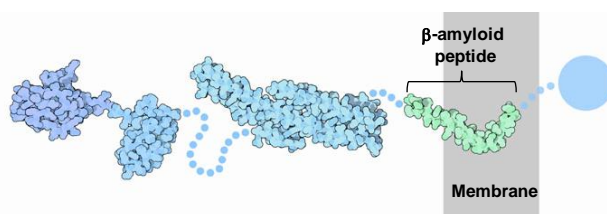
For both cases mentioned above, the ATPase-resveratrol and the ANS-DHQ complexes (Figure 18 and 20), crystallographic the evidence shows the active site of the protein interacting with the polyphenol compound in a 1:1 ratio, which indicates a specific protein-polyphenol interaction. The following examples show polyphenols interacting with certain proteins or peptides, inhibiting its function, as evidenced by the inhibition of their functions that likely results from specific interactions.

Ib.3.3 β -Amyloid peptide-flavonoids

Some polyphenols of the flavonoid family inhibit in a dose dependent manner the β -amyloid₁₋₄₀ and β -amyloid₁₋₄₂ peptide aggregation. β -Amyloid peptides are small peptides that form part of the amyloid precursor protein (APP, a membrane tethered protein) which plays an essential

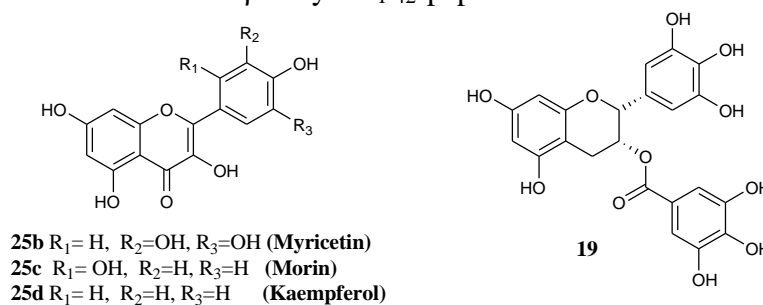
role in neural growth and repair. The function of these small peptides is to anchor the protein to the cell membrane. However, when these small peptides are not bound to the APP protein they leave the membrane, change shape and aggregate into long fibrils. These fibrils form dense plaques that accumulate on nerve cells,³⁵ a process that is associated to major human diseases among which are Alzheimer's disease, Parkinson's disease, and type II diabetes.³⁶

Figure 24. Amyloid precursor protein CPK model (APP)³⁵

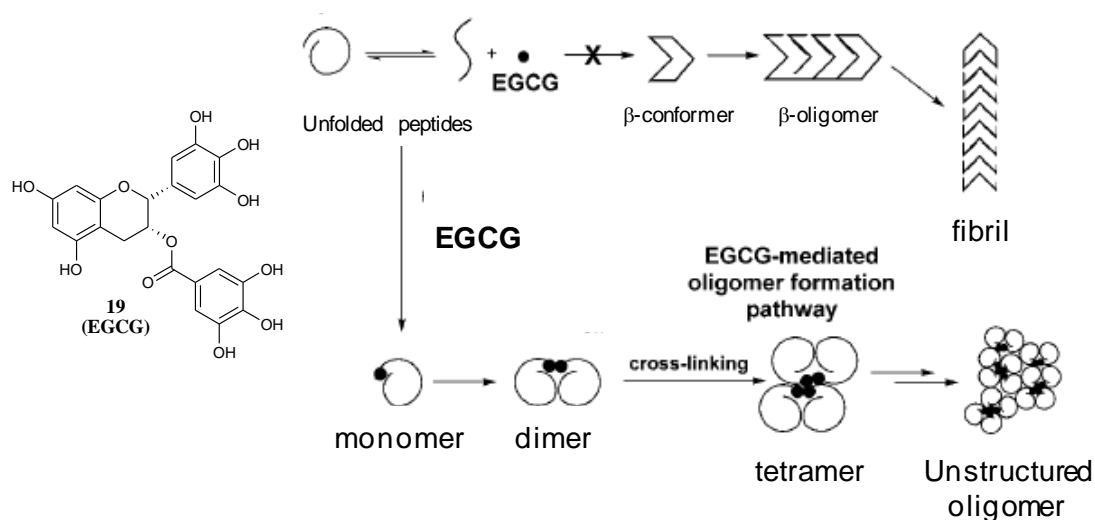


Flavanols with different substitution pattern in the B-ring, such as myricetin (**25b**), morin (**25c**), quercetin (**25a**), kaempferol (**25d**) and the flavanols catechin (**1a**) and epicatechin (**1b**) inhibit the formation of fibrils of the β -amyloid₁₋₄₀ and β -amyloid₁₋₄₂ peptides with effective concentrations (EC_{50}) values between 0.1-1 μ M.³⁷

Figure 25. Flavanols that inhibit the formation of fibrils of the β -amyloid₁₋₄₀ and β -amyloid₁₋₄₂ peptides



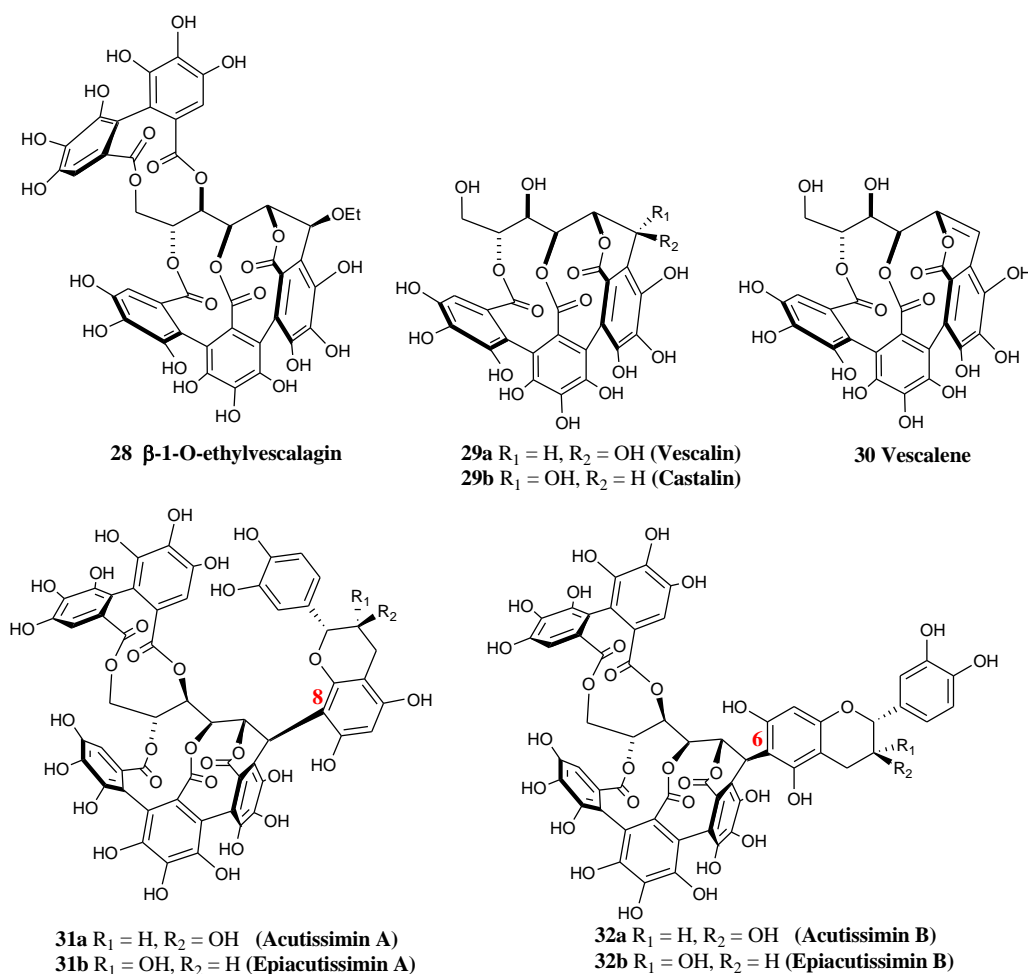
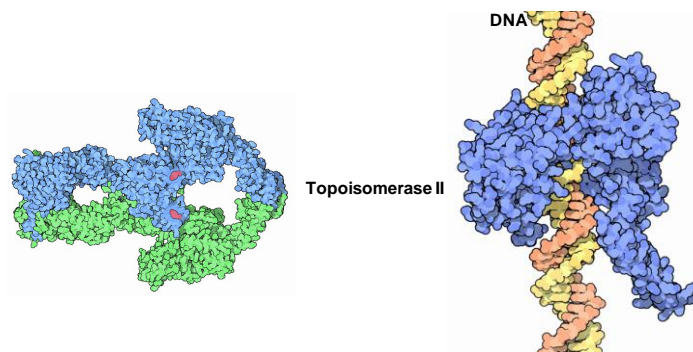
Another flavanol that shows antifibrillogenic properties is epigallocatechin gallate (EGCG, **19**). This flavanol with a pyrogallolic bearing B-ring binds to unfolded β -amyloid peptide and α -synuclein, another amyloidogenic protein implicated in Parkinson's disease. In this case, the authors³⁸ proposed a mechanism in which the inhibitory effect is due to the formation of EGCG (**19**)-stabilized monomers and lower molecular mass oligomers that do not incorporated into the fibril aggregation (Figure 22), hence preventing the formation of toxic aggregates. EGCG (**19**) also shows an inhibitory effect with other amyloidogenic proteins like, Prp^{SC} (proteinaceous Infectious only particle), insulin, calcitonin, as well as a peptide fragment from prostatic acid phosphatase, whose fibrillar aggregates are implicated in the enhancement of HIV-1 infection and urokinase an enzyme required by human tumors to form metastases.³⁹

Figure 26. Model to explain the effect of EGCG over α -synuclein peptide³⁸

The following examples show the inhibition of the function of certain proteins by polyphenols of the C-glucosidic ellagitannin sub-class.

Ib.3.4 Topoisomerase II-ellagitannins

Some C-glucosidic ellagitannins have shown to inhibit human topoisomerase II.⁴⁰ DNA topoisomerase II is an enzyme that acts on the topology of DNA. This class II topoisomerase unwinds and winds DNA by introducing transient DNA double strand breaks. This allows DNA to control the synthesis of proteins, and facilitates DNA replication. This enzyme is an anticancer target in chemotherapy treatments.⁴¹ In vitro testing showed vescalagin (**10**), castalagin (**11**), β -1-O-ethylvescalagin (**28**), vescalin (**29a**), castalin (**29b**), vescalene (**30**), acutissimins A (**31a**) and B (**32a**), as well as epiacutissimins A (**31b**) and B (**32b**) to inhibit decatenation of kDNA (standard bioassay) between 1-10 μ M. The best results of the series being vescalin (**29a**) with 96% inhibition at 1 μ M and vescalene (**30**) with 97% inhibition at 10 μ M. However, in cellulo assays showed vescalagin (**10**) to be the most effective of the series.¹²¹ These ellagitannins showed in vitro to have a higher activity than the VP-16 drug (currently used in chemotherapy treatments, 3.7% inhibition at 1 μ M of VP-16 and 6.5% inhibition at 10 μ M of VP-16).

Figure 27. Ellagitannins that inhibit human topoisomerase II⁴⁰**Figure 28.** Topoisomerase II CPK model and topoisomerase-DNA⁴²

Ib.3.5 Squalene epoxidase and proteasome activity vs. catechin

Catechin (**1a**) derivatives showed to be both potent and selective inhibitors of rat squalene epoxidase (a rate limiting enzyme of cholesterol biogenesis)⁹ and to inhibit proteasome activity (responsible for the degradation of most cellular proteins).⁴³

In the previous examples, the studies were performed using pure protein or peptide samples with polyphenols. The following examples show polyphenols to inhibit more complex systems like the HSV virus and the cellular cytoskeleton of cells.

Ib.3.6 *Herpes simplex virus-ellagitannins*

Research concerning C-glucosidic ellagitannins showed that vescalagin (**10**), castalagin (**11**), grandinin (**26**), roburin B (**27a**), and D (**27b**) inhibit selectively *Herpes simplex virus* (HSV) strains resistant to acyclovir (one of the most commonly used antiviral drugs). Of the series the most active compound was shown to be vescalagin (**10**), with an IC_{50} of 0.4 nM.⁴⁴

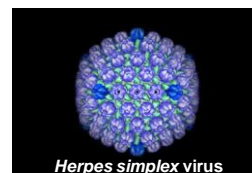


Figure 29. C-glucosidic ellagitannins that inhibit *Herpes simplex virus* (HSV) strains

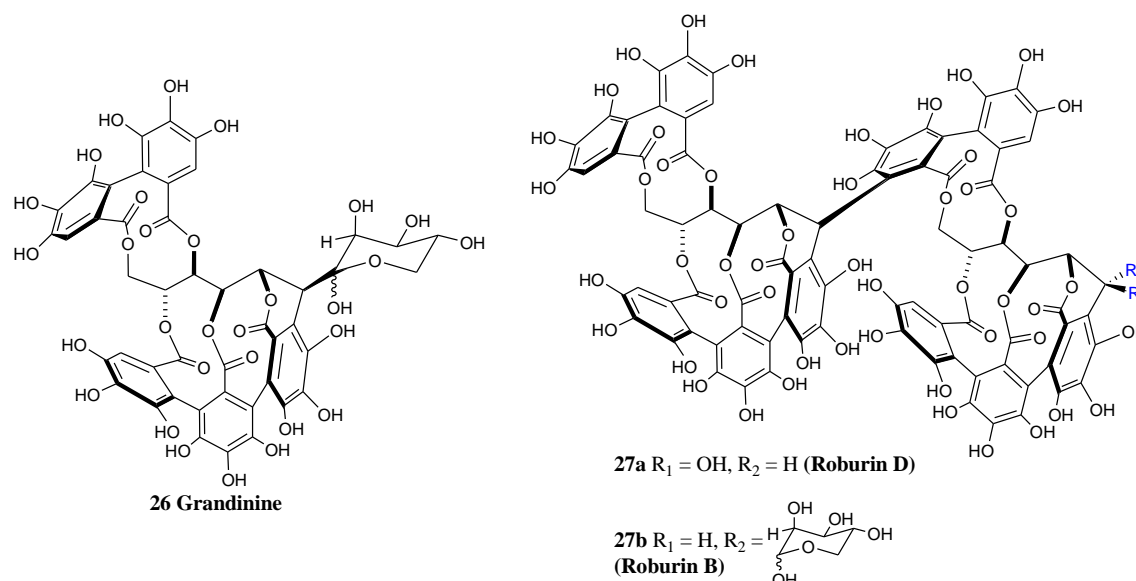
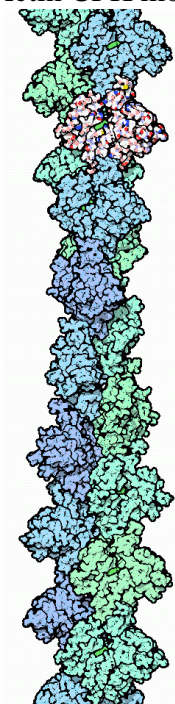


Figure 30.⁴⁵
F-Actin CPK model

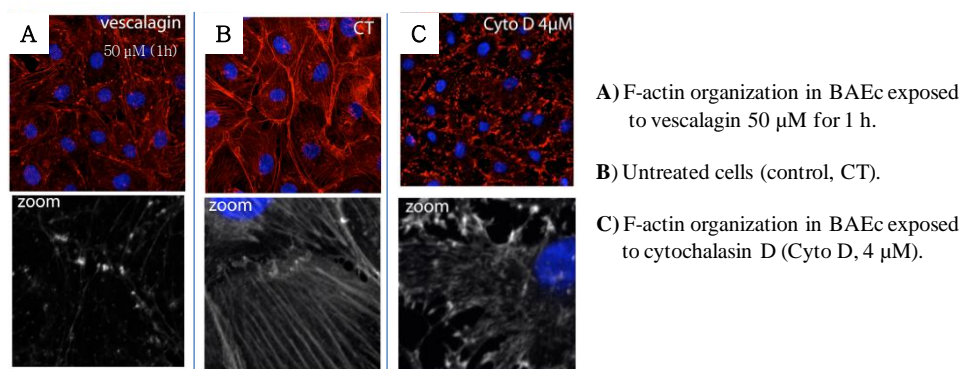


Ib.3.7 *Actin-ellagitannins*

Within the framework of a collaborative study between Quideau's and Génot's teams at the IECB, vescalagin (**10**), castalagin (**11**), and their congeners vescalin (**29a**) and castalin (**29b**) were tested for their activity concerning the actin protein.⁴⁶ Actin is one of the most abundant structural proteins in eukaryotic cells. It forms the microfilaments of the cytoskeleton and participates in many important cellular functions like cell shape, motility, cytokinesis, adhesion, and gene expression. These functions are linked to actin by the equilibrium between monomeric globular actin (G-actin) and the polymeric fibrillar actin (F-actin) in an adenosine triphosphate (ATP) dependent process.⁴⁷⁻⁴⁹ Of the series, vescalagin (**10**) showed to be the most potent compound in presence of actin in its fibrillar form, binding to fibrillar actin (F-actin) and winding the filaments into

fibrillar aggregates. More specifically, in cellulo testing with bovine aortic endothelial cells (BAEc) and vescalagin (**10**) at a concentration of 50 μM showed a disappearance of the internal stress fiber network of the actin cytoskeleton; this behavior was not observed for the negative control cells. The perturbation seemed different from that observed for the cells tested with cytochalasin D (inhibitor of G-actin polymerization, see Figure 31). Furthermore, dissolution of focal adhesion was observed, which suggested an effect of vescalagin over cell adhesion (one of the functions in which is involved F-actin). Dissolution of stress fibers induced by vescalagin (**10**) affected cell morphology. Mitosis was also affected for cells treated with vescalagin (**10**), becoming impaired for a concentration of **10** at 100 μM . The study of the actin-vescalagin (**10**)/vescalin (**29a**) interaction was also achieved by surface plasmon resonance (SPR) studies and constitutes part of this work (Chapter III).

Figure 31. In cellulo effect of vescalagin over the F-actin organization in BAEc⁴⁶



The evidence concerning polyphenol-protein interaction is gathered thanks to a large variety of techniques. Most techniques take advantage of the physico-chemical properties of the molecules involved in order to measure the changes produced over these properties as a consequence of the interaction. Each technique has advantages and disadvantages when compared to another technique, which is why they are mostly complementary. The technique chosen for our study is surface plasmon resonance, which will be discussed further ahead. Before, some of the techniques used to study intermolecular interaction are briefly discussed.

Ic. Techniques used to Study Polyphenol-Protein Interaction

Ic.1 Commonly used techniques to measure protein-ligand interaction

Among the analytical techniques used to study polyphenol-protein interactions are: **microcalorimetry**, which measures the change in enthalpy involving reversible bimolecular interactions,⁵⁰ **fluorescence quenching**, which takes advantage of the intrinsic fluorescence of proteins and the quenching of fluorescence exerted by polyphenolic compounds in close

proximity to the protein,⁵¹ **equilibrium dialysis** that permits to study bimolecular systems in solution at the equilibrium,²⁵ **enzyme inhibition**,²⁸ **precipitation**,^{21,26} **dynamic laser light scattering and electron microscopy**, which allows to study particle size distribution of polyphenol-protein precipitates,²² **circular dichroism**, which analyses changes in secondary and tertiary structure of proteins caused by interaction with polyphenols. This is, by measuring variations in the absorption of left and right circularly polarized light of chromophores that are chiral or placed in a chiral environment^{52,53} and **mass spectrometry**,⁵⁴ among others. The aforementioned techniques give mostly information of the strength and stoichiometry of the complex between polyphenols and proteins. Techniques that allow localization of a ligand within the proteins structure are NMR and X-ray. **NMR** studies uses one dimension or two dimension experiments to determine the proximity between the molecular partners and gives information of the region of the protein or peptide that is affected by the proximity of the ligand.^{23,24,53} However, this technique is limited by the use of isotopically labeled protein and the upper limit for protein size, which is why these NMR investigations usually concern small proteins or model peptides.⁵⁵ **X-ray diffraction** analysis of protein-ligand complex gives a structural print that furnishes information about the binding site and direct interactions with the protein residues involved. However, this implies the use of very pure protein samples in large quantities and the formation of stable crystals that diffract well. This co-crystallization can be difficult and not always possible.⁵⁶

Besides X-ray diffraction and enzyme inhibition, other analytical techniques used to study polyphenol-protein interactions are limited in differentiating specific from unspecific interactions. This lack of adequate techniques prompted Quideau and co-workers to develop new analytical tools based on surface plasmon resonance (SPR, BIAcore GE Healthcare), a highly sensitive and well established technique for measuring protein ligand interaction in real time. This SPR tool is thus presented as an alternative tool for polyphenol-protein interaction studies in the following section.

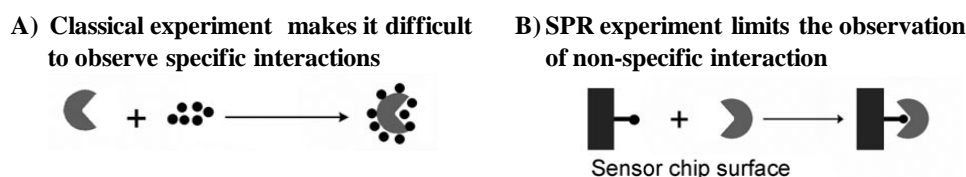
Ic.2 SPR as an alternative technique in the study of polyphenol-protein interaction

The research team of Stéphane Quideau has been interested in the chemistry of polyphenolic compounds and their roles in biology. More specifically, the focus of the team in this area concerns polyphenols such as ellagitannins, gallotannins and flavonoids, as well as the mode of action of these types of polyphenolic compounds towards certain types of proteins.

As stated in the previous section, the main problematic concerning the study of polyphenol-protein interaction is the coating of the proteins surface by polyphenolic molecules under the

conditions regularly used to conduct the experiments and under which the polyphenol is present in molar excess in comparison to the protein (see Figure 32A). Taking this problematic into consideration, Quideau and co-workers presented as an alternative the immobilization of the polyphenol molecule on to a sensor surface in the aim limiting the observation of non-specific interactions (see Figure 32B). The surface plasmon resonance sensor was chosen as the detection system for the interaction studies, for it has the advantage of being a very sensitive technique that uses little amounts of both partners.^{57,58}

Figure 32. Non-specific protein-polyphenol interaction vs. immobilized polyphenol



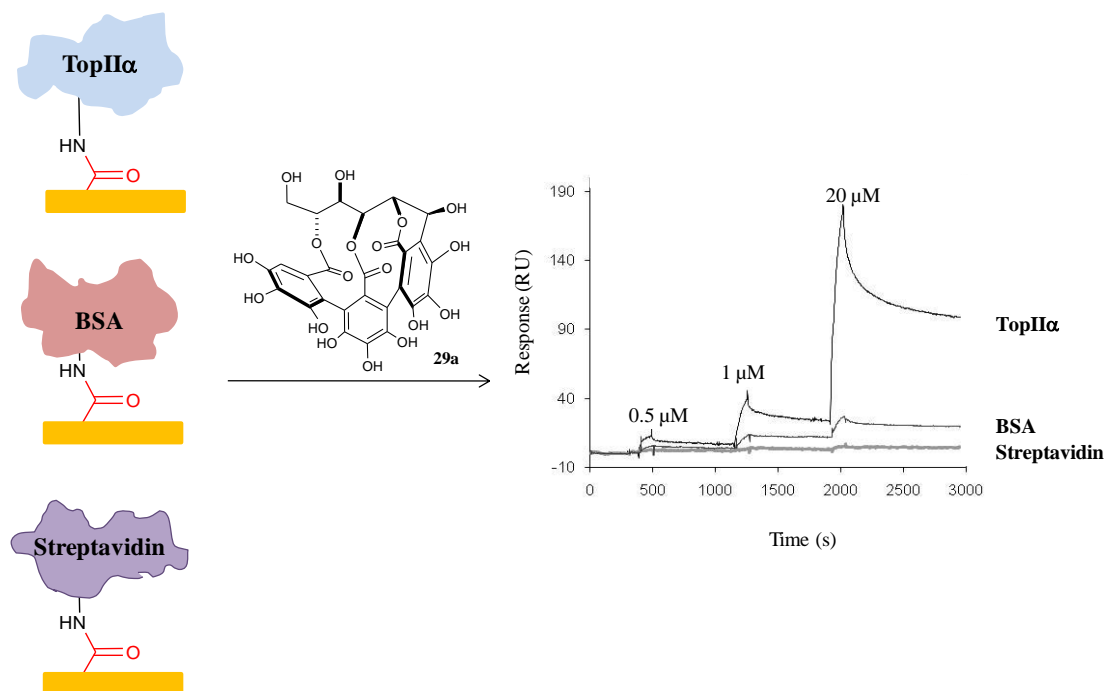
Surface plasmon resonance (SPR) is an optical technique with detectors or SPR sensors that are usually used for the detection and quantification of macromolecular interactions. In this technique, one of the interacting partners is immobilized to the sensor surface (referred to as ligand) and the molecular interaction with another partner (referred to as analyte) is analyzed in solution.⁵⁹ In classical SPR experiments, the protein is bound covalently to the sensor chip surface by well established chemical reactions or by the use of affinity tags.^{59,60} The analyte (in our case the polyphenol) is eluted and allowed to interact with the protein. Under these conditions, the polyphenol is in excess in comparison to the protein, and the system is under the same conditions as those described above and under which it is difficult to discriminate specific from non-specific interactions (Figure 33A). This situation should be avoided in a reverse experiment, during which the protein becomes the analyte used in excess compared to the immobilized polyphenol. Despite the protein being in excess, the SPR technique still allows to use very small amounts of protein for the assays. In this regard, a proof-of-concept study of polyphenol-protein interaction by SPR was successfully performed with the vescaline-TopII α interaction as model.⁶¹ Both the classical SPR experiment and the reverse SPR experiment were compared.

Ic.3 Classical SPR experiment vs. reverse SPR experiment

For the classical SPR experiment, the TopII α protein was immobilized onto the SPR sensor surface by means of covalent binding, taking advantage of the inherent reactivity of the lysine residues of the protein. The same procedure was repeated to immobilize two control proteins

(BSA and streptavidin) commonly used in this kind of experience to discern non-specific type interactions. The results obtained for the classical SPR experiment are shown in Figure 33.

Figure 33. Classical SPR experiment TopII α , BSA, streptavidin vs. vescalin (**29a**)

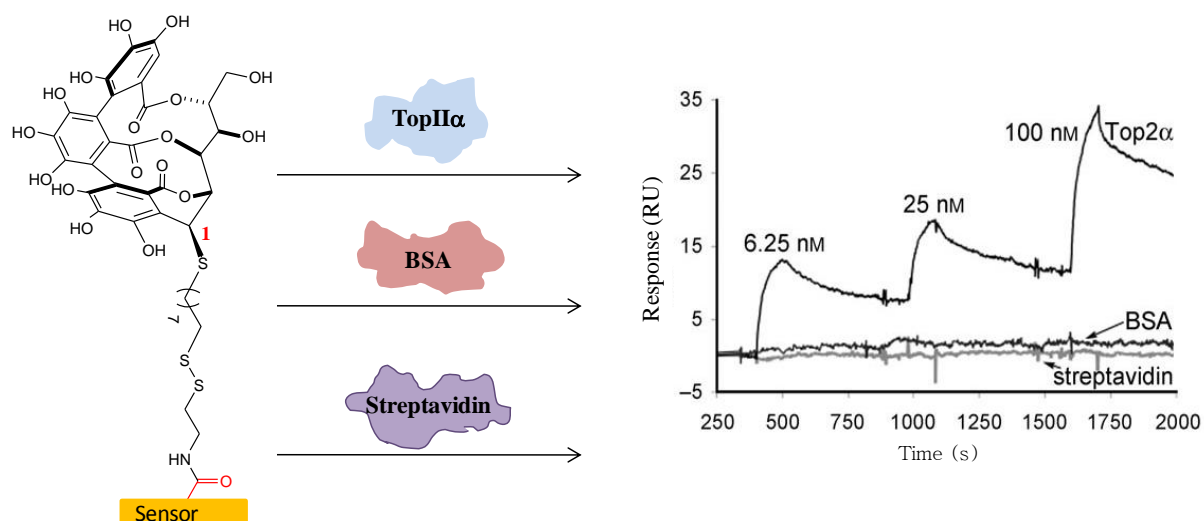


The binding was monitored in real time and measured in relative units (RU), which are proportional to the molar mass of the analyte (see appendix). Binding was observed between vescalin (**29a**) and all three proteins, with a preference for the vescalin-TopII α system as expected. However, the SPR response obtained for the TopII α -vescalin system (175 RU, Figure 33) is much higher than expected (22 RU) for a simple 1:1 binding mechanism, which suggested non-specific accumulation of the polyphenolic molecules over the protein surface. These results were compared with those of the reverse SPR experiment.

For the reverse SPR experiment, modification of vescalin (**29a**) with a long nucleophilic arm was necessary. Vescalin (**29a**) was chemically transformed into a sulfhydryl thioether deoxyvescalin derivative³⁹ and covalently bonded by a disulfide bond to a sensor chips surface (Figure 34). The affinity of TopII α to the immobilized vescalin (Figure 34) was monitored. The SPR response increased in a dose dependent manner indicating binding. This combined with the lack of SPR response for the proteins BSA, and streptavidin suggested specificity of the TopII α binding for vescalin (Figure 34). Furthermore, the SPR response obtained for the TopII α -vescalin system was lower than expected for a 1:1 binding mechanism. The authors suggested that steric hindrance caused by a high density of immobilized vescalin and/or the protein's size interferes with binding. Nonetheless, the fast

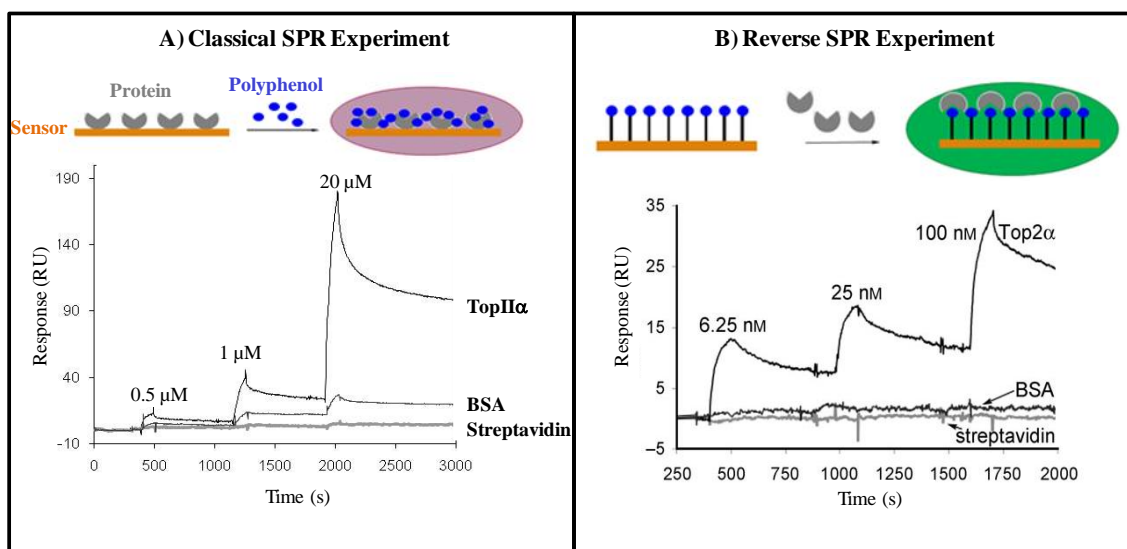
association rates and slow dissociation rates observed indicated binding affinity at the subnanomolar level.

Figure 34. Reverse SPR experiment: immobilized TopII α , BSA, streptavidin vs. vescalin



Comparison of both the classical SPR experiment and the reverse SPR experiment with this TopII α -vescalin model is shown in the following figure. A 35 RU response was obtained when TopII α was injected in solution to the immobilized polyphenol, while a 175 RU response was obtained when the polyphenol was injected. These results demonstrate that the reverse experiment is more suitable to limit the observation of non-specific interactions. This mode of analysis (reverse experiment) has also the advantage of increasing the sensibility of the technique, since the SPR response is proportional to the molar mass of the analyte (passing in solution).⁵⁹

Figure 35. Comparison of classical SPR experiment and the reverse SPR experiment



This proof-of-concept study gave rise to further developments of this tool throughout this thesis. Based on the team's experience, representative polyphenols were chosen among major families: flavonoids, hydrolysable tannins (ellagitannins) and procyanidins. The polyphenol-protein pairs were selected from the basis of the knowledge in their transformation by chemical means, and their known biological activity. The polyphenol-protein pairs that will be discussed throughout this work are the following: Vescalagin/vescalin-TopII α , vescalagin/vescalin-actin, (epi)catechin-ANS.

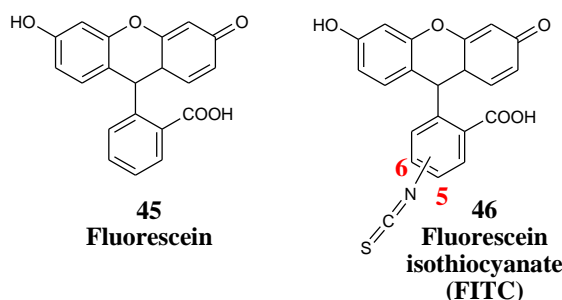
While in vitro assays such as the ones discussed in the previous section are important to understand polyphenol-protein interactions at the molecular level, it is crucial to investigate the effect that a polyphenol of interest may have in systems more representative of the in vivo state, such as the cell. Both C-glucosidic ellagitannins vescalagin (**10**) and vescalin (**29a**) showed an effect over the actin cytoskeleton of bovine aortic endothelial cells (BAEc),⁴⁶ which is why we were interested in localizing vescalagin (**10**) and vescalin (**29a**) within the cell. Fluorescent tagging of bioactive compounds is a technique commonly used to visualize the localization of bioactive compounds in the cellular environment. To this aim, fluorescently tagged derivatives of **10** and **29a** were prepared and used for confocal-microscopy assays with BAEc. These assays will be the subject of Chapter IV. The following section presents some examples of fluorescently tagged polyphenols involved in in cellulo assays.

Id. Polyphenol-fluorescent adducts and their use in cellulo studies

The process of fluolabeling consists in modifying the compound of interest to bear a fluorescent ending linker.⁶² Many fluorescent tags are commercially available and the literature is rich with examples of linkers used to anchor the fluorescent tag to the bioactive compound. However, some combinations of bioactive compound and fluorescent tag may lead to either lost in bioactivity,⁶³ fluorescence quenching,^{64,65} or both. Fluorescein (**45**) is one of the most commonly used fluorophores in biological applications. It has its absorption maxima at 490 nm and emission maxima at 512 nm and possesses good solubility in water. Its excitation maxima at 490 nm is close to the 488 nm spectral line of the argon laser, which makes it a good fluorophore for confocal laser scanning microscopy. Many fluorescein derivatives are available in the market, most of them have been designed to tune over specific wavelengths of the electromagnetic spectrum, circumventing the negative aspects of photobleaching and pH sensitivity or synthesized for specific applications.^{62,66-68} Within the fluorescent tagging of proteins, the most popular fluorophore is fluorescein isothiocyanate (FITC, **46**), because it can be easily installed by reacting with amine or thiol ending residues

from proteins. Its absorption and emission maxima are in good proximity of those of fluorescein (494 nm and 512 nm respectively).⁶²

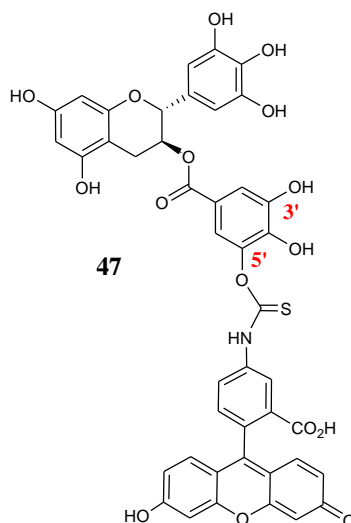
Figure 36. Structures of fluorescein (**45**) and fluorescein isothiocyanate (FITC, **46**)



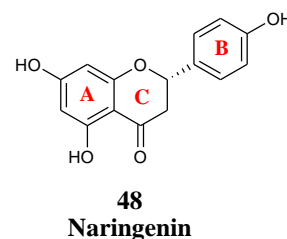
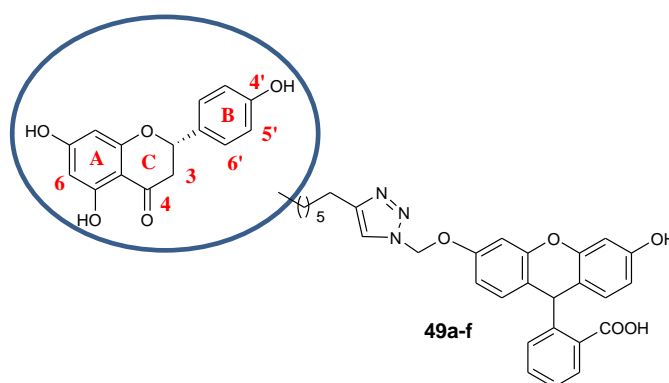
In the following section are presented a few examples of the design, synthetic strategy and rationalization of the bioassays concerning fluorescently marked polyphenolic compounds.

Examples of fluorescent tagging of polyphenols and their localization in cellulo

In 2008, Han *et al.*⁶⁹ reported labeling of EGCG (**19**), in which FITC (**46**) was coupled to the position 3'' or 5'' of the EGCG galloyls moiety (Figure 38) to give adduct **47**. This EGCG-FITC adduct was used in the study of the intracellular trafficking of the EGCG within L-929 cells (murine fibroblast cell line). Briefly, suspended L-929 cells was treated with the EGCG-FITC adduct **47** (65 μ M); by means of confocal microscopy compound **47** was observed at the cell membrane, incorporating into the cytoplasm and after 0.5 h penetrating into the nucleus. With time (up to 4 h of treatment) the EGCG-FITC adduct (**47**) was observed to concentrate in the nucleus of the suspended cells. FITC (**46**, 50 μ M) could not penetrate the membrane of viable cells by itself. Comparable results were also obtained over cultured L-929 cells as a monolayer when treated with EGCG-FITC (**47**) at 130 μ M (IC₅₀ aprox. 350 μ M), except that the absorption of **47** by the cell was slower (between 2 and 4 h of treatment, with apoptosis after 24 h). They also verified that FITC (**46**) does not penetrate the cell's membrane under these conditions. Though they stated that the pattern of cellular response of **47** seems somewhat different to that of **19**, these observations afforded the authors an additional argument that supported the hypothesis that EGCG (**19**) might penetrate the cytoplasm through binding to specific receptors in the membrane, forming complexes which would then pass the nucleus barrier in a time controlled manner.

Figure 37. Han *et al.*, epigallocatechin-3-O-gallate-3''-FITC (EGCG-FITC)⁶⁹

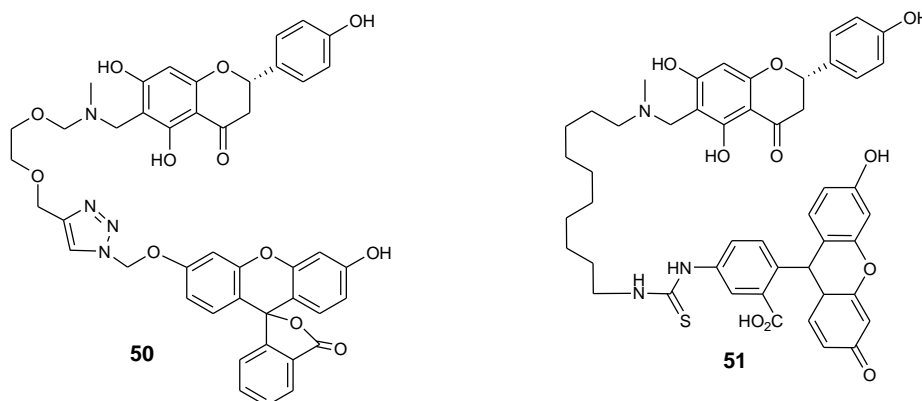
Another polyphenol of the flavanone type that was subject to fluolabeling is naringenin (**48**). In 2008, Chen *et al.*,⁶³ reported the synthesis of a series of naringenin-fluorescein derivatives and their use concerning the biodisponibility of naringenin (**48**) in living *Ribozomium* cells (genus of soil bacteria that associates with the roots of legumes forming a nitrogen fixing endosymbiotic system). More specifically, they were interested in the interaction between naringenin and nod-D gene proteins, because genetics evidence indicates the binding of naringenin (**48**) plays an important role in the production of nodulation signaling molecules. For this purpose, six naringenin-fluolabeled derivatives (**49a-f**) were prepared by varying the position of anchoring for the fluorescent linker to the naringenin skeleton.

**Figure 38.** Chen *et al.*, naringenin-fluorescein derivatives⁶³

All six naringenin-fluorescein derivatives (**49a-f**) kept proper fluorescent properties for the biological studies. However, bioassays revealed that compound **49a** (C-6 derivative) conserved only 9% of naringenin's biological activity, while compounds **49b-f** (B- and C-ring modified) were inactive. Keeping the anchoring of the fluorescent tag to naringenin's A-

ring, they prepared two other naringenin-fluorescein derivatives: one with a PEG-type linker in order to increase solubility (compound **50**) and a second one without the motif 1,2,3-triazole unit to verify that this motif wasn't interfering with the activity (compound **51**).

Figure 39. Naringenin PEG-type linker and aliphatic linker fluorescein derivatives



Both compounds **50** and **51** conserved good fluorescent properties, compound **51** was not active. However, compound **50** maintained 20% of the biological activity observed for naringenin (**48**) which was sufficient to perform the biodisponibility studies. Confocal microscopy analysis of *Rhizobium* cells treated with naringenin-fluorescein adduct **50** confirmed its penetration in the cell while maintaining viability.

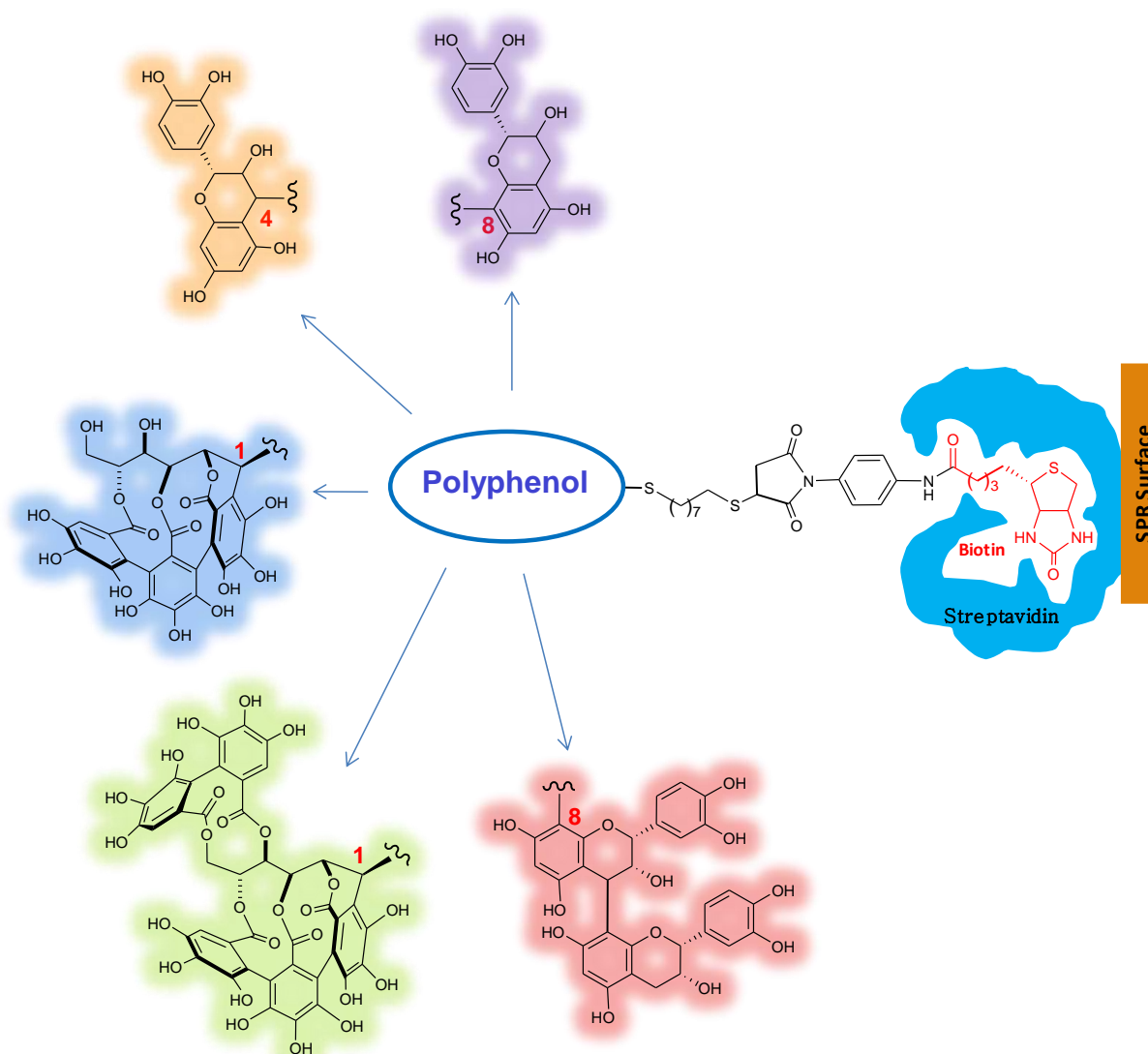
As may be noted from the work of Chen *et al.*⁶³, knowledge of the structure-activity relationship of the natural compound to be modified is of most importance in the development of an efficient fluorescently tagged derivative. In their experience, out of eight different naringenin-fluorescein adducts prepared, only one remained active enough to allow its detection in the biological system of study. In the studies of Han *et al.*⁶⁹, the EGCG-fluorescein derivative (**47**) seemed to have a different mechanism of action than the EGCG (**19**) itself. In accordance, it is considered best to keep available all the phenolic functions of the molecule, because these are possible interaction sites with the target. Also, it is important to verify that the behavior of the fluorescently tagged molecule remains similar to that observed for the non-modified compound during bioassays and that the effect is not due to the fluorescent tag alone.

The following chapters will be structured as follows: **Chapter II** concerns the hemisynthesis of polyphenols-biotin adducts (catechin, epicatechin, vescaline, vescalagin and B-type procyanidin), **Chapter III** concerns the use of the mentioned modified polyphenols for protein-polyphenol interaction studies by SPR with different proteins (TopII α , actin, BSA, among others), and **Chapter IV** covers the hemisynthesis of vescalagin- and vescaline-

fluorescein adducts and the in vitro and in cellulo assays performed concerning the interactions between actin and the ellagitannin pair vescalagin (**10**) and vescalin (**29a**).

Chapter II

Polyphenol Derivatization for Surface Plasmon Resonance Studies

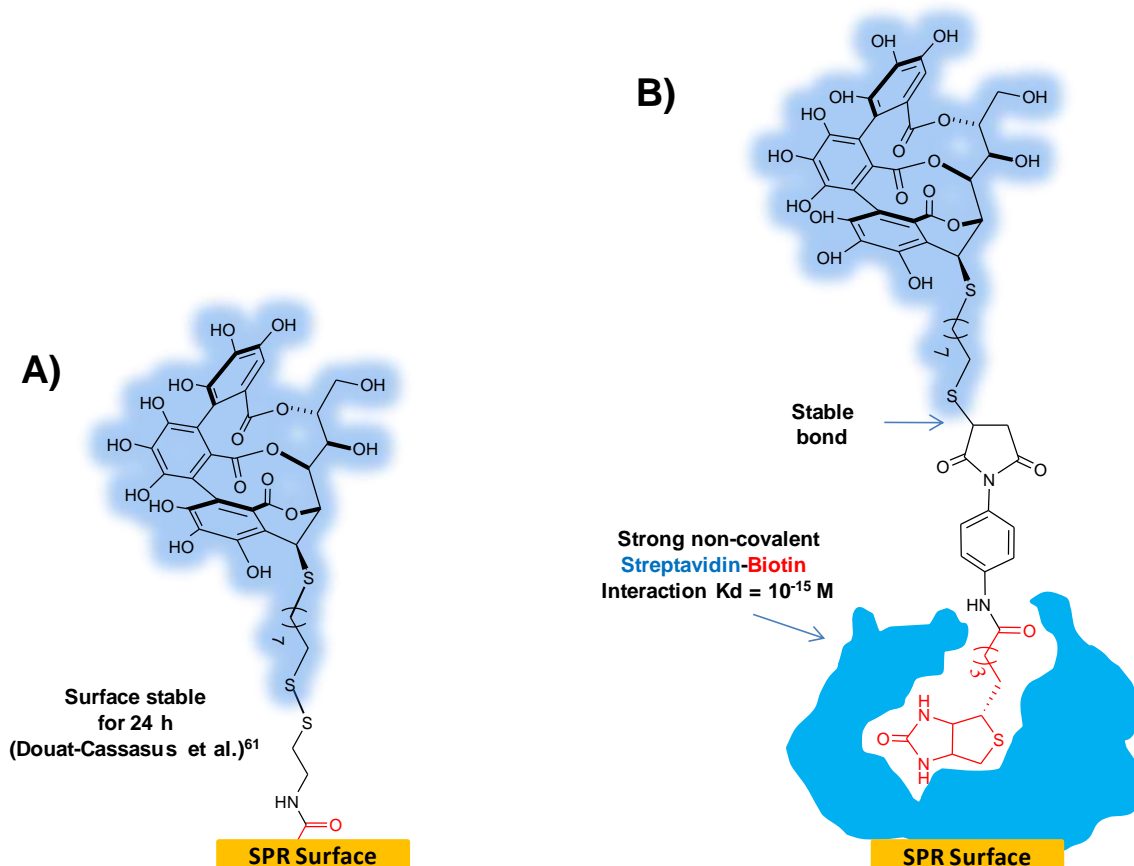


This chapter is dedicated to the description of the preparation of polyphenol-biotin conjugates for SPR studies. The polyphenols that have thus been modified are of the following types: C-glucosidic ellagitannins, flavan-3-ols and B-type procyanidins. Each polyphenol was chemically modified to possess a functional group suitable for immobilization to the SPR sensor. The design and synthetic strategy developed is discussed below.

IIa. Design of Polyphenol-Biotin Conjugates

Vescalin-bearing SPR surfaces (Figure 41A) had already been prepared by Quideau's team in a proof-of-concept study. This initial immobilization of vescalin (**29a**) on to a SPR surface was achieved via a disulfide covalent bond.⁶¹ The SPR studies performed with this disulfide immobilized vescalin showed that thus immobilizing this polyphenol over the SPR surface limits the observation of non-specific type interactions with proteins. However, this vescalin-bearing SPR surface was stable only for about 24 h, which rendered the experiments conducted with this type of surface unreliable through time. We hypothesized that this instability was consequence of the fragility of the disulfide covalent bond.

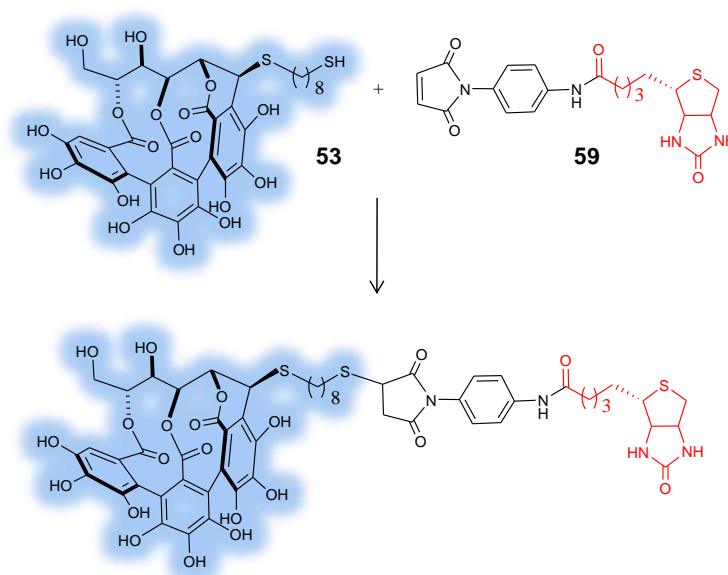
Figure 40. Alternative immobilization chemistries for polyphenols over SPR sensors



To improve the lifetime of these polyphenolic-SPR surfaces, we envisioned the commonly used biotin-streptavidin mode of immobilization because of its well-known stability.^{59,70} To

take advantage of the sulfhydryl thioether deoxyvescalagin previously developed (**53**),⁶¹ a suitable biotin derivative was chosen. A maleimide derivative of biotin (**59**) would be coupled by a Michael-type addition to the thiol function of **53** (Scheme 4).^{71,72} This applied to other ellagitannins would afford ellagitannin-biotin conjugates for immobilization over streptavidin coated SPR surfaces, as illustrated with vescalalin in Figure 41B. Though first developed for C-glucosidic ellagitannins vescalalin (**29a**) and vescalagin (**10**), this strategy could also be adapted to other polyphenols, as will be presented in the following sections of this chapter.

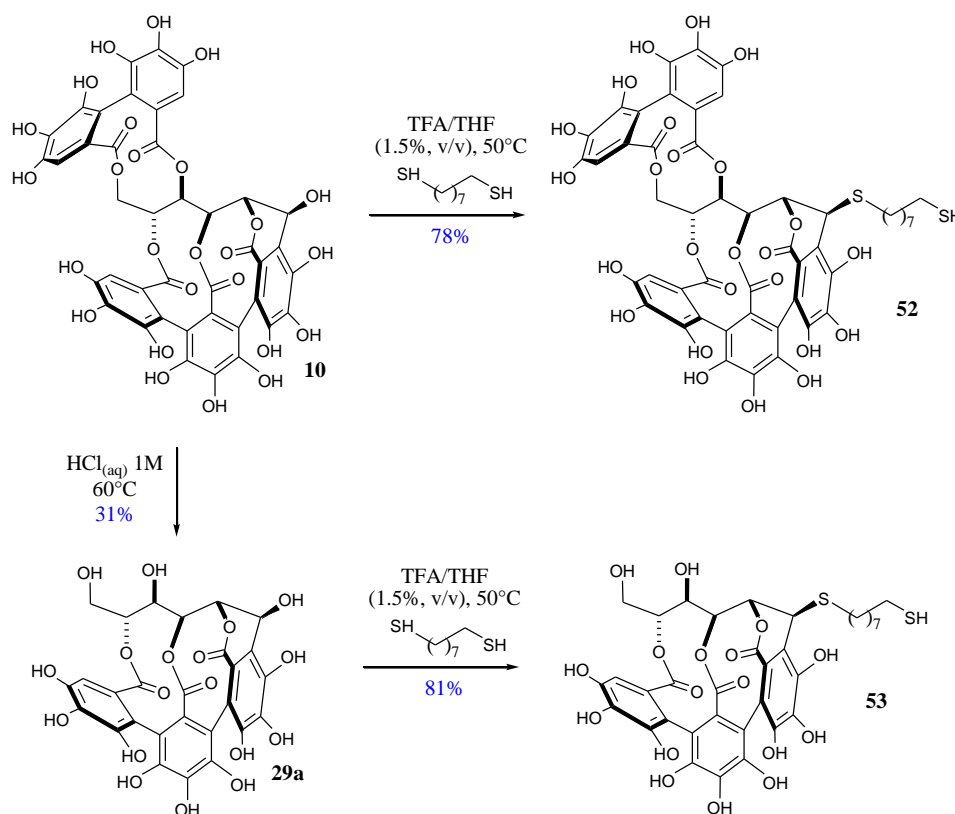
Scheme 4. Vescalin-biotin conjugate formation by Michael-type coupling



IIb. Hemisynthesis of Vescalagin- and Vescalin-Biotin Conjugates

The synthesis of vescalagin- and vescalalin-biotin conjugates was performed in two main steps: the C-glucosidic ellagitannins were transformed into the corresponding sulfhydryl thioether deoxyderivatives,⁶¹ followed by Michael addition to a previously prepared biotin-maleimide derivative.

Vescalagin (**10**), readily available from oakwood, was modified into the sulfhydryl thioether deoxyvescalagin **52** using the same strategy as that previously developed for the vescalalin analog.^{61,40} A solution of **10** in THF-TFA (1.5%, v/v) was heated at 55°C in the presence of octanedithiol to obtain compound **52** in 78% yield. Vescalin (**29a**) was obtained in 31% yield from acid hydrolysis of vescalagin (**10**) in 1M HCl at 60°C, conditions adapted from Scalbert *et al.*^{73,74} Vescalin (**29a**) was submitted to the same conditions as described for **10**, to obtain sulfhydryl thioether deoxyvescalin **53** in 81% yield.⁶¹

Scheme 5. Sulfhydryl thioether deoxy- vescalagin (**52**) and vescalin (**53**) hemisynthesis

The methodology for the derivatization of commercially available biotin (**58**) with N-(4-aminophenyl)maleimide (**57**) was adapted from a procedure published by Keana *et al.*⁷⁵ N-(4-aminophenyl)maleimide (**57**) was obtained in two steps. A solution of 1,4-phenylenediamine (**55**) in THF was allowed to react with maleic anhydride (**54**) for 12 h, to give a yellow precipitate. This precipitate was washed with cold THF to afford the monomaleamidic derivative **56** in 95% (Scheme 6). Keana *et al.*⁷⁵ achieved the cyclization of compound **56** through activation of the carboxylic acid with N,N'-dicyclohexylcarbodiimide (DCC) and N-hydroxybenzotriazole (HOBT) in CH₂Cl₂ at room temperature, obtaining compound **57** in 63% yield. However, in our hands, the use of these reaction conditions led to a lower 23% yield. Other reaction conditions were tested in an attempt to improve the yield of the reaction (Table 1). More satisfactory results (entry 6) were obtained when the activation of the carboxylic acid of **56** was performed in MeCN with N,N,N',N'-tetramethyl-O-(1H-benzotriazol-1-yl)uronium hexafluorophosphate (HBTU) and HOBT as coupling reagents, in the presence of diisopropylethylamine (DIEA) with microwave irradiation (50 watts). Under these conditions, compound **57** was obtained in 38% yield.

Scheme 6. Preparation of biotin maleimide derivative

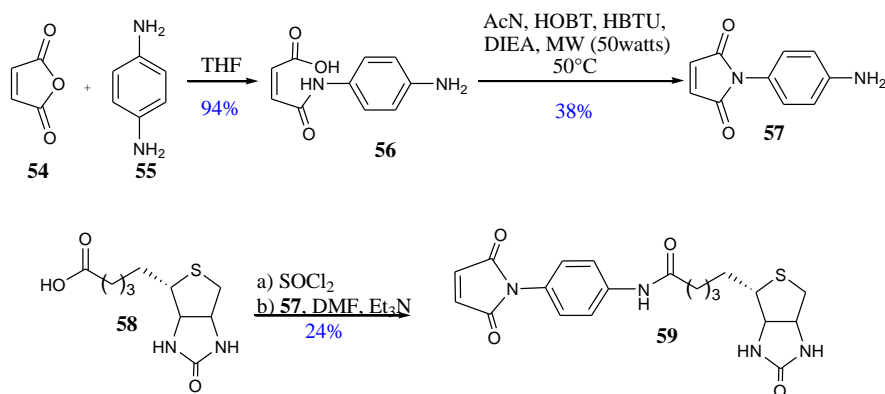


Table 1. Reaction conditions tested for cyclization of compound 56

Entry	Solvent	Reagents	Temperature (°C)	Yield
1	CH ₂ Cl ₂	HOBT/DCC ⁷³	0 to 25	23%
2	CH ₂ Cl ₂	HOBT/DIC	0 to 25	12%
3	MeCN	HOBT/HBTU/DIEA	25	27%
4	MeCN	HOBT/HBTU/DIEA	50	25%
5	Acetone	HOBT/HBTU/DIEA	50°C (50 watts)	20%
6	MeCN	HOBT/HBTU/DIEA	50°C (50 watts)	38%

N-(4-aminophenyl)maleimide (**57**) was then coupled with commercially available biotin (**58**). The carboxylic acid function of biotin (**58**) was previously activated with thionyl chloride (SOCl₂). The resulting acyl chloride was dried and dissolved with a solution of **57** and Et₃N in dry DMF. Semi preparative HPLC purification of the reaction mixture furnished **59** in 24% yield over two steps. With the electrophilic biotin maleimide derivative (**59**) available, the biotinylation of the nucleophilic sulfhydryl thioether deoxyellagitannins **52** and **53** could be performed.

The coupling between the thiol function of sulfhydryl thioether deoxyellagitannin derivatives **52** and **53** with biotin-maleimide derivative (**59**) was achieved by a Michael-type addition using a methodology adapted from Le Gac *et al.*⁷¹ A solution of sulfhydryl thioether deoxyvescalagin (**52**) was allowed to react with biotin maleimide derivative **59** in equimolar quantities. Due to the low solubility of **59**, the reaction was performed using DMSO as the solvent. Deuterated DMSO-*d*₆ was chosen in order to follow the reaction by ¹H NMR. The disparition of the signal corresponding to the protons of the maleimide moiety double bond indicated completion of the reaction (Figure 41). The same procedure was used for the coupling of sulfhydryl thioether deoxyvescalin (**53**) with **59**. The compounds were

precipitated from the DMSO- d_6 solution with a CHCl_3 - Et_2O mixture to afford biotin derivatives **60** and **61** in 95% and 92% yield, respectively.

Scheme 7. Coupling of compounds **52** and **53** respectively with compound **59**

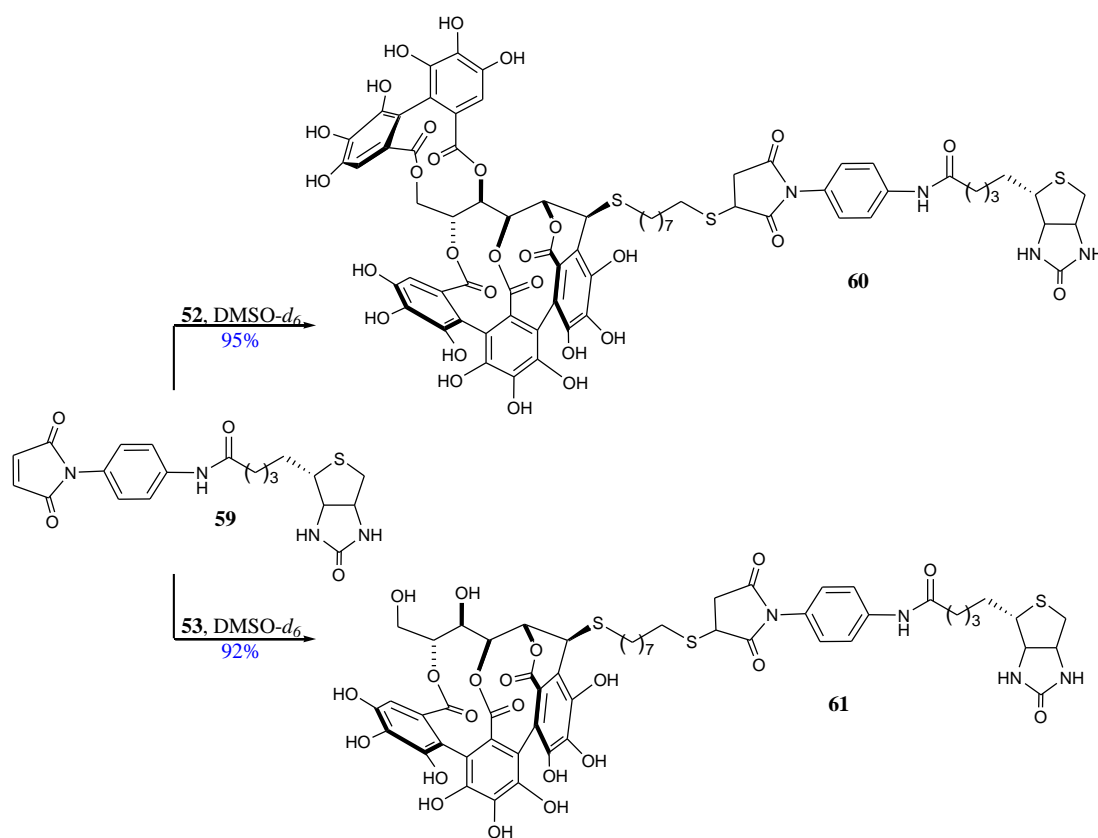
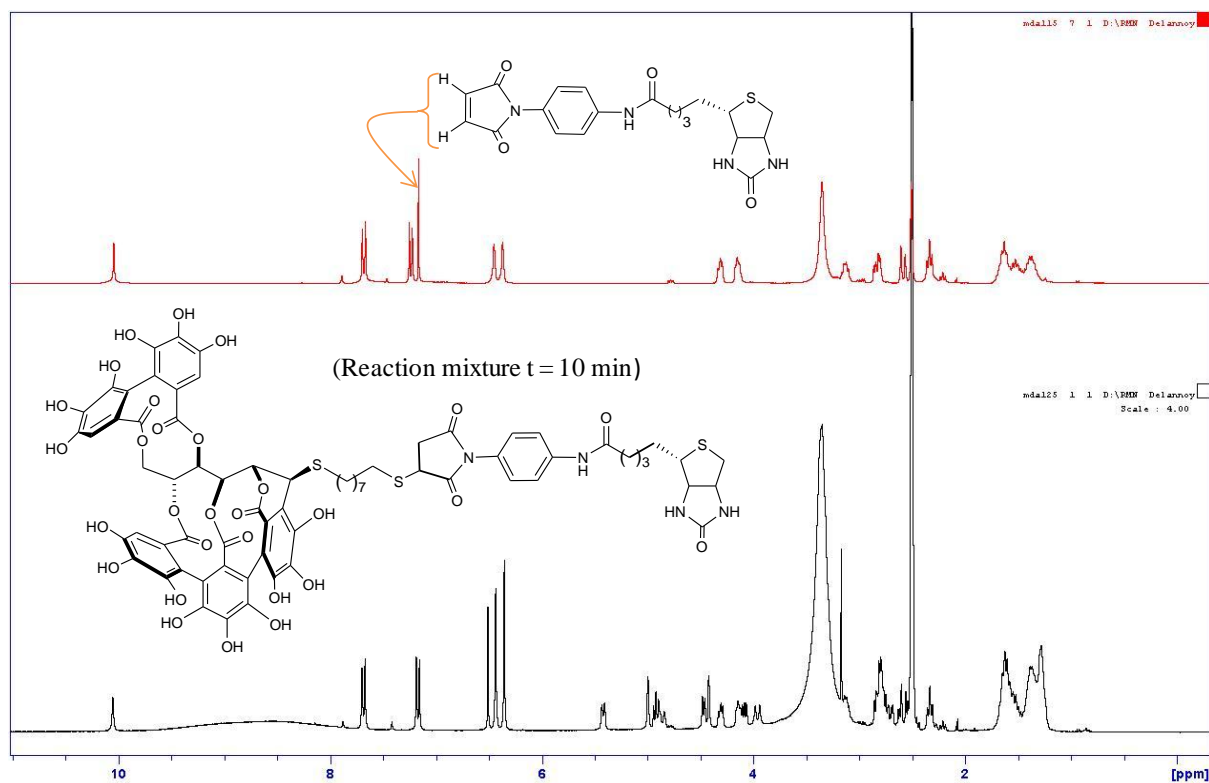


Figure 41. ^1H NMR of the formation of **52** and ^1H NMR of **59** in $\text{DMSO-}d_6$



The hemisynthesis of catechin- and epicatechin-biotin conjugates was also envisioned using the same type of linker and biotin derivative.

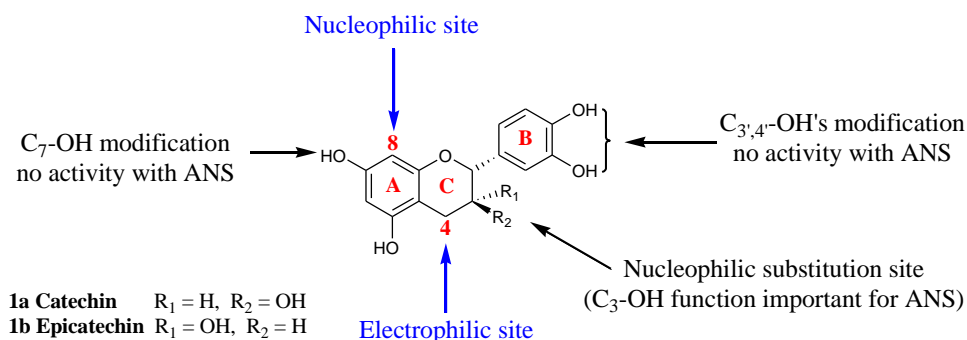
IIc. Hemisynthesis of Catechin- and Epicatechin- Biotin Conjugates

Given the reactivity of these flavonoids, different possibilities were available for the anchoring of the primary thiol ending linker. These options as well as the synthetic strategy used are discussed in this section.

At what position of the (epi)catechin skeleton should we anchor the linker?

Catechin (**1a**) and epicatechin (**1b**) were previously derived by our team in the hands of Céline Chalumeau to bear an aliphatic linker through the A-ring and B-ring respectively.^{34,76} The mentioned derivatives concerned the development of affinity resins for *Vitis vinifera* derived proteins such as anthocyanidin synthase (ANS). The work carried out with these affinity resins allowed to determine that the phenol function on both the A- and B-rings of catechin were crucial for recognition of the flavonoid by the ANS enzyme (activity). On the other hand, catechin derived through C-8 (A-ring) showed to maintain recognition by the ANS enzyme (Figure 42) and even its transformation. Another possibility to modify these flavan-3-ols is to exploit the electrophilicity of the C-4 benzylic position. Since no information had been obtained for the ANS protein with a catechin C-ring derivative, we were interested in building derivatives of these flavonoids through this position. Finally, the secondary alcohol at C-3 could be used in nucleophilic substitution reactions. However, this C₃-OH has been reported to be important for ANS recognition.³¹

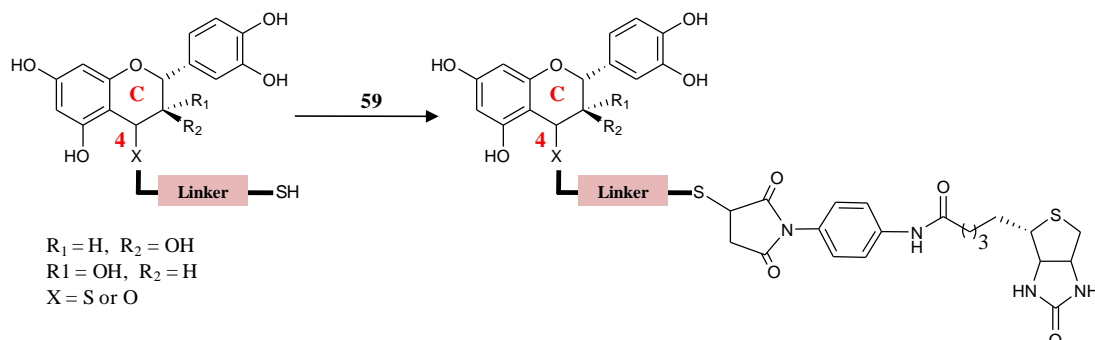
Figure 42. Catechin and epicatechin possible positions for derivatization



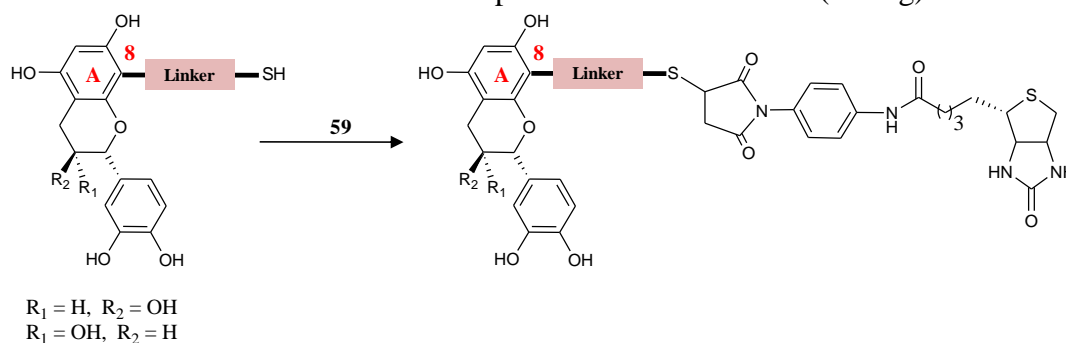
Even though, SPR experiments only serve to evaluate the affinity of the ANS protein for catechin and epicatechin (and not the activity), we preferred to remain prudent by not installing the linker at positions known to be important for ANS activity. This narrowed down the plausible options for derivatization to C-4 (C-ring, Scheme 8) and C-8 (A-ring, Scheme 9). The nature of the linker between the flavonoid and the biotin would be kept as similar as possible to the octanedithiol linker used for the ellagitannin derivatization. The linker should

bear a thiol ending function for its coupling to biotin maleimide **59** (Scheme 4, page 52). These precautions are taken in order to compare as less biased as possible the strength of interaction of polyphenols from different families with the proteins tested. Keeping in mind the comparable reactivity of both epimers, the synthetic strategy developed was assumed applicable to both catechin and epicatechin.

Scheme 8. Catechin and epicatechin derivatization (C-ring)



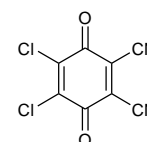
Scheme 9. Catechin and epicatechin derivatization (A-ring)



IIc.1 C-Ring derivatization of catechin (**1a**) and epicatechin (**1b**)

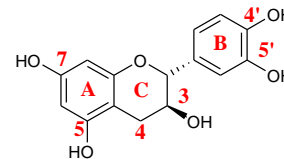
C-Ring derivatization of catechin (**1a**) at position C-4 is most commonly achieved by oxidation with 2,3-dichloro-5,6-dicyano-*p*-benzoquinone (DDQ) in presence of a nucleophile. This methodology has been well documented by several authors for its regio- and stereoselectivity, as well as, its compatibility with a wide range of oxygenated nucleophiles, such as the OH,⁶³ OMe,⁷⁷ OC(O)CH₃,⁷⁸ allyl alcohol,⁷⁹ O(CH₂)₂OH,⁷⁷ OBn,⁸⁰ with satisfactory to excellent results. In this section are presented preliminary tests that were initially performed with the more naturally available catechin (**1a**). Once a viable synthetic path was validated for catechin (**1a**), it was applied to epicatechin (**1b**).

Figure 43. Structure of DDQ



IIc.1.1 Approach without the use of protecting groups on the catechin skeleton

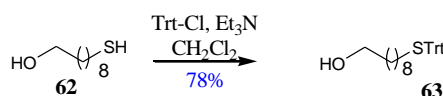
We were interested in developing a simple protective-group-free approach for the C-4 oxidation of catechin with DDQ. To our knowledge, this type of modification has not been performed so far without the use of protecting groups for catechin. The oxidations of 5,7,3',4'-O-protected catechin derivatives with DDQ achieved



by Hayes *et al.*,⁷⁹ Tückmantel and Kosikowski^{77,79,80} and Saito *et al.*⁸⁰ showed that the reaction can be carried out without protection of the hydroxyl group at C-3. The work of Kondo and Oyama,⁸¹ with the flavanone naringenin 4'-glucopyranoside (with an analogue substitution pattern at the A-ring to that of catechin) showed that the reaction can be carried out without protection of the hydroxyl groups of the phloroglucinol moiety (A-ring). On the other hand, the catechol moiety (B-ring) has been reported to be sensitive to oxidation in the presence of DDQ, leading to the corresponding ortho-quinone derivative.^{82,83} Nevertheless, this quinone derivative could be reduced back to the catechol with NaBH₄, or Na₂S₂O₄.⁸³⁻⁸⁵ In general, the nucleophilic agent is used to capture the quinone methide intermediate formed by the reaction of DDQ with the corresponding flavonoid.⁷⁸ The use of octanedithiol as nucleophile had the upside of providing the desired compound in one step. However, oxidation of the thiol is possible in presence of DDQ, before it can act as nucleophile. THF was chosen as solvent, since it is a polar aprotic solvent that dissolved well all the reactants and had been used in similar reaction conditions.⁷⁷

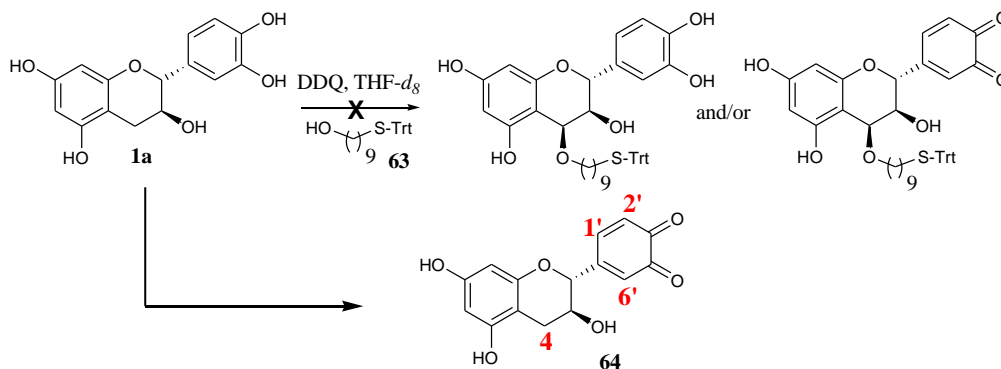
To avoid the possible thiol oxidation side reaction, small modifications were performed on a commercially available building block, 9-mercaptononan-1-ol. The primary thiol was protected by formation of a thioether bond with a trityl group (-C(Ph)₃), removable under mild acidic conditions.⁸⁶ Selective protection of the thiol function of 9-mercaptononan-1-ol (Scheme 10) was carried out by exploiting the higher acidity of the thiol (pK_a 10-11) as compared to that of the primary alcohol function (pK_a 15-16) and the high nucleophilic character of the resulting thiolate in presence of Et₃N, as reported by Demirtas *et al.*⁸⁷ Nucleophilic substitution with the trityl chloride (Trt-Cl) was performed by slow addition of the 9-mercaptononan-1-ol to a solution of trityl chloride (1 equiv.) and Et₃N (1 equiv.) in CH₂Cl₂. After purification by column chromatography of the reaction mixture, compound **5** was obtained in 78% yield.

Scheme 10. Protection of the primary thiol of 9-mercaptonona-1-ol

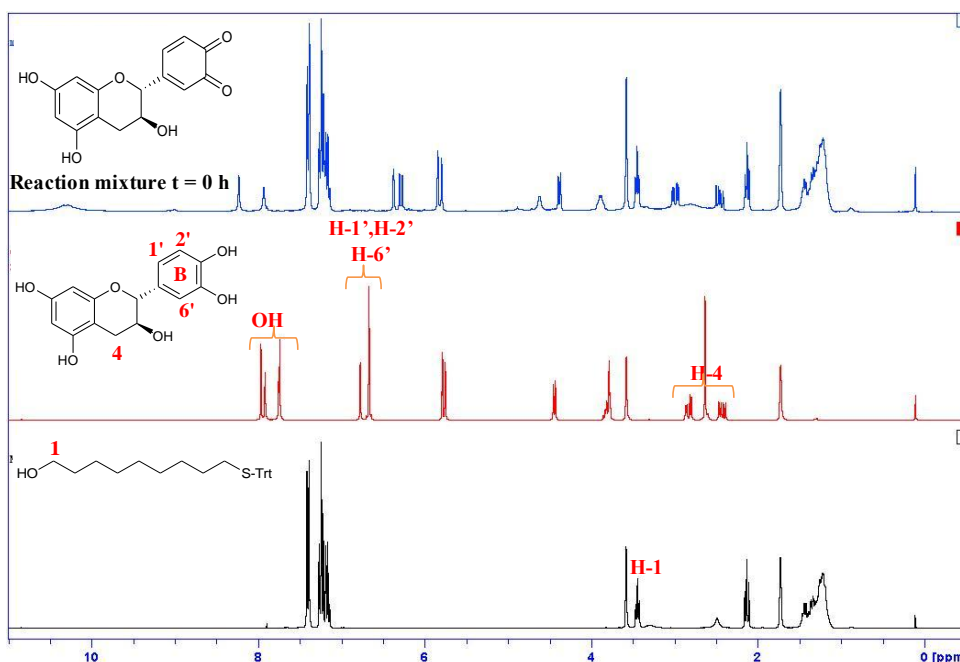


Expecting the oxidation of the catechin C-4 position by DDQ to take place, the protecting group free approach was explored. The reaction was performed in a NMR tube with deuterated THF- d_8 in order to follow the evolution of the reaction by ^1H NMR. In a regular NMR tube fitted with a septum and under Argon (Ar) atmosphere was prepared a solution of catechin (**1a**) and **63** in THF- d_8 . To this solution was then added DDQ (2 equiv.) as solution in THF- d_8 .

Scheme 11. Catechin derivatization: unprotected approach



The color of the reaction mixture's color changed from colorless to green, which is thought to be associated with the formation of a charge-transfer complex between DDQ and an aromatic compound.⁸⁸ In the ^1H NMR of the reaction mixture (Figure 44) at $t = 0$ h was observed a significant upfield shift for the signals of the protons corresponding to the catechol moiety (H-1', H-2', H-6'); as well as the disparition of two of the signals for the phenolic protons (OH). This suggested that the oxidation of the B-ring to the corresponding ortho-quinone had occurred. No change was observed for both, the signals corresponding to the protons at position C-4 of catechin (H-4, figure 44) and the signal that corresponds to the protons adjacent to the alcohol function of **63** (H-1, Figure 44). This indicated that the expected ether bond was not formed. No further change was observed even after prolonged reaction time, or addition of more equivalents of DDQ. These observations led to the conclusion that the most probable compound to have been obtained was compound **64**, in which the catechol moiety of catechin is oxidized to the o-quinone (Scheme 11). No further pushing of the reaction conditions was attempted. Since at least the catechol moiety of **1a** needs to be protected before oxidation with DDQ, the efforts were directed towards a protecting group approach.

Figure 44. ^1H NMR comparison of reaction mixture and starting materials

IIc.1.2 Approach using protecting groups on the catechin skeleton

The most common protecting group used in the derivatization of catechin (**1a**) and epicatechin (**1b**) is the O-benzyl (OBn) protecting group. However, the removal of O-benzyl protecting group under neutral conditions ($\text{H}_2/\text{Pd/C}$) is incompatible with the thiol ending linker (palladium poisoning by sulfur containing compounds).⁸⁶ Nonetheless, protecting groups like methoxymethyl ether (MOM),⁶³ acetyl (OAc),⁸⁹ as well as silyl derivatives such as tertbutyldimethylsilyl (TBDMS)⁹⁰ have been used in general flavonoid derivation. For the use **63** as nucleophile, the p-methoxybenzyl (PMB) group was chosen as protecting group because the removal conditions were similar to that of the S-trityl (S-Trt) of the linker. However, protection of the catechin phenols with p-methoxybenzyl bromide (PMB-Br) proved to be difficult leading us to envision other protecting groups. Among which O-acetyl (O-Ac), O-benzyl (O-Bn), O-triethylsilyl (O-TES) and O-tertbutyldimethylsilyl (O-TBDMS) were the protecting groups tested. The O-silylated derivatives were the best suited for the synthetic strategy proposed. The tests performed with the different protecting groups mentioned are presented in this section.

The formation of 5,7,3',4'-O-p-methoxybenzyl catechin (Scheme 12) was undocumented in the literature at the time with the exception of a patent.⁹¹ However, benzylation of the phenolic and alcoholic functions of catechin is well documented in the literature. The methodology reported by Boyer and co-workers,⁹² using benzyl bromide (Bn-Br), potassium carbonate (K_2CO_3) in dimethylformamide (DMF) had been successfully reproduced in our laboratory.⁷⁶ The attempts performed for O-PMB protection of catechin are summarized in

Table 2. In all cases, a complex mixture of products was obtained. It was then decided to change the nature of the protecting group to the O-acetyl protecting group.

Scheme 12. Protection of catechin phenols with PMB protecting group

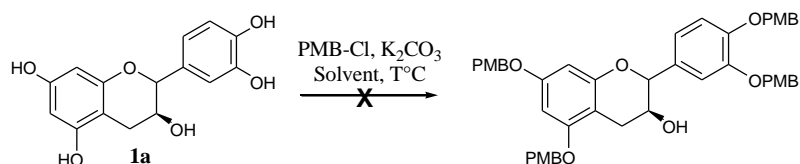
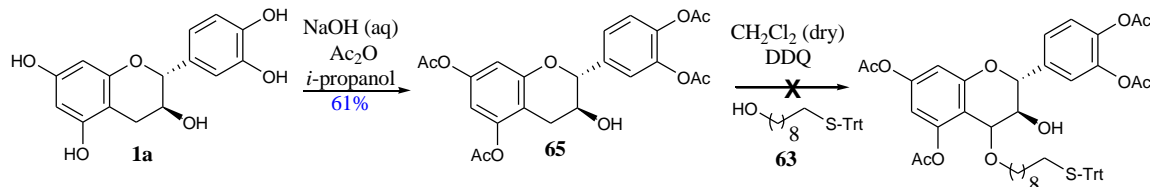


Table 2. Essays for protection of catechin phenols with p-methoxybenzyl (PMB)

Entry	Solvent	Reactants			T (°C)	Time
1	Acetone	PMB-Cl	K ₂ CO ₃	KI	21 to 70	3 days
2	DMF	PMB-Cl	K ₂ CO ₃	KI	21 to 80	3 days
3	DMF	PMB-Cl	NaH	-	0 to 21	4 days
4	THF	PMB-OH	DIAD	PPh ₃	0 to 30	24 h

Keeping in mind mild deprotection conditions for the final deprotection step, selective acetylation of catechin's phenol groups was of interest. At the time these tests were carried out, no experimental protocol for the preparation of 5,7,3',4'-O-acetyl catechin (**65**) was found. Later on, in 2010, a different procedure than the one used here was published by Raab *et al.*⁸⁹, in which **65** is obtained in 35% yield, using Et₃N and acetylchloride in DMF. Formation of the O-acetylated catechin derivative was achieved following an unpublished procedure developed in the 90's by Prof. Jean Moulines. To a catechin solution in isopropanol at 0°C was added powdered NaOH (12 equiv.) and water. The heterogeneous mixture was allowed to reach room temperature and then, acetic anhydride (Ac₂O, 12 equiv.) was added. 5,7,3',4'-O-acetylated (**65**) was obtained in 61% yield.

Scheme 13. 5,7,3',4'-O-acetyl catechin synthesis and oxidation attempt with DDQ

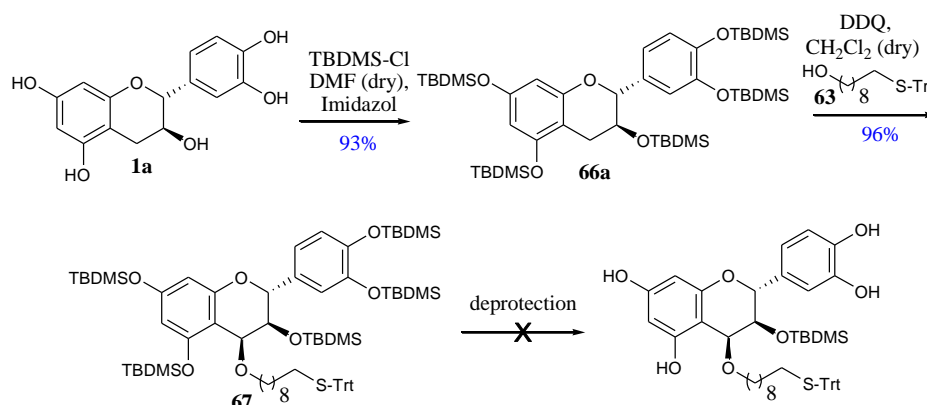


Using the methodology reported by Hayes *et al.*⁷⁹, compound **65** was engaged in the oxidation reaction with DDQ. Compound **65** and compound **63** (2 equiv.) were dissolved in CH₂Cl₂ (dry, distilled) and allowed to react with DDQ (2 equiv.). TLC monitoring and ¹H NMR of the reaction mixture confirmed that both starting materials remained unchanged. It was hypothesized that the electron-withdrawing effect of the O-acetyl groups ortho and para

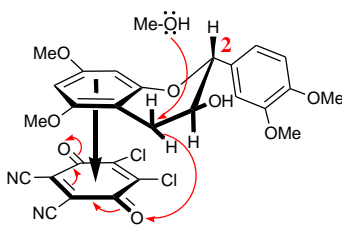
to the C-4 benzylic position prevented the formation of a reacting complex with DDQ. This prompted us towards silylated electron donating protecting groups.

Silylation of the phenol functions, as well as the secondary alcohol was performed in one pot following a protocol reported by De Groot *et al.*⁹³. To a catechin solution in dimethylformamide (DMF, freshly distilled) was added t-butyldimethylsilyl chloride (TBDMS-Cl, 7 equiv.) and imidazole (7 equiv.). The reaction mixture was stirred for 18 h. Purification over column chromatography of the reaction mixture furnished **66a** in 93% yield. The oxidation of silylated catechin derivative **66a** was achieved following the methodology reported by Hayes *et al.*⁷⁹ To a solution of **66a** and **63** (3-5 equiv.) in dry, distilled CH₂Cl₂ was added DDQ (2 equiv.). The reaction mixture turned dark green upon addition of DDQ and slowly changed color to pink as the reaction progressed. TLC analysis showed the reaction to reach quasi completion after 3 h. Column chromatography purification of the reaction mixture furnished **67** in 96% yield. The expected 4 β configuration was confirmed by ¹H NMR analysis.

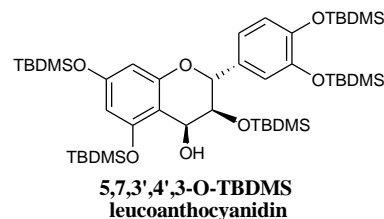
Scheme 14. 5,7,3,3',4'-O-dimethyterbutylsilyl catechin synthesis



In general, DDQ dehydrogenation mechanism goes through an initial formation of a charge-transfer complex.⁸⁸ On the basis of the formation of this charge-transfer complex, Steekamp *et al.*⁹⁴ suggested a reaction mechanism to explain the high regio- and stereo-selectivity concerning the oxidation of flavanols (Figure 45). In their model, formation of a complex is favored between DDQ and the more electron rich phloroglucinol moiety. The β -selectivity was explained by repulsive interactions between H-2 and H-4 in the β -face (axial position) and the incoming DDQ molecule. With positioning of the DDQ molecule over the α -face, the attack of the nucleophile is then more favorable over the β -face.

Figure 45. Dehydrogenation mechanism proposed by Steekamp, *et al.*⁹⁴

The deprotection of per-O-silylated-4-ether catechin derivatives has not been reported in the literature. However, our team has achieved desilylation of a similar compound: 5,7,3',4',3-O-penta TBDMS leucoanthocyanidin (Figure to the right) using the methodology reported by Kaburagi and Kishi.⁹⁵ Based on this methodology, desilylation of compound **67** was attempted. Compound **67** was treated with tetra-*n*-butylammonium fluoride (TBAF, 5 equiv.) in THF (0.03 mol/mL) and the desilylation took place. However, these conditions also resulted in cleavage of the C-4 ether bond of **67**. It was hypothesized that the C-4 ether bond of desilylated **67** was probably unstable under the basic reaction media. With this in mind, it was thought to perform the deprotection step using acidic sources of fluorine: HF_(aq) in MeCN^{79,96} and 3HF-Et₃N/ in THF.⁹⁷ The conditions tested for deprotection of compound **67** are summarized in the table below.

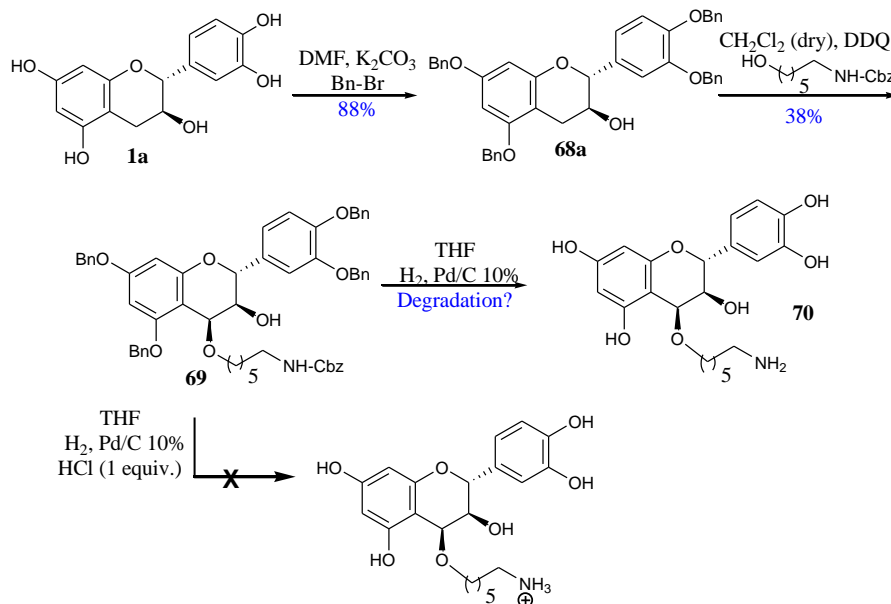
**Table 3.** Essays for removal of O-TBMDS groups of compound **67**

Entry	Solvent	Reagent	T(°C)	Time
1	THF	TBAF ⁹²	0 to 25	2 h
2	MeCN-THF (1:1, v/v)	HF (aq) 40% ^{77,93}	0 to 25	5 h
3	THF	3HF-Et ₃ N ⁹⁴	0 to 25	19 h

Aqueous HF conditions (entry 2) led to the same results than the use of TBAF. This was confirmed by TLC analysis and ¹H NMR of the reaction mixture. Deprotection attempts with 3HF-Et₃N in THF (entry 3) seemed promising, since the cleavage of the linker during the course of the reaction was minimized when compared to entries 1 and 2. Unfortunately, the composition of the reaction mixture changed during its drying under vacuum, resulting once more in cleavage of the C4-O-linker bond. Under acidic conditions, the protonation of the oxygen of the C4-ether bond could be the driving force for the cleavage. To confirm whether the breaking of the C4-O bond was a consequence of the acidity (HF) or basicity (TBAF) of the reaction conditions, an O-benzyl derivative that could be deprotected under neutral conditions was prepared. A primary amine was envisioned to perform the Michael addition of

the modified polyphenol to biotin maleimide (**59**), a protected amine was therefore considered compatible with the removal of O-benzyl protecting groups.

Scheme 15. 5,7,3',4'-O-benzyl catechin synthesis and oxidation of **68a** in presence of DDQ



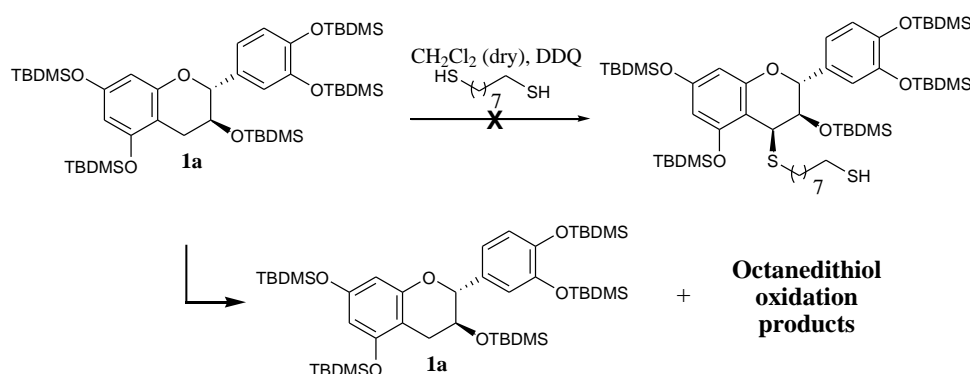
Protection of the catechin phenolic functions was achieved in gram scale using conditions previously described by Boyer, *et al.*⁹² Compound **68a** was obtained in 88% yield. A commercially available N-benzoylaminohexanol linker was chosen. The benzoyl (Bz) protected amine was orthogonal to the coupling conditions and could be removed in one pot with the O-benzyl groups under neutral conditions. Coupling of the linker to 5,7,3',4'-O-benzylated catechin (**68a**) by oxidation with DDQ was achieved using a similar procedure to the one described in the previous section. Compound **69** was obtained in 38% yield. Removal of the O-benzyl protecting groups was attempted under classical conditions. A solution of **69** in THF in presence of Pd/C (10%) was allowed to react under hydrogen atmosphere at room temperature for 20 h. ^1H NMR of the reaction mixture showed disappearance of the benzyl and benzoyl signals and the signal pattern was in accordance with what would be expected for compound **70**. Unfortunately, the instability of the formed product prevented us from performing further experiments to confirm its structure. It was conjectured that the instability observed for compound **70** could have been related to the presence of the free amine in the linker moiety. An attempt to protonate the amine in situ during the reaction was done by addition of HLC in dioxane (1 equiv.) to the reaction media. ^1H NMR of the reaction mixture material recovered showed a complex mixture.

These experiences suggested that the instability was related to the acidic and/or basic conditions to which was submitted the catechin-4-ether derivative. It seemed inappropriate to use such a fragile bonded linker to immobilize these polyphenols to the sensor chips surface.

The approach to use a thioether bond to anchor the linker to the C-4 position of catechin (**1a**) was then carried out. Carbon and sulfur having similar electronegativity form a less polarizable C-S bond when compared to the C-O bond, and therefore should be less sensitive to cleavage.⁹⁸

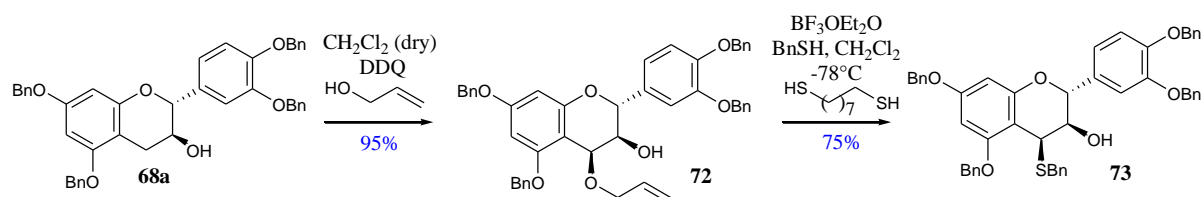
Given the difficulties presented with the C-4-ether bonded linker catechin derivatives, it was of interest to rapidly test whether the direct oxidation of per-O-TBDMS catechin (**66a**) to the C-4-thioether was possible with DDQ. The fact that thiols are better nucleophiles than alcohols encouraged us to try the oxidation of **66a** with DDQ using octanedithiol as nucleophile. Efforts were made towards the full activation of the substrate before addition of the thiol. The reaction was carried out in a regular NMR tube fitted with a septum and under Ar atmosphere. A solution of catechin in THF-*d*₈ and DDQ (2 equiv.) was shaken for 20 min and controlled by ¹H NMR every 10 min (the solutions color was pale green). After 20 min, octanedithiol was added (1 equiv.) with no change. After 30 min, more octanedithiol (5 equiv.) was added, the immediate formation of an insoluble orange precipitate was observed.

Scheme 16. Direct oxidation to the C-4 thioether with DDQ



The immediate formation of an insoluble precipitate with no detection of octanedithiol in solution by ¹H NMR suggested the oxidation of the thiol to be very fast. Since direct introduction of the octanedithiol with DDQ was not a possibility, it was necessary to introduce the octanedithiol by nucleophilic substitution over a previously oxidized C-4 position. Hayes *et al.*⁷⁹ showed efficient nucleophilic exchange between the 4-O-allyl of **72**, using BF₃·OEt₂ as the activating agent for different nucleophiles, including thiols.

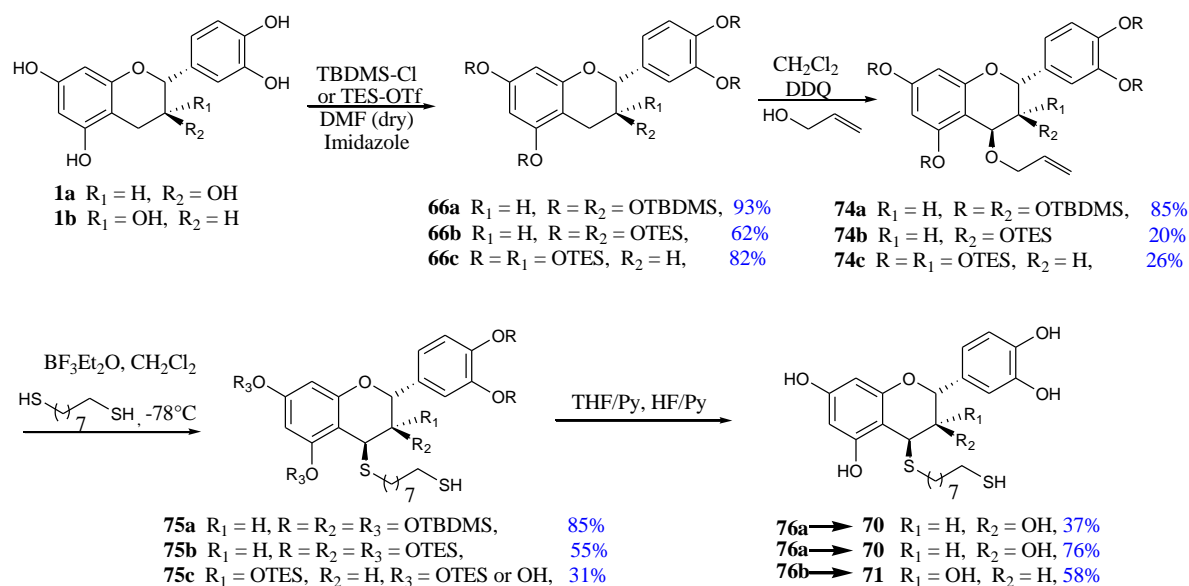
Scheme 17. Hayes *et al.*⁷⁹ 4β-phenylthioether catechin derivative (**73**)



Keeping in mind the compatibility of the protecting group with the octanedithiol linker, the penta-O-TBDMS catechin (**66a**) was used for this synthetic approach. However, some difficulties presented during the removal the C3-O-TBDMS bond led us to try also the more labile O-triethylsilyl (O-TES) analog. Finally, the deprotection problem solved, both O-TES and O-TBDMS analogs furnished the desired C-4 substituted catechin derivative. The same protocol was applied for the transformation of both catechin (**1a**) and its epimer epicatechin (**1b**).

Protection of the phenols and secondary alcohol of catechin (**1a**) and epicatechin (**1b**) with either TES-OTf or TBDMS-Cl was performed following the aforementioned De Groot *et al.* methodology with satisfactory results (Scheme 18).⁹³ Oxidation of the per-O-silylated flavan-3-ol derivative was achieved in presence of DDQ with allyl alcohol as mentioned in the previous sections.⁷⁹ After purification of the reaction mixture over column chromatography, compound **74a** was obtained as the major fraction in 85% yield, the remaining 15% of the material recovered was composed of a mixture of partially deprotected products.^{77,80} In the case of the O-TES analogs **74b** and **74c**, partial deprotection was more important given the lower yields for the oxidation of these analogs.

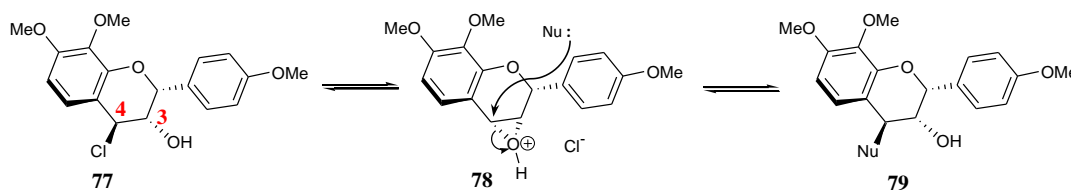
Scheme 18. Catechin (**1a**) and epicatechin (**1b**) C-4 derivatization



Nucleophilic substitution of the C-4-O-allylic unit of compounds **74a-c** was promoted by activation of the ether bond with BF₃·Et₂O, following the methodology reported by Hayes *et al.*⁷⁹ To solutions of compounds **74a-c** and octanedithiol (3 equiv.) in dry CH₂Cl₂ at – 78 °C was added BF₃·Et₂O (1.5 equiv.) dropwise. After half an hour, TLC analysis showed completion of the reaction. Compounds **75a-c** were obtained in 85%, 55% and 31% yield, respectively. The lower yield in the case of the O-TES derivatives was mostly due to partial deprotection. ¹H NMR of the pure compounds **75a-c** showed H-4 with a coupling constant

consistent with a 3,4-cis configuration, indicating retention of the configuration at C-4. However, with such secondary benzylic ether species, the expected reaction mechanism would be through a unimolecular mechanism ($\text{S}_{\text{N}}1$), that is, through a carbocationic intermediate. In this case, a mixture of stereoisomers could be expected. The other option would be through a bimolecular nucleophilic substitution mechanism ($\text{S}_{\text{N}}2$), where products should then present inversion of the configuration. None of these basic mechanisms were in accordance with the obtention of compounds **75a-c**, for which complete retention of the configuration was observed. In a similar situation, Coetzee *et al.*⁹⁹ explained the retention of configuration at C-4 of compound **79** via a neighboring group participation (Scheme 19). Compound **77**, possessing a chloride atom at C-4, first suffers intramolecular displacement by the hydroxyl group at C-3 to give a transient protonated epoxide derivative (**78**). The resulting epoxide derivative **78** has a hindered α face that directs preferentially the nucleophilic attack over the β face. Oyama *et al.*⁷ also justified the retention of configuration for a 3-O-acetyl catechin derivative by this neighboring group mechanism.

Scheme 19. Neighboring group mechanism proposed by Coetzee *et al.*⁹⁹

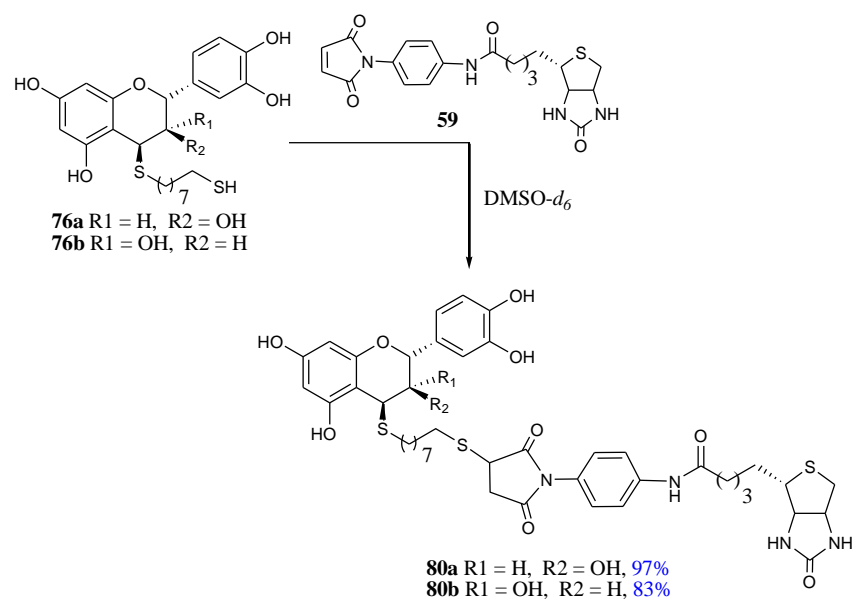


The removal of the O-TBDMS groups hadn't been documented for a C-4-thioether catechin derivative. Similar conditions to those depicted on Table 3 were tested. Kaburagi and Kishi's⁹⁵ methodology was applied to compound **75a** (Table 4, entry 1) to furnish the C3-O-TBDMS derivative and/or degradation products. In order to favor deprotection of the secondary C3-O-TBDMS group, acidic sources of fluorine were tested.⁸⁶ 3HF-Et₃N in THF⁹⁷ (entry 2) removed effectively the phenolic TBDMS groups but didn't affect the C3-O-TBDMS group. Similar results were observed with the use of KF/18-crown ether^{100,101} in THF or DMSO (entry 3). However, complete desilylation was achieved for both O-TBDMS and O-TES analogs using HF-pyridine in THF with additional pyridine^{102,103} to regulate the acidity of the reaction media (entries 6-8).

Table 4. Conditions tested for desilylation of compound **75a-c**

Entry	Comp.	Solvent	Reagent	Equiv.	Time (h)	Result
1	75a	THF	TBAF	10	$\frac{1}{2}$ 2 $\frac{1}{2}$ - 4	Partial deprotection or decomposition
2	75a		3HF-Et ₃ N	18	24	C3-OTBDMS
3	75a	THF or DMSO	KF-crown ether	50	20	C3-OTBDMS
4	75a		HF(70%)-Py 7:1 to 1:2 (v/v)	346	24	C3-OTBDMS
5	75a		1:0 (v/v)	135	1/2	Decomposition
6	75a	THF	4:1 (v/v)	23	24	37% (76a)
7	75b		1:1 (v/v)	11	72	76% (76a)
8	75c		1:1 (v/v)	12	72	58% (76b)

Comparing the overall yields of the four-step synthesis described above (Scheme18), we find that the overall yield is 25% for the OTBDMS protecting group strategy, while that of the OTES protecting group strategy is of only 5%. With catechin and epicatechin modified with a thiol ending linker in hand, it was then possible to use these derivatives for the coupling with biotin maleimide derivative **59**.

Scheme 20. Flavonoid-biotin conjugates (C-ring)

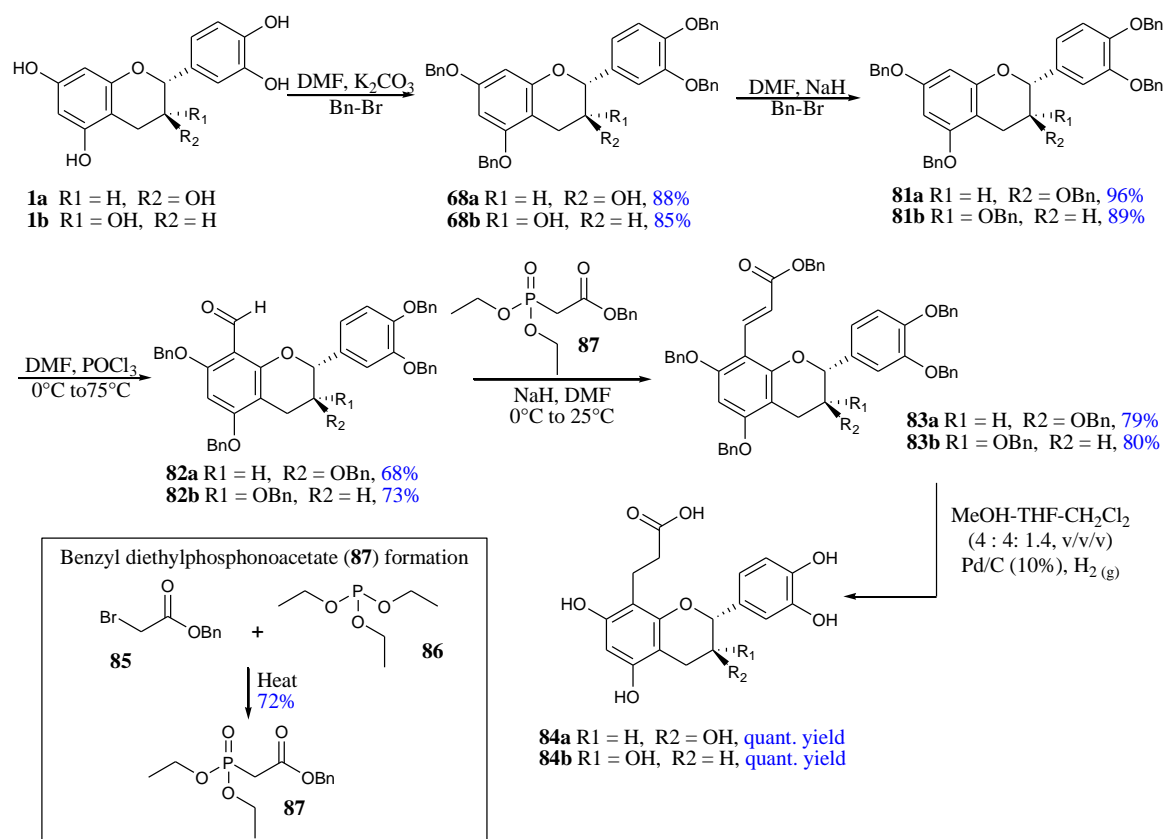
The coupling of catechin and epicatechin derivatives **76a** and **76b** with biotin-maleimide derivative (**59**) was achieved using the methodology adapted from Le Gac *et al.*⁷¹ (analogous to the procedure used to obtain the ellagitannin-biotin conjugates). Biotin conjugates **80a** and **80b** were obtained in 97% and 83% yields respectively.

IIc.2 A-Ring derivatization of catechin (1a) and epicatechin (1b)

For the derivatization of catechin (**1a**) and epicatechin (**1b**) through their A-ring, the inherent nucleophilicity of position C-8 was exploited to install a carboxylic acid ending linker, following the methodology developed by Chalumeau *et al.*³⁴ This carboxylic acid ending linker would then be modified to bear the desired primary thiol function.

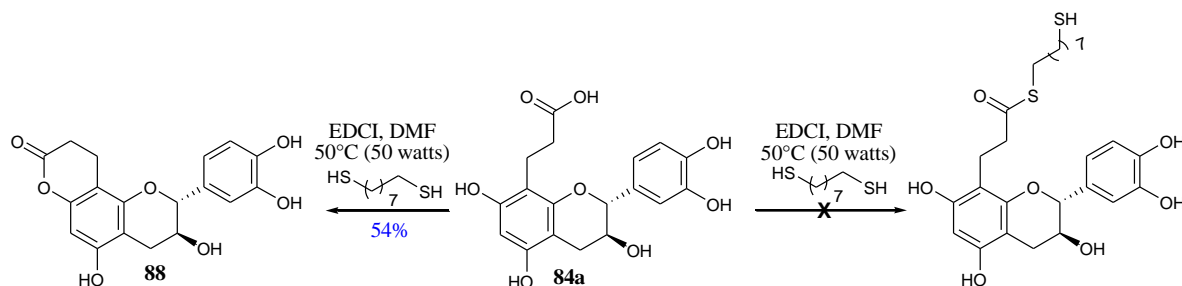
Selective formylation at the C-8 position required prior protection of the phenol and secondary alcohol functions of the flavan-3-ols (Scheme 21). This protection was achieved by etherification with Bn-Br following the two-step procedure reported by Boyer *et al.*^{92,104} Per-O-benzyl catechin (**81a**) and epicatechin (**81b**) were obtained in 83% and 89% yield respectively. Formylation was achieved regioselectively at C-8 by an electrophilic aromatic substitution reaction. Compounds **81a** and **81b** were each allowed to react in DMF and in the presence of phosphoryl chloride (POCl₃) to furnish formylated derivatives **82a** (68%) and **82b** (68%).¹⁰⁴ The installation of the linker required the synthesis of the non-commercially available benzyl diethylphosphonoacetate (**87**). Compound **87** was obtained by an Arbuzov-type reaction. Following a procedure reported by O'Leary *et al.*¹⁰⁵, **87** was directly obtained by distillation in 72% yield from a triethyl phosphite (**86**)-benzyl 2-bromoacetate (**85**) mixture. In a Horner-Wadsworth-Emmons reaction, benzyl diethylphosphonoacetate (**87**) and formylated flavan-3-ol derivatives (**82a** and **82b**) were each allowed to react in DMF and in presence of sodium hydride (NaH) to obtain derivatives **83a** (66%) and **83b** (79%).³⁴ It was more convenient to remove the O-benzyl protecting groups before installation of the thiol ending linker. Therefore, reduction of the linker's double bond, as well as O-benzyl removal was achieved in one pot via hydrogenolysis in the presence of Pd/C (10%) to furnish functionalized catechin and epicatechin derivatives **84a** and **84b** in quantitative yield.

Scheme 21. Derivatization of flavanols at C-8 (C-Ring)³⁴



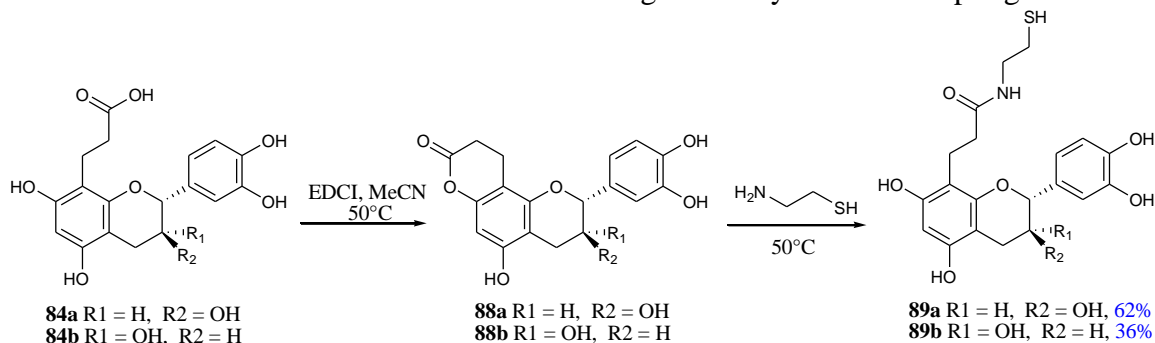
It was envisioned to introduce the primary thiol function by transforming the carboxylic acid of derivatives **84a-b** to the corresponding sulfhydryl thioester derivatives. Classical activation of the carboxylic acid with N-(3-dimethylaminopropyl)-N'-ethylcarbodiimide (EDCI) in presence of octanedithiol failed to furnish the expected thioester (Scheme 22).¹⁰⁶ This was a consequence of the formation of a lactone by intramolecular attack of the phenolic OH at C7. This lactone formation has already been observed in the work of Céline Chalumeau. In her case, heating and microwave activation (50 watts) was sufficient to enable the coupling with a secondary amine (amino-PEGA resin).³⁴ In our case, these conditions did not furnish the desired thioester. It was found in the literature that the reaction equilibrium from carboxylic acid and thiol towards the formation of thioesters is disfavored in comparison to their ester analogs.¹⁰⁷

Scheme 22. Attempt for thioester formation



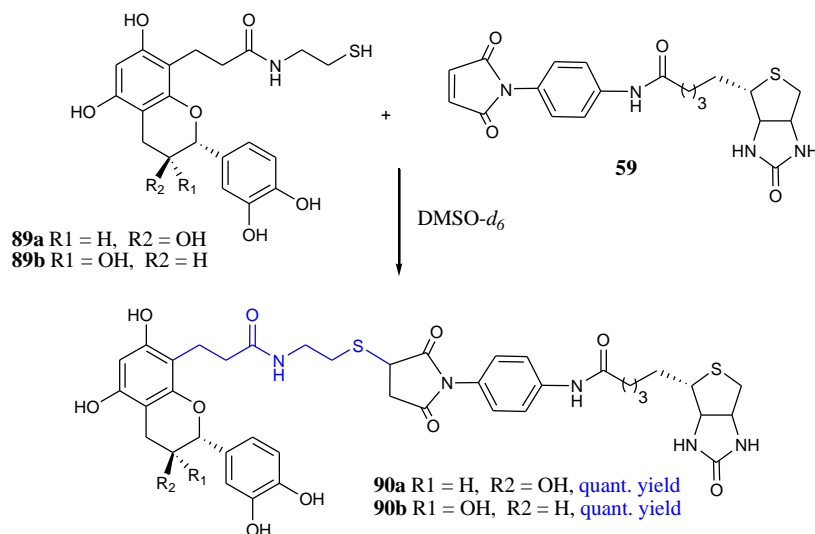
The possibility of forming a more stable intramolecular ester (lactone **88**) prohibits the formation desired of the thioester. Increasing the nucleophilicity of the thiol by forming the thiolate ion was not a viable option, since the basic character of the thiolate ion would also deprotonate the phenols providing multiple possible products. This led us to change the nature of the linker. As previously mentioned, lactone **88** has been successfully transformed to the amide derivative by microwave activation at 50 °C.³⁴ It was decided to use an aliphatic-type linker bearing a thiol in one end and a primary amine in the other end. Cysteamine meets these requirements. Functionalized catechin and epicatechin (**84a** and **84b**) were each allowed to react with the EDCI coupling agent in MeCN at 50°C until complete formation of the lactone (TLC monitoring), then cysteamine was added. Compounds **89a** and **89b** were obtained in 62% and 36%, yields respectively.

Scheme 23. Introduction of thiol ending linker: cysteamine coupling



The coupling of functionalized catechin and epicatechin **89a-b** with biotin-maleimide derivative (**59**) was achieved using the methodology adapted from Le Gac *et al.*⁷¹ as described in the previous sections. Biotin conjugates **90a-b** were both obtained in quantitative yield.

Scheme 24. Flavonoid-biotin conjugates preparation

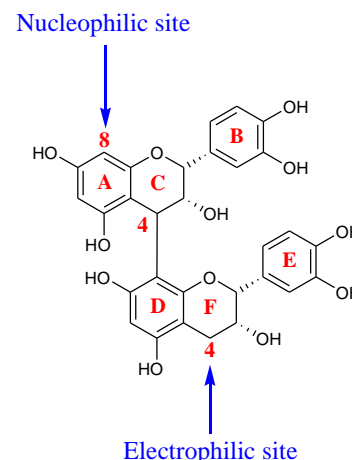


Two versions of catechin and epicatechin biotin adducts (**80a-b**, **90a-b**) were thus available for the intended polyphenol-protein studies by SPR. In order to include a polyphenol model of the procyanidin family, it was decided to prepare procyanidin biotin conjugates using a strategy analog to that followed for the obtention of the (epi)catechin-biotin adducts.

IId. Hemisynthesis of B-Type Procyanidins Biotin Conjugates

As discussed in Chapter I, there are different types of naturally occurring B-type procyanidins.⁴ We were particularly interested in the B-2 procyanidin (epicatechin-4→8-epicatechin) due to an ongoing collaboration with Catherine Renard and Carine Le Bourvellec from INRA the unit of “Sécurité et Qualité des Produits d’Origine Végétale” at the University of Avignon, France, concerning procyanidin-pectin interactions. The reactivity of B-type procyanidins is similar to that of its monomeric units, catechin and epicatechin. Therefore, we proposed to derivatize the B-type procyanidin analogously (Figure 46), by exploiting the electrophilicity of the C-4 benzylic position (F-Ring, C4-F) and the nucleophilicity of the C-8 position (A-ring, C-8A). This section will concern the description of the attempts we performed to prepare these B-type procyanidin derivatives.

Figure 46. B-2 procyanidin sites for derivatization.



IId.1 F-Ring derivatization of B-type procyanidin

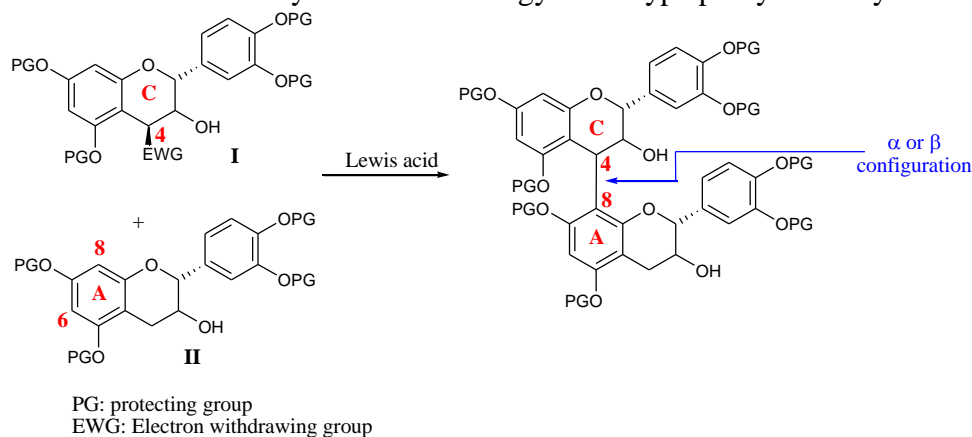
The strategy envisioned for F-ring derivatization of the B-type procyanidin consisted in oxidation of position C4-F with DDQ, followed by nucleophilic substitution with octanedithiol. A B-type O-protected procyanidin derivative was obtained by synthesis. As stated in the previous section, the protecting group that was compatible with the derivatization strategy envisioned was the O-TBDMS group. To our knowledge, B-type procyanidins have not been previously synthesized using per-O-TBDMS protection. It is important to mention that preliminary tests were performed with the more accessible catechin dimer (B-3). In the following section, we present the obtention of per-O-TBDMS B-type procyanidin derivatives.

IId.1.1 Hemisynthesis of per-O-TBDMS B-type procyanidin derivatives

The most common technique used to access these dimers of flavanols recalls the methodology used to obtain sulfhydryl thioesters of catechin and epicatechin **76a** and **76b** (Scheme 18, page 66). Nucleophilic substitution is achieved between an O-protected C-4-EWG (electro withdrawing group) (epi)catechin derivative (**I**) with an O-protected (epi)catechin derivative

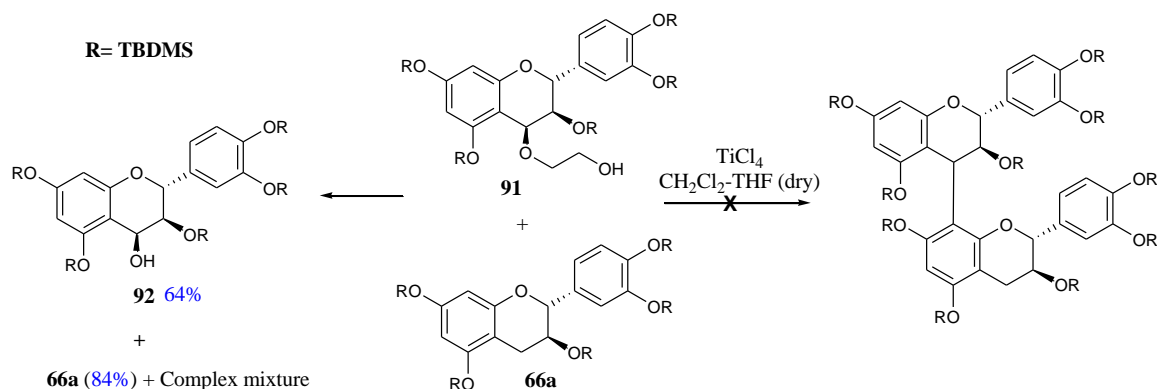
(II) in the presence of a Lewis acid (Scheme 25). The C-8A position, being more nucleophilic and less sterically hindered than the C-6A position, will preferentially attack the electrophilic C-4 position of I, which regioselectively leads to C4→C8 products. This methodology has been employed by several authors,^{7,77,80,106-108} for which the protecting group used was the benzyl protecting group.

Scheme 25. Commonly used methodology for B-type procyanidin synthesis



The natural B-2 isomer (epicatechin-4→8-epicatechin) possesses a β -configuration at the interflavan C4→C8 bond. In general, mixtures of stereoisomers are obtained when the methodology described above is used. Tuckmantel *et al.*⁷⁷ reported obtention of the single natural B-2 isomer by the use of a C-4-O-CH₂CH₂OH epicatechin derivative and TiCl₄ as the Lewis acid. The aforementioned reaction conditions are also applicable to form the B-3 derivative (catechin-4→8-catechin), as shown by the work of Tarascou *et al.*¹⁰⁹ Interested in the obtention of the natural isomer in its pure form, we tested this methodology with our per-O-TBDMS derivatives **91** and **66a** (Scheme 26) without success. Instead, the C4-OH derivative (**92**) was obtained.

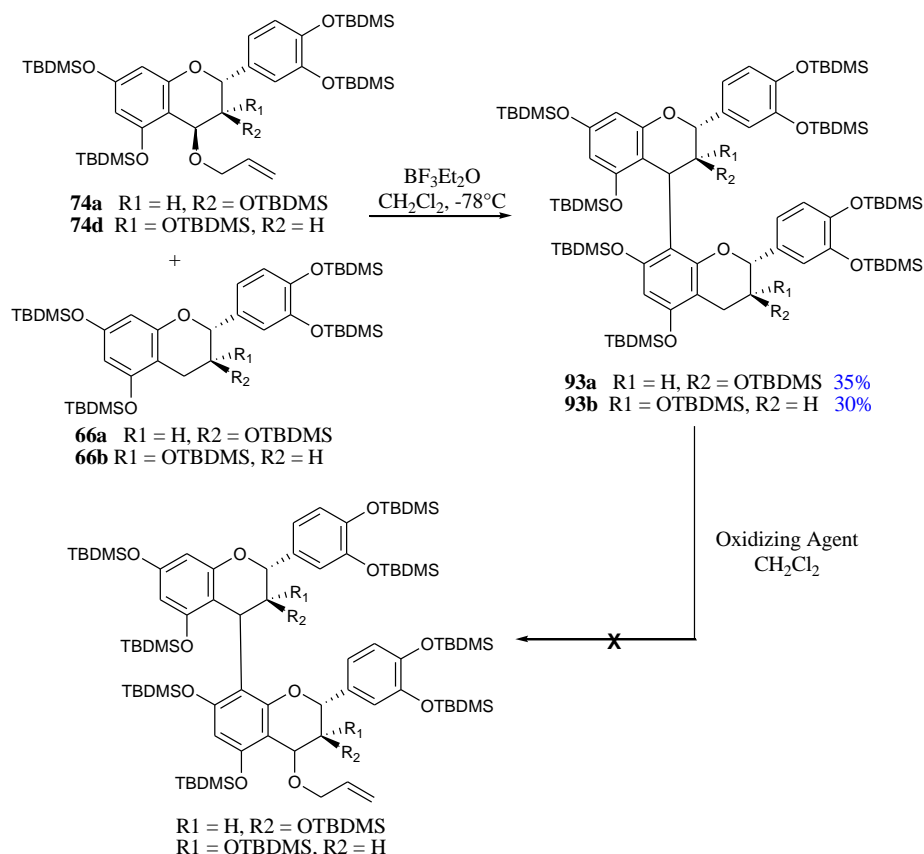
Scheme 26. Attempt of B-type procyanidin hemisynthesis⁷⁷



Since the glassware was flame dried, the solid starting materials were vacuum dried overnight and the solvents were dried and freshly distilled before the reaction, it was hypothesized that

adventitious water came from the handling of the TiCl_4 , which is hygroscopic. It was then decided to use the conditions adapted from those used by Hayes *et al.*⁷⁹ using $\text{BF}_3 \cdot \text{OEt}_2$ as the Lewis acid. These conditions were used successfully for similar nucleophilic substitution reactions within this work (Scheme 18). Per-O-TBDMS-4-O-allyl catechin (**74a**) was allowed to react at -78°C in presence of $\text{BF}_3 \cdot \text{OEt}_2$ with **66a** and the expected per-O-TBDMS B-3 procyanidin derivative (**93a**) was obtained in 35% yield.

Scheme 27. Hemisynthesis of per-O-TBDMS B-type procyanidin derivative and attempt for F-ring derivatization



Using the same procedure, the B-2 derivative (**93b**) was obtained in 30% yield. Both compounds were obtained as mixtures of the α/β isomers, such as reported in the literature.⁷⁹ The ratio for both species was estimated by ^1H NMR as 1:0.5 for the B-3 derivative (**93a**) and as 1:0.3 for the B-2 derivative (**93b**). The low yields (30-35%) are due to undesired self-condensation reactions between two or more units of **74a** or **74b** (or **66a-b**), respectively. A common strategy to avoid this side-reaction is to protect position C-8 with a bromine group (Br).^{77,109,110} However, we desired not to add additional steps to our synthesis. With the per-O-TBDMS B-type procyanidin derivative available, the oxidation step could be tested next.

Referring to the literature, only one report was found for oxidation of a B-type procyanidin in presence of DDQ within the work of Saito *et al.*¹¹¹ However, no procedure was described by the authors. Following Hayes *et al.* methodology (Table 5, entry 1)⁷⁹, oxidation of **93a** with

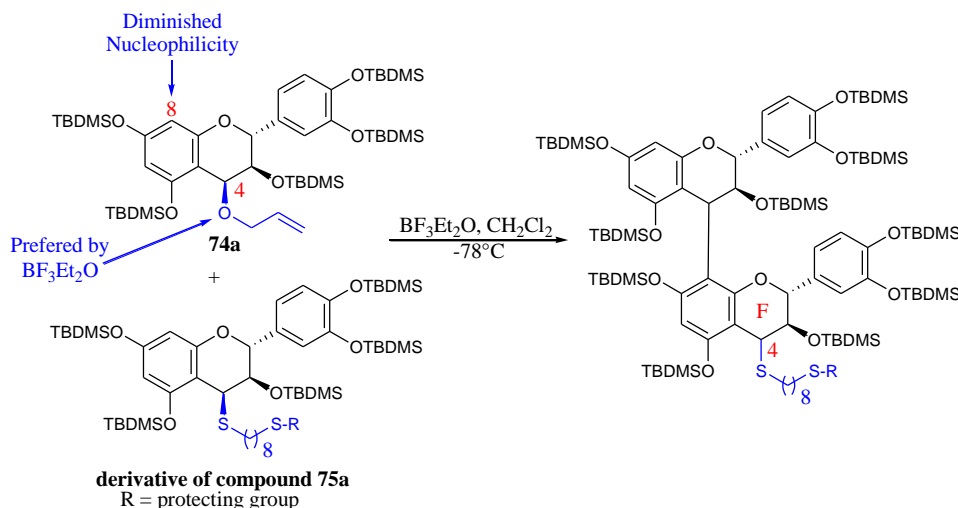
DDQ (2 equiv.) was attempted in the presence of allyl alcohol in CH_2Cl_2 . Under these conditions, no reaction was observed. Addition of more equivalents of DDQ or concentration of the reaction mixture resulted in complex mixtures. No difference was observed when the same procedure was applied to B-2 derivative (**93b**). Other oxidizing agents typically used for benzylic carbon oxidation were also tested. When the same reaction conditions were applied using the milder tetra-o-chloro benzoquinone (chloranil)⁸⁸ no reaction occurred (Table 5, entry 2). Oxidation with metallic one-electron oxidants, such as AgBF_4 ¹¹² and ceric ammonium nitrate (CAN)^{113,114} was also attempted. No reaction occurred when AgBF_4 was used (entry 3) and partial deprotection of the silylethers was observed using CAN (entry 4). However, no oxidation was observed at the C-4F position neither for **93a** nor **93b**.

Table 5. Conditions tested for C4-F ring oxidation

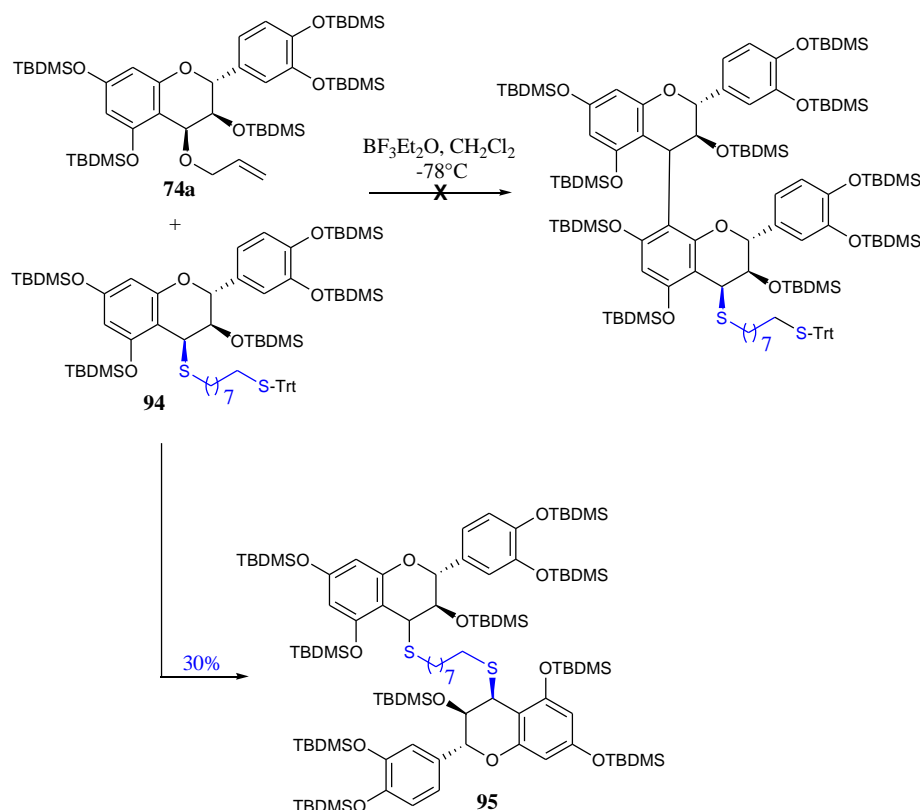
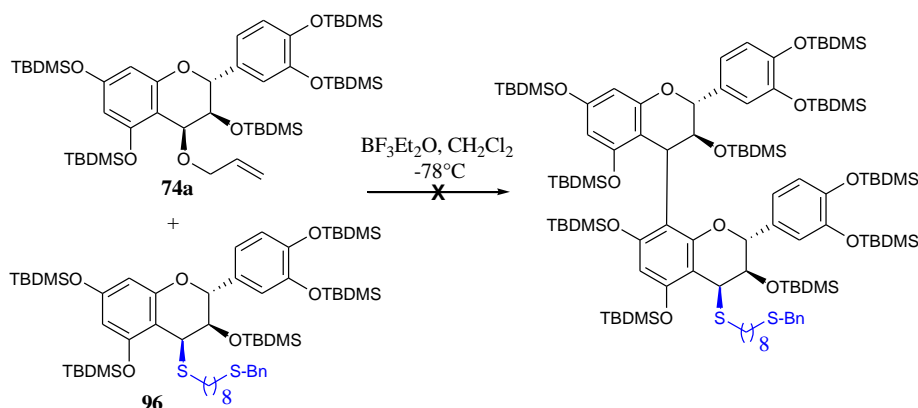
Entry	Oxidizing Agent	Solvent	Nucleophile	T (°C)	Outcome
1	DDQ	CH_2Cl_2	Allyl alcohol	0 to 25	No reaction or Complex mixture
2	Chloranil	CH_2Cl_2	Allyl alcohol	0 to 40	No reaction
3	AgBF_4	THF	Allyl alcohol	0 to 60	No Reaction or Partial Deprotection
4	CAN	$\text{DMF}/\text{CH}_2\text{Cl}_2$	Allyl alcohol	0 to 60	Partial Deprotection

In the literature, derivatization at the C-4F position of B-type procyanidins concerns the introduction of another (epi)catechin unit or units to access trimeric, tetrameric (and so on) procyanidins. The most common procedure involves the use of a monomeric catechin or epicatechin unit activated at C-4 that reacts with the dimeric procyanidin used as the nucleophile.^{110,115} This suggests that selective oxidation at the C4-F position of a dimeric reaction partner is not an easy task. Given the difficulties found to selectively oxidize position C4-F, an alternative approach was envisioned, and based on coupling of two orthogonally C-4 functionalized units. Inspired by the work of Ohmori *et al.*¹¹⁰, selective activation of the C4-O bond of compound **74a** was envisioned (Scheme 28). The C4-O bond is activated by $\text{BF}_3 \cdot \text{Et}_2\text{O}$ in the presence of a catechin derivative possessing a C4-S bond less reactive to $\text{BF}_3 \cdot \text{Et}_2\text{O}$. The same authors mentioned in previous work¹¹⁶ that C-4-oxygenated catechin derivatives are less nucleophilic (at C-8) than C-4-S derivatives. This approach would allow rapid obtention of a C-4F functionalized procyanidin.

Scheme 28. C-C coupling of C4- activated catechin units by Lewis acid activation



The C4-S nucleophilic partner was chosen to be a derivative of sulfhydryl thioether (**75a**). However, the thiol function needs to be protected prior to dimer formation. The protecting group chosen was the S-trityl protecting group because of its easy removal under acidic conditions, also compatible with a one-pot deprotection of the O-TBDMS groups. The coupling reaction was carried out following the method of Ohmori *et al.*¹¹⁶ (similar to the previously used Hayes *et al.*⁷⁹ methodology). A solution of **74a** and **94** (3 equiv., Scheme 29) in CH₂Cl₂ (dist., dry) was allowed to cool to -78°C (with molecular sieves in powder). To this solution was added BF₃Et₂O (1 equiv., dist.). TLC monitoring indicated completion of the reaction after 19 h. However, under these conditions the expected dimer was not obtained. Instead, a compound which could be **95**, as suggested by ¹H NMR and mass analyses, was isolated in 12% yield. The rest of the fractions isolated from the reaction mixture were composed of complex mixtures of compounds. The obtention of **95** suggested that deprotection of the S-trityl group of **94** occurred during the reaction. The resulting nucleophilic thiol performs preferentially the nucleophilic attack at the C-4 position of the activated form of compound **74a**. This was not completely unexpected since S-trityl deprotection has been reported to occur in the presence of BF₃·OEt.⁸⁶ Due to the fact that the S-trityl protecting group was inappropriate for this reaction, installation of a more stable protecting group was attempted. We then prepared benzyl-thioether derivative (**96**), the S-benzyl being also removable under acidic conditions.⁸⁶ Then we attempted the coupling using the same conditions as above,¹¹⁶ but again, no reaction occurred (Scheme 30).

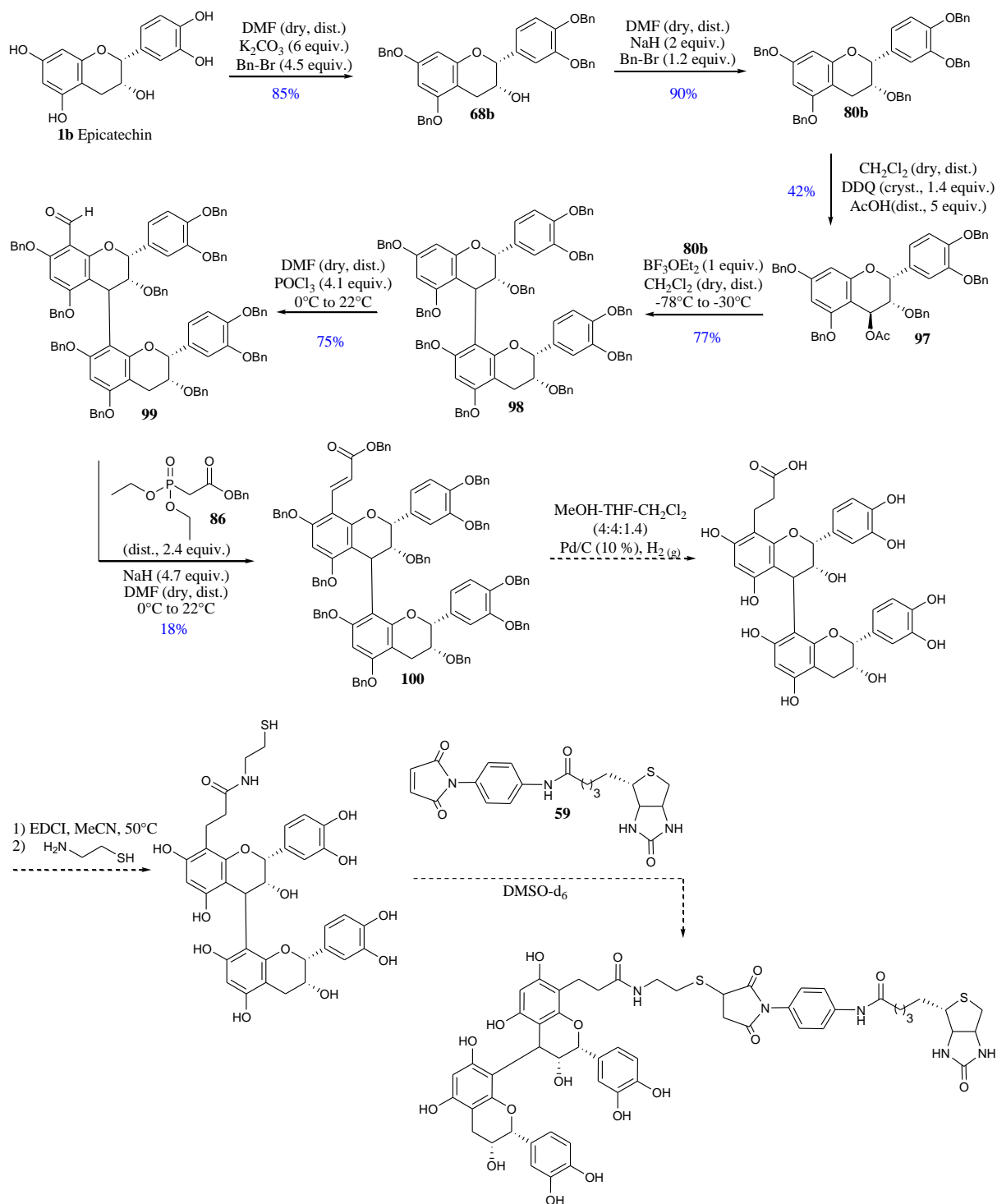
Scheme 29. Attempt to a form B-type C-4F functionalized derivative**Scheme 30.** Attempt to form B-type C-4F functionalized derivative

The same reaction was carried out by rapidly increasing the temperature of the reaction mixture from -78°C to -30°C . TLC monitoring showed no evolution after 20 h of reaction time. Further increment of the temperature to room temperature afforded several products of complex nature. These results led us to conclude that protection of the C-8 position is crucial in order to stop the formation of complex mixtures. Thus, these coupling tests were not explored any further. We then pursued the C8-A derivatization approach. The perspectives envisioned for this C8-A approach are discussed in the following section.

IId.2 A-Ring derivatization of B-type procyanidin

Concerning the A-ring derivatization of B-type procyanidins, the preparation of the more classical per-O-benzyl B-2 derivative was envisioned. Derivatization of the C8-A position is proposed following the approach for the derivatization of catechin and epicatechin (A-ring) discussed in Chapter II, section IIc.2 (page 69). The synthetic strategy is presented in the following figure. This work is currently underway. However, no results are available so far and therefore form part of the perspectives of this work.

Scheme 31. B-type procyanidin A-ring derivatization

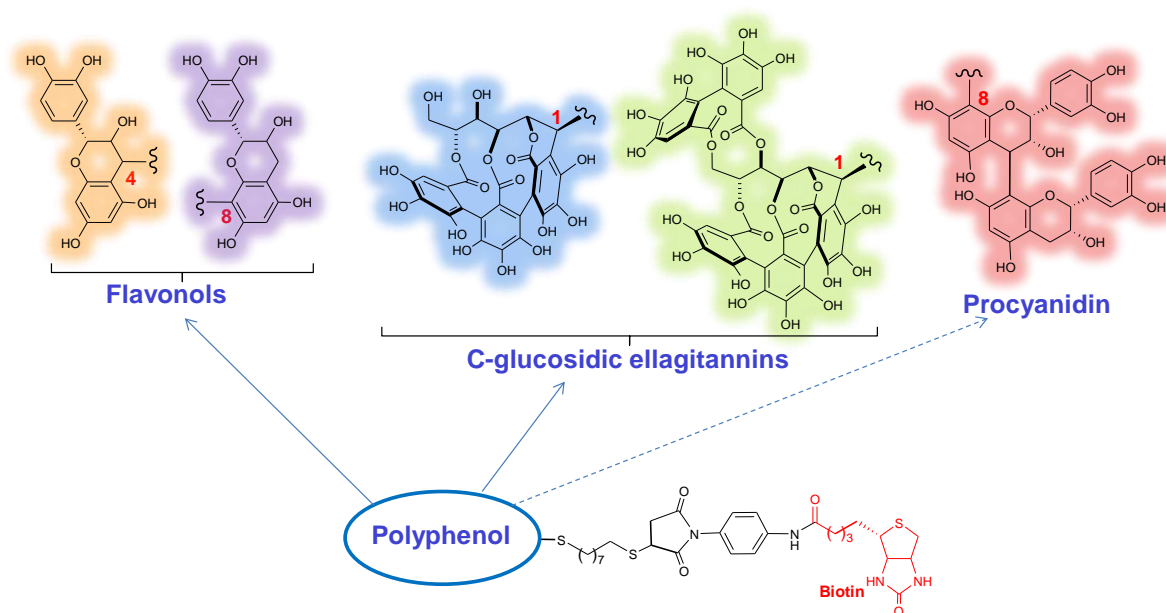


IIe. Conclusion

Derivatization of two C-glucosidic ellagitannins was achieved by nucleophilic substitution at the benzylic C-1 position without the use of protecting groups, using octanedithiol as nucleophile. The sulfhydryl thioether deoxyellagitannins obtained (**52** and **53**) were then coupled successfully to previously prepared biotin maleimide (**59**) by Michael addition to furnish the biotinylated conjugates **60** and **61**.

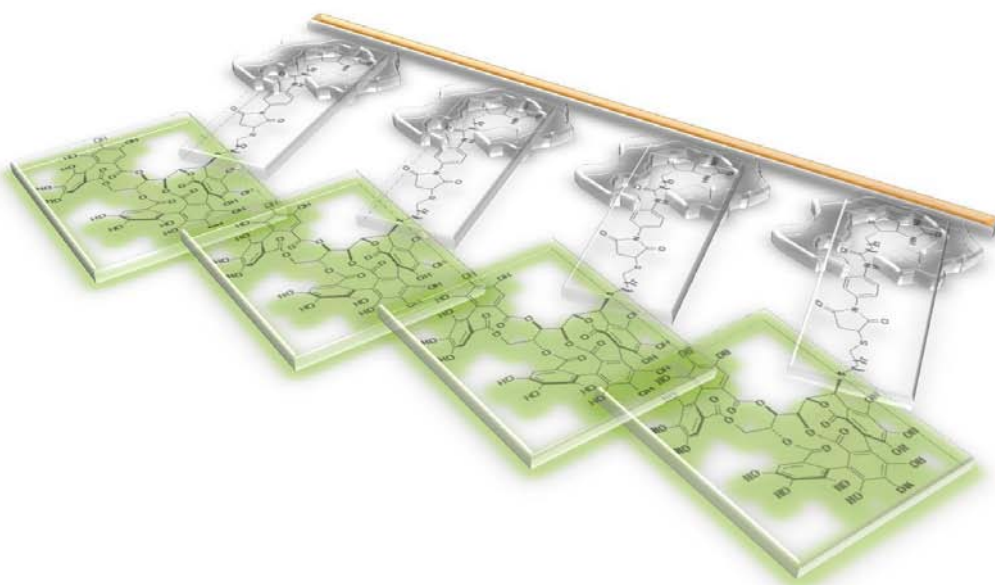
The derivatization of catechin and its epimer at C-3, epicatechin, was achieved at two positions of the flavonoid skeleton (C4-C ring and C8-A ring). Position C-4 was derivatized by means of a four-step synthesis. Different strategies were studied, including variations in the choice of linker and protecting group for phenolic, aliphatic alcohol and thiol functions. Of the different strategies studied, the choice of a sulfhydryl thioether flavonoid derivative was the more appropriate (analogous to the ellagitannin derivatives). Obtention of these derivatives was achieved through t-butyldimethylsilyl (and/or triethylsilyl) protecting group chemistry. The final deprotection step could yet be improved by better regulation of the pH of the reaction media towards neutral pH.

Derivatization of B-type procyanidins at benzylic C4-F position was not possible using the conditions analogous to flavonoid derivatization. The results obtained suggest loss in selectivity of oxidation with DDQ at position C-4F, resulting in complex mixtures. Other oxidizing agents tested did not furnish the desired C4-F functionalized dimer. Obtention by coupling of orthogonal C-4 activated catechin units was also attempted without success. Protection of the C-8 position of the electrophilic partner seems crucial. Derivatization over the C-8 position is envisioned and under study.



Chapter III

Polyphenol-Protein Interaction Studies by Surface Plasmon Resonance

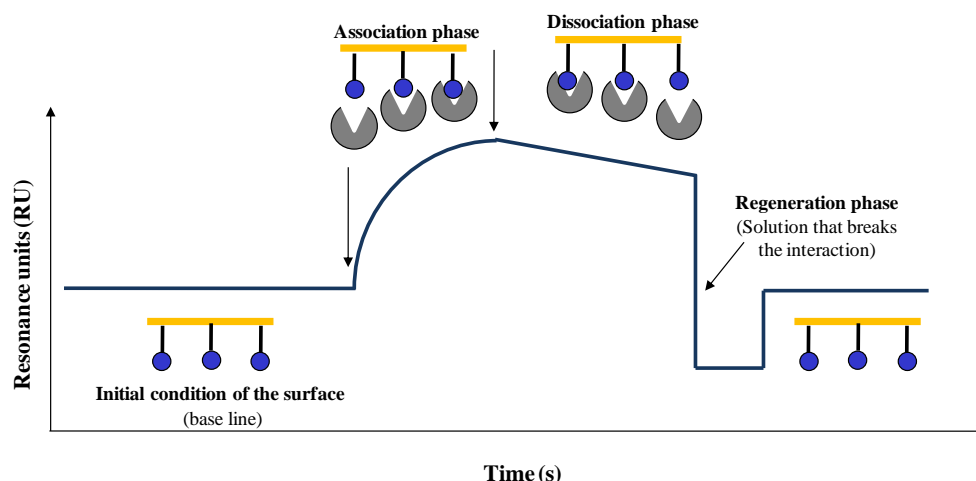


This chapter concerns the immobilization of the polyphenol-biotin adducts presented in the previous chapter over SPR sensor chip surfaces and the use of the resulting SPR sensor chip systems to evaluate their interaction with different proteins, including TopII α , actin, and bovine serum albumin (BSA).

IIIa. Generalities about the analysis of intermolecular interactions by SPR

Surface plasmon resonance (SPR) is a phenomenon that occurs at the interface between metallic surface and an aqueous solution when the electrons at the surface of the metal are excited by incident light of a specific wavelength and at a specific angle (SPR angle). The incident light generates a surface electromagnetic wave (surface plasmons) that propagates perpendicular to the surface of the metal and into the aqueous solution. This wave is very sensitive to any change produced at the proximity of the metal-aqueous interface, which is why any change at the interface will cause a change in the SPR angle. Based on this principle, SPR allows to study intermolecular interactions between, SPR surface-bound molecules (ligand) and a second molecule present in solution (analyte).⁵⁹ Briefly, the SPR surface-bound ligand gives a constant SPR response (base line, see Figure below) because a constant flow of buffer solution (running buffer) is injected on to the surface. A fixed quantity of analyte solution (of known concentration) is injected on to the SPR surface-bound ligand, and the formation of analyte-ligand complex at the interface (**association phase**, Figure 47) causes a change in the SPR angle, which is followed in real time. The SPR response is proportional to the molar mass of the analyte and is measured in relative units (RU, relative to the initial baseline) vs. time (seconds, s). This graph is called a sensorgram (Figure 47). Once the injection of the analyte solution is finished, the SPR response remains either constant because the analyte remains bound to the ligand at the interface, or diminished as a consequence of natural dissociation of the ligand-analyte complex (**dissociation phase**). In general, a **regeneration phase** is needed to bring the surface to its initial state, which consists in forcing the dissociation of the complex by injection of a denaturing agent, such as detergents, acid or basic solutions, a solution with an important ionic strength (1M), or increase of the temperature of the media. These phases are shown in the following figure (for more details about SPR see the appendix section).

Figure 47. Phases of a sensorgram



The sensorgrams presented in this chapter are the result of the subtraction of three sensorgrams. To the sensorgram obtained for the analyte-ligand surface system is subtracted a sensorgram obtained for the analyte-reference surface system (surface without ligand, treated under the same conditions). To the resulting sensorgram is subtracted the sensorgram obtained for running buffer injected onto the ligand and reference surface systems, under the same conditions. This double referencing is done to remove instrument noises and the buffer's contribution to the SPR signal.¹¹⁷

Each SPR sensor chip is divided into four separate flow cells, of which, one is kept blank to use as reference surface and the three remaining flow cells are used to immobilize different ligands (polyphenols). Since we were interested in studying the behavior of different polyphenols towards the same protein, it was important to immobilize equimolar or similar quantities of each polyphenol respectively over different flow cells of the same sensor chip. Because the SPR response is dependant of the molar mass of the molecules⁵⁹, equimolar quantities of different polyphenols (with different molar mass), correspond to different values of SPR response (RU). Taking only into account the mass difference between the polyphenols, the proportionality between the molar mass (MM) and the SPR response (RU) was used to determine how many RU's corresponded to equimolar quantities of each type of polyphenol-biotin adduct. For example, if 79 RU of vescalagin-biotin adduct (MM 1509 g/mol) were immobilized in one flow cell of a sensor chip, 63 RU's of vescalagin-biotin adduct (MM 1207 g/mol) should be immobilized on the neighbor flow cell to have equimolar quantities of both polyphenols.

$$\frac{X}{79 \text{ RU of Vescalagin-biotin adduct immobilized}} = \frac{1207 \text{ g/mol (MM Vescalagin-biotin adduct)}}{1509 \text{ g/mol (MM Vescalagin-biotin adduct)}}$$

X = 63 RU of vescalagin-biotin adduct (**57**) are equivalent to 79 RU of Vescalagin-biotin adduct (**56**)

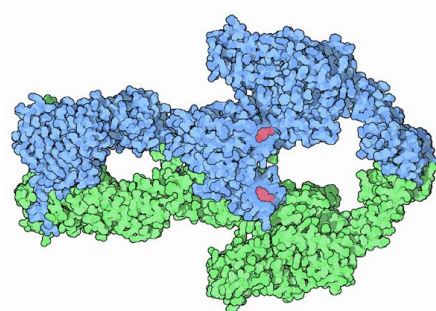
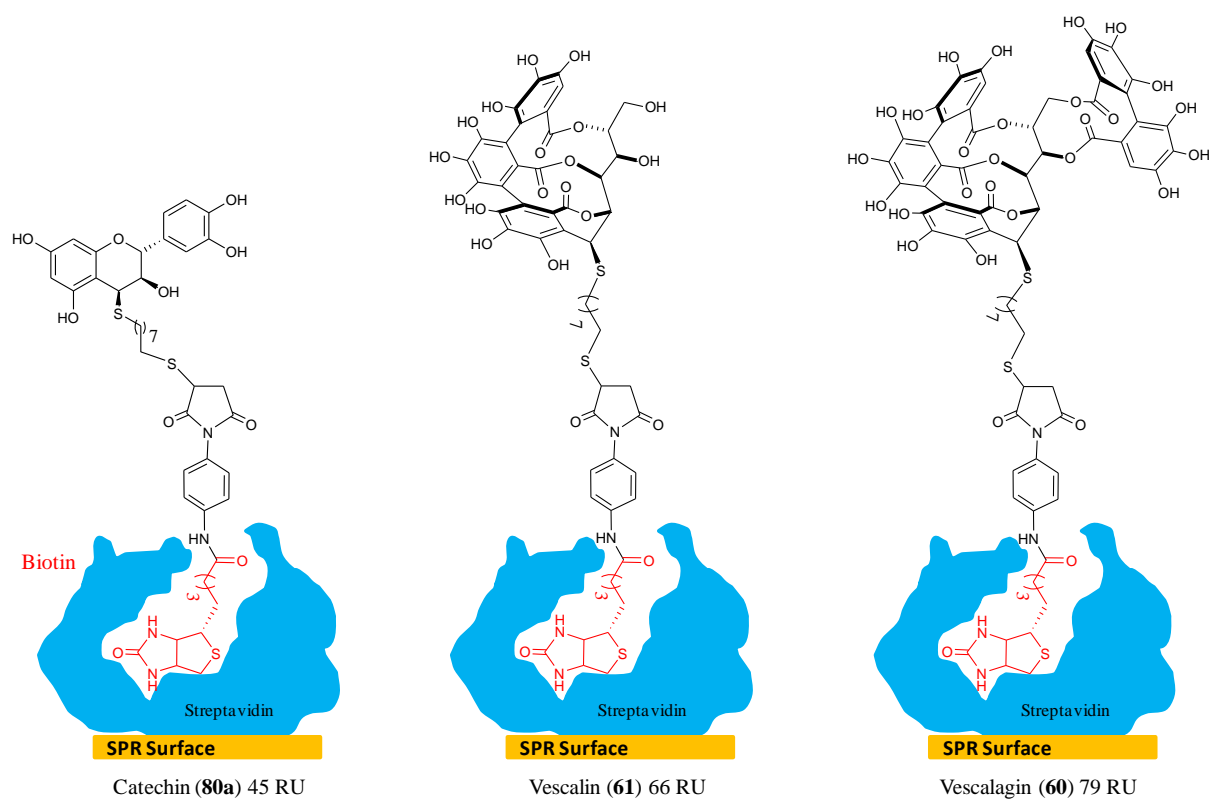
Each biotinylated polyphenol is immobilized on the streptavidin coated SPR surface by injecting a known quantity (in μL) of polyphenol-biotin adduct solution of known concentration (nM). The quantity of polyphenol is quantified in RU following the sensorgram produced by this procedure. In the following section, the results presented concern equimolar or similar quantities of each polyphenol in separate flow cells of the same sensor chip (three polyphenols by sensor chip). A protein solution was injected over all flow cells at once and the SPR response (RU) was measured in real time.

IIIc. Polyphenol-Protein Interaction Studies

As mentioned in Chapter I, both C-glucosidic ellagitannins vescaline (**29a**) and vescalagin (**10**) have been reported in the literature as inhibitors of the TopII α enzyme; therefore, we used this known interaction as a model to validate the use of our biotin-streptavidin bound polyphenol-SPR surfaces in the study of polyphenol-protein interaction.⁵⁹ We were also interested in knowing whether TopII α was capable of differentiating between different types of polyphenols of the same family, such as **60** and **61**, and of different families, such as **80a** (Figure 48) since this would suggest a certain specificity.

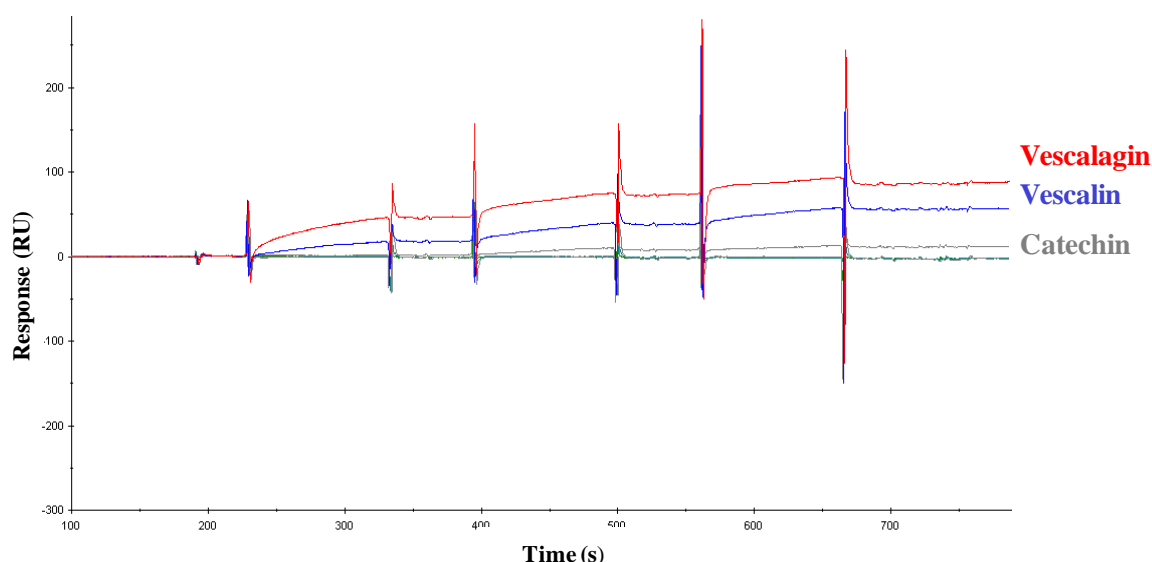
IIIc.1 Topoisomerase II α (TopII α) vs. Vescalagin/ Vescaline/ Catechin

45 RU of catechin-biotin adduct (**80a**), 66 RU of vescaline-biotin adduct (**61**) and 79 RU of vescalagin-biotin adduct (**60**) were immobilized respectively on to streptavidin coated surfaces, using a SAHC 80m sensor chip and following standard procedure recommended by the manufacturers (see Chapter V, Section Vd.2). One flow cell was left blank (streptavidin) to use as reference surface.

Figure 48. Representation of **80a**, **60** and **61** immobilized over streptavidin coated surfaces

Human TopIIα (from *E. coli* containing a clone of the human Topoisomerase II gene) solutions were prepared from a commercial solution (4.08 μM TopIIα, in sodium phosphate 15 mM, pH 7.1, NaCl 700 mM, EDTA 0.1mM, DTT 0.5mM, glycerol 50%) diluted with running buffer (sodium phosphate 50 mM, pH 7, NaCl

150 mM, P20 0.005%)⁵⁹ to obtain the desired concentrations of 6.25, 12.5 and 25 nM. Binding assays were performed at a constant flow rate of 20 μL/min,¹¹⁸ of running buffer at 23°C. Briefly, running buffer was allowed to flow for 3 min before injecting the protein solution; then, injections of TopIIα at 6.25, 12.5, 25 nM solutions were performed in increasing order of concentration and without regeneration of the surface in between injections (titration mode).^{61,119,120} This mode of injection allows to study the interaction at different concentrations of protein, without “damaging the surface” with a possibly non effective regenerating agent. Each concentration was injected over a period of 1.75 min (35 μL) allowing 60 s between injections of protein to allow dissociation of the polyphenol-protein complex. The sensorgram obtained is presented below; Table 6 shows the values of SPR response at the maximum of the curve for each concentration of TopIIα.

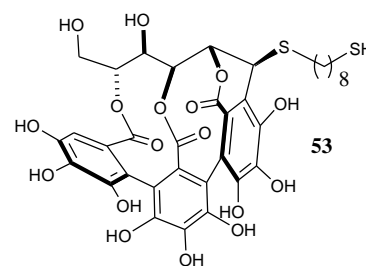
Figure 49. Sensorgram obtained for TopII α injections over polyphenol immobilized surfaces**Table 6.** SPR response observed for immobilized polyphenols vs. concentration of TopII α

Polyphenol	Level of Immobilization (RU)	SPR Response-TopII α		
		6.25 nM	12.5 nM	25 nM
Catechin	45	2	8	11
Vescalin	66	19	37	59
Vescalagin	79	47	76	87

In Figure 49, we can observe that for equimolar levels of **80a**, **61** and **60**, the SPR response was observed to increase in a dose-dependent manner for the three successive injections of TopII α at 6.25, 12.5, 25 nM, suggesting binding of TopII α to the polyphenol-surfaces. We can also observe that the SPR response is greater for the vescalagin-TopII α system than for the corresponding vescalin and catechin systems. This suggests a preference of the enzyme for vescalagin (**56**), which is in accordance with our previous reports.^{40,121}

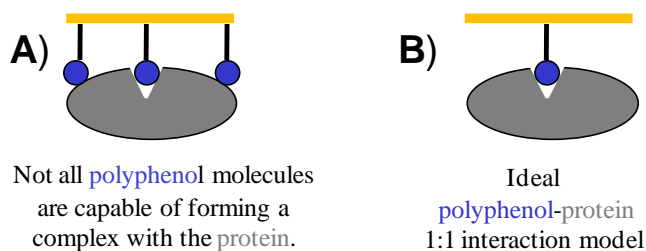
As mentioned in section IIIa, the SPR response observed is proportional to the molar mass of the analyte (the protein) and can be estimated using cross-multiplication as exemplified in the same section. We can thus estimate the maximum SPR response expected for a fixed quantity of SPR surface-bound ligand (polyphenol) during its binding to a protein of known molar mass and compare this theoretical value to the observed SPR response. For 66 RU of immobilized vescalin-biotin adduct (**61**) the estimated theoretical maximum SPR response is 9536 RU (see appendix, page 215), which is significantly higher than the SPR response that was observed of 59 RU (Table 6). Similar results were observed for **60** and **80a**.

These results are comparable to those obtained in the previous report for the vescalin-TopII α system⁶¹, in which the low SPR response was



explained via steric hindrance caused by the high density of **53** (72 RU, figure at the bottom of previous page) at the interface and/or by the protein size, interfering with binding.

Figure 50. Protein size vs. polyphenols immobilized over SPR surface



To rationalize our results, the density of vescaline derivative (**61**) used in our assay was compared to the density of vescaline derivative (**53**) used in the aforementioned study.⁶¹ For this, it was necessary to take into account the difference in molar mass of the two vescaline derivatives **61** and **53**. Using the proportionality between SPR response and molar mass, we estimate that the 66 RU of **61** (MM 1207 g/mol) used in our assay corresponded to a surface that contained approximately 35% less vescaline than the one used in the aforementioned study with **53** (MM 793 g/mol). Since our 35% less dense vescaline-bound-surface did not furnish a higher SPR response, it is possible that the low SPR response obtained is not due to the high density of polyphenol at the interface, but more likely a consequence of the proteins size (Figure 50). To confirm this hypothesis, we repeated the experience using a sensor chip with 52 RU of **80a**, 48 RU of **61** and 61 RU of **60**. The results obtained are presented in the table below.

Table 7. SPR response depending on the level of immobilized polyphenol with TopII α

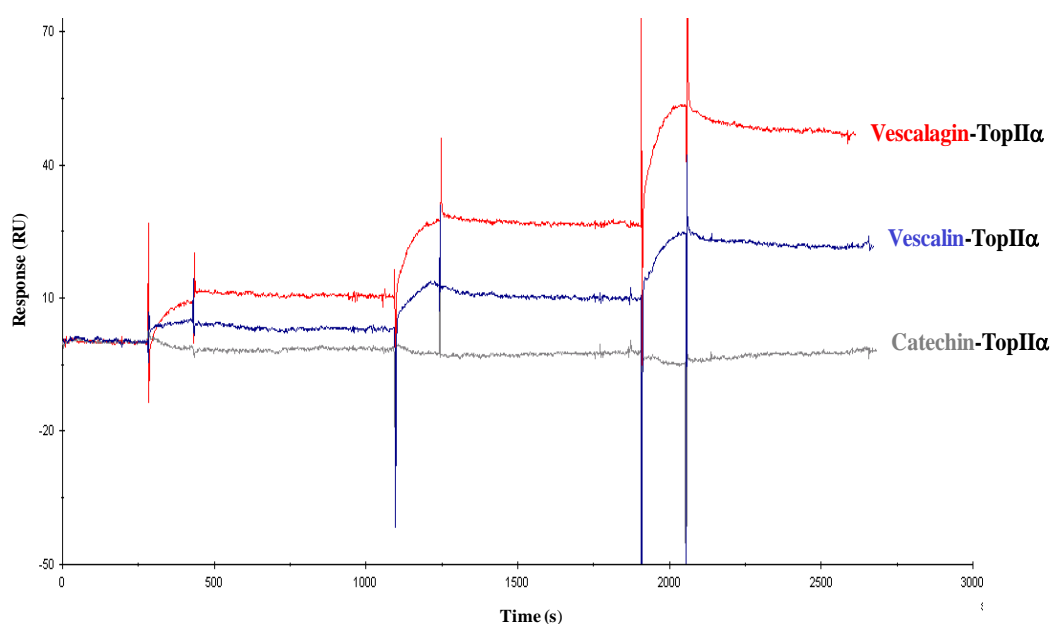
Polyphenol		Level of Immobilization (RU)	SPR Response-TopII α		
			6.25 nM	12.5 nM	25 nM
Catechin	(80a)	52	8	12	14
Catechin	(80a)	45	2	8	11
Vescalin	(61)	66	19	37	59
Vescalin	(61)	48	7	11	11
Vescalagin	(60)	79	47	76	87
Vescalagin	(60)	61	15	33	41

In Table 7, we can observe that for each polyphenol (**80a**, **61**, **60**), the SPR response observed was lower for the less dense surface, suggesting that the magnitude of the SPR response is most probably a consequence of steric hindrance due to the large size of the protein molecules (174,385 Da, about 100 times bigger than the polyphenols). We can imagine that only a few of the polyphenol molecules at the interface are capable of interacting with the available protein (Figure 50A) and that a much less dense surface should be used to favor the ideal 1:1 interaction model (at saturation, Figure 50B). However, given the loss of

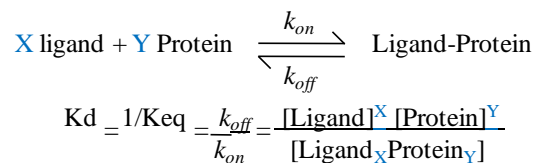
sensitivity observed for the lower density systems, we believe this kind of system should be studied with a much more sensitive SPR apparatus. Or, if our SPR apparatus is used another option would be to inject much more concentrated solutions of protein. However, this would render the experiments more difficult, because the other components in the TopII α commercial solution interfere with the SPR response for concentrations above 25 nM of TopII α . Dialysis of the protein commercial solution against the running buffer may solve this problem, because the dialysis would eliminate the components that interfere with the SPR signal. Unfortunately, the quantity available of protein is another limiting factor. The low density surface (aprox. 5 RU) has to be tested and forms part of one of the perspectives of this work, aimed at properly determining the polyphenol-protein stoichiometry forming the complex.

The dissociation phase of the sensorgram shown in Figure 49 gives useful qualitative information about the stability of the complex formed. We can observe that the SPR response remains constant after each protein injection, suggesting that the polyphenol-TopII α complex does not dissociate. To confirm this hypothesis, the experience was repeated allowing 500 s of dissociation time (instead of 60 s). The sensorgrams corresponding to this assay is shown in the figure below. We can observe that the result is a quasi constant SPR response during the 500 s dissociation time, suggesting once more that a stable complex is formed between vescalagin or vescalin and TopII α .

Figure 51. Comparison of SPR response for polyphenols-TopII α interaction



The affinity between a protein and its ligand (in our case, a polyphenol) is commonly quantified using the dissociation constant (K_d) of the protein-ligand complex, which is defined by the following equation:



K_d = dissociation constant of the protein ligand complex

K_{eq} = the equilibrium constant

k_{on} = on or forward rate constant

k_{off} = off or backward rate constant

X and Y = stoichiometry of ligand (X) and of protein (Y).

We can determine the K_d for the ligand-protein system, if we can obtain the on rate constant (k_{on}) and the off rate constant (k_{off}) for the reaction. This information can be obtained from the sensorgram of a binding assay of the ligand-protein system under specific conditions. These conditions are met when the maximal SPR response (RU_{max}) is obtained, which corresponds to the concentration of protein (the analyte in our case) at which all the available ligand molecules are complexed with the protein.¹¹⁸ For our polyphenol-TopIIα systems, this condition to calculate the K_d value is not met, because of the hypothesis aforementioned of steric hindrance due to protein size. Moreover, at least three replicates of the assay are necessary, to verify the reproducibility of the sensorgram and to obtain an average value of dissociation constant (K_d). This implies the need for efficient regeneration of the SPR surface. The ideal regenerating agent is one that will break the polyphenol-TopIIα complex without affecting the capability of the polyphenol molecules at the interface to interact with the protein. This is verified by the obtention of superposable sensorgrams for repeated cycles. This procedure is described in the following section.

Regeneration of polyphenol-TopIIα complex

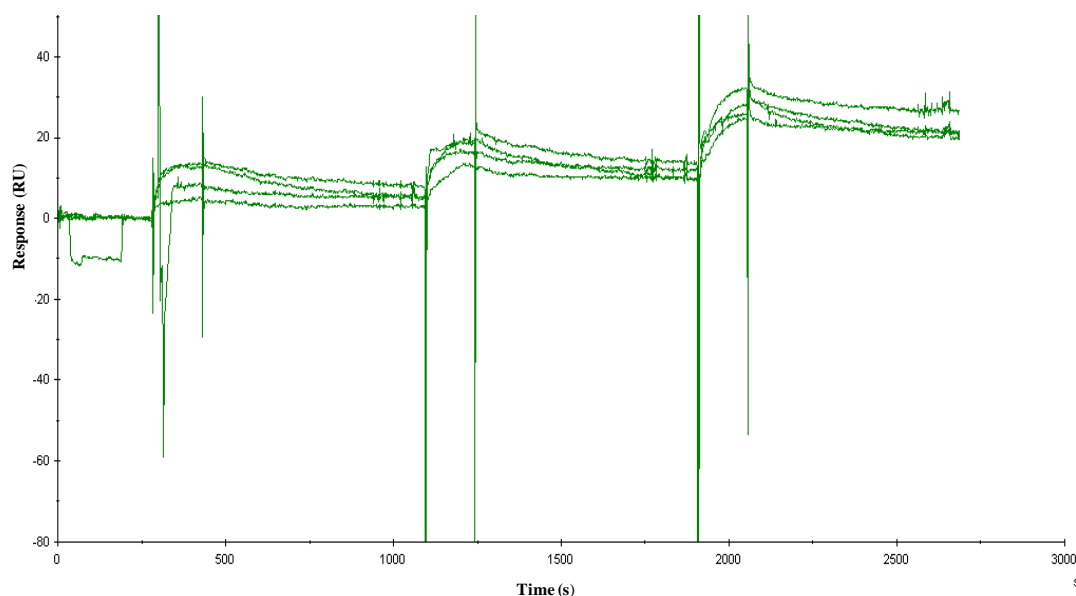
Regeneration was attempted with a classical regenerating agent¹¹⁸, sodium dodecyl sulfate (SDS), which was injected after TopIIα injections and under the same conditions. Briefly, 20 μL of SDS 0.05% solution (in H₂O milliQ) was injected at 20 μL/min, followed by a 20 μL buffer injection. Then, the binding assay with TopIIα was repeated as previously described. Table 8 shows the SPR response at the maximum of the curve for each TopIIα concentration. The values obtained for the same surface with freshly immobilized ligands are also included for comparison.

Table 8: SPR response before and after regeneration with SDS 0.05%

TopII α (nM)	Obtained values (RU)					
	Catechin 80a (45 RU)		Vescalin 61 (66 RU)		Vescalagin 60 (79 RU)	
	Before	After	Before	After	Before	After
6.25	2	4	19	17	47	17
12.5	8	7	37	33	76	28
25.0	11	11	59	51	87	40

From these values, we observe that the systems are still capable of interacting with TopII α after regeneration with SDS 0.05%. However, we notice from Table 8 that, before and after the SDS 0.05% injection, the RU's of protein bound respectively to catechin (**80a**) and vescalin (**61**) are similar, but not identical.

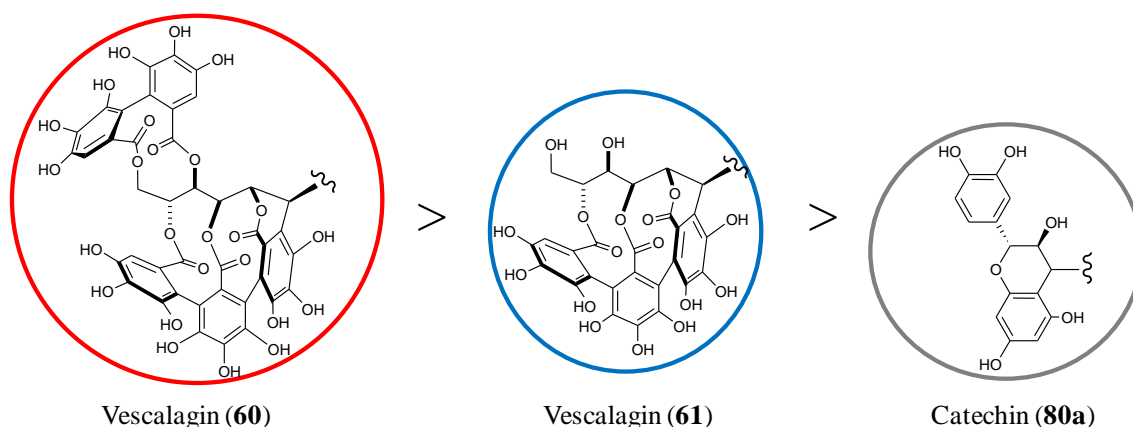
Figure 52. Regeneration cycles with SDS 0.05% for vescalin-biotin adduct (**61**) surface



In Figure 52 is presented the sensorgram of 4 repetitions the vescalin (**61**)-TopII α system over the same SPR surface. Though we observe similar SPR responses for each cycle, the sensorgrams are not superposable, which is interpreted as inefficient regeneration. In the particular case of the vescalagin derivative **60**, the SPR response after SDS 0.05% is much lower than for the freshly immobilized surface. This could be a consequence of the surface being “damaged” by the SDS regenerating agent or that this agent was not efficient in breaking the vescalagin-TopII α complex. Therefore, less vescalagin molecules are available for interacting with the protein, hence the lower SPR response. Since the complex formed is stable even after 500 s, we are more in agreement with the latter. Finding a better regenerating agent forms part of the perspectives of this project.

With the results obtained so far, we can argue that the protein is capable of differentiating between polyphenols belonging to the same family, such as vescalalin and vescalagin and more markedly, between polyphenols belonging to different families, such as the flavanol catechin. Furthermore, given the fast association rate and slow dissociation rate of the polyphenol-TopII α complex at nanomolar concentrations, we can conclude that there is a high binding affinity between the C-glucosidic ellagitannins TopII α , with a preferred affinity of the protein for vescalagin as suggested by both the higher SPR response during the association phase and the difficulty to regenerate the surface.

Figure 53. Decreasing order of SPR response.



One could argue that the SPR response decreasing in the order **60** > **61** > **80a** could be related to the decreasing number of hydroxyl functions and aromatic rings, that modulate their contribution to hydrophilic and hydrophobic interactions with the protein in the same order (**60** > **61** > **80a**). This would mean that the interaction observed would be of a non-specific nature. If this were the case, we should basically observe the same pattern of SPR responses whichever the protein tertiary structure or size. Therefore, we repeated the experience with other proteins of different sizes and structures. These proteins were bovine serum albumin (BSA, globular, 66 KDa),^{26,61} myoglobin (globular, 17 KDa), streptavidin (tetrameric, 54 KDa)⁶¹ and collagen type I (fibrillar, approx. 300 KDa).¹⁹

IIIc.2. Other proteins vs. Vescalin/Vescalagin/Catechin

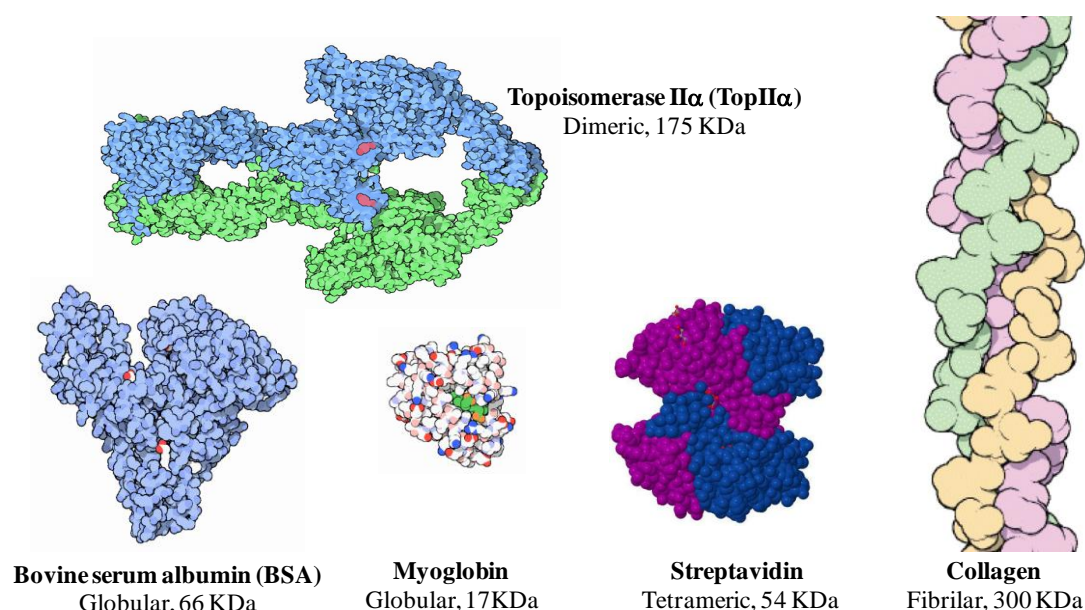
52 RU of catechin-biotin adduct (**80a**), 63 RU of vescalalin-biotin adduct (**61**) and 81 RU of vescalagin-biotin adduct (**60**) were immobilized respectively on to streptavidin coated surfaces, using a SAHC 80m sensor chip, following standard procedure. Binding assays were performed with a flow rate of 20 μ L/min at 23°C. Briefly, running buffer was allowed to run over all surfaces for 3 min, after which time 50 μ L of protein solution 6.25 nM was injected (2.5 min). Afterwards, buffer was allowed to run for 500 s (dissociation time) and the

procedure was repeated for 12.5 nM and 25 nM protein solution. If no formation of complex was observed, the surface was rinsed by three buffer injections, and a different protein was injected. On the contrary, if complex formation was observed, two pulses (20 μ L \times 2) of SDS 0.05% were performed to regenerate the surfaces. The results are summarized in the table below.

Table 9. Binding assays between proteins (6.25, 12.5, 25 nM) and immobilized polyphenols

Protein (Characteristic, MM)	Catechin (80a) (52 RU)	Vescalin (61) (72 RU)	Vescalagin (60) (Fc4 85 RU)
	Interaction?		
BSA (Globular, 66 KDa)	No	No	No
Myoglobin (Globular, 17KDa)	No	No	No
Streptavidin (Tetrameric, 54 KDa)	No	No	No
Collagen Type I (Fibrillar, 300 KDa)	No	No	No
TopII α (Dimeric, 175 KDa)	Yes	Yes	Yes

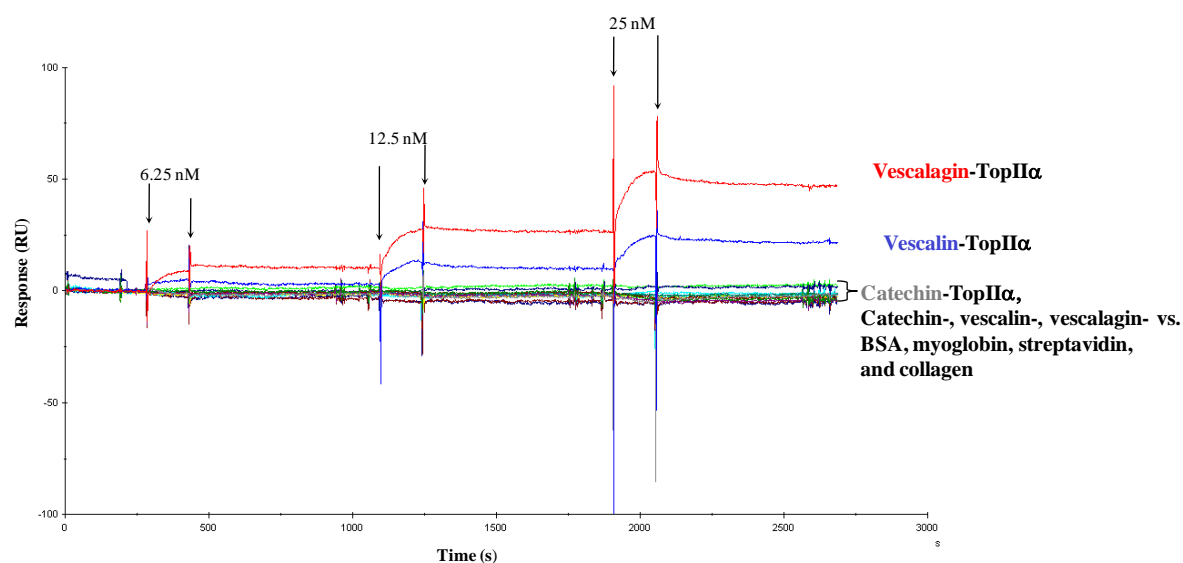
Figure 54. Corey-Pauling-Koltun (CPK) space filling model of proteins from table 9 ^{42,122-125}



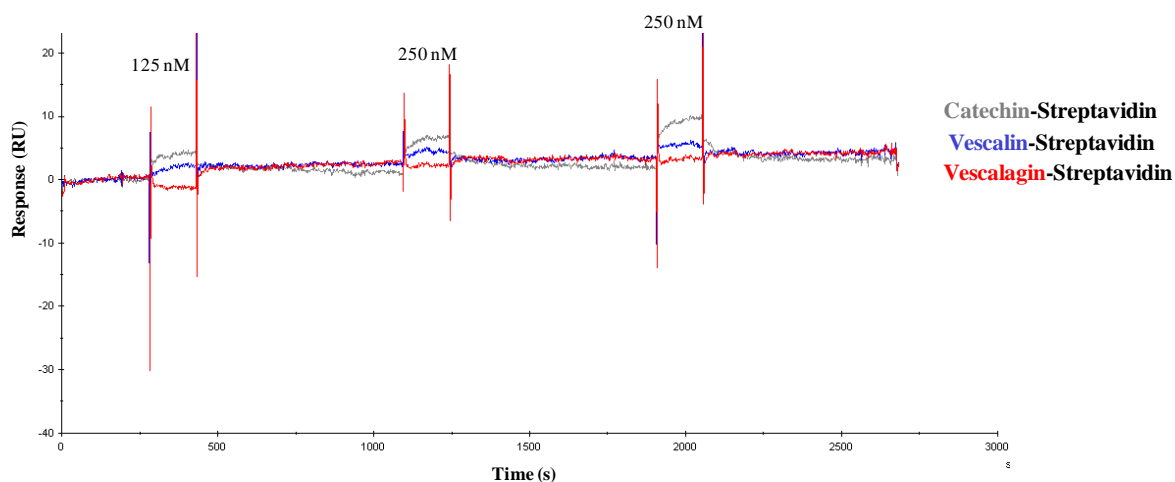
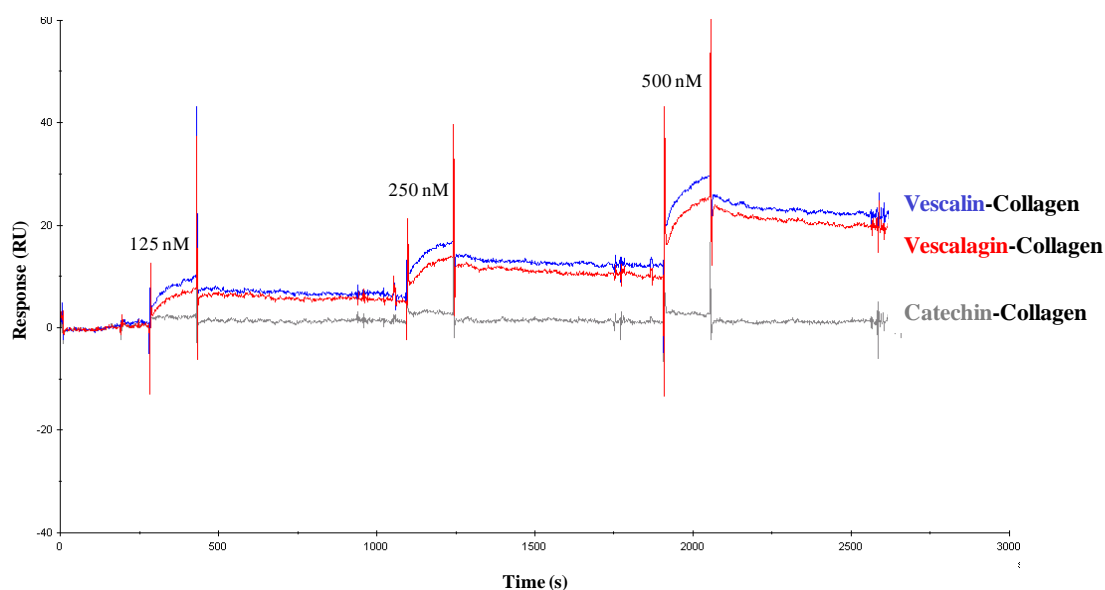
No difference in the SPR response was observed during the injection of BSA, myoglobin, streptavidin or collagen type I solutions at 6.25, 12.5 and 25 nM (Figure 55, between the arrows), which suggests that these proteins do not interact with **60**, **61** and **80a**. TopII α was injected under the same conditions at the end of the assay with the aforementioned proteins to verify that the polyphenols were well immobilized over the surface. A positive SPR response was observed for the polyphenol-TopII α systems. These results show that under the same experimental conditions the proteins tested interact differently with polyphenols, providing further evidence that the pattern observed for TopII α and the polyphenols **60**, **61** and **80a** is

not simply due to the number of phenolic functions, and in a more general sense, proving the usefulness of this SPR tool for protein-polyphenol binding assays.

Figure 55. Proteins vs. immobilized catechin (**80a**), vescalin (**61**), vescalagin (**60**)



At higher concentrations (125, 250, 500 nM), binding was observed between the polyphenols and streptavidin with fast dissociation (Figure 56), and more markedly with collagen type I with slow dissociation (Figure 57). These results suggest a “loss in selectivity” of the polyphenols for the TopIIα at higher concentrations of protein, because other proteins like streptavidin and collagen type I, also give a positive SPR response. Nonetheless, there is still some selectivity between the polyphenols and the proteins within the range of 125-500 nM, because at the same concentrations, the globular proteins BSA and myoglobin did not associate to the polyphenols tested. From Figure 56 and 57 we can observe that the elongated fibrillar collagen type I protein, showed a preference for the ellagitannin-type polyphenols **60** and **61**, while the tetrameric globular streptavidin showed a preference for the flavanol-type polyphenol **80a**, which suggest that there is complementarity between the structures of both the polyphenol and the protein. In general, these results show the importance of using low concentrations of protein in order to detect specific interactions between the polyphenols and proteins, and indirectly the importance of coupling this technique to others in order to make conclusions about the specificity of the interaction.

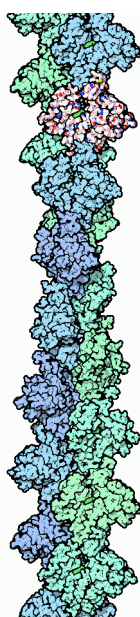
Figure 56. Streptavidin (125, 250, 500 nM) vs. catechin (**80a**), vescalin (**61**), vescalagin (**60**)**Figure 57.** Collagen (125, 250, 500 nM) vs. catechin (**80a**), vescalin (**61**), vescalagin (**60**)

Within the framework of our collaborative project with Elizabeth Génot's team at the IECB, *in vitro* and *in cellulo* assays suggested that vescalagin interacts with the fibrillar actin (F-actin, polymer) rather than with globular actin (G-actin, the monomer), these actins being major constituents of the eukaryotic cell cytoskeleton, as discussed in more details in Chapter IV).⁴⁶ To verify this apparent preference of vescalagin to bind to F-actin, we relied on our SPR tool.

IIIc.3 Actin vs. Vescalagin

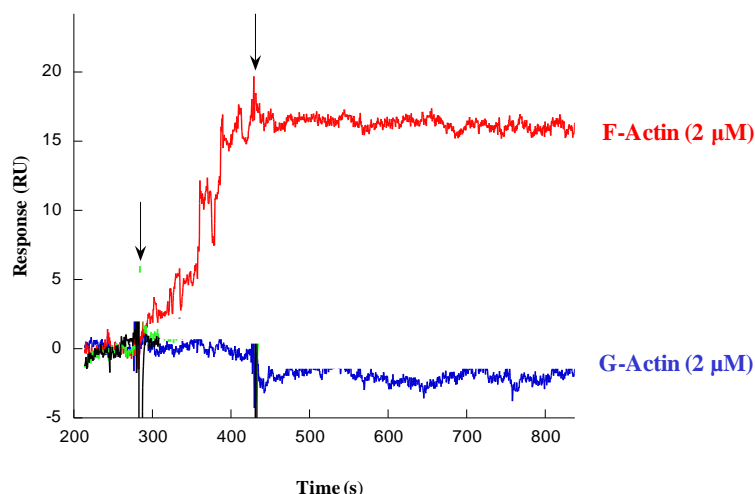
**G-actin model**

70 RU and 217 RU of vescalagin-biotin adduct (**60**) were immobilized respectively on to a streptavidin coated sensor chip surface (Xantec SAD 200m) using the standard protocol. Commercial G-actin powder (α -Actin, from rabbit skeletal muscle) was dissolved with G-buffer (Tris-HCl 5 mM, pH = 8.0, and CaCl_2 0.2 mM) to give a 238 μM G-actin solution. This solution was diluted with running buffer (Phosphate 10 mM Buffer, pH = 7, NaCl 150 mM, CaCl_2 0.2 mM, ATP 0.2 mM, P20 0.005%)¹²⁶ to obtain 2 μM and 4 μM G-actin solutions respectively. Binding experiments were performed at 25°C with a constant 20 $\mu\text{L}/\text{min}$ flow of running buffer, which was allowed to run for 3 min before injecting 50 μL of G-actin solution at 2 μM and 4 μM in that order. No difference was observed between the reference flow cell and the vescalagin-coated (**60**) flow cell, suggesting no interaction between vescalagin and G-actin.

**F-Actin model**

F-actin solutions were prepared respectively from G-actin 2 μM and 4 μM solutions by addition of 10 % F-buffer (Tris-HCl 5 mM, pH = 7.5, KCl 500 mM, MgCl_2 20 mM, 10 mM ATP) and 20% mol/mol of phalloidin to stabilize the fibers (Chapter V, Section Vd.3).¹²⁶ Binding experiments were performed under the same conditions as described above for G-actin. Figure 58 shows an increase in the SPR response during injection of F-actin 2 μM solution, suggesting binding of the protein to vescalagin (**60**). After the injection of the F-actin solution (dissociation phase), the quasi constant SPR response suggests slow dissociation of the vescalagin/F-actin complex. Furthermore, the SPR response was observed to increase with the concentration from “2 μM ” to “4 μM ” of F-actin. Similar results were obtained for both the higher (217 RU) and lower (70 RU) density systems, with lower sensitivity observed for the higher density one system. These results provide further evidence that vescalagin binds to fibrillar F-actin, but not to the monomer G-actin.⁴⁶

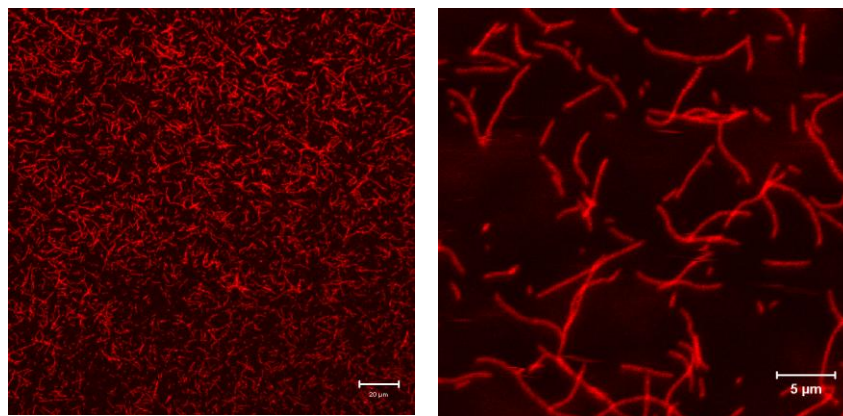
Figure 58. G-actin and F-actin (2 μM , 4 μM) vs. Vescalagin (**60**, 70 RU)

**Table 10.** SPR response for vescalagin (**60**) G-actin and F-actin systems

Protein	Concentration	Vescalagin 60 (70RU)	Vescalagin 60 (217RU)
SPR response (RU)			
G-Actin	2 μ M	-	-
	4 μ M	-	-
F-Actin	2 μ M	50	17
	4 μ M	100	50

It is important to mention that the preparation of the F-actin solutions turned out to be crucial to observe the intermolecular complex by SPR. When the assays were carried out using F-actin polymerized without phalloidin (used to stabilize the fibers), the vescalagin (**60**)-F-actin complex was not observed. Since phalloidin is added to favor the equilibrium towards the fibrillar form of actin¹²⁶ we hypothesized that the F-actin concentration was too low to observe the formation of the complex with vescalagin. The assay was then performed by using a “pure” F-actin/phalloidin stabilized solution, in which fibers had been separated of any residual G-actin and phalloidin by centrifugation. The pellet containing the fibers was re-suspended in running buffer and injected over the vescalagin (**60**) SPR system. Unfortunately, this methodology rendered the assays difficult to reproduce. In most cases, the low change in the refractive index at the interface during F-actin injection suggested that very little protein had been injected. This F-actin batch had been prepared using marked phalloidin (Alexa 534), allowing to verify the formation of F-actin fibers by confocal microscopy (Figure 59). It was hypothesized that given the “jellified” nature of the resulting F-actin pellet, it was too difficult to obtain reproducible homogeneous solutions.

Figure 59. F-actin (0.02 μ M) solution image from confocal microscopy

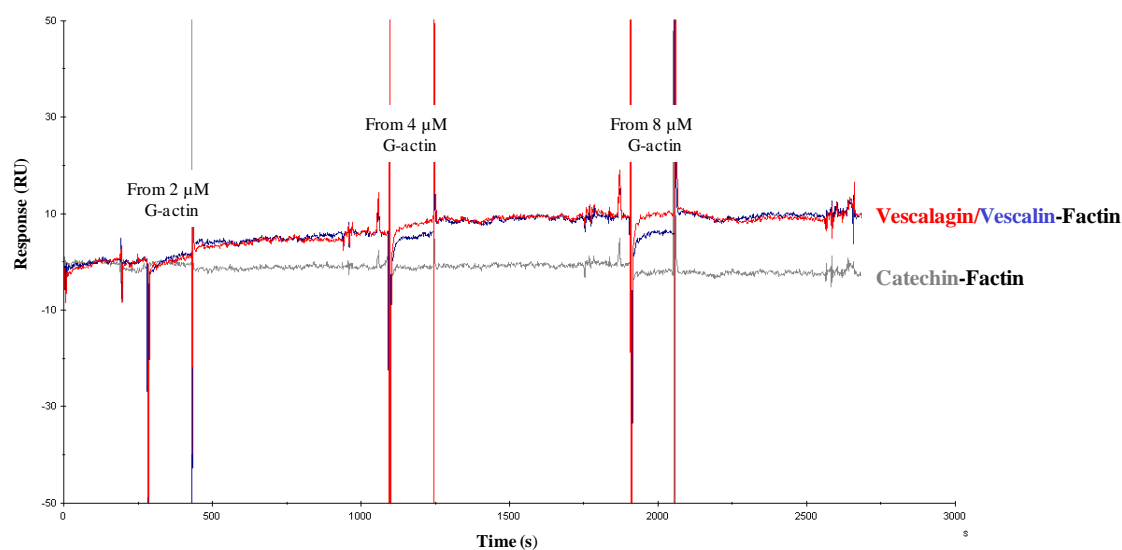


Finally, the use of an F-actin solution from G-actin polymerization in presence of phalloidin and without centrifugation (see Chapter V, Section Vd.3) allowed the observation of the vescalagin/F-actin complex by SPR in a more reproducible manner, probably because a more concentrated and homogeneous F-actin solution was thus obtained. It was verified that none of the other components of the F-actin solution were responsible for the SPR response observed.

We were interested in knowing whether vescalin-biotin adduct (**61**) would respond in the same manner as vescalagin-biotin adduct (**60**) towards G- and F-actin. Catechin (**80a**) was also included in order to compare the results with the ones presented in Chapter II, Section IIc.2.

Actin vs. Vescalagin/Vescalin/Catechin

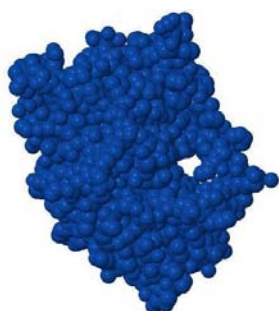
41 RU of catechin-biotin adduct (**80a**), 55 RU of vescalin-biotin adduct (**61**) and 77 RU of vescalagin-biotin adduct (**60**) were immobilized respectively on to streptavidin coated surfaces (SAHC 80m sensor chip), following standard procedure. Binding assays were performed under the same conditions as described above. F-actin solutions were prepared respectively from 2, 4 and 8 μM G-actin solutions (see Chapter V, Section Vd.3) and injected in increasing order of concentration over the SPR system. The SPR response was observed to increase during each injection of protein over the ellagitannin flow cells (**60**, **61**), while no change in SPR response was observed for the catechin (**80a**) flow cell. These results suggest that F-actin interacts with vescalagin (**60**) and vescalin (**61**), but not with the flavanol catechin (**80a**). Furthermore, the similar magnitude of SPR response observed between the vescalagin/F-actin and vescalin/F-actin systems suggests this protein binds to both C-glucosidic ellagitannins without any particular preference under these conditions. These results are in agreement with in cellulo and in vitro assays performed for both ellagitannins. However, in these studies vescalagin showed an effect at much lower concentrations than vescalin (unpublished results).

Figure 60. Polyphenol/ F-actin binding assays**Table 11.** SPR response for Vescalagin/Vescalin/Catechin vs. F-Actin

F-Actin	Catechin (80a) 41 RU	Vescalin (61) 55 RU	Vescalagin (60) 77 RU
2 μM	-	4.5	4.5
4 μM	-	9	9
8 μM	-	9	9

To complete our study, we wanted to study the catechin-anthocyanidin synthase (ANS) system. ANS is a protein that plays a role in the biosynthetic pathway of anthocyanidins (see Chapter I). It is known to transform catechin (**1a**)³² and co-crystallization of this enzyme with the flavonoid dihydroquercetin (Figure 20, page 34) allowed to identify the interaction site of the protein.³¹ Since the catechin-ANS system constitutes a specific polyphenol-protein interaction, we would expect to measure this specificity using our SPR system, expecting a positive response for the catechin (**80a**) flow cell and no SPR response for both vescalatin (**61**) and vescalagin (**60**). Because this protein can degrade easily, it is very difficult to handle the protein during the multiple steps between its production and the injection in the SPR system. For this reason, the exploratory studies were at first performed with catechin-biotin adducts only (**80a** or **90a**).

IIIc.4. ANS vs. Catechin



**Anthocyanidin Synthase
(ANS)**

24 RU of catechin-biotin adduct (**80a**) was immobilized on to a streptavidin coated SPR sensor surface (SAHC 80m) following the standard procedure (Chapter V, Section Vd.2). The composition of the running buffer was adapted from the buffer reported by Wellman *et al.*:³² sodium phosphate 200 mM, pH = 6, Glycerol 10%, 2-oxoglutarate 100 μ M, $[\text{NH}_4]_2[\text{Fe}][\text{SO}_4]$ 50 μ M, sodium ascorbate 2.5 mM, P20 0.005%; glycerol was added to increase protein stability over time, the co-substrates 2-oxoglutarate, $[\text{NH}_4]_2[\text{Fe}][\text{SO}_4]$ and sodium ascorbate were added for preliminary experiments, though it is not known whether they are necessary for recognition and P20 is a surfactant added to reduce adsorption of molecules to flow system.¹¹⁸ N-terminal His₆-tagged recombinant ANS from *Vitis vinifera* (partially purified by using Ni-chelating affinity chromatography) was dialyzed against the running buffer and diluted to obtain the desired concentrations. Binding assays were performed at 23°C with a constant flow of 20 μ L/min of running buffer by injecting ANS solutions at 0.5, 25 and 50 nM and 1 μ M in increasing order of concentrations, following the procedure described in the previous sections. Between 0.5-25 nM ANS, no change in the SPR response was observed during protein injection, suggesting no interaction. However, between 50 nM-1 μ M, ANS was binding to the streptavidin coated reference surface. Since the catechin (**80a**) flow cell also contains this streptavidin coating any positive SPR response showed by this flow cell can not be considered conclusive.

The lack of SPR response between 0.5-25 nM of ANS and the reported Michaelis constant K_m of 175 μM (for ANS *Gerbera*-catechin)³² suggest that the binding between catechin and ANS would be observed for a concentration of ANS in the micromolar range. However, the high magnitude (636 RU) of non-specific binding of the protein to the streptavidin over the surface masks any interaction that the protein might have with the immobilized **80a**. Since this difficulty was not observed for the previous proteins analyzed, it was hypothesized that this was a consequence of the protein's properties. To circumvent this problem, the assay was repeated for ANS 1 μM , modifying the ionic strength or the pH of the running buffer (Table 12).

Table 12. Effect of salinity and pH of running buffer over the catechin-ANS interaction

Running buffer composition	ANS (μM)	SPR Response
Running Buffer 1		
Sodium phosphate 200mM, pH = 6, Glycerol 10%, 2-oxoglutarate 100 μM , $[\text{NH}_4]_2[\text{Fe}][\text{SO}_4]$ 50 μM , Sodium ascorbate 2.5 mM, P20 0.005%.	0.5 nM, 25 nM 50 nM to 1 μM	- Interacts with reference surface
Running Buffer 2		
Sodium phosphate 200 mM, pH = 6, Glycerol 10%, 2-oxoglutarate 100 μM , $[\text{NH}_4]_2[\text{Fe}][\text{SO}_4]$ 50 μM , Sodium ascorbate 2.5 mM, P20 0.005% + 200 mM NaCl.	1 μM	-
Running Buffer 3		
Sodium phosphate 200 mM, pH = 6, Glycerol 10%, 2-oxoglutarate 100 μM , $[\text{NH}_4]_2[\text{Fe}][\text{SO}_4]$ 50 μM , Sodium ascorbate 2.5 mM, P20 0.005% + 125 mM NaCl.	1 μM	-
Running Buffer 4		
Sodium phosphate 200 mM, pH = 6, Glycerol 10%, 2-oxoglutarate 100 μM , $[\text{NH}_4]_2[\text{Fe}][\text{SO}_4]$ 50 μM , Sodium ascorbate 2.5 mM, P20 0.005% + 50 mM NaCl.	1 μM	Interacts with reference surface
Running Buffer 5		
Sodium phosphate 200 mM, pH = 7 , Glycerol 10%, 2-oxoglutarate 100 μM , $[\text{NH}_4]_2[\text{Fe}][\text{SO}_4]$ 50 μM , Sodium ascorbate 2.5 mM, P20 0.005%	1 μM	Interacts with reference surface

The use of a running buffer containing 200 mM NaCl (**running buffer 2**) reduced the interaction of ANS with the reference surface. However, no interaction was observed between catechin and ANS under these conditions. To determine whether the ionic strength was too strong to allow the protein to approach the interface, the assay was performed with a running buffer containing 125 mM NaCl (**running buffer 3**), but furnished similar negative results. Further decrease of the ionic strength to 50 mM (**running buffer 4**) showed again interaction

of ANS with the reference surface, and similar results were obtained when the assay was performed using sodium phosphate buffer pH 7 (**running buffer 5**). We hypothesized that the lack of SPR response for the catechin-ANS system could be a consequence of one or several of the following factors: non-specific binding of the protein to the streptavidin matrix, instability of the protein in the running buffer, inappropriate position of the biotin-ending linker on the catechin skeleton or lack of sensitivity in SPR response due to low immobilization level or steric hindrance. These factors are discussed separately as follows.

It is worth mentioning that the assays were performed with freshly produced, purified and dialyzed protein in the running buffer, as storage in the binding buffer was not feasible due to precipitation upon defrosting. Also, the use of co-substrates for the running buffer caused precipitation and changes of the color of the buffer after 24 h, making it no longer suitable for the BIAcore experiments. This is because the presence of a precipitate may cause damage to the BIAcore microfluidic system and the change in color of the buffer may be due to oxidation of the iron (II) co-substrate to iron (III) which generally gives a yellow coloration in aqueous solution.

Non-specific binding to the SPR-surface's matrix

In an attempt to find a more suitable SPR surface, other commercially available SPR surfaces, such as SAHC80m, SA, CM5, C1, CM3 (Table 13) were tested by injecting a 50 nM solution of ANS (50 μ L) at 20 μ L/min, using a running buffer of intermediate ionic strength based on the observations presented in Table 12 (Sodium phosphate 20mM, pH = 6, NaCl 100 mM, 2-oxoglutarate 100 μ M, $[\text{NH}_4]_2[\text{Fe}][\text{SO}_4]$ 50 μ M, sodium ascorbate 2.5 mM, Twin (P20) 0.005%). A similar running buffer containing DMSO 9% was also tested. In the following table are presented the maximal value of SPR response (RU) observed during the ANS 50 μ M injection.

Table 13. SPR response for ANS (50 nM) vs. surface of different sensor chips

Entry	Buffer	SPR response (RU)				
		SAHC 80m	SA	CM5-cysteine	C1	CM3
1	Sodium phosphate 20mM, pH = 6, NaCl 100 mM, 2-oxoglutarate 100 μ M, $[\text{NH}_4]_2[\text{Fe}][\text{SO}_4]$ 50 μ M, Sodium ascorbate 2.5 mM, Twin (P20) 0.005%.	636	152	144	1812	950
2	Sodium phosphate 20mM, pH = 6, NaCl 100 mM, 2-oxoglutarate 100 μ M, $[\text{NH}_4]_2[\text{Fe}][\text{SO}_4]$ 50 μ M, Sodium ascorbate 2.5 mM,	-	35	45	-	-

Twin (P20) 0.005%

+ **DMSO 9%**

The experiences that have been described in this Chapter were performed using streptavidin coated SAHC 80m sensor chips (Xantec®). In Table 13, we can observe that ANS binds significantly to this surface (entry 1, SAHC 80m, 636 RU), but it binds to a lesser extent to the BIAcore streptavidin coated SA sensor chip (entry 1, SA, 152 RU). Since streptavidin coated sensor chips are prepared by immobilizing streptavidin on to dextran coated sensor chips, we also tested the binding of ANS to the surface of commercially available dextran coated sensor chips. The results show that ANS binds more significantly to dextran coated sensor chips, such as CM3 (entry 1, 1812) and C1 (entry 1, 950 RU), but it binds less to the CM5-cysteine modified-dextran surface (entry 1, 144 RU). These results suggest that the non-specific binding of ANS to the streptavidin coated surfaces may be a consequence of the presence of more residual dextran on the SAHC 80m sensor chips than on the SA BIAcore® one. Then, we repeated the experience using the surfaces that interacted less with ANS (SA and CM5-cysteine), but using a running buffer to which was added 9% DMSO. As shown in entry 2, the addition of 9% DMSO to the running buffer reduced significantly the binding of ANS in both cases, 35 RU on the SA sensor chip and 45 RU on the CM5-cysteine sensor chip. It was then decided to use the SA sensor chip with the running buffer containing 9% DMSO for the catechin-ANS binding assays. However, it was necessary to test the stability of ANS in this running buffer before performing the binding assays.

Stability of ANS in the running buffer

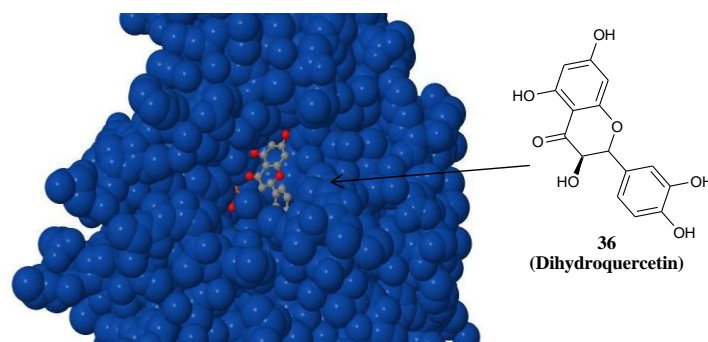
ANS activity assays were performed by Hélène Carrie (graduate student) promptly after dialysis of the protein in the buffer containing 9% DMSO. In parallel, the protein was tested under classical conditions^{34,76} for comparison (see appendix for details). Briefly, the assays consisted in measuring the proteins capacity to transform the substrate catechin (**1a**) to the dimer **34** (Scheme 3, page 33). The results were analyzed by LC/MS analysis. The results showed that ANS remained 25% active when it was dialyzed against the buffer containing 9% DMSO, and 46% active when it was dialyzed against the buffer containing 5% DMSO. The percentage of activity for ANS of 25% and 46% was calculated relative to the activity of ANS under classical conditions (see appendix for details). The activity of ANS dialyzed against the buffer containing 5% DMSO was studied over time and upon storage at 4°C and room temperature. The results showed that the activity of ANS diminished rapidly over time, meaning 50% loss of activity when ANS was kept 1 h at room temperature and 15 % loss in

activity when ANS was kept 1 h at 4°C (relative to initial activity, see appendix for details). It was thus decided to perform the binding assays by SPR using the buffer containing 5% DMSO.

Position of the biotin-ending linker in the catechin skeleton

Structure-activity studies revealed that ANS did not transform the catechin substrate when the hydroxyls of the catechol B-ring or the hydroxyl group at position C-7 (A-ring) are modified.^{34,76} However, there is no information about modifications made at the C-ring C-4 position. Though the co-crystal structure of ANS in presence of DHQ (Figure 20, page 34) would indicate that a C-4 substituted flavanol is capable of interacting with the protein,³¹ we surmised that the orientation of the catechin-biotin adduct **80a** (Figure 48, page 85) could be inappropriate to allow its entrance in the ANS interaction site. We then preferred to synthesize the catechin-biotin adduct **90a**, anchored by the A-ring C-8 position, since other C-8 modified catechin species were shown during structure-activity studies to interact with ANS.^{34,76} **90a** would provide a positive control of the ANS-catechin interaction during the SPR binding assays.

Figure 61. Orientation of DHQ (**36**) in interaction site of ANS¹¹⁵



To summarize the above, binding assays by SPR would be best performed using SA (BIAcore®) streptavidin coated surfaces with the following running buffer: sodium phosphate 20mM, pH = 6, NaCl 100 mM, 2-oxoglutarate 100 μM, [NH₄]₂[Fe][SO₄] 50 μM, sodium ascorbate 2.5 mM, Twin (P20) 0.005%, DMSO 5%. Catechin-8-biotin adduct (**90a**) would be immobilized at a higher density of immobilization to improve sensibility and to confirm a positive SPR response for the ANS-catechin interaction. The preliminary results are presented in the following section.

ANS vs. Catechin-8-biotin adduct

89 RU of catechin-biotin adduct (**90a**) was immobilized over a streptavidin coated SPR surface (SA BIAcore®) using standard procedure. Binding assays were performed at a constant flow of 20 μL/min of running buffer: sodium phosphate 20mM, pH = 6, NaCl 100

mM, 2-oxoglutarate 100 μ M, $[\text{NH}_4]_2[\text{Fe}][\text{SO}_4]$ 50 μ M, sodium ascorbate 2.5 mM, P20 0.005%, DMSO 5%. ANS solutions at 200, 400 and 600 nM were injected over the SPR system following the procedure described in the previous sections. A positive SPR response was observed for each injection of protein (Figure 63), increasing when the protein concentration was increased, and thus suggesting efficient binding of ANS to catechin (**90a**). These results are in accordance with the activity and affinity testes previously described.^{34,76}

Figure 62. Catechin-8-Biotin (89 RU) vs. ANS (Co-S)

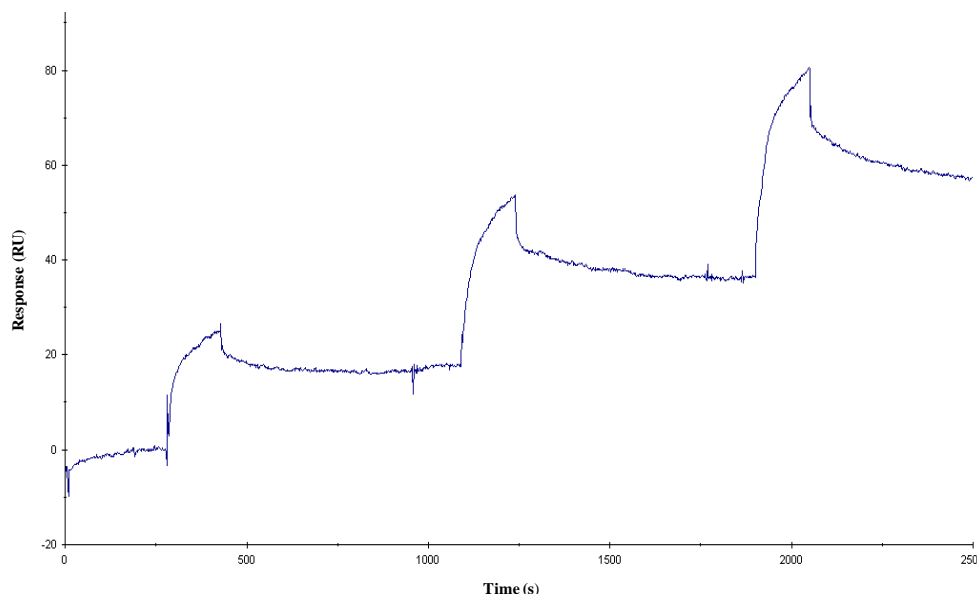


Table 14. ANS-Catechin-8-Biotin interaction results (with Co-S)

ANS	Catechin (90a) 89 RU
200 nM	25 RU
400 nM	53 RU
600 nM	80 RU

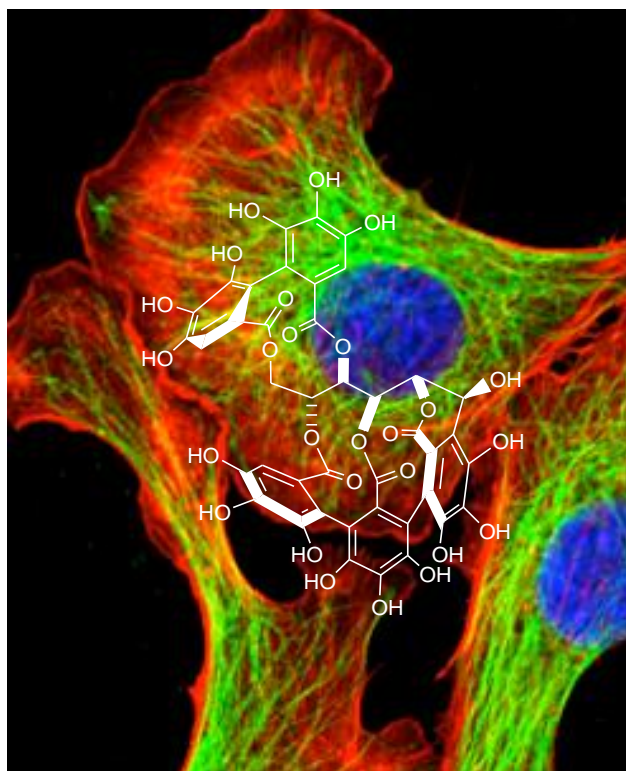
The observation of the catechin (**80a**)-ANS complex encouraged us to repeat the assay under the same conditions with other polyphenols. We envisioned an assay aimed at comparing catechin-8-biotin adduct (**90a**), catechin-4-biotin adduct (**80a**) and epicatechin-8-biotin adduct (**90b**) to complete this structure-affinity relationship studies concerning the flavanol-ANS interaction. We also envisioned another assay comparing catechin-8-biotin adduct (**90a**), vescalatin-biotin adduct (**61**) and vescalagin-biotin adduct (**60**) to confirm whether if by this SPR-based technique, ANS is capable of differentiating between the flavanol (catechin) and the ellagitannins (vescalatin and vescalagin). These studies form part of the perspectives of this work.

Conclusion

The polyphenol-biotin adducts synthesized were successfully immobilized onto streptavidin coated SPR surfaces, which could be used for qualitative studies months after immobilization. The binding studies performed showed that a protein like topoisomerase II α is capable of differentiating between polyphenols from the same family (vescalagin vs. vescalin) and more drastically between polyphenols of different families (*C*-glucosidic ellagitannins vs. flavanols). At the same concentration of protein and under the same conditions, other proteins of different molecular weight and structure (BSA, myoglobin, streptavidin and collagen type I) did not bind to either of the polyphenols tested. This suggests a certain level of specificity for the polyphenol-TopII α system. Furthermore, the vescalagin (**60**)-SPR system was used to discern that vescalagin-biotin adduct (**60**) binds to fibrillar actin (F-actin) and not to globular G-actin. Moreover, the comparison between vescalagin (**60**) and vescalin (**61**) showed both *C*-glucosidic ellagitannins to bind to F-actin, which is in accordance with other assays performed in collaboration with Elizabeth Génot's team.

Chapter IV

Fluorescent Labeling of Vescalagin and Bioassays: Vescalagin-Actin Interaction Studies



In the previous chapter, we studied the interaction between the C-glucosidic ellagitannins vescalagin (**10**) and vescalin (**29a**) with the actin protein by SPR. It was showed that vescalagin (**10**) and vescalin (**29a**) had a certain affinity for actin, but only in its fibrillar form (F-Actin). Parallel to these SPR studies and in order to visualize its localization in cellulo, this vescalagin/vescalin-actin interaction was being studied by confocal microscopy, in collaboration with Elizabeth Génot's team at the European Institute of Chemistry and Biology (IECB). This study required fluorescently marked vescalagin (**10**) and vescalin (**29a**). This chapter describes the hemisynthesis of fluorescent vescalagin and vescalin derivates and their application in bioassays aimed at unveiling the consequences in cellulo of interactions between these polyphenolic compounds and the actin protein.

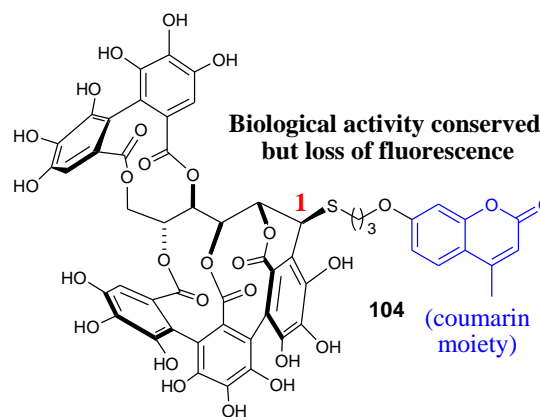
IVa. Design of Vescalagin-Fluorescent Conjugate

Three important factors have to be taken into account in order to efficiently design and develop an appropriate fluorescently tagged derivative of these bioactive polyphenols (and natural compounds in general): the position of anchoring of the fluorescent tag, the type of fluorophore to be used and the length of the linker to form the polyphenolic-fluorescent adduct. These factors and how they applied to the development of a vescalagin-fluorescein conjugate are presented in this section.

IVa.1 At which position of the vescalagin skeleton should we anchor the fluorescent tag?

Within the context of the bioactivity of polyphenols, it is important to take into account the impact that may have the structure modification of the bioactive compound on the activity of the native compound. Our team had earlier synthesized and tested in cellulo a vescalagin-coumarin conjugate (**104**). The bioassay results obtained for conjugate **104** were positive, since they showed that the introduction of a relatively large, medially hydrophobic substituent such as a coumarin unit at the vescalagin's C-1 position did not alter its activity. Moreover, the C-1 vescalagin's (**10**) position is not only appropriate for anchoring the fluorescent tag, but also is susceptible to the attack of all kinds of

Figure 63. Vescalagin-coumarin conjugate **104**

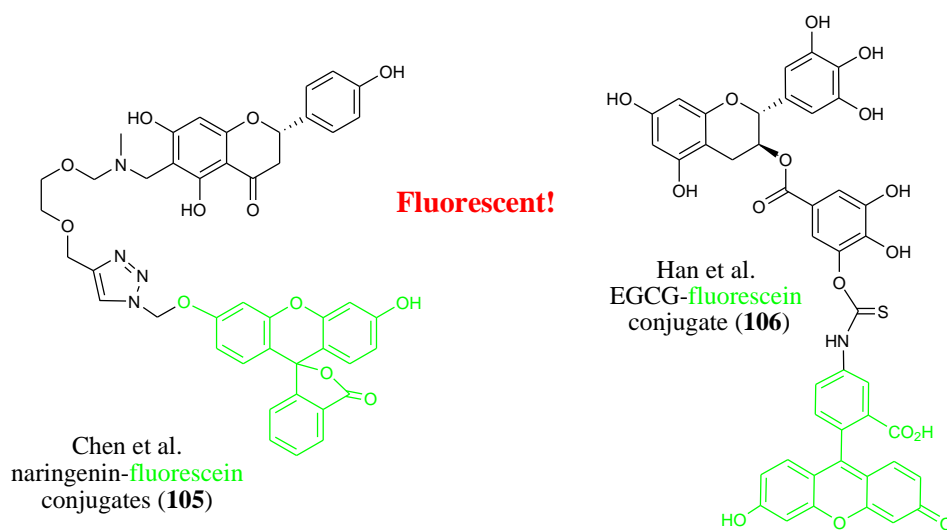


nucleophilic species without the need of any protective chemistry; simply by taking advantage of the remarkable chemoselectivity expressed at C-1.⁴⁰ Unfortunately, the coumarin moiety of the conjugate (**104**) lost its fluorescent properties once coupled to vescalagin (**10**), because of some fluorescence quenching due to the proximity of the vescalagin's phenolic moieties to the coumarin unit.^{51,65} Therefore, the choice of the fluorescent tag and its linker to the vescalagin molecule in the development of a vescalagin-fluorescent conjugate is crucial.

IVa.2 What kind of fluorescent tag should we use?

An alternative to coumarin (Figure 63) as fluorescent tag is the fluorescent organic compound fluorescein (Figure 64), which is one of the most commonly used fluorophores in biological applications due to a good overall efficiency/price ratio;⁶² furthermore, the literature shows examples of flavonoid-fluorescein conjugates that possess good fluorescent properties after coupling with the polyphenolic molecule. In the work of Chen *et al.*⁶³ eight positional naringenin-fluorescein conjugates (**105**) were synthesized, all of which maintained good fluorescent properties. Though these authors used twelve-atom-long spacers between the fluorophore and naringenin, Han *et al.*⁶⁹ coupled epigallocatechin gallate (EGCG) to fluorescein isothiocyanate (FITC, **107**, Figure 65) by a two atom long spacer and the EGCG-FITC conjugate (**106**) still possessed good fluorescent properties for confocal microscopy studies. This evidence suggested the fluorescein family to be a better choice of fluorophores for polyphenolic ellagitannin tagging rather than coumarin.

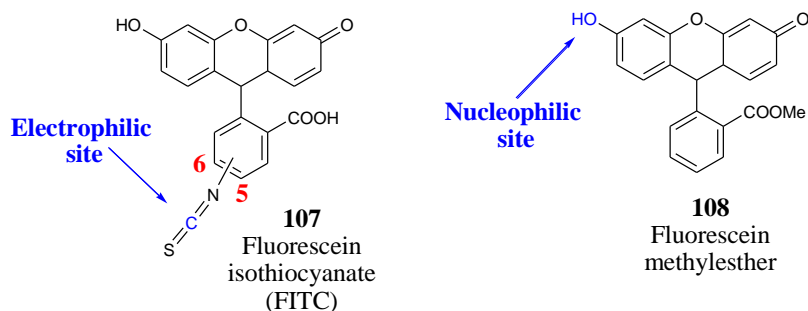
Figure 64. Flavonoid-Fluorescein conjugates by Chen *et al.*⁶³ and Han *et al.*⁶⁹



Previously, our team also performed some attempts to introduce a fluorescein methylester (**108**) tag on the vescalagin's C-1 position without success (see following section). In these

attempts, fluorescein methylester (**108**) nucleophilicity of the phenolic function was exploited for installation of the linker. As an alternative, FITC (**107**) was chosen for its readily available electrophilic site (the carbon of the isothiocyanate function). This has also the advantage of keeping in its native form both the phenol and the carboxylic acid function of the fluorescein moiety which could provide better solubility to the final vescalagin-fluorescein conjugate.

Figure 65. FITC and Fluorescein methylester structures and reactive sites

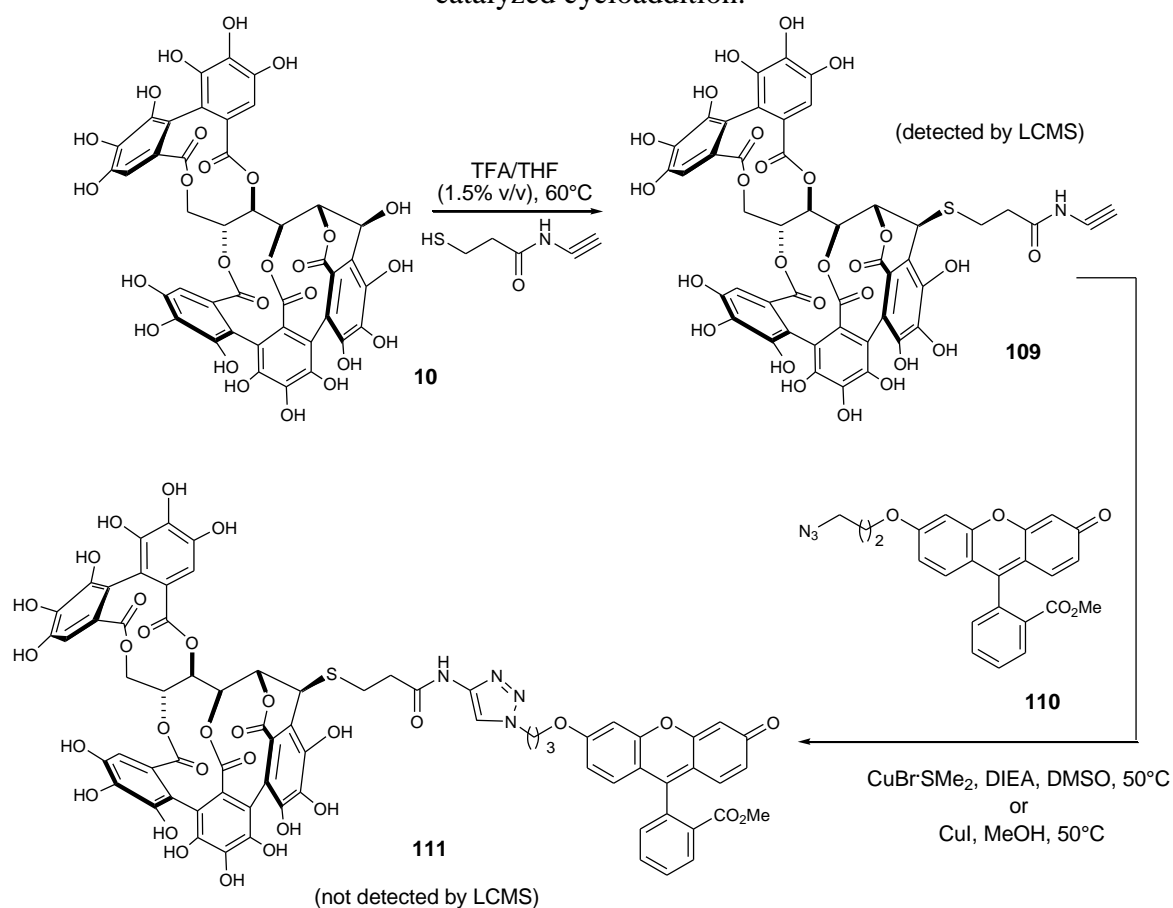


IVa.3 What kind of linker should we use?

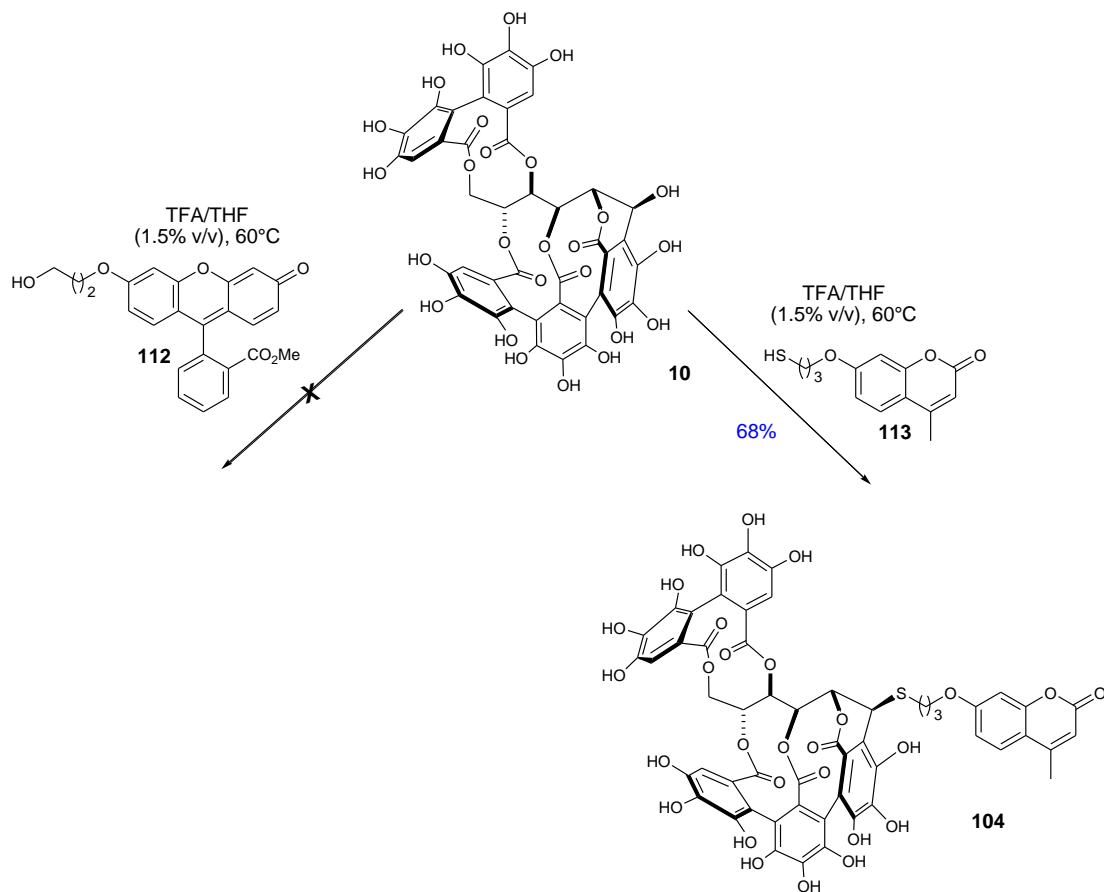
The mechanism by which does proceed the quenching of fluorescence of coumarin when coupled to vescalagin (conjugate **104**) is not known. Nonetheless, occurrence of this quenching phenomenon requires contact or at least a proximity between the fluorophore (coumarin) and the quencher (vescalagin).^{51,65} The quenching was possibly a consequence of the use of the short three-atom-long linker between the phenol-rich vescalagin and the coumarin unit, and therefore could be avoided by the use of a longer linker. Based on this reasoning, the length of the linker was then fixed to be at least eight atoms long inspired by Chen's *et al.* conjugates.⁶³

Concerning the design of the linker, two strategies were previously attempted by our team, in the hands of Stéphane Chasaing. One strategy (Scheme 32), was based on Huisgen Cu (I) catalyzed cycloaddition (click chemistry) between fluorescein methyl ester derivative with an azido terminating linker (**110**) and vescalagin acyl derivative (**109**). However, this attempt was unsuccessful probably because of the small scale of the reaction. The other strategy (Scheme 33), was based on nucleophilic attack of the primary alcohol of fluorescein methyl ester derivative (**112**) on the vescalagin's C-1 position under classical conditions (THF-TFA 1.5%, 60°C). Unfortunately, this attempt was unsuccessful probably because the acidity of the reaction media necessary for the activation of the C-1 benzylic alcohol diminished the nucleophilicity of the primary alcohol of **112**. Nonetheless, the latter strategy was successful when the nucleophile was a primary thiol group, as shown by the obtention of vescalagin-coumarin adduct (**104**).

Scheme 32. Previous attempt of introduction of fluorescent tag by Huisgen Cu (I) catalyzed cycloaddition.

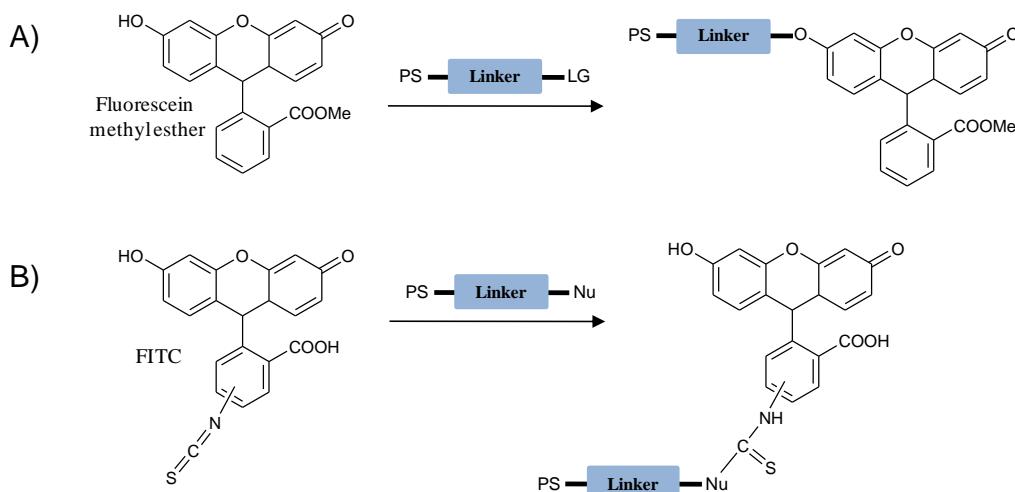


Scheme 33. Introduction of fluorescent tag by nucleophilic substitution



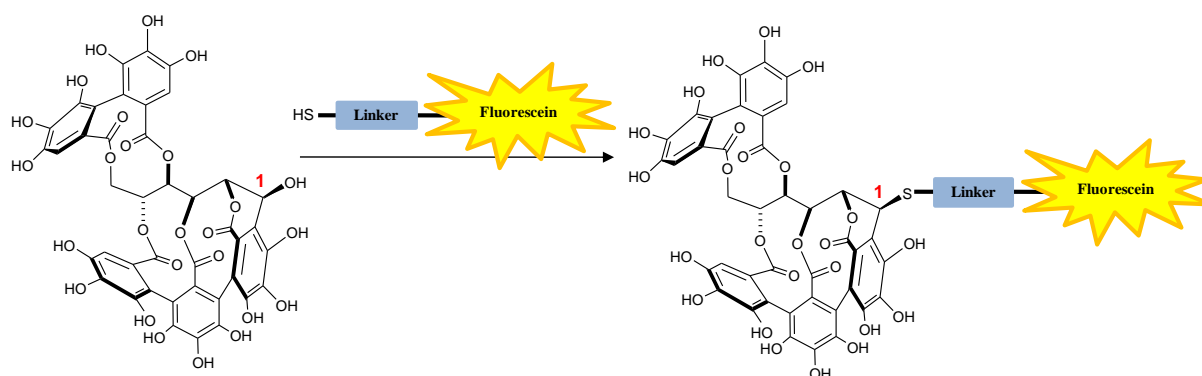
Based on these previous experiences, it was concluded that the linker needs to be a bifunctional linker, possessing in one end a primary thiol function for the coupling step with vescalagin. The opposite end of the linker should possess a function with good leaving group capacity susceptible to nucleophilic substitution by the fluorescein phenol group (Scheme 34A); or it should possess another nucleophilic function capable of attacking the FITC's isothiocyanate electrophilic carbon (Scheme 34B). To summarize, the synthetic strategy can be divided into two synthetic steps:

Scheme 34. Step 1: Installation of the linker on the fluorescent moiety



(PS: protecting group for thiol, LG: leaving group, Nu: nucleophile)

Scheme 35. Coupling of the nucleophilic fluorescein derivative with vescalagin



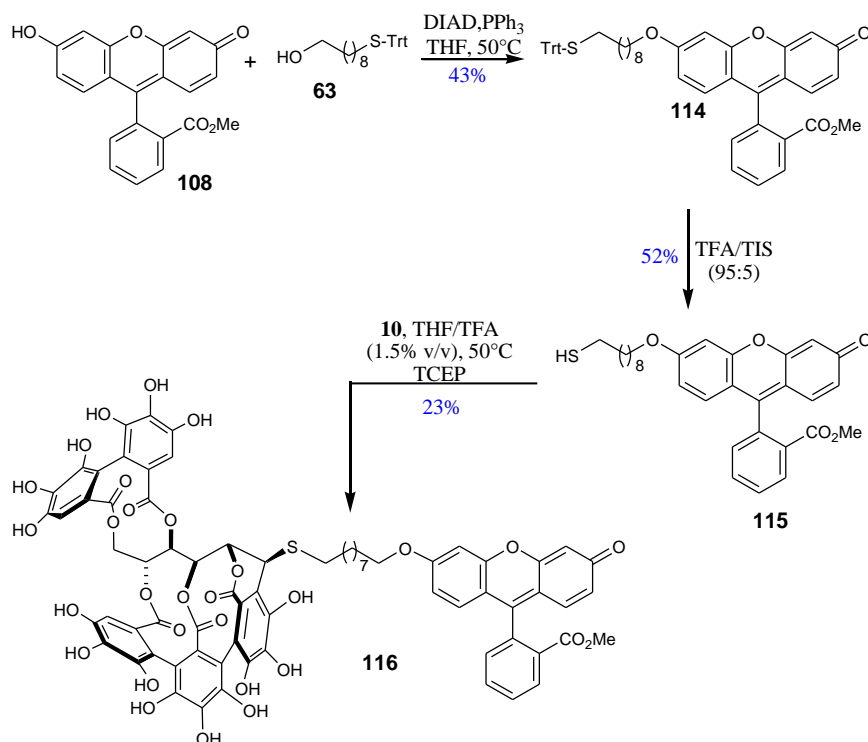
IVb. Hemisynthesis of Vescalagin-Fluorescein Conjugate

Three vescalagin fluorescein conjugates were obtained by hemisynthesis, one of which possessing the desired characteristics (fluorescence and solubility) to serve as a tool for the actin-vescalagin interaction studies by confocal microscopy. The synthetic strategy for the obtention of these vescalagin fluorescein conjugates is described in this section.

IVb.1 Hemisynthesis of vescalagin-Fluorescein Conjugate I

In a first approach, a nucleophilic fluorescein derivative equipped with a simple nine-carbon-long aliphatic linker was envisioned, inspired by the naringenin-fluorescein conjugates developed by Chen *et al.*⁶³ As a linker, was used compound **63** bearing a primary alcohol ending function (leaving group) and a thiol function masked by a thioether bond, with a trityl group (-C(Ph)₃) to avoid any competing reaction with the primary thiol (Scheme 10, page 58).^{86,87}

Scheme 36. Hemisynthesis of vescalagin-fluorescein conjugate I



As previously discussed, the nucleophilicity of the phenolic position of fluorescein methylester (**108**) can be exploited in order to install aliphatic linker **63** over this position. For this, Mitsunobu conditions were relied upon to enhance the leaving group's capacity of the primary alcohol of **63** under mild conditions.¹²⁷ For this reaction, a protocol adapted from a report by Sigmund *et al.*¹²⁸ on the fluorescent tagging of nucleotides was used. A solution of **63** in anhydrous THF was allowed to react with triphenylphosphine (PPh₃) and diisopropyl azodicarboxylate (DIAD) in presence of fluorescein methylester (**108**) at 50°C. Purification of the reaction mixture furnished **114** as a bright orange oil in 43% yield. Removal of the S-trityl protecting group is achieved under acidic conditions (5% TFA, v/v) in the presence of triisopropylsilane (TIS) to capture the acid-labile triphenylcarbocation generated during the reaction.⁸⁶ Inspired by the deprotection of thio-trityl groups on peptides realized by Bernardes *et al.*,¹²⁹ compound **114** was simply dissolved in a TIS-TFA (95:5, v/v) solution and after 1 h,

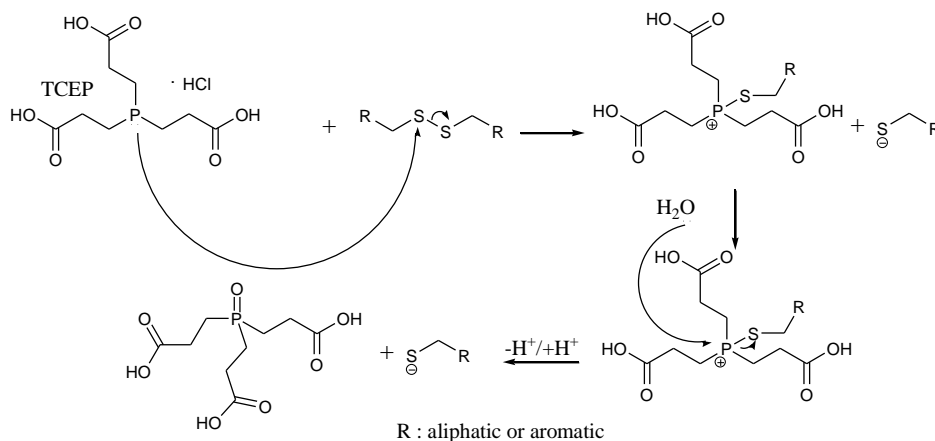
the solvent was evaporated and the reaction mixture purified to furnish compound **115** as an orange oil in 52% yield. With this nucleophilic fluorescein derivative ready, the coupling with vesicalagin (**10**) could take place.

Some difficulties encountered in this synthesis

Many thiols are rapidly oxidized to give the resulting disulfide.¹³⁰ Compound **115** formed the corresponding disulfide upon storage to give a thiol-disulfide mixture. This mixture was engaged in the coupling with vesicalagin (**10**). A specific reducing agent for disulfides was used to regenerate thiol **115** in situ during the reaction.

As previously shown by the work of Quideau *et al.*⁴⁰ vesicalagin's (**10**) inherent reactivity at position C-1 allows a large variety of nucleophiles to attack this electrophilic site by a S_N1 type reaction mechanism without the use of protecting groups. This reactivity was exploited in the coupling reaction of vesicalagin (**10**) with the fluorescein nucleophilic derivative **115**. A solution of vesicalagin (**10**) in THF-TFA (1.5%, v/v) was heated to 50°C and allowed to react with **115** (thiol-disulfide mixture) in presence of tris(2-carboxyethyl)phosphine (TCEP, 1 equiv.) to cleave the disulfide of **115** in situ during the reaction.¹³¹ Since the reaction was carried out under anhydrous conditions the source of H_2O necessary for the reduction of the disulfide¹³² by the trialkylphosphine comes advantageously from the release of one mol of H_2O during the nucleophilic substitution on the vesicalagin (**10**).

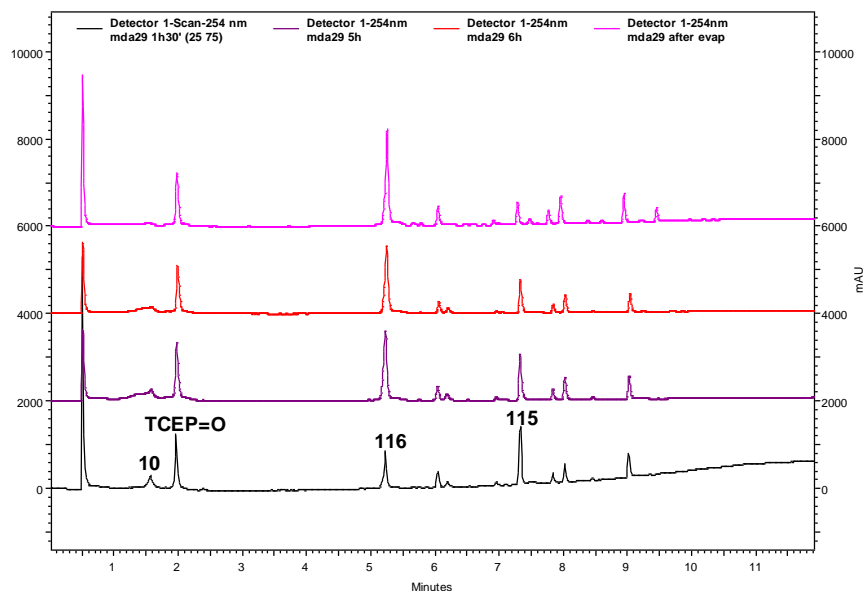
Scheme 37. Disulfide bond cleavage proposed mechanism¹³²



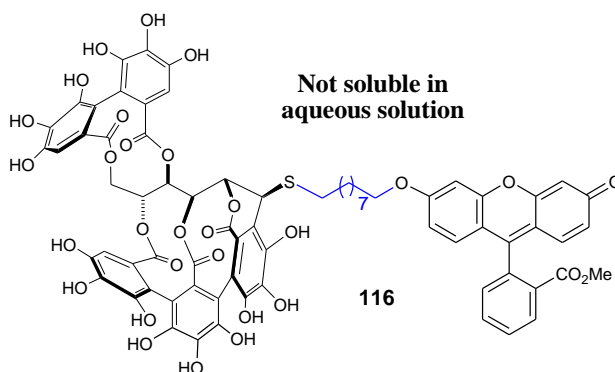
HPLC monitoring of the reaction showed the apparition of a new product with a retention time of $R_t = 5.21$ min, with an UV profile similar to that of fluorescein's derivative **115** ($\lambda_{max} = 443$). After 6 h, HPLC monitoring indicated the quasi completion of the reaction. Purification of the reaction mixture by semi-preparative HPLC furnished compound **116** as a yellow powder in 23% yield. The low yield of compound **116** was attributed to the use of only 1 equivalent of fluorescent thiol (**115**) relative to 1 equiv. of vesicalagin (**10**); because,

vescalagin (**10**) under similar conditions using 10 equiv. of octanedithiol as nucleophile furnished 78% yield of analog derivative (Chapter II, Section IIb).

Figure 66. HPLC monitoring of reaction mixture of coupling step between vescalagin (**10**) and **115**. Chromolith® Performance RP-18e column (4.6 × 100 mm, 5 µm), 3.0 mL.min⁻¹: 0-10 min: 0% to 100% of MeCN/TFA 0.1%



Unfortunately, vescalagin-fluorescein conjugate **116** was insoluble in aqueous solutions and therefore inappropriate for bioassays in cellulo. To increase the solubility of the vescalagin-fluorescein conjugate in water it was envisioned to use a polyethylene glycol linker.⁶¹ A commercially available building block, 2-(2-(2-chlorethoxy)-ethoxy)-ethanol (**117**), was modified to allow its installation on fluoresceins methyl ester.

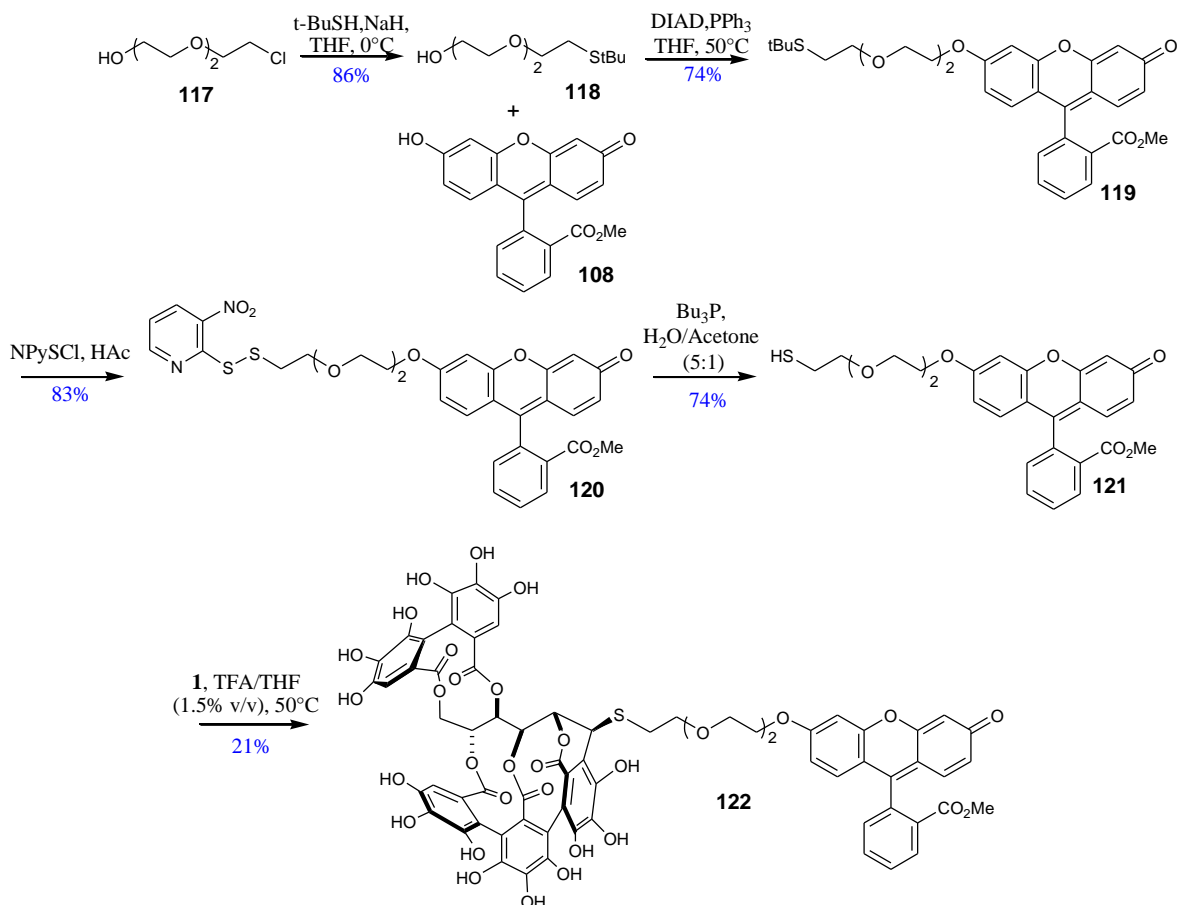


IVb.2 Hemisynthesis of vescalagin-Fluorescein Conjugate II

Commercially available 2-(2-(2-chlorethoxy)-ethoxy)-ethanol (**117**) was modified to contain a thiol function masked as a ter-butyl thiol ether. This was conveniently accomplished by directly substituting the chloride with an appropriate thiolate ion. Following the procedure reported by Brown *et al.*,¹³³ a solution of t-butylthiol was cooled at 0°C and allowed to react with sodium hydride (NaH, 1 equiv.) in order to generate the sodium thiolate. Once the release of hydrogen had ceased, 2-(2-(2-chlorethoxy)-ethoxy)-ethanol (**117**) was added to the

mixture. Purification of the reaction mixture furnished compound **118** in 86% yield. ^1H NMR and ^{13}C NMR data and mass analysis were in accordance to that reported by the authors.¹³³

Scheme 38. Hemisynthesis of vescalagin-fluorescein conjugate II



Compound **118** was coupled under Mitsunobu conditions to the fluorescein methylester (**108**) by means of the same procedure as described for the fluorescein derivative **114**.¹²⁸ A solution of **118** in anhydrous THF was allowed to react with PPh_3 and DIAD in presence of the fluorescein methylester **108** at 50°C . Purification of the reaction mixture furnished a bright orange solid that was identified as compound **119** (74%). Of the different methodologies reported⁸⁶ for removing a S-t-butyl group, treatment with 3-nitro-2-pyridinesulphenyl chloride (NpsCl) was chosen because it was one of the mildest methods proposed (compared to HF or mercury salts) and because this deprotection methodology had been used successfully in other projects of our team. Removal of the S-t-butyl group was achieved in two steps: formation of a disulfide by treatment with NpsCl, followed by reduction of the disulfide by tributylphosphine (PBu_3). In a first step (Scheme 38), following a protocol reported by Pastuszak and Chimiak;¹³⁴ compound **119** was dissolved in acetic acid and allowed to react with a source of R-S^+ (NpsCl, 1.1 equiv.). The site of cleavage of the thioether bond is governed by the stability of the carbocation formed, favoring the cleavage of the S-t-butyl bond. After 3 h, acetic acid was removed by co-evaporation under reduced

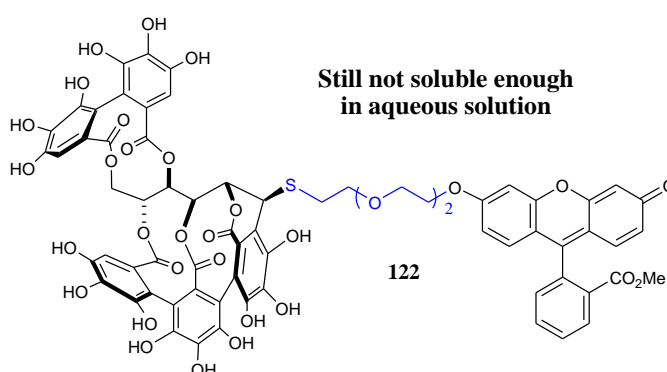
pressure with cyclohexane. Purification of the reaction mixture afforded compound **120** in 83% yield as an orange solid. The second step consisted in the reduction of the disulfide bond. This cleavage of the disulfide bond is commonly done in peptide chemistry by reduction with 2-mercaptoethanol, thioglycolic acid, cysteine or dithiothreitol (DTT). Another alternative is treatment of the disulfide in the presence of water with trialkyl phosphines, more specifically tri-*n*-butylphosphine (PBU₃). In this case, PBU₃ was the reagent of choice for its effectiveness in the reduction of simple organic disulfides.¹³² Thus, following the methodology reported by Humphrey and Potter,¹³⁵ compound **120** was dissolved in a mixture of acetone-H₂O (5:1, v/v) and was allowed to react with (Bu₃P, 1 equiv.) at room temperature for 4 h. Purification of the reaction mixture afforded compounds **121** in 74% yield as an orange solid.

As for the fluorescein-thiol derivative **115** (previous section), compound **121** also rapidly oxidized to form the corresponding disulfide after O=PBU₃ was removed from the reaction mixture. Despite our efforts to obtain the thiol in pure form (HPLC purification with acidified solvents, re-submission of the disulfide to reduction with PBU₃ and use of degassed solvents during the work-up) during the handling of the sample, some disulfide nevertheless formed. However, it was observed that the disulfide-thiol ratio remained at a 1:1 as calculated from ¹H NMR. It was decided then to carry out the coupling with vescalagin (**10**) using this thiol-disulfide (1:1) mixture of **121**.

The coupling between vescalagin (**10**) and the fluorescein derivative **121** was performed using the protocol described for the obtention of conjugate **116** (THF-TFA 1.5%, v/v, solution heated to 50°C).⁴⁰ Monitoring of the reaction progress by HPLC showed the apparition of a new product with retention time Rt =

5.61 min, with an UV profile similar to that of fluorescein ($\lambda_{\text{max}} = 442$ nm). After 19 h, HPLC monitoring indicated quasi completion of the reaction. Purification of the reaction mixture by semi-preparative HPLC

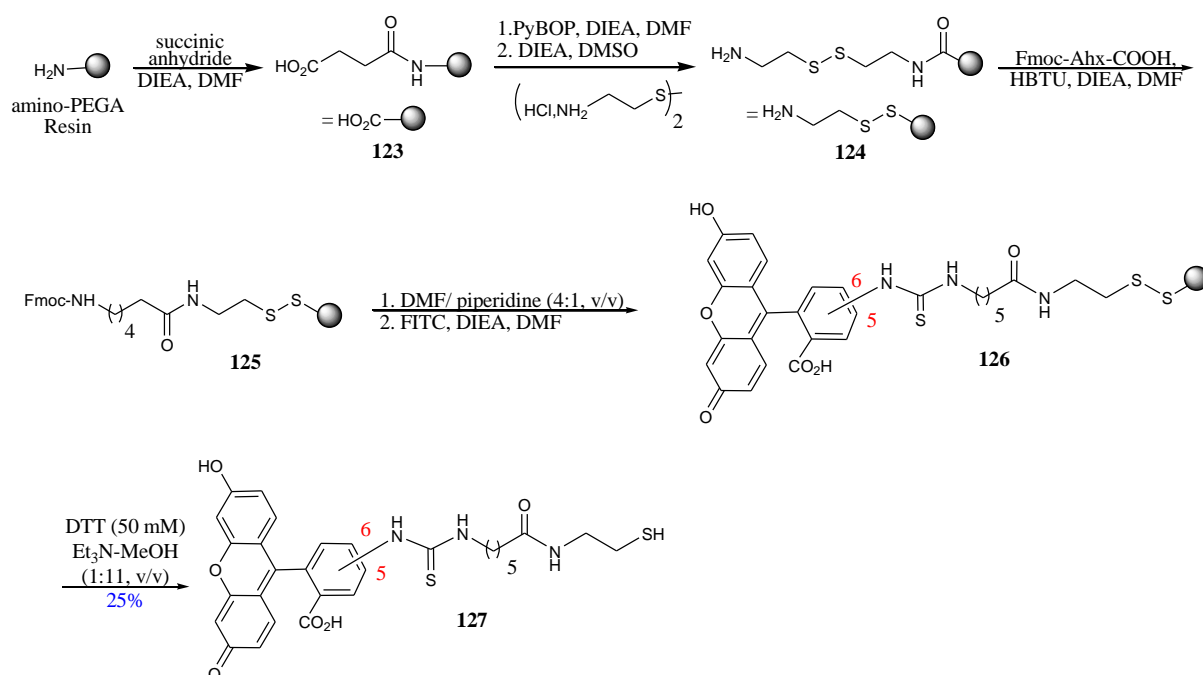
furnished compound **122** in 21% yield as a dark orange solid. Despite the presence of the polyethylene glycol linker, the vescalagin-fluorescein conjugate **122**, was still highly hydrophobic, only soluble in MeOH (7mg > 3mL) and partially soluble in CDCl₃, MeCN and DMSO. Another option to increase the solubility in aqueous solution of the desired vescalagin-fluorescein derivative is to keep both the phenol and carboxylic acid functions of the fluorescein unit. To this aim, we decided to use FITC (**107**) as the starting fluorophore.



IVb.3 Hemisynthesis of vescalagin-Fluorescein Conjugate III

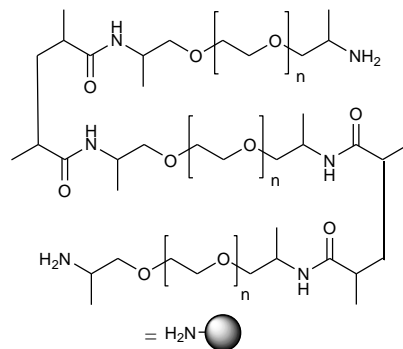
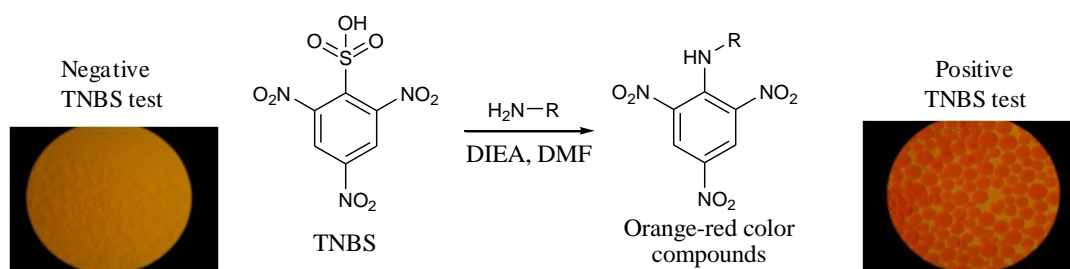
Thus we next directed our efforts towards the preparation of a vescalagin-fluorescein derivative using FITC (**107**) as the starting fluorophore. Because FITC (**107**) is most commonly used in protein and peptide tagging,⁶² the synthesis of the hydrophilic nucleophilic fluorescein tag with this fluorophore was performed using solid-phase synthesis.^{136,137} In solid phase synthesis, the molecules are bound to a bead (resin) which allows the removal of excess reagents by simply washing them away. Given the experience of Quideau's group in this field of chemistry, a fluorescein tag possessing a thiol-ending, thirteen-atom-long linker was synthesized in six steps. This was performed by coupling of commercially succinic anhydride, N-Fmoc protected cystamine and 5(6)-fluorescein isothiocyanate (**107**) on amino-PEGA resin as solid support (Scheme 39). The thiol ending function was introduced in the linker moiety masked as a cystamine, from with the reactive primary thiol will be released upon cleavage from the solid support by disulfide reduction. Each step was controlled using the 2,4,6-trinitrobenzenesulfonic acid (TNBS) color test for primary amines.¹³⁸

Scheme 39. Synthesis of hydrophilic nucleophilic fluorescein Tag III



Amino PEGA resin¹³⁹ is a highly polar solid support with good swelling properties in polar solvents. It is composed of bis-aminopropyl-polyethylene glycol di-acryloyl (70-80%) copolymerized with bis-aminopropyl-polyethylene glycol mono-acryloyl (5-10%) and its reactive functionalities are secondary amine groups (Figure 67). With the purpose of introducing a cystamine, the amino-PEGA resin was allowed to react with succinic anhydride in DMF in the presence of di-*iso*-propylethyl amine (DIEA). After washing with DMF, MeOH, and CH₂Cl₂, a small portion of the resin was submitted to the TNBS test; the lack of change of color of the resin indicated completion of the coupling reaction and therefore obtention of carboxylic acid functionalized resin **123**.

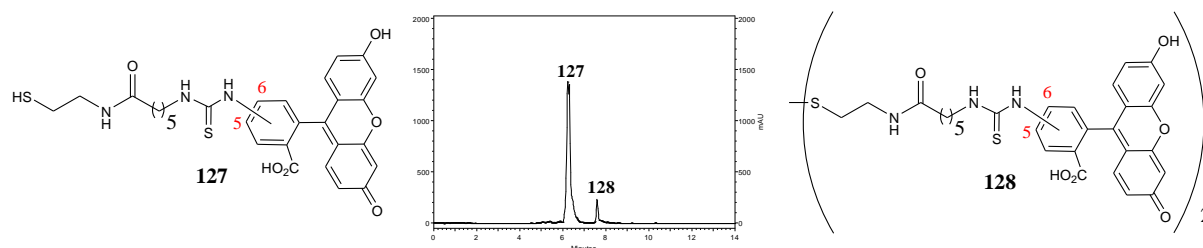
Figure 67. Amino PEGA Resin

Scheme 40. TNBS color test reaction¹³⁸

Following a protocol modified from that of Li *et al.*¹⁴⁰ carboxylic acid resin **123** was activated with (benzotriazol-1-yloxy)tripyrrolidinophosphonium hexafluorophosphate (PyBOP) and DIEA in DMF for 20 min and coupled with cystamine previously dissolved in DMSO in presence of DIEA. After washing the resulting resin, the TNBS reagent changed the coloration of the resin from white to red, indicating successful obtention of resin **124**. Inspired by the work of Jullian *et al.*,¹³⁷ the resulting cysteamine resin **124** was coupled to Fmoc-Ahx-COOH (an alkyl spacer that has been formerly used in combination with FITC) using N,N,N',N'-tetramethyl-O-(1H-benzotriazol-1-yl)uronium hexafluorophosphate (HBTU) as the activating agent in DMF and in presence of DIEA. After washings and verification through the TNBS control test, the Fmoc protecting group was removed with DMF-piperidine (4/1, v/v) solution. The terminal amine group was then free to perform a nucleophilic attack over the isothiocyanate electrophilic carbon of 5(6)-FITC to form a thiourea. The reaction was carried out by allowing to react deprotected resin **125** swollen in DMF with 5(6)-FITC (**107**) in the presence of DIEA overnight. After the washings, the resulting resin **126** was orange.

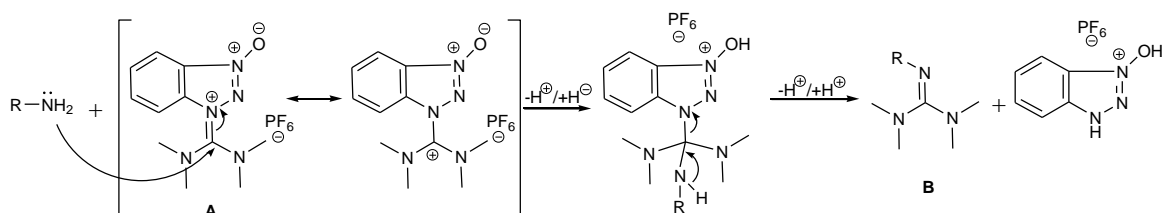
Cleavage of the nucleophilic fluorescein derivative from resin **127** was carried out with a methodology adapted from Hummel and Hindsgaul¹⁴¹ (reductive treatment of cystamine's disulfide bond with dithiothreitol (DTT, 50 mM) in MeOH-Et₃N (11:1, v/v) solution). HPLC analysis of the MeOH washings of the resin indicated the reaction to be clean (Figure 68). In the chromatogram (Figure 69) we notice one major compound, as two peaks with very close retention times ($R_{t1} = 6.24$ min, $R_{t2} = 6.31$ min); which was attributed to the 5(6)-FITC derivative (**127**) positional isomers, obtained in 25% overall yield. The second peak in the chromatogram consisted of the disulfide of the desired product **127** as shown by mass spectrometric analysis.

Figure 68. HPLC trace of reaction mixture from resin **126** MeOH washings after disulfide cleavage. Chromolith® Performance RP-18e column (4.6 × 100 mm, 5 μm), 3.0 mL.min⁻¹: 0-10 min: 0% to 75% of MeCN/TFA 0.1%



Difficulties encountered during the synthesis

In the first attempt to perform the synthesis of **127** (Table 15, entries 1-3), only traces of this compound were obtained. At first, we believed the cleavage of the disulfide bond to release **127** from resin **126** was unsuccessful because of the intense orange color of the resin. Since the use different cleaving reagents (DTT and mercaptoethanol)¹⁴² and change in reaction conditions (solvent, pH)¹⁴⁰ did not furnish compound **127**, it was suspected that the problem was due to a coupling step previous to the FITC introduction. However, it was found from the work of Li *et al.*¹⁴⁰ that the coupling step between the carboxylic acid resin **123** and cystamine could be the limiting step of the reaction sequence (Scheme 39, page 117). The coupling agent N-HBTU **A** (Scheme 41) bears an iminium salt function with a positive carbon, which is known in some cases to react with amines to form a stable guanidine side products **B**.¹⁴³

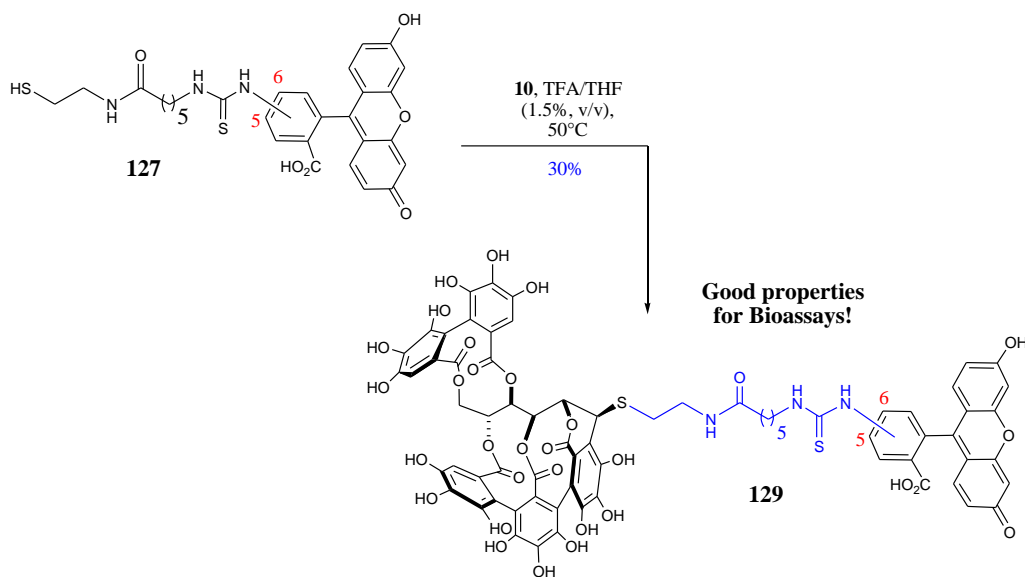
Scheme 41. N-HBTU plausible side reaction¹⁴³

Taking this into consideration, the reaction sequence was carried out using the phosphonium salt PyBOP as the coupling reagent for the cysteamine coupling to resin **123**. The solvent was also changed to DMSO for better dissolution of the cysteamine salt in the presence of Et₃N. The yield of the overall reaction was increased to 25%, which was sufficient to continue with the coupling step of **127** with vescalagin (**10**).

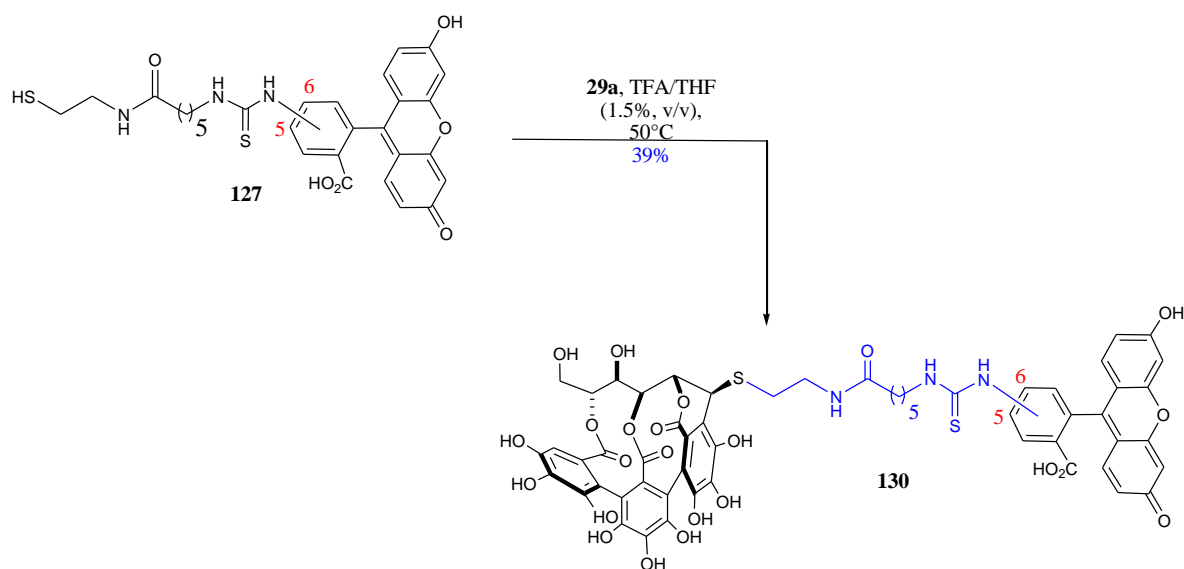
Table 15. Essays performed to improve the formation of compound **127**

Entry	Coupling reagent	Solvent	Cleaving reagent	Yield
1			DTT-Et ₃ N-MeOH ¹⁴¹	
2	HBTU	DMF	Mercaptoethanol ¹⁴²	Trace
3			DTT-Tris Buffer (pH 8) ¹⁴⁰	
4	PyBOP	DMSO	DTT-Et ₃ N-MeOH ¹⁴¹	15%-25%

Nucleophilic substitution at the C-1 position of vescalagin (**10**) was finally performed with compound **127** as described in the previous sections, (THF-TFA 1.5%, v/v solution at 50°C). The desired vescalagin-fluorescein derivative **129** was obtained in 30% yield after semi-preparative purification. The solubility in water of this vescalagin-fluorescein conjugate **6** was adequate to allow bioassays in aqueous media. Also, it possessed good fluorescence properties, with absorption maxima at 456 nm and emission at 520 nm. These properties permitted in cellulose localization through confocal microscopy to further pursue the actin-vescalagin interaction studies.

Figure 69. Formation of vescalagin-fluorescein conjugate III**IVc. Hemisynthesis of vescalin-Fluorescein Conjugate**

The vescalagin (**10**) congener vescalin (**29a**) also demonstrated an interesting effect on actin. As part of the comparative structure-activity study between these ellagitannins and actin proteins, it was thus also of interest to construct a fluorescent vescalin conjugate. As discussed in Chapter II, the reactivity at C-1 of vescalagin (**10**) and vescalin (**29a**) is very similar. Vescalin (**29a**) was then allowed to react with compound **127** in THF-TFA (1.5%, v/v) solution at 50°C for 8 h to afford compound **130** in 39% yield after semi-preparative HPLC purification.

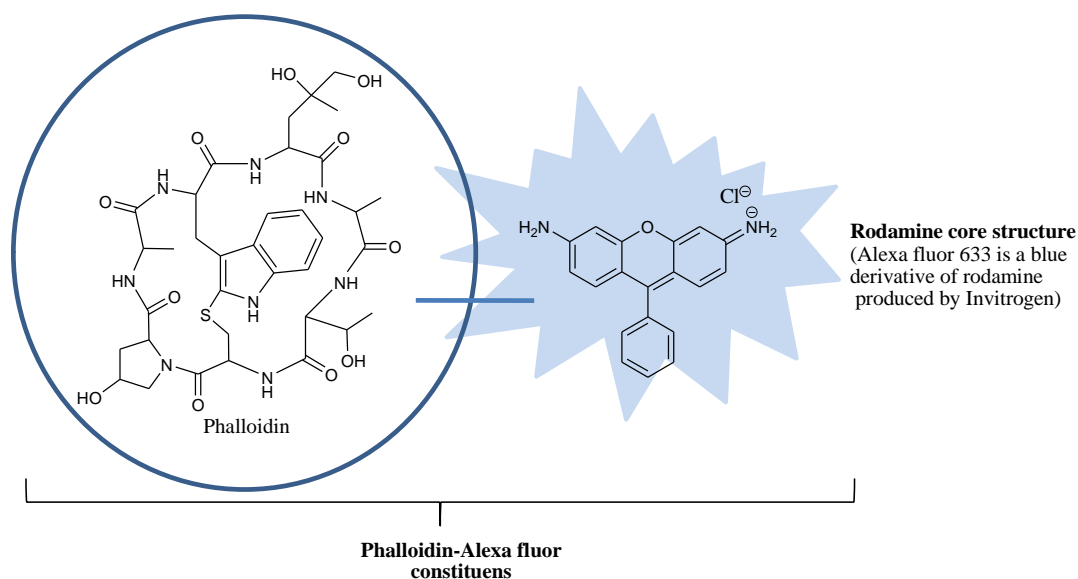
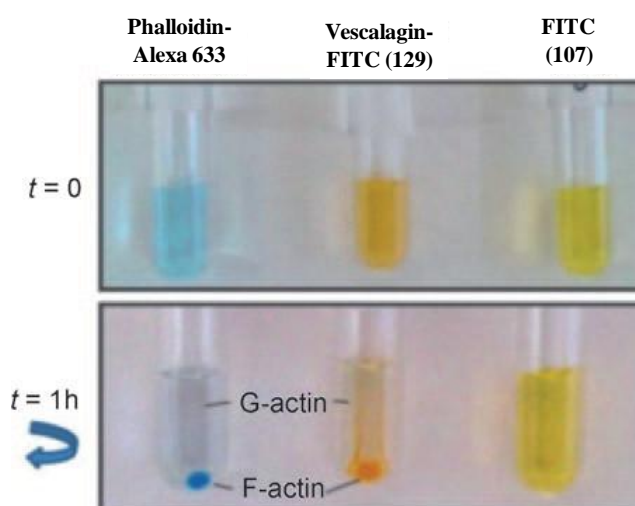
Scheme 42. Vescalin (**29a**) coupling with fluorescein derivative **127**

IVd. Actin-vescalagin interaction studies: application of vescalagin-fluorescein derivative **129**

Our collaboration with Elizabeth Génot's team led us to perform *in vitro* and *in cellulo* bioassays with vescalagin. These studies showed that this ellagitannin binds to fibrillar actin (F-actin) and winds these actin filaments into fibrillar aggregates. This effect disturbs the important functionalities of the actin network in eukaryotic cells (motility, adhesion, morphology). As discussed in the previous chapter, SPR experiments enabled us to collect evidence of this vescalagin-F-actin interaction. In this section, we will discuss the application of the vescalagin-fluorescein conjugate **6**, in the visualization of this effect *in vitro* and *in cellulo*.⁴⁶ The studies that concern the vescalin-actin interaction with the use of the vescalin-fluorescein conjugate **130** are underway.

IVd.1 *In vitro* assays

In the aim of visualizing the molecular association between vescalagin-fluorescein conjugate **129** and fibrillar actin, a polymerization assay from a globular actin solution in presence of **129** was performed under classical polymerization conditions.¹²⁶ As a control, the same experiment was performed in parallel in the presence of fluorescent phalloidin (phalloidin-Alexa633, Figure 70), a compound commonly used in the staining of F-actin filaments. After 30 min of incubation, both samples were spun at 48000 rpm (for 30 min), conditions that allow to separate the newly formed actin fibers as a pellet from the remaining G-actin still in the solution. As it can be observed in the Figure 71 (bottom, tube in the middle), the actin fibers that polymerized in presence of **129** furnished an orange pellet (same color as FITC derivative **129**), showing co-precipitation of F-actin and fluorescent vescalagin **129**. Similar results were obtained with the fibers that polymerized in the presence of blue phalloidin-Alexa fluor 633 (Figure 71 bottom, left tube). This evidences again a direct molecular interaction between vescalagin and F-actin.

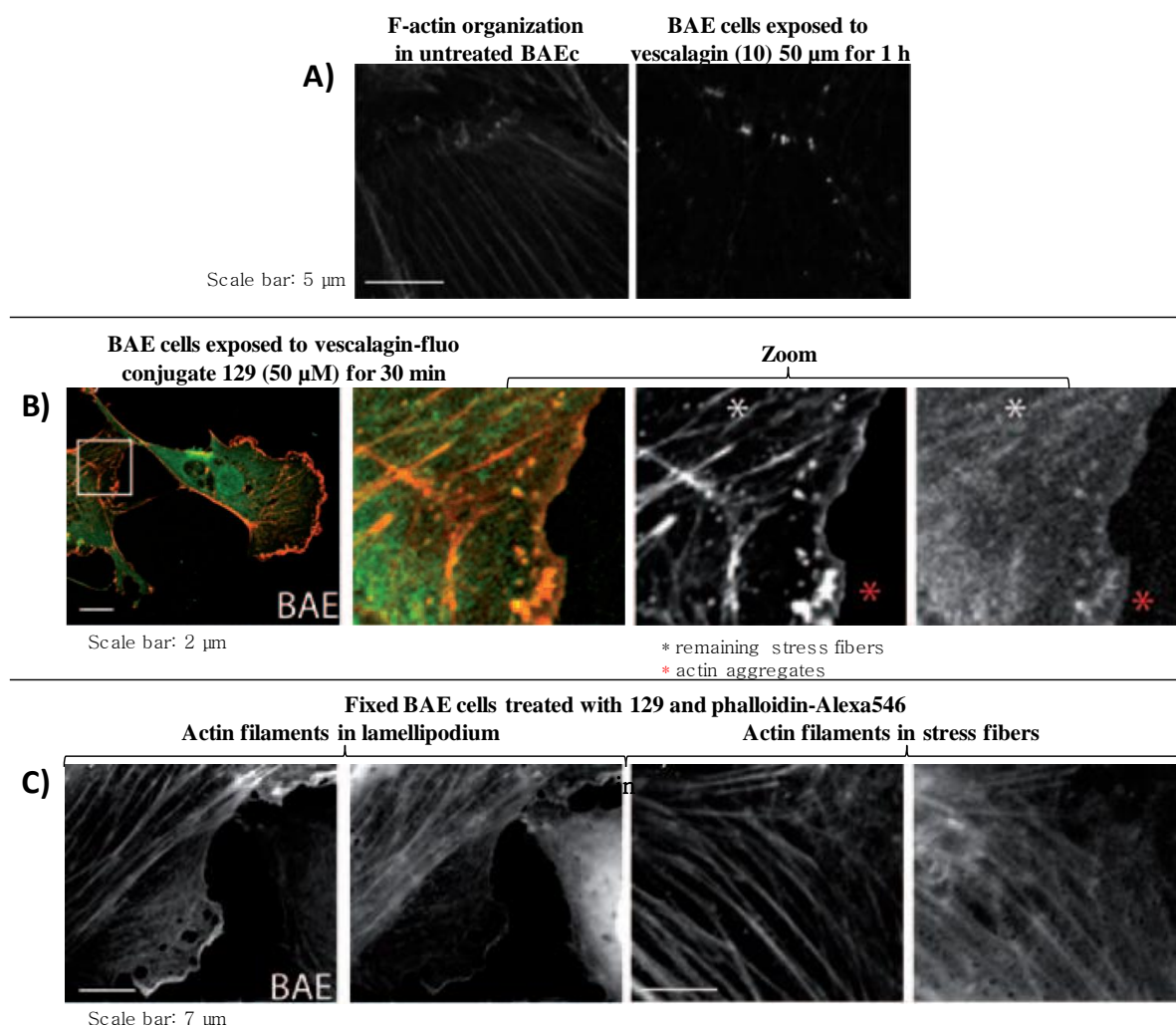
Figure 70. Structure of phalloidin and core structure of its fluorescent tag Alexa633**Figure 71.** F-actin polymerization in presence of phalloidin (blue, left), **129** (orange, middle) and FITC (orange, right)

IVd.2 *In cellulo* assays

In Figure 72A (left), is shown the F-actin organization in untreated living bovine aortic endothelial cells (BAEc, a representative model of the *in vivo* state) and the disturbances caused by vescalagin (**10**) at 50 μM on this F-actin organization (left). First, the effect of **129** on BAEc was compared to the effect of vescalagin (**10**) on the same cell type (Figure 72B, third from left to right). Both vescalagin (**10**) and **6** showed similar disturbance of the actin cytoskeleton. In order to visualize the effect of vescalagin in cellulo, BAEc were treated with vescalagin-fluorescein conjugate **129** at 50 μM for 30 min (Figure 72B). This experience

confirmed the penetration of **129** into BAEc plasma membrane as shown by the colocalization of compound **129** fluorescence with F-actin internal stress fibers and aggregates in the cells cytoskeleton (Figure 72B second and third figure).

Figure 72. Effect of vescalagin-fluorescent conjugate 129 over BAE cells (BAEc)



In order to better visualize the target, the experiment was repeated over fixed cells (Figure 72C); this makes the observation of the cell easier because they are not in constant movement. BAEc were treated with paraformaldehyde (action that kills the cells, which stops its movement) and after permeabilization of the cell membrane (with the use of MeOH) both fluorescent phalloidin-Alexa546 (known to bind F-actin)¹²⁶ and vescalagin conjugate **129** were added. This experience showed that when the actin-destabilization effect was “turned off” by fixation of the cell, **129** was shown to highlight the entire cytoskeleton of the cell, similar as to phalloidin-Alexa456. From this experience, we can conclude that vescalagin-fluorescein conjugate **129**, binds to actin fibers (F-actin) in cellulo.

IVe. Conclusions

Three new nucleophilic fluorescein derivatives were synthesized and coupled to vescalagin to furnish three new fluorescent vescalagin conjugates. Varying the nature of the linker and of the fluorescein derivative, one vescalagin-fluorescein conjugate (**129**) displayed appropriate solubility and fluorescent properties for confocal microscopy applications. The effect of this vescalagin-fluorescein conjugate (**129**) on actin proved useful in the elucidation of the nature of the vescalagin-actin intermolecular interaction, showing its pronounced preference for actin filaments (F-actin) through both in vitro and in cellulo bioassays. These findings were in accordance and are therefore complementary to the observations obtained from the SPR analysis of the vescalagin-F-actin molecular interaction.

The synthetic methodology that we developed was also validated for the vescalagin congener, vescalin which was similarly modified to obtain a fluorescent derivative (**130**).

General Conclusion

The SPR technique allows to analyze polyphenol-protein interactions in real time, while discriminating specific from non-specific interactions when the polyphenol is immobilized on to the SPR surface. For which, the polyphenol needs to be modified to introduce a linker with an anchoring function. Careful consideration is needed when choosing the position on the polyphenol skeleton to anchor this linker, because it can affect the affinity of the protein for the polyphenol. Four polyphenols were modified to bear a linker with a biotin anchoring function, which was the used to immobilize these polyphenols to a SPR surface by a biotin-streptavidin non-covalent but strong and stable interaction. The resulting polyphenol-bound SPR surfaces are stable during several weeks, which has the advantage of providing **surfaces that could be used in screening applications**. These systems can be used to compare qualitatively the affinity of one polyphenol for different proteins, and the affinity of different polyphenols for one protein, with up to three different polyphenols that may be tested in the same experience. The screening applications may be of interest in diverse fields like pharmacy, nutrition and cosmetics, for example. The polyphenol-bound SPR surface is thus a useful and complementary tool to the analytical techniques used nowadays in polyphenol-protein interaction studies, which in general share in common the knowledge of the identity of both the protein and the polyphenol implicated in the problematic under study, a condition that is not necessary for SPR analysis.

The transformations performed over five different polyphenols used in this work (vescalagin, vescalalin, catechin, epicatechin and B-2 procyanidin) are the result of the study of both the reactivity of polyphenol (towards chemical transformation) and its affinity with the proteins under study (positioning of the linker on the polyphenol skeleton). The synthetic approach used to install the biotin-ending-linker that allows the immobilization of the polyphenol on to streptavidin coated SPR surfaces, but could also be used for streptavidin affinity resins or nanobeads, for example. The same synthetic approach was used successfully for the installation of a fluorescent linker in the case of the *C*-glucosidic ellagitannins, which shows the versatility of functions that can be anchored in the same manner on to these polyphenols. More particularly, the vescalagin-fluorescein conjugate **129** prepared was useful in the study of certain aspects of in vitro vescalagin-actin interaction studies and moreover in the study of its biodisponibility in cellulo. The fluorescent studies, as well as, the SPR studies carried out for the vescalagin-actin system allowed to confirm that vescalagin is as an anti-actin agent, that **could be used in F-actin fluorescent tagging applications**, in cellulo for systems where the currently used F-actin fluorescent tags like phalloidin-Alexa derivatives, for example, show no effect.

Chapter V

Experimental Section



Va. Materials and methods

(-)-Vescalagin (**10**) was extracted from *Quercus robur* heartwood and purified as previously described^{147,148}. Commercially available reagents were obtained from Sigma-Aldrich or VWR and used as received unless otherwise noted. Fmoc-6-aminohexanoic acid (Fmoc-Ahx-OH) was purchased from Bachem. Amino PEGA resin and 2-(1*H*-Benzotriazole-1-yl)-1,1,3,3-tetramethylaminium hexafluorophosphate (HBTU) were purchased from Novabiochem. (+)-Catechin and (-)-epicatechin were purchased from Sigma Aldrich. All organic solvents for solid phase synthesis were of analytical quality. Solvents for solution phase reactions were either dispensed from a solvent purification system that passes solvents through packed columns of dry neutral alumina [dichloromethane (DCM)] or activated molecular sieves [dimethyl formamide (DMF), or purified by distillation from sodium/benzophenone [tetrahydrofuran (THF)] under N₂, or CaH₂ under Ar [dichloromethane (CH₂Cl₂)] immediately before use. Trifluoroacetic acid (TFA) from Sigma-Aldrich was of spectrophotometric grade (99%). HPLC-quality acetonitrile (CH₃CN) and MilliQ water were used for HPLC analyses and purification. Evaporations were conducted under reduced pressure at temperatures less than 40 °C unless otherwise noted. Reactions were monitored by analytical thin-layer chromatography using Merck silica gel 60 F254 plates. Compounds were visualized with an UV lamp (λ 254 nm) and staining with phosphomolibdenic acid solution in EtOH (10% v/v).

Vb. Purification and analysis

Purification

Flash chromatography was performed under positive pressure using 40-60 μ m silica gel (Merck) and the indicated solvents. RP-HPLC analyses were carried out on a Thermo Spectra system with P1000 XR pumps, an AS3000 autosampler and a UV 6000 LP diode array detector. The solvent systems and the type of column used are given for each compound in the synthetic procedures (Chapter V, Section Vc). Effluent was monitored by UV/Vis detection at 254 and 280 nm. Semi-preparative HPLC purifications were performed on a Varian ProStar system. The solvent system was A = 0.1% TFA in H₂O and B = 0.1% TFA in CH₃CN with SD-1 Dynamax® pumps at a flow rate of 17 mL.min⁻¹, and a Varian UV-Vis Prostar 325 diode array detector. Column effluent was monitored by UV/Vis detection at 254 nm, 230 and 442 nm. The columns used: Varian Microsorb RP-18 column (250 mm \times 21.5 mm, 5 μ m) or Macherey-Nagel NUCLEODOR C-18 Pyramid column (250 mm \times 10, 5 μ m) and solvent systems used, are specified in Chapter V, Section Vc for each compound.

NMR Analysis

^1H NMR spectra were recorded at 23 °C on a Bruker Avance II 300 MHz spectrometer or on a Bruker DPX 400 MHz spectrometer. Chemical shifts (δ) are reported in parts per million (ppm) and referenced to residual protons in the NMR solvent. Data are reported as follows: chemical shift, multiplicity (s = singlet, d = doublet, t = triplet, m = multiplet), coupling constant (J) in Hertz (Hz), and integration. ^{13}C NMR spectra were recorded at 23 °C on a Bruker Avance II 300 MHz spectrometer (75 MHz) or on a Bruker DPX spectrometer (100 MHz). Chemical shifts (δ) are reported in parts per million (ppm), referenced to carbon resonances in the NMR solvent. Carbon multiplicities were determined by DEPT135 experiments. Structural connectivities were determined by HMQC, HMBC and COSY experiments.

IR analysis

IR spectra were recorded with a FT-IR Bruker Equinox spectrometer (Zn/Se) or FT-IR Thermo Scientific Nicolet 6700 spectrometer (Ge).

Mass analysis

Electrospray ionization (ESI) mass spectrometric low- and high-resolution data (MS, HRMS) were obtained from the Mass Spectrometry Laboratory at the European Institute of Chemistry and Biology (IECB), Pessac, France.

Melting point

Melting points were obtained in open-ended capillary tubes with a Digital BÜCHI B-540 melting point apparatus.

Optical rotation

Optical rotations were recorded using a polarimeter KRÜSS P3001.

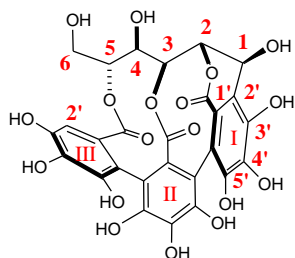
Fluorescence spectra

Fluorescence spectra were taken in a JASCO J-815 CD spectrometer with a 4 QS window Hellma, 10 × 10 mm cell.

UV-Vis spectra

UV-Vis spectra were recorded from analytical HPLC analysis detection, in the solvent composition given by elution of each compound.

Vc. Synthetic procedures

29a**(-)-Vescalin**

- CAS : 34112-28-2
- MM : 632.4
- EM : 632.0650
- MF : C₂₇H₂₀O₁₈

A solution of (-)-vescalagin (**10**, 41 mg, 0.044 mmol) in aqueous HCl 1M (20 mL), under Ar atmosphere, was allowed to stir at 60°C for 15 h (a white solid precipitates during the reaction). After this time HPLC monitoring indicated completion of the reaction. The solvent was evaporated under reduced pressure to give a light brown solid. This solid was purified by semi-preparative RP-HPLC (0-20 min: 0% to 20% MeOH/HCOOH 0.1%, column: Pyramid, flow rate: 1mL/min) to furnish, after lyophilization, **29a** (8.5 mg, 31%) as an off-white amorphous powder.

Retention time: 5.3 min.

Method: 0-20 min: 0% to 20% MeOH-HCOOH 0.1%.

Column: Macherey-Nagel Pyramid C-18 (4.6 × 250 mm, 5 μm).

Flow rate: 1mL/min.

Detection: 244 nm.

[α]_D = - 11.6°, 13.6 mM, H₂O (Lit.¹⁴⁹ - 15.2° 3M in H₂O).

¹H NMR (300 MHz, D₂O): δ 8.44 (s, O-H), 6.88 (s, H_{III}-2'), 5.41 (s, H-2), 5.12 (bs, H-5), 4.84 (s, H-1), 4.55 (d, *J* = 6.6, H-3), 3.95 (t, *J* = 7.4, H-4), 4.00-3.87 (m, H-6).

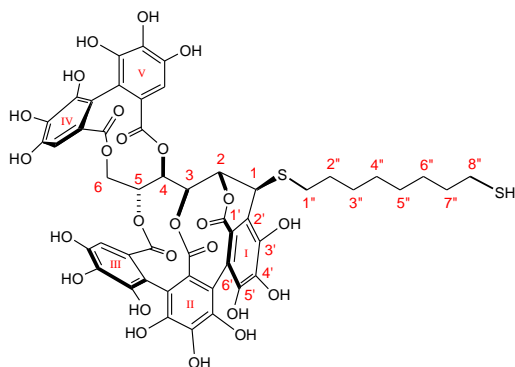
¹³C NMR (75 MHz, D₂O): δ 169.8 (C_I=O), 168.3, 168.2 (C_{III}=O, C_{II}=O), 148.9, 146.5, 145.7, 145.2, 145.1, 139.5 (2C), 137.2, 135.8 (C-3'I-III, C-4'I-III, C-5'I-III), 128.3, 126.3, 124.8 (C-1'I-III), 118.3, 116.7, 115.3, 114.5, 113.7, 110.0 (C-6'I-III, C-2'I-III), 77.5 (C-5), 75.7 (C-2), 72.2 (C-3), 69.1 (C-4), 65.5 (C-1), 62.3 (C-6).

IR (Ge): 3367, 1729, 1208, 1059 cm⁻¹.

UV/Vis: λ_{max} 244 nm.

MS (ESI) *m/z* (rel. intensity): 631 [M-H]⁻, (100).

(-)-Sulfhydryl thioether deoxyvescalagin



- New product
- MM : 1095.0
- EM : 1094.1457
- MF : C₄₉H₄₂O₂₅S₂

(-)-Vescalagin (**10**) (39 mg, 0.04 mmol) was dissolved with an anhydrous/degassed solution of THF-TFA (1.5%, v/v, 15 mL), under Ar atmosphere. To this solution 1,8-octanedithiol (76 μ L, 0.41 mmol) was added. The reaction mixture was heated to 55 °C and let under stirring for 6 h, after which time HPLC monitoring (0-25 min: 0% to 100% MeCN-TFA 0.1%) indicated quasi completion of the reaction. The reaction mixture was concentrated under vacuum to provide a residue, which was dissolved in water (20 mL). This aqueous solution was extracted with diethyl ether (3 \times 5 mL). The resulting aqueous phase was then lyophilized to furnish pure **52** as an off-white amorphous powder (34 mg, 78 %).

mp: 219 °C (decomp.).

Retention time: 14.9 min.

Method: 0-25 min: 0% to 100% MeCN-TFA 0.1%.

Column: Varian Microsorb C-18 (10 \times 250 mm, 5 μ m).

Flow rate: 1mL/min.

Detection: 252 nm and 312 nm.

[α]_D = - 23.6°, 0.4 mM, MeOH.

¹H NMR (300 MHz, MeOD-*d*₄): δ 6.76 (s, H-2'III), 6.64 (s, H-2'IV), 6.57 (s, H-2'V), 5.60 (d, *J* = 7.1, H-5), 5.26 (s, H-2), 5.17 (t, *J* = 7.2, H-4), 4.97 (dd, *J* = 2.2, 13.0, H-6a), 4.64 (d, *J* = 7.4, H-3), 4.30 (d, *J* = 1.6, H-1), 4.01 (d, *J* = 12.6, H-6b), 2.87 (t, *J* = 7.3, H-1''), 2.47 (t, *J* = 7.1, H-8''), 2.47 (t, *J* = 7.1, H-2''), 1.56 (q, *J* = 7.5, H-7''), 1.4 (m), 1.33 (bs) (H-3''-H-6'').

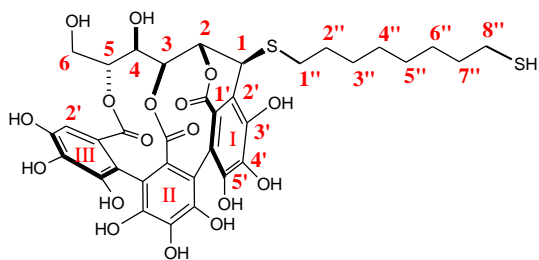
¹³C NMR (75 MHz, MeOD-*d*₄): δ 170.4 (C_V=O), 168.0 (C_{III}=O), 167.5 (C_{IV}=O), 166.6 (C_I=O), 166.0 (C_{II}=O), 148.0 (Cq), 146.3, 146.2, 146.1 (C-3'III-V), 145.3 (Cq), 145.1 (Cq), 145.0 (Cq), 144.9 (Cq), 144.6, 144.4 (Cq, C-3'I), 139.1 (C-4'I or II), 138.4 (C-4'IV), 137.6 (C-4'III), 137.0 (C-4'V), 136.1 (C-4'I or II), 128.0 (Cq), 127.0 (Cq), 125.3 (Cq), 124.9 (C-1'III), 124.5 (C-1'I), 117.9 (C-2'I), 117.2 (C-6'IV), 116.0 (Cq), 115.5 (C-6'V), 115.3, 115.2 (Cq, C-6'III), 114.0 (Cq), 109.4, 109.3 (C-2'III, C-2'IV), 108.0 (C-2'V), 77.6 (C-2), 71.8 (C-5), 71.4 (C-3), 70.5 (C-4), 66.1 (C-6), 44.1 (C-1), 35.2 (C-7''), 32.6 (C-1''), 30.8 (C-2''), 30.2, 30.0, 29.8, 29.3 (C-3'' - C-6''), 25.0 (C-8'').

IR (Zn/Se): 3365, 2925, 2857, 1735, 1313, 1176 cm⁻¹.

UV/Vis: λ_{max} 252 nm, $\lambda_{\text{max}2}$ 312 nm.

HRMS (ESI-TOF) *m/z*: [M+Na]⁺ calcd. C₄₉H₄₂O₂₅S₂Na, 1117.1354; found, 1117.1335.

(-)-Sulfhydryl thioether deoxyvescalin



- CAS : New product
- MM : 792,8
- EM : 792,1394
- MF : C₃₅H₃₆O₁₇S₂

(-)-Vescalin (**29a**, 11.3 mg, 0.018 mmol, from two hydrolysis of vescalagin) was dissolved in an anhydrous/degassed (Ar) solution of TFA in THF (12 mL, 1.5% v/v) and 1,8-octanedithiol (34 μ L, 0.18 mmol) was added. The reaction mixture was heated to 55 °C and let under stirring for 5 h, after which time HPLC monitoring (method A) indicated completion of the reaction. The reaction mixture was concentrated under vacuum to provide a pale yellow solid, which was dissolved in water (20 mL). This aqueous solution was extracted with diethyl ether (3 \times 5 mL). The resulting aqueous phase was then lyophilized to furnish pure **53** as an off-white amorphous powder (11.6 mg, 81 %)

Retention time: 6.6 min.

Method: 0-20 min: 0 to 20% MeOH-HCOOH 0.1%.

Column: Macherey-Nagel Pyramid C-18 (4.6 \times 250 mm, 5 μ m).

Flow rate: 1mL/min.

Detection: 236 nm.

$[\alpha]_D^{25} = +56.3^\circ$ (2.2 mM in MeCN-H₂O, 30/6, v/v).

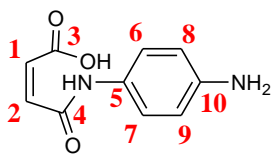
¹H NMR (300 MHz, MeCN-*d*₃/D₂O): δ 6.72 (s, H-2'III), 5.32 (s, H-2), 4.99 (bs, H-5), 4.46 (d, $J = 6.8$, H-3), 4.10 (s, H-1), 3.89-3.74 (m, H-4, H-6), 2.75-2.68 (m, H-1''), 2.45 (t, $J = 7.0$, H-8''), 1.60-1.25 (m, H-2''- H-8'').

¹³C NMR (75 MHz, MeCN-*d*₃/D₂O): δ 168.6, 166.8, 166.4 (C_{I-III}=O), 147.2, 145.7, 144.6, 144.3, 143.9, 136.1, 134.9, (C-3'I-III, C-4' I-III, C-5' I-III), 128.1, 126.1, 124.7 (C-1'I-III), 117.5, 115.8, 114.6, 113.7, 113.2 (C-6'I-III, C-2'II-III), 109.0 (C-2'I), 74.7 (C-5, C-2), 73.7 (C-3), 69.0 (C-4), 62.0 (C-6), 43.5 (C-1), 34.5 (C-7''), 32.2 (C-1''), 30.1, 29.6, 29.4, 29.3, 28.8 (C-2''- C-6''), 24.8 (C-8'').

IR (Ge): 3317, 2927, 2854, 1730, 1203, 1042 cm⁻¹.

UV/Vis: λ_{\max} 236 nm.

MS (ESI) m/z (rel. intensity): 791 [M-H]⁻, (100).

56**3-(4-aminophenylcarbamoyl)acrylic acid**

- CAS : 71603-06-0
- MM : 206.1
- EM : 206.0691
- MF : C₁₀H₁₀N₂O₃

To a solution of 1,4-phenylenediamine (2.17 g, 20.1 mmol) in 40 mL of THF was added dropwise over 1 h, a solution of maleic anhydride (2.00 g, 20.4 mmol) in 15 mL of THF. After 12 h, the resulting yellow precipitate was collected, washed with cold THF and dried to give the monomaleamidic acid derivative **56** (3.91 g, 94%) as a bright yellow solid.

mp: 162 °C (decomp.) (lit.⁷⁵ 163–162 °C, decomp.).

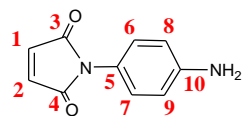
TLC (AcOEt - MeOH, 1:1, v/v): R_f = 0.7.

¹H NMR (300 MHz, DMSO-*d*₆): δ 10.5 (s, 1H), 7.30 (d, *J* = 8.7, H-6 - H-9), 6.54 (d, *J* = 8.7, H-6 - H-9), 6.48 (d, *J* = 12.4, H-1 or H-2), 6.28 (d, *J* = 12.3, H-1 or H-2).

¹³C NMR (75 MHz, DMSO-*d*₆): δ 166.1, 162.5 (C₃=O, C₄=O), 146.0 (Cq), 132.0, 131.9 (C-1, C-2), 126.8 (Cq), 121.5, 113.8 (C-6 - C-9).

IR (Zn/Se): 3800-2200, 1681, 1654, 1556 cm⁻¹.

MS (ESI) *m/z* (rel. intensity): 207 [M+H]⁺, (100).

57**1-(4-aminophenyl)-1H-pyrrole-2,5-dione**

- CAS : 29753-26-2
- MM : 188.2
- EM : 188.0586
- FM : C₁₀H₈N₂O₂

To a 10 mL microwave reaction vessel, containing a solution of **56** (25 mg, 0.12 mmol) in MeCN (5 mL) were added HOBt (19 mg, 0.14 mmol), HBTU (46 mg, 0.12 mmol) and DIEA (0.041 μ L, 0.24 mmol). The reaction mixture was then irradiated (50 W maximum power, 50 °C, 10 min ramp, hold 1 h) at atmospheric pressure. The mixture was rapidly cooled down to room temperature by passing compressed air through the microwave cavity. The resulting suspension was then filtered off at 0 °C and the filtrate was evaporated to dryness. The residue was purified by flash column chromatography on silica gel, eluting with CH₂Cl₂–EtOAc (7:3, v/v), to furnish **57** as red crystals (8.5 mg, 38%).

mp: 173-174 °C (Lit.⁷⁵ 172-173°C).

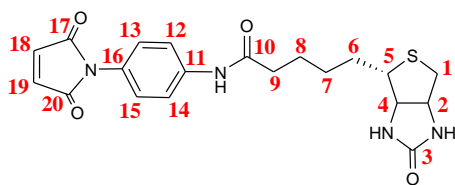
TLC (CH₂Cl₂:AcOEt, 7:3 v/v): R_f = 0.7.

¹H NMR (300 MHz, CDCl₃): δ 7.06 (dt, J = 2.6, 8.8, H-6 - H-9), 6.81 (s, H-1, H-2), 6.72 (dt, J = 2.6, 8.8, H-6 - H-9), 3.79 (s, NH₂).

¹³C NMR (75 MHz, CDCl₃): δ 170.2 (C₃=O, C₄=O), 146.6 (Cq), 134.2 (C-1, C-2), 127.7 (CH), 121.6 (Cq), 115.4 (CH).

IR (Zn/Se): 3358, 3046, 1708, 1518 cm⁻¹.

MS (ESI) m/z (rel. intensity): 189 [M+H]⁺, (100).



- CAS : 1312312-14-3
- MM : 414.5
- EM : 414.1362
- FM : C₂₀H₂₂N₄O₄S

Biotin (107 mg, 0.44 mmol) was dissolved in 0.7 mL of thionylchloride (under Ar atmosphere). The reaction mixture was stirred for 30 min, after which time the excess of SOCl₂ was evaporated under reduced pressure, and dried under vacuum. The residue was then dissolved in dry DMF (0.3 mL) and a solution of **57** (85 mg, 0.45 mmol) and Et₃N (62 μ L, 0.44 mmol) in dry DMF (1 mL) was added dropwise. The reaction mixture was stirred 30 min. After partial removal of the solvent under vacuum, the resulting residue was directly purified by semi-preparative HPLC (0-25 min: 0 to 50% MeCN/TFA 0.1%, Microsorb column, flow rate 17 mL/min) to furnish, after lyophilization, **59** (44 mg, 24%) as a pale yellow powder.

mp: 250–252 °C (lit.⁷⁵ 247–250 °C).

Retention time: 19.2 min.

Method: 0-25 min: 0 to 50% MeCN-TFA 0.1%.

Column: Varian Microsorb C-18 (10 \times 250 mm, 5 μ m).

Flow rate: 1mL/min.

Detection: 252 nm, 313 nm.

$[\alpha]_D$ = – 160.4°, 2.2 mM, DMSO.

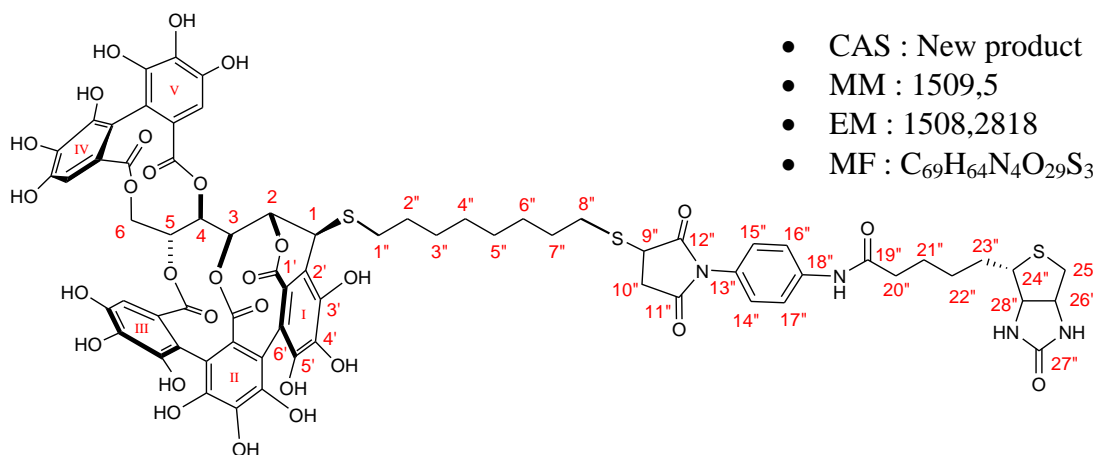
¹H NMR (300 MHz, DMSO-*d*₆): δ 10.03 (s, C₁₀-N-H), 7.67 (d, *J* = 8.8, H-12, H-14), 7.23 (d, *J* = 8.8, H-13, H-15), 7.16 (s, H-18, H-19), 6.44 (s, C₃-N-H), 6.36 (s, C₃-N-H), 4.33-4.29 (m, H-2), 4.16-4.12 (m, H-4), 3.16-3.10 (m, H-5), 2.83 (dd, *J* = 5.0, 12.4, H-1a), 2.55 (d, *J* = 12.4, H-1b), 2.33 (t, *J* = 7.3, H-9), 1.64-1.24 (m, H-6 - H-8).

¹³C NMR (75 MHz, DMSO-*d*₆): δ 171.4 (C₁₀=O), 170.1 (C-17, C-20), 162.7 (C₃=O), 138.8 (C-11), 134.6 (C-18, C-19), 127.3 (C-13, C-15), 126.1 (C-16), 119.2 (C-12, C-14), 61.0 (C-4), 59.2 (C-2), 55.4 (C-5), 39.8 (C-1), 36.2 (C-9), 28.2, 28.1 (C-6, C-7), 25.1 (C-8).

IR (Ge): 3418, 3295, 2940, 1704, 1531 cm⁻¹.

UV/Vis: $\lambda_{\max 1}$ 252 nm, $\lambda_{\max 2}$ 313 nm.

MS (ESI) *m/z* (rel. intensity): 415 [M+H]⁺, (100).



To a solution of **52** (27 mg, 0.025 mmol) in DMSO-*d*₆ (1mL), under Ar atmosphere, was added **59** (9.4 mg, 0.023 mmol). The mixture was stirred for 7 h, after which time ¹H NMR analysis indicated completion of the reaction. The desired reaction product was conveniently precipitated out of the reaction mixture using Et₂O-MeOH (20 mL, 3:1, v/v) to directly furnish pure **60** (36 mg, 95%) as an off-white solid.

mp: 186–188 °C.

Retention time : 10.64 min

Method: 0-5 min: 0 to 40% then 5-30 min: 40% MeCN-HCOOH 0.1%.

Column: Varian Microsorb C-18 (10 × 250 mm, 5μm).

Flow rate: 1mL/min.

[α]_D = − 97.6°, 0.8 mM, DMSO.

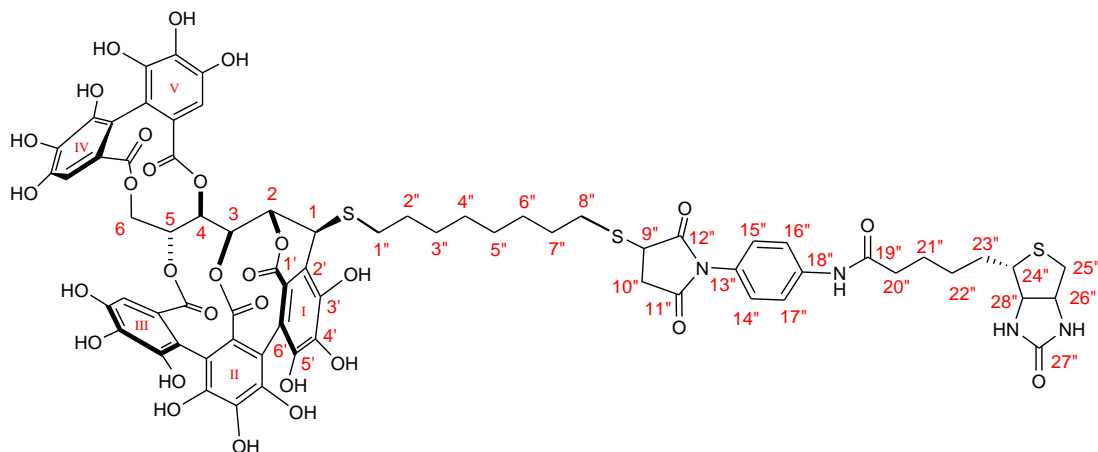
¹H NMR (300 MHz, DMSO-*d*₆): δ 10.05 (s, N-H), 7.68 (d, *J* = 8.8, H-16'', H-17''), 7.17 (d, *J* = 8.8, H-14'', H-15''), 6.51 (s, H-2''III), 6.43 (s, H-2''IV, 27''-N-H), 6.35 (s, H-2''V, 27''-N-H), 5.42 (d, *J* = 7.4, H-5), 4.99 (s, H-2), 4.92 (t, *J* = 7.1, H-4), 4.87 (d, *J* = 16.0, H-6), 4.47 (d, *J* = 7.4, H-3), 4.42 (s, H-1), 4.30 (m, H-26''), 4.14 (m, H-28''), 4.08 (dd, *J* = 4.1, 9.1, H-9''), 3.96 (d, *J* = 12.5, H-6), 3.3.14 - 3.09 (m, H-24''), 2.85-2.70 (m, H-1'', H-8'', H-25a''), 2.65 (dd, *J* = 4.0, 18.3, H-10''), 2.58 (d, *J* = 12.5, H-25b''), 2.33 (t, *J* = 7.2, H-20''), 1.64-1.28 (m, H-2''-H-7'').

¹³C NMR (100 MHz, DMSO-*d*₆): δ 176.1, 174.5 (C₁₁''=O, C₁₂''=O), 171.5 (C₁₉''=O), 168.2 (C_V=O), 165.9 (C_{III}=O), 165.7 (C_{IV}=O), 165.1 (C_{II}=O), 163.1 (C_I=O), 162.8 (C₂₇''=O), 147.1, 144.9, 144.8, 144.7 (C-3''II or C-5''I-V), 144.5, 144.4 (C-3''III-V), 144.1, 143.6 (C-3''II or C-5''I-V), 142.5 (C-3''I), 139.3 (C-13''), 137.0 (C-4''I or II), 136.1 (C-4''IV), 135.5 (C-4''III), 134.8 (C-4''V), 133.2 (C-4''I or II), 127.4 (C-14'', C-15''), 126.9 (C-18''), 125.9, 125.0 (C-1''II-V), 123.8 (C-1''I), 123.4, 123.3 (C-1''II-V), 119.3 (C-16'', C-17''), 115.6 (C-6''IV), 115.5 (C-2''I), 114.4 (C-2''II or C-6''I-II), 114.2 (C-6''III), 114.1 (C-6''V), 111.7 (C-2''II, C-6''I-II), 107.2 (C-2''IV), 106.6 (C-2''III), 105.2 (C-2''V), 74.6 (C-2), 69.8 (C-5), 69.5 (C-3), 68.4 (C-4), 64.5 (C-6), 61.1 (C-28''), 59.2 (C-26''), 55.4 (C-24''), 42.4 (C-1), 40.0 (C-25''), 39.7 (C-9''), 36.2 (C-10'', C-20''), 30.9 (C-1''), 30.7 (C-8''), 29.1, 28.7 (2C), 28.6, 28.4, 28.3, 28.1, 25.1 (C-2'' - C-7'', C-21'' - C-23'').

IR (Ge): 3728, 3702, 3625, 3598, 3203, 1748, 1168, 1022 cm⁻¹.

UV/Vis: λ_{max} 242 nm.

HRMS (ESI-TOF) *m/z*: [M+H]⁺ calcd. for C₆₉H₆₅N₄O₂₉S₃ 1509.2897, found 1509.2955.



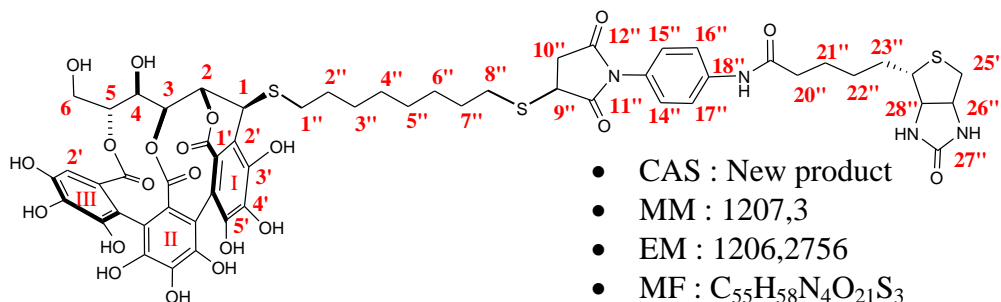
NMR signal assignments of vescalagin-biotin conjugate

Position	δ_H (mult., J in Hz)	δ_C (mult.)	HMQC ^a	HMBC ^b
Vescalagin moiety				
Glucose ^[7,8]				
1	4.42 (s)	42.4	C-1	C-1', C-2', C-3', C-1'' H-2, H-3, H-1''
2	4.99 (s)	74.6	C-2	C-4, C-2', C _I =O H-4
3	4.47 (d, 7.4)	69.5	C-3	C-5, C _{II} =O
4	4.92 (t, 6.9)	68.4	C-4	C-2, C-5, C _V =O H-2
5	5.42 (d, 7.4)	69.8	C-5	C _{III} =O H-3, H-4
6	3.96 (d, 12.5) 4.87 (d, 16.0)	64.5	C-6	
Aromatics ^[7,8]				
1' _I	-	123.8	-	H-1
1' [III-V]	-	125.9, 125.0, 123.4, 123.3	-	-
2' [I-III] and 6' [III]	-	114.3, 114.4, 115.5, 111.7	-	H-1, H-2
2' _{III}	6.51 (s)	106.6	C-2' _{III}	C-3' _{III} , C-4' _{III} , C-6' _{III} , C _{III} =O
2' _{IV}	6.43 (s)	107.2	C-2' _{IV}	C-3' _{IV} , C-4' _{IV} , C-6' _{IV} , C _{IV} =O
2' _V	6.35 (s)	105.2	C-2' _V	C-3' _V , C-4' _V , C-6' _V , C _V =O
3' _I	-	142.5	-	H-1
3' [III-V]	-	144.5, 144.4 (2C)	-	-
3' _{II} and 5' [I-V]	-	147.1, 144.9, 144.8, 144.7, 144.1, 143.6	-	-
4' [I-III]	-	137.0, 133.2, 136.1	-	-
4' _{III}	-	135.5	-	H-2' _{III}
4' _{IV}	-	136.1	-	H-2' _{IV}
4' _V	-	134.8	-	H-2' _V
6' _{III}	-	114.2	-	H-2' _{III}
6' _{IV}	-	115.6	-	H-2' _{IV}
6' _V	-	114.1	-	H-2' _V
Carbonyls				
C _I =O	-	163.1	-	H-2

Chapter V: Experimental section

C _{II} =O	-	165.1	-	H-3
C _{III} =O	-	165.9	-	H-2' _{III} , H-5
C _{IV} =O	-	165.7	-	H-2' _{IV} , H-4
C _V =O	-	168.2	-	H-2' _V
Biotin maleimide moiety				
9''	4.08 (dd, 4.1, 9.8)	39.7	C-9''	C-8'', C-10'' - C-12'' H-8'', H-10'' H-9''
10''	2.65 (d, 4.0, 18.3)	36.2	C-10''	C11'', C-12''
11'' - 12''	-	176.1, 174.5	-	H-9'', H-10''
13''	-	126.9	-	H-14'' - H-17''
14'' - 15''	7.17 (d, 8.8)	127.4	C-14'', 15''	C-13'' - C-15'', C-18'' H-14'', H-15''
16'' - 17''	7.68 (d, 8.8)	119.3	C-16'', 17''	C-13'', C-16'' - C-18'' H-16'', H-17''
18''	-	139.3	-	H-16'', H-17''
19''	-	171.5	-	H-20''
20''	2.33 (t, 7.2)	36.2	C-20''	C-19''
21'' - 23''	1.64 - 1.28 (m)	29.1, 28.7 (2C), 28.6, 28.4, 28.3, 28.1, 25.1	C-21'' - 23''	H-21'' - 23''
24''	3.14 (m)	55.4	C-24''	H-28'', H-26''
25''	2.58 (d, 12.5) 2.83 (d, 16.0)	40.0	C-25''	C-24'', C-26'', C-28'' H-26'', H-28''
26''	4.30 (m)	59.2	C-26''	H-25'', NH
27''	-	162.8	-	H-26'', NH
28''	4.14 (m)	61.1	C-28''	H-25'', NH
Linker moiety				
1'', 8''	2.85-2.70 (m)	30.9 30.7	C-1'' C-8''	H-1 H-9'', C-9''
2'' - 7''	1.64 - 1.28 (m)	29.1, 28.7 (2C), 28.6, 28.4, 28.3, 28.1, 25.1	C-2'' - 7''	H-2'' - 7''
Amides (NH)				
NH	10.05 (s)	-	-	C-16'', C-17'', C ₁₉ =O
NH	6.43 (s) 6.45 (s)	-	-	C ₂₇ =O, C-26'', C-28''

^aCarbons directly bonded to the protons resonating at the ppm value indicated in the δ_{H} column. ^bCarbons are two, three, or even four bonds away from the protons indicated in the left column.



To a solution of **53** (8.1 mg, 0.01 mmol) in DMSO-*d*₆ (0.6 mL), under Ar atmosphere, was added **59** (3.9 mg, 0.01 mmol). The mixture was shaken for 30 min, after which time ¹H NMR analysis indicated completion of the reaction. The desired product was conveniently precipitated out of the reaction mixture using Et₂O-MeOH (40 mL, 8:1, v/v) to directly furnish pure **61** (11 mg, 92%) as a brown amorphous powder.

Retention time : 24.3 min

Method: 0-25min: 0 to 50% then 25-30min: 50% to 100% MeCN-HCOOH 0.1%.

Column: Varian Microsorb C-18 (10 × 250 mm, 5μm).

Flow rate: 1mL/min.

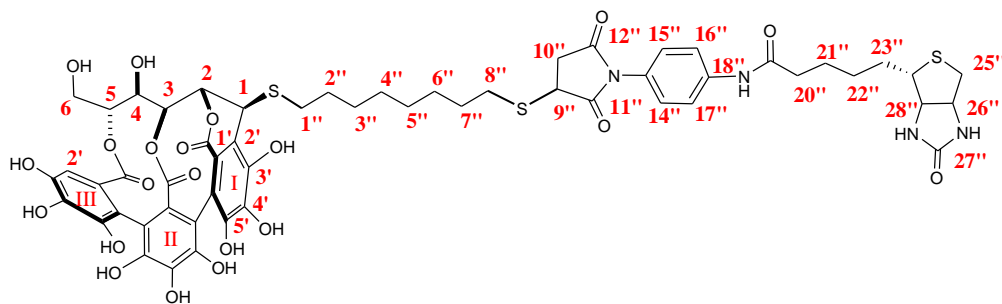
¹H NMR (400 MHz, DMSO-*d*₆): δ 10.07 (s, C₁₉"-N-H), 7.69 (d, *J* = 8.7, H-16", H-17"), 7.17 (d, *J* = 8.7, H-14", H-15"), 6.53 (s, H-2'III), 6.44 (s, C₂₇"-N-H), 6.36 (s, C₂₇"-N-H), 5.14 (s, H-2), 4.92 (td, *J* = 2.8, 7.8, H-5), 4.32-4.29 (m, H-26"), 4.21 (d, *J* = 7.0, H-3), 4.16-4.13 (m, H-28"), 4.08 (dd, *J* = 4.0, 9.0, H-9"), 4.06 (bs, H-1), 3.74-3.65 (m, H-6), 3.67 (t, *J* = 7.4, H-4), 3.55-3.50 (m, H-6), 3.33 (dd, *J* = 9.1, 18.2, H-10a"), 3.15-3.10 (m, H-24"), 2.82 (dd, *J* = 5.1, 12.4, H-25"), 2.75-2.63 (m, H-1", H-8", H-10b"), 2.58 (d, *J* = 12.5, H-25"), 2.33 (t, *J* = 7.0, H-20"), 1.59-1.12 (m, H-2" - H-7", H-21" - 23").

¹³C NMR (100 MHz, DMSO-*d*₆): δ 176.1, 174.5 (C₁₁"=O, C₁₂"=O), 171.4 (C₁₉"=O), 166.4 (C_{III}=O), 165.7 (C_{II}=O), 163.4 (C_I=O), 162.7 (C₂₇"=O), 147.1 (Cq), 144.9 (Cq), 144.2 (C-3'III), 143.3 (Cq), 142.5 (C-3'I), 139.3 (C-18"), 136.5 (Cq), 134.8 (C-4'III), 133.2 (Cq), 127.3 (C-14", C-15"), 126.8, 126.4 (Cq, C-13"), 124.8 (Cq), 124.0 (C-1'I), 119.3 (C-16", C-17"), 115.3 (C-2'I), 114.4 (Cq), 114.0 (Cq), 113.8 (C-6'III), 111.9 (Cq), 106.7 (C-2'III), 73.1 (C-2, C-5), 72.1 (C-3), 68.4 (C-4), 61.1 (C-28"), 60.9 (C-6), 59.2 (C-26"), 55.4 (C-24"), 42.8 (C-1), 39.8 (C-25"), 39.6 (C-9"), 36.2 (C-10", C-20"), 30.9, 30.6 (C-1", C-8"), 29.3, 28.6, 28.5, 28.3, 28.2 (2C), 28.1, 27.8 (C-2"- C-7", C-22"- C-23"), 25.1 (C-21").

IR (Ge): 3338, 1708, 1199, 1023 cm⁻¹.

UV/Vis: λ_{max} 238 nm.

HRMS (ESI-TOF) *m/z*: [M+Na]⁺ calcd. for C₅₅H₅₈N₄O₂₁S₃Na 1229.2682, found 1229.2653.



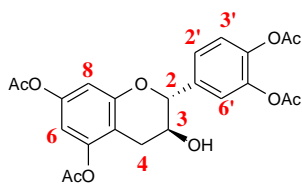
NMR signal assignments of vescalin-biotin conjugate

position	δ_{H} (mult., J in Hz)	δ_{C} (mult.)	HSQC ^a	HMBC ^b
Vescalin moiety				
Glucose				
1	4.06 (bs)	42.8	C-1	C-1', C-2', C-3', C-1'' H-2, H-3
2	5.14 (s)	73.1	C-2	C-1, C-4, C-2', C _I =O H-3
3	4.21 (d, 7.0)	72.1	C-3	C-1, C-2, C _{II} =O
4	3.67 (t, 7.4)	68.4	C-4	C-5 H-2
5	4.92 (td, 2.8, 7.8)	73.1	C-5	H-4
6	3.55-3.50 (m) 3.74-3.65 (m)	60.9	C-6	-
Aromatics				
1' _I	-	124.0	-	H-1
1' _[II-III]	-	126.8 or 126.4 and 124.8	-	-
2' _I	-	115.3	-	H-1, H-2
2' _{II} and 6' _[I-II]	-	114.4, 114.0, 111.9	-	-
2' _{III}	6.53 (s)	106.7	C-2' _{III}	C-3' _{III} , C-4' _{III} , C-6' _{III} , C _{III} =O
3' _I	-	142.5	-	H-1
3' _{II} , 4' _I , 4' _{II} , 5' _[I-III]	-	147.1, 144.9, 144.2, 143.3, 136.5, 133.2	-	-
3' _{III}	-	144.2	-	H-2' _{III}
4' _{III}	-	134.8	-	H-2' _{III}
6' _{III}	-	113.8	-	H-2' _{III}
Carbonyls				
C _I =O	-	163.4	-	H-2
C _{II} =O	-	165.7	-	H-3
C _{III} =O	-	166.4	-	H-2' _{III}
Biotin maleimide moiety				
9''	4.08 (dd, 4.0, 9.0)	39.6	C-9''	C-1'', C-8'', C-10'' - C-12'' H-10''
10''	2.75-2.63 (m) 3.33 (dd, 9.1, 18.2)	36.2	C-10''	C11'', C-12'' H-9''
11'' - 12''	-	176.1, 174.5	-	H-9'', H-10''
13''	-	126.8 or 126.4	-	H-16'', H-17''
14'' - 15''	7.17 (d, 8.7)	127.3	C-14'', 15''	C-18'', C-14'', C-15'' H-14'', H-15''

Chapter V: Experimental section

16'' - 17''	7.69 (d, 8.7)	119.3	C-16'', 17''	C-13'', C-16''- C-18'' H-16'', H-17''
18''	-	139.3	-	H-14'' - H-17''
19''	-	171.4	-	H-20''
20''	2.33 (t, 7.0)	36.2	C-20''	-
21'' - 23''	1.59-1.12 (m)	29.3, 28.6, 28.5, 28.3, 28.2 (2C), 28.1, 27.8, 25.1	C-21''- 23''	H-21''- 23''
24''	3.15-3.10 (m)	55.4	C-24''	H-28'', H-26'', H-25''
25''	2.58 (d, 12.5) 2.82 (dd, 5.1, 12.4)	39.8	C-25''	H-28'', H-26''
26''	4.32-4.29 (m)	59.2	C-26''	H-25'', NH (27'')
27''	-	162.7	-	H-26'', N-H (27'')
28''	4.16-4.13 (m)	61.1	C-28''	H-25'', NH (27'')
Linker moiety				
1'', 8''	2.75-2.63 (m)	30.9, 30.6	C-1'', C-8''	H-9'', H-1
2'' - 7''	1.59-1.12 (m)	29.3, 28.6, 28.5, 28.3, 28.2 (2C), 28.1, 27.8, 25.1	C-2'' - 7''	H-2'' - 7''
Amides (NH)				
19''-NH	10.07 (s)	-	-	-
27''-NH	6.44 (s) 6.36 (s)	-	-	C _{27''} =O, C-26'', C-28''

^aCarbons directly bonded to the protons resonating at the ppm value indicated in the δ_{H} column. ^bCarbons are two, three, or even four bonds away from the protons indicated in the left column.

65**5, 7, 4', 5'-O-acetyl catechin**

- CAS : 20728-86-3
- MM : 458,4
- ME : 458,1213
- FM : C₂₃H₂₂O₁₀

(+)-catechin (329 mg, 1.13 mmol) was dissolved with 6 mL of *i*-propanol (under Ar atmosphere). After cooling at 0°C, NaOH (549 mg, 13.7 mmol) was added followed by dropwise addition of H₂O (1 mL). The heterogeneous mixture was allowed to stir at room temperature for 30 min, then Ac₂O (1.3 mL, 13.7 mmols) was added dropwise at 0°C. The mixture was stirred at room temperature for 9 h, after which time TLC monitoring indicated completion of the reaction. The mixture was diluted with cold H₂O (20 mL) and the *i*-propanol was evaporated under reduced pressure. The resulting aqueous layer was extracted with CH₂Cl₂ (10 mL × 3) and the joined organic layers were extracted with brine (10 mL × 2) and dried over Na₂SO₄. The solvent was evaporated under reduced pressure to give a foamy off-white solid. This solid was purified by silica gel column chromatography eluting with pure Et₂O, to afford **65** as a white solid (316 mg, 61%).

mp: 84-87 °C.

TLC (Et₂O): R_f = 0.6.

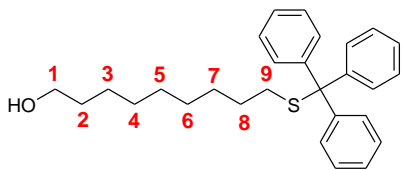
¹H NMR (300MHz, Acetone-*d*₆) δ 7.38 (dd, *J* = 1.9, 8.6, H-2'), 7.33 (d, *J* = 2.0, H-6'), 7.25 (d, *J* = 8.3, H-3'), 6.58 (d, *J* = 2.2, H-6 or H-8), 6.56 (d, *J* = 2.3, H-6 or H-8), 4.85 (d, *J* = 8.2, H-2), 4.54 (d, *J* = 5.3, O-H), 4.14 - 4.05 (m, H-3), 2.92 (dd, *J* = 5.5, 16.4, H-4), 2.61 (dd, *J* = 9.0, 16.4, H-4), 2.30 (s, OAc), 2.27 (bs, OAc), 2.23 (s, OAc).

¹³C NMR (75 MHz, Acetone-*d*₆) δ 169.4 (C=O), 169.0 (C=O), 168.7 (2C=O), 156.0 (Cq), 150.8 (Cq), 150.7 (Cq), 143.3 (Cq), 143.2 (Cq), 138.5 (Cq), 126.4, 124.1, 123.3 (C-2', C-3', C-6'), 113.1 (Cq), 109.5, 108.2 (C-6, C-8), 82.3 (C-2), 67.3 (C-3), 29.5 (C-4), 20.9 (CH₃, OAc), 20.6 (CH₃, OAc), 20.5 (CH₃, OAc), 20.5 (CH₃, OAc).

IR (Zn/Se): 3500, 3064, 2937, 1729, 1260, 1206 cm⁻¹.

UV/Vis: λ_{max1} 264 nm, λ_{max2} 280 nm.

MS (ESI) *m/z* (rel. intensity): 481 [M+Na]⁺, (100).

63**9-(tritylthio)nonan-1-ol**

- CAS : New product
- MM : 418.6
- EM : 418.2330
- MF : C₂₈H₃₄OS

To a solution of tritylchloride (Trt-Cl) (742 mg, 2.7 mmol) in dry CH₂Cl₂ (5 mL), under Ar, were added Et₃N (371 μ L, 2.7 mmol) and 9-mercaptonona-1-ol (500 μ L, 2.7 mmol). The reaction mixture was stirred overnight, after which time, the reaction mixture was washed with brine (5 mL \times 3). The organic layer was then dried with Na₂SO₄ and concentrated under reduced pressure to give a colorless oil. This colorless oil was purified by silica gel chromatography eluting with CHCl₃-MeOH (98:2, v/v), to furnish **63** as a white solid (870 mg, 78%).

m.p: 37-38 °C.

TLC (CH₂Cl₂-MeOH, 98:2 v/v): R_f = 0.5.

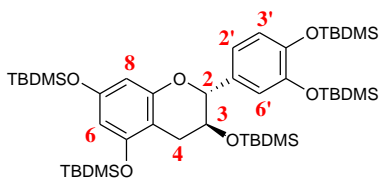
¹H NMR (300MHz, CDCl₃) δ 7.43-7.39 (m, C-H, Trt), 7.30-7.17 (m, C-H, Trt), 3.63 (t, *J* = 6.6, H-1), 2.13 (t, *J* = 7.3, H-9), 1.57-1.17 (m, H-2-H-8).

¹³C NMR (75MHz, CDCl₃) δ 145.2 (Cq), 129.7 (CH), 127.9 (CH), 126.6 (CH), 66.5 (QC), 63.1 (C-1), 32.9, 32.1, 29.4, 29.2, 29.1, 28.7, 25.8 (C-2-C-8);

IR (Zn/Se): 3333, 2928, 700 cm⁻¹.

UV-Vis: λ_{max} 250 nm.

HRMS (ESI-TOF) *m/z*: [M+Na]⁺ calcd. for C₂₈H₃₄NONaS, 441.2228; found, 441.2219.

66a**per-O-TBDMS catechin**

- CAS : 1174718-36-5
- MM : 861,6
- EM : 860,5114
- MF : C₄₅H₈₄O₆Si₅

(+)-catechin (418 mg, 1.44 mmol) was dissolved with 10 mL of DMF (dry, distilled), under Ar atmosphere. To this solution, imidazole (686 mg, 10 mmol) and tertbutyldimethylsilyl chloride (TBDMSCl) (1.5 g, 10 mmol) were added. The reaction mixture was stirred for 18h after which time TLC monitoring indicated quasi completion of the reaction. The mixture was diluted with Et₂O (30 mL) and extracted with H₂O (10 mL × 3) and brine (10 mL). The organic layer was dried over Na₂SO₄ and the solvent evaporated under reduced pressure, to give a yellow oil. This oil was purified by silica gel column chromatography with cyclohexane-AcOEt (95:5, v/v), to afford **66a** as a white solid (1.15 g, 93%).

mp: 121-122°C (Lit.⁷⁶ 121-122°C).

[α]_D = +19.5°, 8.3 mM, acetone.

TLC (Cyclohexane-CH₂Cl₂, 1:1 v/v): R_f = 0.7.

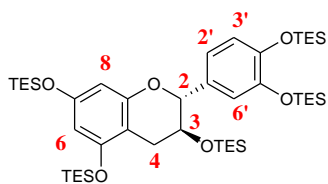
¹H NMR (300MHz, Acetone-*d*₆) δ 6.97 (bs), 6.91 (2bs, H-2', H-3', H-6'), 6.03 (d, *J* = 2.3, H-6), 6.01 (d, *J* = 2.3, H-8), 4.57 (d, *J* = 8.3, H-2), 3.99 (td, *J* = 5.6, 8.7, H-3), 3.01 (dd, *J* = 5.7, 16.1, H-4), 2.55 (dd, *J* = 9.0, 16.0, H-4), 1.04 (s, Ar-O-TBDMS), 1.02 (s, Ar-O-TBDMS), 1.01 (s, Ar-O-TBDMS), 0.98 (s, Ar-O-TBDMS), 0.79 (s, C3-O-TBDMS), 0.27-0.22 (s, O-TBDMS), 0.02 (s, C3-O-TBDMS), 0.24 (s, C3-O-TBDMS).

¹³C NMR (300MHz, Acetone-*d*₆) δ 156.8 (Cq), 155.8 (Cq), 155.2 (Cq), 147.3 (2Cq), 134.0 (Cq), 121.8, 121.6, 121.2 (C-2', C-3', C-6'), 106.6 (Cq), 104.3, 102.0 (C-6, C-8), 82.4 (C-2), 70.2 (C-3), 31.6 (C-4), 26.4, 26.2, 26.1 (3C), 19.1, 18.8 (2C), 18.7, 18.5, -2.7, -3.7 (2C), -3.8, -3.9, -4.0, -4.1, -4.2, -4.5, -4.9 (O-TBDMS).

IR (Zn/Se): 1255, 1004, 837 cm⁻¹.

UV/Vis: λ_{max1} 247 nm, λ_{max2} 274 nm.

MS (ESI) *m/z* (rel. intensity): 861 [M+H]⁺, (30) and 1744 [M+H]⁺, (100).

66b**per-O-TES catechin**

- CAS : New product
- MM : 861,6
- EM : 860,5114
- MF : C₄₅H₈₄O₆Si₅

(+)-catechin (674 mg, 2.3 mmol) was dissolved with 22 mL of DMF (dry, distilled), under Ar atmosphere. To this solution imidazol (1.09 g, 16.0 mmol) and triethylsilyl triflate (TESOTf) (3.64 mL, 16.1 mmol) were added. The reaction mixture was stirred for 4h, after which time TLC monitoring indicated completion of the reaction. The mixture was diluted with Et₂O (85 mL) and extracted with H₂O (10 mL × 3) and brine (10 mL). The organic layer was dried over Na₂SO₄ and the solvent evaporated under reduced pressure to give a yellow oily residue. This residue was purified by silica gel column chromatography with cyclohexane-AcOEt (95:5, v/v), to afford **66b** as a pale yellow oil (1.23 g, 62%).

TLC (Cyclohexane-AcOEt (95:5, v/v)): R_f = 0.3.

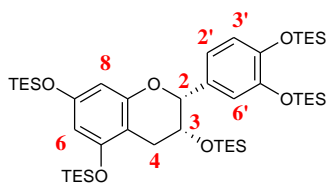
¹H NMR (300MHz, Acetone-*d*₆) δ 6.94 (d, J = 1.2, H-6'), 6.89, 6.88 (2bs, H-2', H-3'), 6.05 (d, J = 2.3, H-6), 6.03 (d, J = 2.3, H-8), 4.61 (d, J = 7.9, H-2), 4.00 (td, J = 5.4, H-3), 2.97 (dd, J = 5.5, 16.1, H-4), 2.58 (dd, J = 8.6, 16.1, H-4), 1.07-0.72 (m, O-TES), 0.57-0.36 (m, C3-O-TES).

¹³C NMR (75 MHz, Acetone-*d*₆) δ 156.8 (Cq), 155.8 (Cq), 155.4 (Cq), 147.3 (Cq), 147.2 (Cq), 134.0 (Cq), 121.6, 120.9, 120.3 (C-2', C-3', C-6'), 106.4 (Cq), 104.0, 101.8 (C-6, C-8), 82.4 (C-2), 69.9 (C-3), 30.9 (C-4), 7.1, 7.0 (3C), 6.0, 5.8, 5.7, 5.6, 5.4 (C-O-TES).

IR (Zn/Se): 1004, 745 cm⁻¹.

UV/Vis: λ_{max1} 246 nm, λ_{max2} 273 nm.

HRMS (ESI-TOF) *m/z*: [M+Na]⁺ calcd. for C₄₅H₈₄O₆NaSi₅, 883.5006; found, 883.5046.

66c**per-O-TES epicatechin**

- CAS : New product
- MM : 861,6
- EM : 860,5114
- MF : C₄₅H₈₄O₆Si₅

(–)-epicatechin (504 mg, 1.7 mmol) was dissolved with 16 mL of DMF (dry, distilled), under Ar atmosphere. To this solution imidazol (830 g, 12.2 mmol) and triethylsilyl triflate (TESOTf, 2.75 mL, 12.2 mmol) were added. The reaction mixture was stirred for 4h, after which time TLC monitoring indicated completion of the reaction. The mixture was diluted with Et₂O (60 mL) and extracted with H₂O (15 mL × 3) and brine (15 mL). The organic layer was dried over Na₂SO₄ and the solvent evaporated under reduced pressure to give a yellow oily residue. This residue was purified by silica gel column chromatography with cyclohexane-AcOEt (98:2, v/v), to afford **66c** as a colorless oil (1.19 g, 82%).

TLC (Cyclohexane-AcOEt (95:5, v/v): R_f = 0.7.

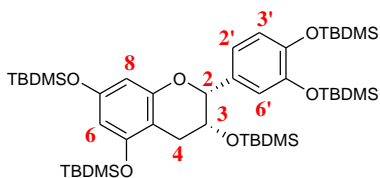
¹H NMR (300MHz, Acetone-*d*₆) δ 7.02 (d, J = 2.0, H-6'), 6.94 (dd, J = 1.8, 8.3, H-2'), 6.84 (d, J = 8.2, H-3'), 6.09 (d, J = 2.3, H-6), 6.02 (d, J = 2.3, H-8), 4.99 (s, H-2), 4.35 (td, J = 2.0, 4.2, H-3), 2.89 (dd, J = 4.0, 16.4, H-4), 2.73 (dd, J = 4.2, 16.5, H-4), 1.06-0.75 (m, O-TES), 0.53-0.39 (m, C3-O-TES).

¹³C NMR (75 MHz, Acetone-*d*₆) δ 156.9 (Cq), 155.7 (Cq), 155.6 (Cq), 147.0 (Cq), 146.7 (Cq), 133.9 (Cq), 121.1, 120.7, 120.2 (C-2', C-3', C-6'), 105.5 (Cq), 103.6, 101.9 (C-6, C-8), 79.3 (C-2), 68.2 (C-3), 29.7 (C-4), 7.1, 7.1, 7.0, 6.0, 5.8, 5.7, 5.7, 5.4 (O-TES)

IR (Zn/Se): 2956, 2912, 2877, 1613, 1296, 1155 cm⁻¹.

UV/Vis: λ_{max1} 260 nm, λ_{max2} 288 nm.

HRMS (ESI-TOF) *m/z*: [M+Na]⁺ calcd. for C₄₅H₈₄O₆NaSi₅, 883.5006; found, 883.5038.

66d**per-O-TBDMS epicatechin**

- CAS : New product
- MM : 861,6
- EM : 860,5114
- MF : C₄₅H₈₄O₆Si₅

(–)-epicatechin (1.08 g, 3.7 mmol) was dissolved with 26 mL of DMF (dry, distilled), under Ar atmosphere. To this solution imidazol (1.76 mg, 26 mmol) and tertbutyldimethylsilyl chloride (TBDMSCl) (3.90 g, 26 mmol) were added. The reaction mixture was stirred for 7 h, after which time TLC monitoring indicated completion of the reaction. The mixture was diluted with Et₂O (100 mL) and extracted with H₂O (100 mL × 3) and brine (100 mL). The organic layer was dried over Na₂SO₄ and the solvent evaporated under reduced pressure to give a colorless oil. This oil was purified by silica gel column chromatography with cyclohexane-Et₂O (95:5, v/v), to afford **66d** as a white sticky solid (3.01 mg, 94%).

TLC (Cyclohexane-Et₂O (95:5, v/v): R_f = 0.6.

¹H NMR (300MHz, Acetone-*d*₆) δ 7.02 (d, *J* = 1.9, H-6'), 6.96 (dd, *J* = 1.8, 8.3, H-2'), 6.88 (d, *J* = 8.2, H-3'), 6.07 (d, *J* = 2.3, H-6), 5.99 (d, *J* = 2.3, H-8), 5.01 (s, H-2), 4.32 (m, H-3), 2.88 (dd, 3.9, 16.4, H-4), 2.75 (dd, 4.1, 12.7, H-4), 1.03 (bs, Ar-O-TBDMS), 1.02 (bs, Ar-O-TBDMS), 1.01 (bs, Ar-O-TBDMS), 1.00 (bs, Ar-O-TBDMS), 0.76 (bs, C3-O-TBDMS), 0.27-0.21 (m, O-TBDMS), -0.09 (s, C3-O-TBDMS), -0.26 (s, C3-O-TBDMS).

¹³C NMR (75 MHz, Acetone-*d*₆) δ 157.0 (Cq), 155.6 (2Cq), 147.1 (Cq), 146.8 (Cq), 134.1 (Cq), 121.4, 121.1, 120.8 (C-2', C-3', C-6'), 105.6 (Cq), 103.9, 102.0 (C-6, C-8), 79.3 (C-2), 68.3 (C-3), 29.6 (C-4), 26.5, 26.4, 26.2 (2C), 26.1, 19.1, 18.9, 18.7, -3.7 (2C), -3.8, -3.9, -4.0, -4.1, -4.8, -4.9 (O-TBDMS).

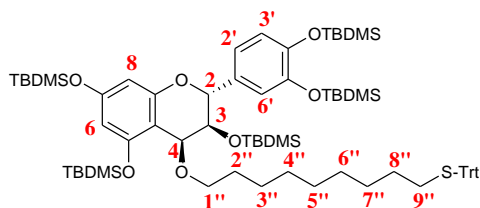
IR (Zn/Se): 2956, 2930, 2895, 2858, 1613, 1255, 1155 cm⁻¹.

UV/Vis: λ_{max1} 261 nm, λ_{max2} 288 nm.

HRMS (ESI-TOF) *m/z*: [M+Na]⁺ calculated for C₄₅H₈₄O₆NaSi₅, 883.5006; found, 883.5005.

67

per-O-TBDMS-4-(9-(tritylthio)nonyloxy) catechin



- CAS : New product
- MM : 1278,2
- EM : 1276,7288
- MF : C₇₃H₁₁₆O₇SSi₅

66a (300 mg, 0.35 mmol) was dissolved with 10 mL of CH₂Cl₂ (distilled), under Ar atmosphere. To this solution **63** (279 mg, 0.67 mmol) was added. After cooling to 0°C, DDQ (160 mg, 0.70) was added all at once with vigorous stirring. The reaction mixture was stirred for 1 h at 0°C and then at room temperature for 3 h, after which time TLC monitoring indicated quasi completion of the reaction. The solvent was evaporated under reduced pressure to give a dark blue solid. This solid was purified by silica gel column chromatography eluting with pure cyclohexane to cyclohexane-AcOEt (8:2, v/v), to afford **67** as a pale yellow sticky solid (430 mg, 96%).

TLC (Cyclohexane-AcOEt (95:5, v/v)): R_f = 0.6.

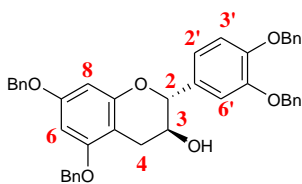
¹H NMR (300MHz, Acetone-*d*₆) δ 7.47 - 7.20 (m, S-Trt), 6.98 (d, *J* = 1.4, H-6'), 6.92 (dd, *J* = 2.3, 8.4, H-2'), 6.89 (d, *J* = 8.2, H-3'), 6.02 (bs, H-6, H-8), 5.16 (d, *J* = 9.9, H-2), 4.70 (d, *J* = 2.5, H-4), 3.94 - 3.85 (m, H-3, H-1''), 3.74 - 3.69 (m, H-1''), 2.16 (t, *J* = 7.3, H-9''), 1.58-1.20 (m, H-2''- H-8''), 1.07 (bs, Ar-O-TBDMS), 1.03 (bs, Ar-O-TBDMS), 1.02 (bs, Ar-O-TBDMS), 1.00 (bs, Ar-O-TBDMS), 0.82 (bs, C3-O-TBDMS), 0.34-0.24 (m, O-TBDMS), -0.01 (bs, C3-O-TBDMS), -0.37 (bs, C3-O-TBDMS).

¹³C NMR (75 MHz, Acetone-*d*₆) δ 157.8 (Cq), 157.0 (Cq), 155.8 (Cq), 147.4 (Cq), 147.3 (Cq), 146.1 (Cq), 134.3 (Cq), 130.4 (C-H, Trt), 128.6 (C-H, Trt), 127.4 (C-H, Trt), 122.4, 121.6, 121.5 (C-2', C-3', C-6'), 108.7 (Cq), 103.6 (Cq), 101.8 (Cq), 77.2 (C-2), 74.6 (C-3), 71.0, 70.9 (C-4, C-1''), 67.2 (QC, Trt), 32.5 (C-9''), 31.2, 29.7, 29.1, 27.5, 27.0 (C-2'' - C-8''), 26.5, 26.4, 26.1, 19.1 (2C), 19.0, 18.8, 18.6, -3.6, -3.7, -3.8 (2C), -3.9, -4.1, -4.2, -5.0 (O-TBDMS).

IR (Zn/Se): 2929, 2857, 1255, 1125, 837, 780 cm⁻¹.

UV/Vis: λ_{max} 270 nm.

HRMS (ESI-TOF) *m/z*: [M+Na]⁺ calcd. for C₇₃H₁₁₆O₇NaSi₅S, 1299.7180; found, 1299.7167.

68a**5, 7, 4', 5'-O-benzyl catechin**

- CAS : 20728-73-8
- MM : 650.8
- ME : 650.2668
- FM : C₄₃H₃₈O₆

(+)-catechin (103 mg, 0.35 mmol) was dissolved with distilled DMF (2 mL), under Ar atmosphere. To this solution dry K₂CO₃ (298 mg, 2.2 mmol) was added at 0°C and stirred for 20 min. Then Bn-Br (193 μ L, 1.6 mmol) was added dropwise and the mixture was allowed to stir for 2 h at 0°C and 24 h at room temperature, after which time TLC monitoring indicated completion of the reaction. The mixture was diluted with AcOEt (30 mL) and extracted with H₂O (10 mL \times 3), brine (10 mL) and dried over Na₂SO₄. The solvent was evaporated under reduced pressure to give a yellow oily residue. This residue was purified by silica gel column chromatography eluting with cyclohexane-AcOEt (8:2 v/v), to afford **68a** as a white solid (200 mg, 88%).

mp: 123–126 °C (lit.¹⁰⁹ 124–126 °C).

TLC (CH₂Cl₂): R_f = 0.3.

[α]_D = + 4.0°, 1.5 M, CH₂Cl₂.

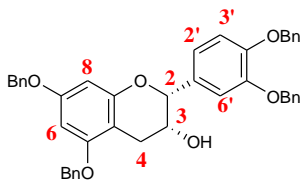
¹H NMR (300MHz, Acetone-*d*₆) δ 7.52 -7.30 (m, Ar-O-Bn), 7.19 (d, *J* = 1.8, H-6'), 7.05 (d, *J* = 8.3, H-3'), 6.98 (dd, *J* = 1.8, 8.2, H-2'), 6.36 (d, *J* = 2.3, H-8), 6.18 (d, *J* = 2.3, H-6), 5.16 (s, O-Bn), 5.14 (s, O-Bn), 5.11 (s, O-Bn), 5.06 (s, O-Bn), 4.69 (d, *J* = 7.6, H-2), 4.09 - 4.04 (m, H-3, O-H), 2.99 (dd, *J* = 5.4, 16.3, H-4), 2.62 (dd, *J* = 8.2, 16.4, H-4).

¹³C NMR (75 MHz, Acetone-*d*₆) δ 159.6 (Cq), 158.6 (Cq), 156.5 (Cq), 149.7 (Cq), 138.7 (Cq, OBn), 138.6 (Cq, OBn), 138.5 (2Cq, OBn), 133.6 (Cq), 129.3 (2C-H, OBn), 129.2 (2C-H, OBn), 128.6 (C-H, OBn), 128.5 (C-H, OBn), 128.4 (2C-H, OBn), 128.3 (C-H, OBn), 128.1 (C-H, Bn), 121.5, 115.3, 115.1 (C-2', C-3', C-6'), 103.4 (Cq), 95.5, 94.2 (C-6, C-8), 82.6 (C-2), 71.7 (CH₂, OBn), 71.6 (CH₂, OBn), 70.5 (2CH₂, OBn), 67.9 (C-3).

IR (Zn/Se): 3428, 3031, 2927, 1618, 1593, 1143, 1117 cm⁻¹.

UV/Vis: $\lambda_{\text{max}1}$ 254 nm, $\lambda_{\text{max}2}$ 274 nm.

MS (ESI) *m/z* (rel. intensity): 651 [M+H]⁺, (70); 1323 [2M+Na]⁺, (75); 1339 [2M+K]⁺, (100).

68b**5, 7, 4', 5'-O-benzyl epicatechin**

- CAS : 20728-73-8
- MM : 650.8
- ME : 650.2668
- FM : C₄₃H₃₈O₆

(–)-epicatechin (2.05 g, 7.07 mmol) was dissolved with distilled DMF (dry, 30 mL), under Ar atmosphere. To this solution was added dry K₂CO₃ (5.9 g, 42.7 mmol) at 0°C and the mixture was stirred for 20 min. Then Bn-Br (4.8 mL, 32.0 mmol) was added dropwise and the mixture was allowed to stir for 2 h at 0°C and 40 h at room temperature, after which time TLC monitoring indicated completion of the reaction. The mixture was diluted with AcOEt (300 mL) and extracted with H₂O (300 mL × 3), brine (300 mL) and dried over Na₂SO₄. The solvent was evaporated under reduced pressure to give a yellow oily residue. This residue was purified by silica gel column chromatography eluting with cyclohexane-AcOEt (8:2 v/v), to afford **68b** as a white solid (3.9 g, 85%).

mp: 131-132 °C (lit.^{76,109} 126-130 °C).

TLC (Cyclohexane-AcOEt, 8:2 v/v): R_f = 0.6.

[α]_D = – 17°, 1.5 M, CH₂Cl₂.

¹H NMR (300MHz, CDCl₃): δ 7.49-7.32 (m, OBn), 7.17 (d, *J* = 1.7, H-6'), 7.03 (dd, *J* = 1.7, 8.5, H-2'), 6.98 (d, *J* = 8.3, H-3'), 6.30 (d, *J* = 2.5, H-8), 6.29 (d, *J* = 2.4, H-6), 5.21 (bs, OBn), 5.19 (bs, OBn), 5.04 (bs, OBn), 5.03 (bs, OBn), 4.93 (s, H-2), 4.23 (bs, H-3), 3.02 (dd, *J* = 2.4, 17.5, H-4), 2.94 (dd, *J* = 4.3, 17.3, H-4).

¹³C NMR (75 MHz, CDCl₃): δ 158.9 (Cq), 158.4 (Cq), 155.4 (Cq), 149.2 (Cq), 149.0 (Cq), 137.4 (Cq, OBn), 137.3 (Cq, OBn), 137.1 (2Cq, OBn), 131.6 (Cq), 128.7 (2C), 128.6 (2C), 128.6, 128.2, 128.1, 128.0 (2C), 127.9, 127.7, 127.6 (2C), 127.4 (2C), 127.3 (CH, OBn), 119.6, 115.2, 113.7 (C-2', C-3', C-6'), 101.1 (Cq), 94.8, 94.2 (C-6, C-8), 78.5 (C-2), 71.5 (CH₂, OBn), 71.4 (CH₂, OBn), 70.3 (CH₂, OBn), 70.1 (CH₂, OBn), 66.5 (C-3), 28.3 (C-4).

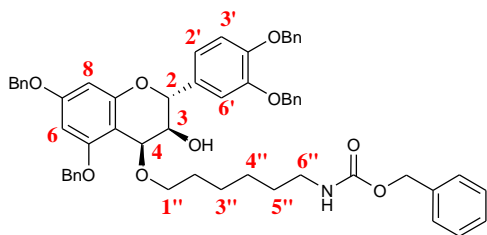
IR (Zn/Se): 3030, 2868, 1617, 1509, 1142, 1114 cm⁻¹.

UV/Vis: λ_{max1} 255 nm, λ_{max2} 270 nm.

MS (ESI) *m/z*: 651 [M+H]⁺, (40); 673 [M+Na]⁺, (60); 1323 [2M+Na]⁺, (100).

69

5, 7, 4', 5'-O-benzyl-4(-oxyhexyl-6''-benzylcarbamate) catechin



- CAS : 20728-73-8
- MM : 900,1
- ME : 899,4033
- FM : C₅₇H₅₇NO₉

68a (103 mg, 0.16 mmol) was dissolved with 5 mL of CH₂Cl₂ (dry, distilled), under Ar atmosphere. To this solution 6-(Z-amino)-1-hexanol (121 mg, 0.48 mmol) was added. After cooling to 0°C, DDQ (91 mg, 0.40) was added all at once with vigorous stirring. The reaction mixture was stirred 0°C for 1 h then at room temperature for 3 h after which time TLC monitoring indicated quasi completion of the reaction. The solvent was evaporated under reduced pressure to give a dark purple residue. This solid was purified by silica gel column chromatography eluting with to cyclohexane-AcOEt (8:2, v/v) to (7:3, v/v), to afford **69** as a pale pink amorphous solid (54 mg, 38%).

TLC (Cyclohexane-AcOEt, 7:3 v/v): R_f = 0.5.

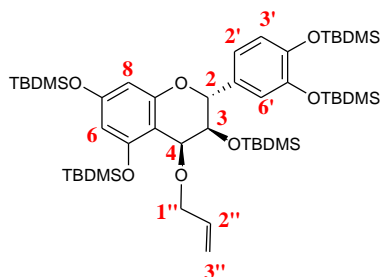
¹H NMR (300MHz, CDCl₃) δ 7.65 -7.39 (m, OBn), 7.29 (d, *J* = 1.7, H-6'), 7.20 (dd, *J* = 1.8, H-2'), 7.15 (d, *J* = 8.2, H-3'), 6.46 (d, *J* = 2.3, H-8), 6.36 (d, *J* = 2.2, H-6), 5.34-5.11 (m, H-2 or H-4, OBn), 4.97 (d, *J* = 3.5, H-2 or H-4), 4.10-3.72 (3m, H-3, H-1''), 3.32 (q, *J* = 6.6, H-6''), 2.65 (d, *J* = 9.6, O-H or N-H), 1.78-1.03 (m, H-2'' - H-5'').

¹³C NMR (75 MHz, CDCl₃) δ 161.0, 158.9, 156.5, 156.4 (Cq, C=O), 149.5 (Cq), 149.3 (Cq), 137.5, 137.4, 136.8, 136.7, 136.6 (Cq, OBn, Cbz), 131.9 (Cq), 128.8, 128.7 (2C), 128.6 (3C), 128.3, 128.2, 127.9 (2C), 127.8, 127.7, 127.6, 127.4 (CH, OBn, NBz), 121.5, 115.0, 114.7 (C-2', C-3', C-6'), 103.6 (Cq), 94.5, 93.5 (C-6, C-8), 71.5, 71.4, 70.6, 70.5, 70.2, 68.6, 66.7 (C-2, C-3, C-4, C-1'', CH₂, OBn and Cbz), 41.1 (C-6''), 30.1, 29.8, 26.6, 25.8 (C-2'' - C-5'').

IR (Zn/Se): 3418, 3352, 3063, 3032, 2928, 2858, 1709, 1614, 1264, 1148 cm⁻¹.

UV/Vis: λ_{max1} 255 nm, λ_{max2} 270 nm.

HRMS (ESI-TOF) *m/z*: [M+Na]⁺ calcd. for C₅₇H₅₇NO₉Na, 922.3925; found, 922.3926.

74a**per-O-TBDMS-4-O-allyl catechin**

- CAS : New product
- MM : 917,6
- EM : 916,5376
- MF : C₄₈H₈₈O₇Si₅

66a (618 mg, 0.72 mmol) was dissolved with 18 mL of CH₂Cl₂ (dry, distilled), under Ar atmosphere. To this solution was added allyl alcohol (2 mL, 29.3 mmol). After cooling to 0°C, DDQ (327 mg, 1.44 mmol) was added all at once with vigorous stirring. The reaction mixture was stirred for 7 h 30 min, after which time TLC monitoring indicated quasi completion of the reaction. The solvent was evaporated under reduced pressure to give a dark beige solid. This solid was purified by silica gel column chromatography eluting with CH₂Cl₂-cyclohexane (1:1, v/v), to afford **74a** as a colorless sticky solid (560 mg, 85%).

TLC (Cyclohexane-CH₂Cl₂, 1:1 v/v): R_f = 0.6

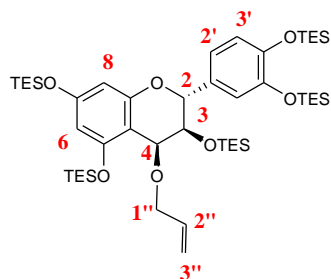
¹H NMR (300MHz, Acetone-*d*₆) δ 6.98 (d, *J* = 1.8, H-6'), 6.93 (dd, *J* = 1.9, 8.2, H-2'), 6.89 (d, *J* = 8.1, H-3'), 6.03 (d, *J* = 2.2, H-6), 6.01 (d, *J* = 2.2, H-8), 5.99-5.89 (m, H-2''), 5.28 (ddd, *J* = 1.9, 3.9, 17.4, H-3''), 5.15 (d, *J* = 9.9, H-2), 5.06 (ddd, *J* = 1.6, 3.7, 10.5, H-3''), 4.75 (d, *J* = 2.7, H-4), 4.43 (ddt, *J* = 1.7, 5.0, 12.8, H-1''), 4.25 (ddt, *J* = 1.7, 5.1, 12.8, H-1'), 3.95 (dd, *J* = 2.7, 9.9, H-3), 1.06 (bs, Ar-O-TBDMS), 1.02 (bs, Ar-O-TBDMS), 0.99 (bs, Ar-O-TBDMS), 0.81 (bs, C3-O-TBDMS), 0.34 (s, O-TBDMS), 0.31 (s, O-TBDMS), 0.24 (s, O-TBDMS), 0.23 (s, O-TBDMS), 0.01 (s, C3-O-TBDMS), -0.39 (s, C3-O-TBDMS).

¹³C NMR (75 MHz, Acetone-*d*₆) δ 157.9 (Cq), 157.1 (Cq), 155.9 (Cq), 147.4 (Cq), 147.3 (Cq), 137.1 (C-2''), 134.2 (Cq), 122.5, 121.6 (C-2', C-3', C-6'), 115.3 (C-3''), 108.3 (Cq), 103.7, 101.8 (C-6, C-8), 77.2 (C-2), 74.4 (C-3), 72.1 (C-1''), 71.3 C-4), 19.1, 19.1, 19.0, 18.8, 18.6, -3.7, -3.7, -3.8, -3.9, -4.1, -4.2, -4.2, -5.1 (O-TBDMS).

IR (Zn/Se): 1255, 1003, 838 cm⁻¹.

UV/Vis: $\lambda_{\text{max}1}$ 261 nm, $\lambda_{\text{max}2}$ 286 nm.

HRMS (ESI-TOF) *m/z*: [M+Na]⁺ calcd. for C₄₈H₈₈O₇NaSi₅, 939.5268; found, 939.5305.

74b**per-O-TES-4-O-allyl catechin**

- CAS : New product
- MM : 917,6
- EM : 916,5376
- MF : C₄₈H₈₈O₇Si₅

66b (1.16 g, 1.3 mmol) was dissolved with 33 mL of CH₂Cl₂ (dry, distilled), under Ar atmosphere. To this solution was added, allyl alcohol (3.4 mL, 50 mmol) and DDQ (611 mg, 2.7 mmol) with vigorous stirring. The reaction mixture was stirred for 24 h, after which time TLC monitoring indicated quasi completion of the reaction. The solvent was evaporated under reduced pressure to give a beige oily residue. This solid was purified by silica gel column chromatography eluting with CH₂Cl₂/cyclohexane (1:1, v/v), to afford **74b** as a colorless sticky solid (239 mg, 20%).

TLC (Cyclohexane-CH₂Cl₂, 6:4 v/v): R_f = 0.4.

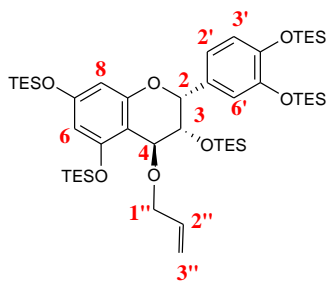
¹H NMR (300MHz, Acetone-*d*₆) δ 6.97 (d, J = 1.8, H-6'), 6.92 (dd, J = 1.9, 8.2, H-2'), 6.88 (d, J = 8.1, H-3'), 6.00 (d, J = 2.2, H-6), 5.94 (d, J = 1.8, H-8), 6.01-5.92 (m, H-2''), 5.29 (ddd, J = 1.8, 3.8, 17.3, H-3''), 5.12 (d, J = 9.9, H-2), 5.07 (ddd, J = 1.7, 3.6, 10.5, H-3''), 4.73 (d, J = 2.8, H-4), 4.42 (ddt, J = 1.6, 5.2, 12.8, H-1''), 4.26 (ddt, J = 1.6, 5.2, 12.8, H-1''), 3.91 (dd, J = 2.8, 9.9, H-3), 1.10-0.74 (m, O-TES), 0.52-0.23 (m, C3-O-TES).

¹³C NMR (75 MHz, Acetone-*d*₆) δ 158.0 (Cq), 157.0 (Cq), 156.1 (Cq), 147.4 (Cq), 147.3 (Cq), 137.2 (C-2''), 134.2 (Cq), 122.3 (C-3'), 120.8, 120.6 (C-2', C-6'), 115.4 (C-3''), 108.2 (Cq), 103.1, 101.6 (C-6, C-8), 77.2 (C-2), 74.6 (C-3), 72.4 (C-1''), 71.5 (C-4), 7.2, 7.0, 6.9, 6.0, 5.8, 5.7, 5.6, 5.3 (O-TES).

IR (Zn/Se): 2956, 2912, 2878, 1610, 1297, 1160 cm⁻¹.

UV/Vis: λ_{max1} 256 nm, λ_{max2} 272 nm.

HRMS (ESI-TOF) *m/z*: [M+Na]⁺ calculated for C₄₈H₈₈O₇NaSi₅, 939.5268; found, 939.5304.

74c**per-O-TES-4-O-allyl epicatechin**

- CAS : New product
- MM : 917,6
- EM : 916,5376
- MF : C₄₈H₈₈O₇Si₅

66c (1.03 g, 1.2 mmol) was dissolved with 30 mL of CH₂Cl₂ (dry, distilled), under Ar atmosphere. To this solution was added allyl alcohol (2.98 mL, 44 mmol) and DDQ (543 mg, 2.4 mmol), with vigorous stirring. The reaction mixture was stirred for 6 h, after which time TLC monitoring indicated quasi completion of the reaction. The solvent was evaporated under reduced pressure to give a beige oily residue. This residue was purified by silica gel column chromatography eluting with CH₂Cl₂/cyclohexane (4:6, v/v), to afford **74c** as a colorless oil (290 mg, 26%).

TLC (Cyclohexane-CH₂Cl₂, 4:6 v/v): R_f = 0.6.

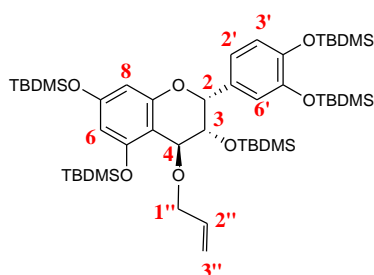
¹H NMR (300MHz, Acetone-*d*₆): δ 7.03 (d, *J* = 1.9, H-6'), 6.96 (dd, *J* = 2.0, 8.6, H-2'), 6.89 (d, *J* = 8.2, H-3'), 6.09 (d, *J* = 2.2, H-6), 6.05 (d, *J* = 2.3, H-8), 6.03-5.96 (m, H-2''), 5.33 (ddd, *J* = 1.8, 3.6, 17.2, H-3''), 5.14 (ddd, *J* = 1.8, 3.4, 11.2, H-3''), 5.12 (bs, H-2), 4.55 (d, *J* = 3.2, H-4), 4.37-4.29 (ddt, *J* = 1.6, 5.4, 13.0, H-1''), 4.08 (dd, *J* = 1.3, 3.2, H-3), 1.09-0.72 (m, O-TES), 0.45-0.25 (m, C3-O-TES).

¹³C NMR (75 MHz, Acetone-*d*₆): δ 157.8 (Cq), 157.5 (Cq), 157.4 (Cq), 147.2 (Cq), 146.9 (Cq), 137.0 (C-2''), 133.5 (Cq), 121.0 (Cq), 120.8 (Cq), 120.5 (Cq), 115.9 (C-3''), 106.3 (Cq), 102.7, 101.5 (C-6, C-8), 75.7 (C-2), 71.6 (C-4), 70.9 (C-1''), 70.3 (C-3), 7.1 (2C), 7.0 (2C), 6.9, 6.0, 5.8, 5.7, 5.6, 5.3 (O-TES).

IR (Zn/Se): 2956, 2912, 2877, 1164, 1105, 744 cm⁻¹.

UV/Vis: λ_{max1} 260 nm, λ_{max2} 288 nm.

HRMS (ESI-TOF) *m/z*: [M+Na]⁺ calcd. for C₄₈H₈₈O₇NaSi₅, 939.5268; found, 939.5280.

74d**per-O-TBDMS-4-O-allyl epicatechin**

- CAS : New product
- MM : 917,6
- EM : 916,5376
- MF : C₄₈H₈₈O₇Si₅

66d (1.31 g, 1.52 mmol) was dissolved with 32 mL of CH₂Cl₂ (dry, distilled). To this solution was added allyl alcohol (4.2 mL, 62 mmol) and DDQ (0.70 g, 3.08 mmol) with vigorous stirring. The reaction mixture was stirred for 18 h, after which time TLC monitoring indicated quasi completion of the reaction. The solvent was evaporated under reduced pressure to give a dark beige solid. This solid was purified by silica gel column chromatography, eluting with CH₂Cl₂-cyclohexane (1:1, v/v), to afford **74d** as a colorless sticky solid (898 mg, 65%).

TLC (Cyclohexane-CH₂Cl₂, 1:1 v/v): R_f = 0.6.

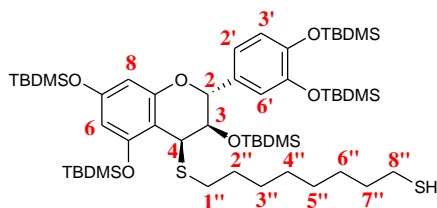
¹H NMR (300MHz, Acetone-*d*₆): δ 7.04 (d, J = 1.9, H-6'), 6.95 (dd, J = 1.8, 8.4, H-2'), 6.91 (d, J = 8.2, H-3'), 6.11-5.95 (m, H-2''), 6.10 (d, J = 2.2, H-6), 6.04 (d, J = 2.2, H-8), 5.33 (ddd, J = 1.8, 3.6, 17.3, H-3''), 5.19 (s, H-2), 5.17 (ddd, J = 1.5, 3.4, 10.4, H-3''), 4.55 (d, J = 3.3, H-4), 4.36 (ddt, J = 1.5, 5.5, 12.9, H-1''), 4.28 (ddt, J = 1.6, 5.0, 12.9, H-1''), 4.08 (dd, J = 1.3, 3.3, H-3), 1.08 (bs, Ar-O-TBDMS), 1.04 (bs, Ar-O-TBDMS), 1.03 (bs, Ar-O-TBDMS), 1.0 (bs, Ar-O-TBDMS), 0.69 (bs, C3-O-TBDMS), 0.36 (s, O-TBDMS), 0.32 (s, O-TBDMS), 0.27 (s, O-TBDMS), 0.24 (bs, O-TBDMS), 0.22 (s, O-TBDMS), -0.08 (s, C3-O-TBDMS), -0.46 (s, C3-O-TBDMS).

¹³C NMR (75 MHz, Acetone-*d*₆): δ 157.8 (Cq), 157.4 (Cq), 157.3 (Cq), 147.2 (Cq), 146.8 (Cq), 136.9 (C-2''), 133.5 (Cq), 121.7, 121.1, 120.7 (C-2', C-3', C-6'), 116.0 (C-3''), 106.3 (Cq), 103.3, 101.6 (C-6, C-8), 75.4 (C-2), 71.5 (C-4), 70.6 (C-1''), 69.7 (C-3), 26.5, 26.4, 26.3, 26.1 (2C), 19.1, 19.0 (2C), 18.9, 18.4, -3.5, -3.6, -3.7, -3.8, -4.0, -4.1, -4.9, -5.0 (O-TBDMS).

IR (Zn/Se): 2930, 2896, 2858, 1293, 1256, 838, 779 cm⁻¹.

UV/Vis: $\lambda_{\text{max}1}$ 263 nm, $\lambda_{\text{max}2}$ 284 nm.

HRMS (ESI-TOF) *m/z*: [M+Na]⁺ calcd. for C₄₈H₈₈O₇NaSi₅, 939.5268; found, 939.5305.

75a**per-O-TBDMS-4-thioetheroctanethiol catechin**

- CAS : New product
- MM : 1037,9
- EM : 1036,5808
- MF : C₅₃H₁₀₀O₆S₂Si₅

74a (328 mg, 0.36 mmol) was dissolved with 6.5 mL of CH₂Cl₂ (dry, distilled), under Ar atmosphere. To this solution was added octanedithiol (200 µL, 1.1 mmol). After cooling to – 78°C, BF₃·Et₂O (69 µL, 0.54 mmol) was added. The mixture was allowed to stir at – 78°C for 1 h, after which time TLC monitoring indicated completion of the reaction. At this temperature, NaHCO_{3(sat)} (1 mL) was added and the mixture was allowed to reach room temperature. The mixture was diluted with CHCl₃ (25 mL) and extracted with H₂O (10 mL) and brine (10 mL). The organic layer was dried over Na₂SO₄ and the solvent was evaporated under reduced pressure to give colorless oil. This oil was purified by silica gel column chromatography eluting from cyclohexane-CH₂Cl₂ (8:2, v/v) to (1:1, v/v), to afford **75a** as clear colorless oil (319 mg, 85%).

TLC (Cyclohexane-CH₂Cl₂, 6:4 v/v): R_f = 0.4.

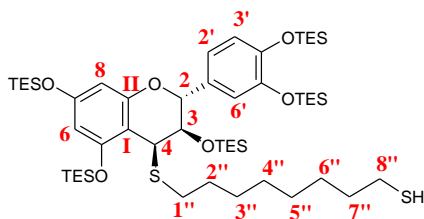
¹H NMR (300MHz, Acetone-*d*₆): δ 6.95 (bs, H-6'), 6.91 (bs, H-2', H-6'), 6.02 (d, *J* = 2.2, H-6), 6.01 (d, *J* = 2.2, H-8), 5.34 (d, *J* = 9.3, H-2), 4.56 (d, *J* = 3.9, H-4), 4.10 (dd, *J* = 3.9, 9.3, H-3), 2.73 - 2.65 (m, H-1''), 2.54 - 2.43 (m, H-1'', H-8''), 1.66 - 1.28 (m, H-2'' - H-7''), 1.08 (bs, Ar-O-TBDMS), 1.02 (bs, Ar-O-TBDMS), 1.01 (bs, Ar-O-TBDMS), 0.99 (bs, Ar-O-TBDMS), 0.83 (s, C3-O-TBDMS), 0.36 (s, O-TBDMS), 0.31 (s, O-TBDMS), 0.24 (s, O-TBDMS), 0.23 (s, O-TBDMS), -0.04 (s, C3-O-TBDMS), -0.39 (s, C3-O-TBDMS).

¹³C NMR (75 MHz, Acetone-*d*₆): δ 157.2 (Cq), 156.5 (Cq), 154.9 (Cq), 147.5 (Cq), 147.4 (Cq), 134.1 (Cq), 122.6, 121.6, 121.5 (C-2', C-3', C-6'), 107.3 (Cq), 103.6, 101.7 (C-6, C-8), 78.3 (C-2), 74.0 (C-3), 43.7 (C-4), 34.8 (C-7''), 31.8 (C-1''), 30.8, 29.8, 29.7, 29.0 (C-2'' - C-6''), 26.5, 26.4, 26.2, 26.1 (O-TBDMS), 24.8 (C-8''), 19.1 (2C), 18.9 (2C), 18.7, -3.7, -3.8 (2C), -3.9 (2C), -4.1, -4.2 (2C), -5.0 (O-TBDMS).

IR (Zn/Se): 2955, 2930, 2857, 1254, 1159, 838, 780 cm⁻¹.

UV/Vis: λ_{max1} 265 nm, λ_{max2} 284 nm.

HRMS (ESI-TOF) *m/z*: [M+Na]⁺ calcd. for C₅₃H₁₀₀O₆NaSi₅S₂, 1059.5699; found, 1059.5738.

75b**per-O-TES-4-thioetheroctanethiol catechin**

- CAS : New product
- MM : 1037,9
- EM : 1036,5808
- MF : C₅₃H₁₀₀O₆S₂Si₅

74b (139 mg, 0.15 mmol) was dissolved with 2.7 mL of CH₂Cl₂ (dry, distilled), under Ar atmosphere. To this solution was added octanedithiol (84 µL, 0.45 mmol). After cooling to – 78°C, BF₃·Et₂O (29 µL, 0.22 mmol) was added. The mixture was allowed to stir at – 78°C for 1 h, after which time TLC monitoring indicated completion of the reaction. At this temperature NaHCO₃(sat) (1 mL) was added and the mixture was allowed to reach room temperature. The mixture was diluted with CHCl₃ (20 mL) and extracted with H₂O (10 mL) and brine (10 mL). The organic layer was dried over Na₂SO₄ and the solvent was evaporated under reduced pressure to give colorless oil. This oil was purified by silica gel column chromatography eluting from CH₂Cl₂-cyclohexane (8:2, v/v) to CH₂Cl₂-cyclohexane (1:1, v/v), to afford **75b** as a colorless oil (86 mg, 55%)

TLC (Cyclohexane-CH₂Cl₂, 1:1 v/v): R_f = 0.5.

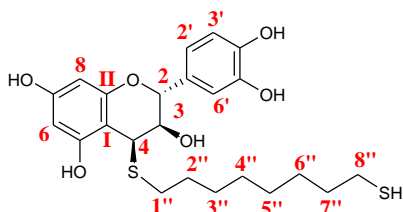
¹H NMR (300MHz, Acetone-*d*₆): δ 6.96 (d, *J* = 1.7, H-6'), 6.92 (dd, *J* = 1.8, 8.2, H-2'), 6.88 (d, *J* = 8.1, H-3'), 6.03 (d, *J* = 2.3, H-6), 6.02 (d, *J* = 2.3, H-8), 5.32 (d, *J* = 9.3, H-2), 4.47 (d, *J* = 3.8, H-4), 4.07 (dd, *J* = 3.8, 9.3, H-3), 2.87-2.63 (m, H-1''), 2.51 (q, *J* = 7.5, H-8''), 1.65-1.29 (m, H-2'' - H-7''), 1.11-0.73 (m, O-TES), 0.53-0.25 (m, C₃-O-TES).

¹³C NMR (75 MHz, Acetone-*d*₆): δ 157.2 (Cq), 156.3 (Cq), 155.0 (Cq), 147.4 (Cq), 147.3 (Cq), 134.1 (Cq), 122.4 (C-3'), 120.8, 120.6 (C-2', C-6'), 107.6 (Cq), 103.4, 101.5 (C-6, C-8), 78.3 (C-2), 74.3 (C-3), 44.3 (C-4), 34.9 (C-7''), 33.2 (C-1''), 30.8, 29.9, 29.8, 29.0 (C-2'' - C-6''), 24.9 (C-8''), 7.2, 7.1, 7.0, 6.9, 6.1, 5.8, 5.7, 5.6, 5.3 (O-TES).

IR (Zn/Se): 2955, 2934, 2913, 2877, 1608, 1158, 1004, 744 cm⁻¹.

UV/Vis: λ_{max1} 255 nm, λ_{max2} 275 nm.

HRMS (ESI-TOF) *m/z*: [M+Na]⁺ calcd. for C₅₃H₁₀₀O₆NaSi₅S₂, 1059.5699; found, 1059.5676.

76a**Catechin-4-thioetheroctanethiol**

- CAS : New product
- MM : 466,1
- ME : 466,6107
- MF : C₂₃H₃₀O₆S₂

75b (80 mg, 0.08 mmol) was dissolved with 0.2 mL of THF (dry), under Ar atmosphere. To this solution was added 1.1 mL of a solution of HF/Py (70%, 117 μ L, 1.35 mmol) in 893 μ L THF/Py (16%, v/v). The mixture was allowed to stir for 3 days after which time TLC monitoring indicated completion of the reaction. The mixture was diluted with AcOEt (20 mL) and extracted with NaHCO₃ (5 mL) and brine (5 mL). The organic layer was dried over Na₂SO₄ and the solvent was evaporated under reduced pressure to give colorless oil. This oil was again dissolved in AcOEt (1 mL) and extracted with NH₄Cl (0.5 mL \times 3) and brine (0.5 mL). The organic layer was dried over Na₂SO₄ and the solvent was evaporated under reduced pressure to give **76a** (28 mg, 76%) as a sticky solid.

TLC (CH₂Cl₂-MeOH, 9:1 v/v): R_f = 0.6.

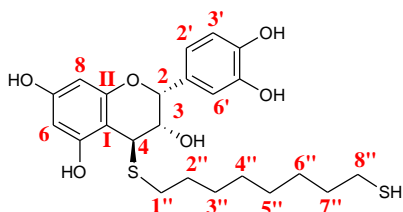
¹H NMR (300MHz, Acetone-*d*₆): δ 8.37 (bs, O-H), 8.19 (bs, O-H), 7.87 (bs, O-H), 6.95 (s, H-6'), 6.81 (bs, H-2', H-3'), 6.04 (d, *J* = 2.3, H-6), 5.83 (d, *J* = 2.3, H-8), 4.91 (d, *J* = 9.7, H-2), 4.34 (d, *J* = 4.4, H-4), 4.14-4.07 (m, H-3), 3.74 (d, *J* = 7.0, C₃-OH), 2.93-2.75 (m, H-1''), 2.50 (q, *J* = 7.5, H-8''), 1.70-2.26 (m, H-2'' - H-7'').

¹³C NMR (75 MHz, Acetone-*d*₆): δ 159.1, 157.3 (C-5, C-7), 156.3 (C_{II}), 145.9, 145.6 (C-5', C-4'), 131.7 (C-1'), 121.0 (C-3'), 116.0 (C-6'), 115.6 (C-2'), 102.7 (C_I), 96.5 (C-6), 95.3 (C-8), 78.9 (C-2), 71.7 (C-3), 45.0 (C-4), 34.8, 34.7 (C-1'', C-7''), 30.7, 29.9, 29.7, 29.0 (C-2'' - C-6''), 24.8 (C-8'').

IR (Zn/Se): 3361, 1622, 1147 cm⁻¹.

UV/Vis: $\lambda_{\text{max}1}$ 247 nm, $\lambda_{\text{max}2}$ 269 nm.

HRMS (ESI-TOF) *m/z*: [M+Na]⁺ calcd. for C₂₃H₃₀O₆NaS₂, 489.1376; found, 489.1388.

76b**Epicatechin-4-thioetheroctanethiol**

- CAS : New product
- MM : 466,1
- ME : 466,6107
- MF : C₂₃H₃₀O₆S₂

75c (50 mg, 0.054 mmol) was dissolved with 0.2 mL of THF (dry). To this solution was added 0.6 mL of a solution of HF/Py (70%, 54.4 μ L, 0.63 mmol) in 537 μ L THF/Py (16%, v/v). The mixture was allowed to stir for 3 days after which time TLC monitoring indicated completion of the reaction. The mixture was diluted with AcOEt (20 mL) and extracted with NaHCO₃ (10 mL) and brine (10 mL). The organic layer was dried over Na₂SO₄ and the solvent was evaporated under reduced pressure to give colorless oil. This oil was again dissolved in AcOEt (1 mL) and extracted with NH₄Cl (0.5 mL \times 3) and brine (0.5 mL). The organic layer was dried over Na₂SO₄ and the solvent was evaporated under reduced pressure to give **76b** (14.6 mg, 58%) as a pale yellow sticky solid.

TLC (CH₂Cl₂-MeOH, 9:1 v/v): R_f = 0.6

¹H NMR (400MHz, Acetone-*d*₆): δ 8.17 (s, O-H), 8.15 (s, O-H), 7.82 (bs, O-H), 7.09 (d, J = 2.3, H-6'), 6.87 (dd, J = 2.3, 10.9, H-2'), 6.82 (d, J = 10.8, H-3'), 6.04 (d, J = 3.1, H-6), 5.91 (d, J = 3.1, H-8), 5.31 (s, H-2), 4.06 (bs, H-4), 3.94 (d, J = 8.0, C3-OH), 2.86-2.68 (m, H-1''), 2.51 (q, J = 9.8, H-8''), 1.75-1.31 (m, H-2'' - H7'').

¹³C NMR (75 MHz, Acetone-*d*₆): δ 158.8, 158.4 (C-5, C-7), 157.1 (C_{II}), 145.5, 145.4 (C-4', C-5'), 132.1 (C-1'), 119.3 (C-3'), 115.6 (C-2'), 115.4 (C-6'), 100.2 (C_I), 96.7 (C-6), 95.6 (C-8), 75.3 (C-2), 71.7 (C-3), 43.2 (C-4), 34.8 (C-7''), 32.8 (C-1''), 30.42, 29.7, 29.5 29.0 (C-2'' - C-5''), 24.8 (C-8'').

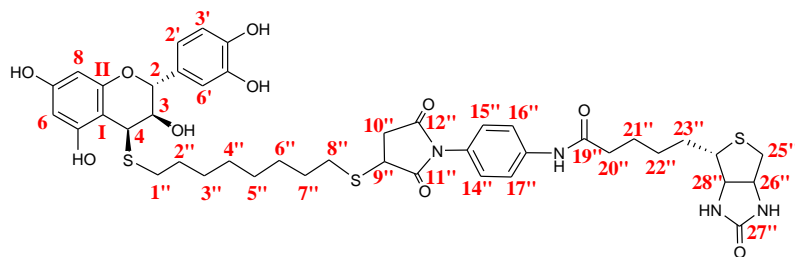
IR (Zn/Se): 3354, 2927, 2854, 1627, 1284, 1149, 824 cm⁻¹.

UV/Vis: $\lambda_{\text{max}1}$ 232 nm, $\lambda_{\text{max}2}$ 279 nm.

HRMS (ESI-TOF) *m/z*: [M+Na]⁺ calcd. for C₂₃H₃₀O₆NaS₂, 489.1376; found, 489.1377.

80a

Catechin-4-biotin adduct



- CAS: New product
- MM: 881,1
- EM: 880,2846
- MF: C₄₃H₅₂N₄O₁₀S₃

To a solution of **76a** (13.1 mg, 0.028 mmol) in DMSO-*d*₆ (1.1 mL), under Ar atmosphere, was added **59** (10.9 mg, 0.026 mmol). The mixture was shaken for 6 h, after which time ¹H NMR analysis indicated completion of the reaction. The desired reaction product was conveniently precipitated out of the reaction mixture using Et₂O-CHCl₃ (32 mL, 7:9, v/v) to directly furnish pure **80a** (24 mg, 97%) as pale pink hygroscopic solid.

Retention time: 25.6 min.

Method: 0-25 min: 0 to 50% then 25-30 min: 50 to 100% MeCN-TFA 0.1%.

Column: Varian Microsorb C-18 (10 × 250 mm, 5μm).

Flow rate: 1mL/min.

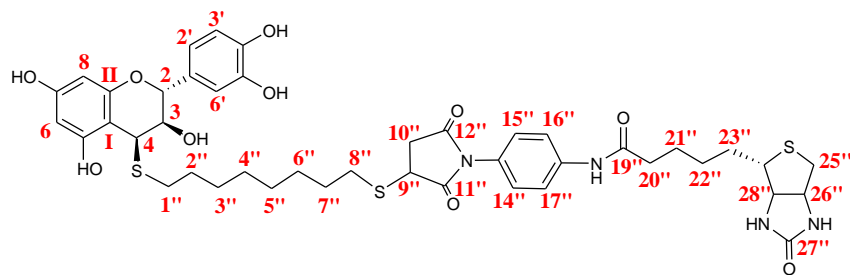
¹H NMR (300 MHz, DMSO-*d*₆) δ 10.05 (s, NH), 9.47 (s, OH-Ar), 9.14 (s, OH-Ar), 8.89 (s, OH-Ar), 7.68 (d, *J* = 8.9, H-16", H-17"), 7.17 (d, *J* = 8.8, H-14", H15"), 6.76 (d, *J* = 1.7, H-6'), 6.70 (d, *J* = 8.1, H-3'), 6.64 (dd, *J* = 1.8, 8.1, H-2'), 6.44 (s, NH), 6.36 (s, NH), 5.88 (d, *J* = 2.2, H-8), 5.61 (d, *J* = 2.1, 1H-6), 4.90 (d, *J* = 5.7, C3-OH), 4.86 (d, *J* = 9.7, H-2), 4.33-4.29 (m, H-26"), 4.18 (d, *J* = 4.0, H-4), 4.19-4.12 (m, H-28"), 4.07 (dd, *J* = 4.1, 9.2, H-9"), 3.92 (q, *J* = 4.7, H-3), 3.29 (d, *J* = 9.2, H10"), 3.17-3.09 (m, H-24"), 2.82 (dd, *J* = 5.1, 12.5, H-25"), 2.77-2.56 (m, H-1", H-8", H-10"), 2.58 (d, *J* = 12.6, H-25"), 2.33 (t, *J* = 7.2, H-20"), 1.64-1.22 (m, H2"-H7", H21"-H23").

¹³C NMR (100 MHz, DMSO-*d*₆) δ 176.1, 174.4 (C-11", C-12"), 171.4 (C-19"), 162.7 (C-27"), 157.8 (C-7), 156.1 (C-2), 154.7 (C-5), 145.1, 144.8 (C-4', C-5'), 139.3 (C-13"), 130.3 (C-1'), 127.3 (C-14", C-15"), 126.8 (C-18"), 119.4 (C-2'), 119.3 (C-16", C-17"), 115.3 (C-6'), 115.0 (C-3'), 101.0 (C_D), 95.1 (C-8), 93.5 (C-6), 77.3 (C-2), 70.2 (C-3), 61.1 (C-28"), 59.2 (C-26"), 55.4 (C-24"), 43.0 (C-4), 36.2 (C-10", C-20"), 32.9 (C-1"), 30.6 (C-8"), 29.6, 29.5, 28.7, 28.6, 28.5, 28.4, 28.2, 28.1, 25.1 (C2"-7", C21"-23").

IR (Ge): 3260, 1708, 1150, 1023 cm⁻¹.

UV/Vis: λ_{max} 239 nm.

MS (ESI) *m/z* (rel. intensity): 881 [M+H]⁺, (100).



NMR signal assignments of catechin-biotin (C-ring) conjugate

position	δ_H (mult., J in Hz)	δ_C (mult.)	HMQC ^a	HMBC ^b
Catechin Moiety				
2	4.86 (d, 9.7)	77.3	C-2	C-4, C-3, C-1', C-2', C-3' C ₃ -OH, H-4, H-2', H-6'
3	3.92 (q, 4.7)	70.2	C-3	H-2, H-4
4	4.18 (d, 4.0)	43.0	C-4	C-3, C-2, C _I , C _{II} , C-5 H-2, H-1''
5	-	154.7	-	H-4, H-6
6	5.88 (d, 2.2)	93.5	C-6	C-8, C _I , C-5, C-7 H-8
7	-	157.8	-	H-8, H-6
8	5.61 (d, 2.1)	95.1	C-8	H-6
1'	-	130.3	-	H-2, H-2', H-3', H-6'
2'	6.64 (dd, 1.8, 8.1)	119.4	C-2'	C-1', C-3', C-4', C-5', C-6', H-2, H-3', H-6'
3'	6.70 (d, 8.1)	115.0	C-3'	C-1', C-2', C-4', C-5' H-2, H-6'
4', 5'	-	145.1, 144.8	-	H-2', H-3', H-6'
6'	6.76 (d, 1.7)	115.3	C-6'	C-1', C-2', C-4', C-5' H ₂ , H-2'
C _I	-	100.1	-	H-8, H-6, H-4
C _{II}	-	156.1	-	H-8, H-4
Biotin maleimide moiety				
9''	4.07 (dd, 4.1, 9.2)	39.5	C-9''	C-10'', C-11'', C-12'' H-10''
10a,b''	3.29 (d, 9.2) 2.77-2.56 (m)	36.2	C-10''	C-11'', C-12'' H-9''
11''- 12''	-	176.1, 174.4	-	H-9'', H-10''
13''	-	126.8	-	H-14''- H-17''
14''- 15''	7.17 (d, 8.8)	127.3	C-14'', C-15''	C-13'', C-14'', C-15'', C-18'', H-14'', H-15''
16''- 17''	7.68 (d, 8.9)	119.3	C-16'', C-17''	C-13'', C-16''- C-18'' N-H (19''), H-16'', H-17''
18''	-	139.3	-	H-14'' - H-17''
19''	-	171.4	-	H-20''
20''	2.33 (t, 7.2)	36.2	C-20''	C-19''
21''-23''	1.64-1.22 (m)	28.2, 28.1, 25.08	C-21'', C-22'', C-23''	-

Chapter V: Experimental section

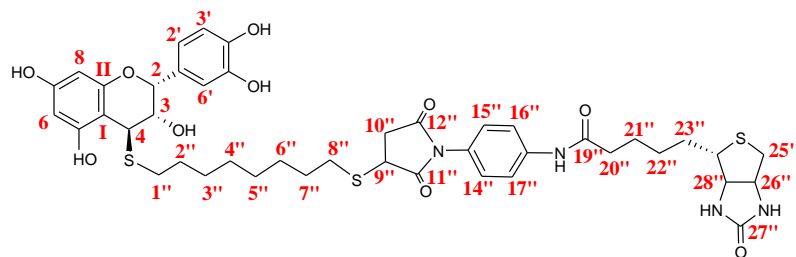
24''	3.17-3.09 (m)	55.4	C-24''	H-26'', H-28''
25a,b''	2.82 (dd, 5.1, 12.5) 2.58 (d, 12.6)	39.9	C-25''	H-26'', H-28'' C-24'', C-26'', C-28''
26''	4.33-4.29 (m)	59.2	C-26''	C-25'', C-24'' NH, H-25''
27''	-	162.7	-	NH, H-26''
28''	4.19-4.12 (m)	61.1	C-28''	C-25'', C-24'' NH
Carbonyls				
C ₁₁ '=O	-	176.1, 174.4	-	H-9'', H-10''
C ₁₂ '=O	-		-	
C ₁₉ '=O	-	171.4	-	H-20''
C ₂₇ '=O	-	162.7	-	NH, H-26''
Hydroxyls (OH)				
5, 7, 4', 5'	9.47 (bs), 9.14 (bs), 8.89 (bs)	-	-	-
3''	4.90 (d, 5.7)	-	-	-
Amides (NH)				
19''-NH	10.06	-	-	C ₁₉ '=O
27''-NH	6.44 (bs) 6.36 (bs)	-	-	C ₂₇ '=O, C-28'', C26''
Linker				
1'', 8''	2.77-2.56 (m)	32.9 30.6	C-1'' C-8''	H-4 H-9''
2''-7''	1.64-1.22 (m)	29.6, 29.5, 28.7, 28.6, 28.5, 28.4	C-2''-C-7''	

^aCarbons correlate with the protons resonating at the ppm value indicated in the δ_{H} column.

^bIndicated carbons and protons correlated with the protons or carbons at the position indicated in the left column.

80b

Epicatechin-4-biotin adduct



- CAS : New product
- MM : 881,1
- EM : 880,2846
- MF : C₄₃H₅₂N₄O₁₀S₃

To a solution of **76b** (11.9 mg, 0.026 mmol) in DMSO-*d*₆ (0.5 mL), under Ar atmosphere, was added **59** (9.9 mg, 0.024 mmol). The mixture was shaken for 4 h min after which time ¹H NMR analysis indicated completion of the reaction. The desired reaction product was conveniently precipitated out of the reaction mixture using Et₂O-CHCl₃ (25 mL, 3:2, v/v) to directly furnish pure **80b** (19 mg, 83%) as pale pink sticky solid.

Retention time: 25.9 min

Method: 0-25 min: 0 to 50% then 25-30 min: 50 to 100% MeCN-TFA 0.1%.

Column: Varian Microsorb C-18 (10 × 250 mm, 5μm).

Flow rate: 1mL/min.

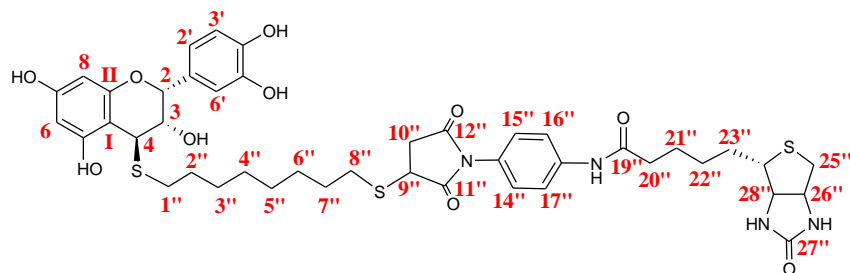
¹H NMR (300MHz, DMSO-*d*₆): δ 10.06 (s, N-H), 9.37 (bs, O-H), 9.09 (bs, O-H), 8.86 (bs, O-H), 7.69 (d, *J* = 8.8, H-16", H-17"), 7.17 (d, *J* = 8.9, H-15", H-14"), 6.91 (d, *J* = 1.5, H-6'), 6.71 (d, *J* = 8.1, H-3'), 6.66 (dd, *J* = 1.5, 8.2, H-2'), 6.44 (bs, N-H), 6.36 (bs, N-H), 5.90 (d, *J* = 2.1, H-8), 5.69 (d, *J* = 2.1, H-6), 5.11 (s, H-2), 5.00 (d, *J* = 3.9, C3-OH), 4.33-4.29 (m, H-26"), 4.12-4.16 (m, H-28"), 4.07 (dd, *J* = 4.1, 9.1, H-9"), 3.84 (s, H-4), 3.81 (bs, H-3), 3.30 (d, *J* = 9.3, H-10"), 3.18-3.09 (m, H-24"), 2.85-2.56 (m, H-1", H-8", H-10", H-25"), 2.33 (t, *J* = 7.2, H-20"), 1.67-1.23 (m, H-2"-H-7", H-21"-H-23").

¹³C NMR (100 MHz, DMSO-*d*₆): δ 176.1, 174.4 (C₁₁"=O, C₁₂"=O), 171.4 (C₁₉"=O), 162.7 (C₂₇"=O), 157.4 (C_{II}, C-7), 155.6 (C-5), 144.7, 144.6 (C-4', C-5'), 139.3 (C-13"), 130.3 (C-1'), 127.3 (C-14", C-15"), 126.8 (C-18"), 119.2 (C-17", C-16"), 117.8 (C-2'), 114.9 (C3', C-6'), 99.0 (C_I), 95.4 (C-8), 93.8 (C-6), 74.0 (C-2), 69.6 (C-3), 61.1 (C-28"), 59.2 (C-26"), 55.4 (C-24"), 42.0 (C-4), 39.8 (C-25"), 39.5 (C-9"), 36.2 (C-10", C-20"), 31.7 (C-1"), 30.6 (C-8"), 30.7, 29.5, 28.6, 28.2, 28.1, 25.1 (C-2"-C-7", C-22"-C-23"), 25.1 (C-21").

IR (Ge): 3268, 1705, 1151, 1022 cm⁻¹.

UV/Vis: λ_{max} 234 nm.

HRMS (ESI-TOF) *m/z*: [M+Na]⁺ calcd. for C₄₃H₅₂N₄O₁₀NaS₃, 903.2737; found, 903.2737.



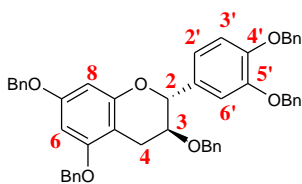
NMR signal assignments of epicatechin-biotin conjugate

position	δ_H (mult., J in Hz)	δ_C (mult.)	HMQC ^a	HMBC ^b
Epicatechin Moiety				
2	5.11 (s)	74.0	C-2	C-4, C-3, C-1', C-2', C-3' C ₃ -OH, H-3, H-2', H-6'
3	3.81 (bs)	69.6	C-3	C-2, C _I O-H, H-4
4	3.84 (s)	42.0	C-4	C-3, C-2, C _I , C _{II} , C-5 H-2, H-1''
5	-	155.6	-	H-4, H-6
6	5.69 (d, 2.1)	93.8	C-6	C-8, C _I , C-5, C-7 H-8
7	-	157.4	-	H-8, H-6
8	5.90 (d, 2.1)	95.4	C-8	H-6
1'	-	130.3	-	H-2, H-2', H-3', H-6'
2'	6.66 (dd, 1.5, 8.2)	117.8	C-2'	C-1', C-3', C-4', C-5', C-6', H-2, H-6'
3'	6.71 (d, 8.1)	114.9	C-3'	C-1', C-4', C-5' H-2'
4', 5'	-	144.6, 144.7	-	H-2', H-3', H-6'
6'	6.91 (d, 1.5)	114.9	C-6'	C-1', C-2', C-4', C-5' H ₂ , H-2'
C _I	-	99.0	-	H-8, H-6, H-4
C _{II}	-	157.4	-	H-8, H-4
Biotin maleimide moiety				
9''	4.07 (dd, 4.1, 9.1)	39.5	C-9''	C-10'', C-8'', C-11'', C-12'' H-10''
10a,b''	3.30 (d, 9.3) 2.85-2.56 (m)	36.2	C-10''	C-9'', C-11'', C-12'' H-9''
11''- 12''	-	176.0, 174.4	-	H-9'', H-10''
13''	-	126.8	-	H-14'' - H-17''
14''- 15''	7.17 (d, 8.9)	127.3	C-14'', C-15''	C-13''- C-15'', C-18'' H-14'' - H-17''
16''- 17''	7.69 (d, 8.8)	119.2	C-16'', C-17''	C-13'', C-16''- C-18'' N-H (19''), H-16'', H-17''
18''	-	139.3	-	H-14'' - H-17''
19''	-	171.4	-	H-20''
20''	2.33 (t, 7.2)	36.2	C-20''	C-19''
21''- 23''	1.67-1.23 (m)	29.5, 28.6, 28.2, 28.1, 25.1	C-21'', C-22'', C-23''	-

Chapter V: Experimental section

24''	3.18-3.09 (m)	55.4	C-24''	H-26'', H-28''
25''	2.85-2.56 (m)	39.8	C-25''	H-26'', H-28'' C-24'', C-26'', C-28''
26''	4.33-4.29 (m)	59.2	C-26''	C-25'', C-24'' NH, H-25''
27''	-	162.7	-	NH, H-26''
28''	4.12-4.16 (m)	61.1	C-28''	C-25'', C-24'' NH, H-25''
Carbonyls				
C ₁₁ '=O	-	176.1, 174.4	-	H-9'', H-10''
C ₁₂ '=O	-		-	
C ₁₉ '=O	-	171.4	-	H-20''
C ₂₇ '=O	-	162.7	-	NH, H-26''
Hydroxyls (OH)				
5, 7, 4', 5'	9.37 (bs), 9.09 (bs), 8.86 (bs)	-	-	-
3''	5.00 (d, 3.9)	-	-	C-2
Amides (NH)				
19''-NH	10.06	-	-	C ₁₉ '=O, C-18'', C-17''
27''-NH	6.44 (bs) 6.36 (bs)	-	-	C ₂₇ '=O, C-28'', C26''
Linker				
1'', 8''	2.85-2.56 (m)	31.7 30.6	C-1'' C-8''	H-4 H-9''
2''-7''	1.67-1.23 (m)	30.7, 29.5, 28.6, 28.2, 28.1, 25.1	C-2''-C-7''	-

^aCarbons correlate with the protons resonating at the ppm value indicated in the δ_{H} column. ^bIndicated carbons and protons correlated with the protons or carbons at the position indicated in the left column.

81a**per-O-benzyl catechin**

- CAS : 85443-49-8
- MM : 740.9
- EM : 740.3138
- MF : C₅₀H₄₄O₆

Under Ar atmosphere **68a** (4.03 g, 6.19 mmol) was dissolved with DMF (10 mL, dry, distilled). In a separate flask NaH (60% suspended in oil, 505.5 mg, 12.6 mmol) was washed with n-pentane (3 × 4 mL), dried under vacuum and suspended with DMF (5 mL). Both solutions were allowed to cool in an ice bath (0°C) and the **68a** solution was added dropwise to the NaH solution. Then, Bn-Br (0.8 mL, 6.68 mmol) was added to the mixture, which was allowed to stir at 0°C for 2 h; after which time TLC analysis indicated completion of the reaction. At 0°C, H₂O (4 mL) was added slowly until no more H₂(g)↑ was observed. The reaction mixture was diluted with AcOEt (100 mL) and extracted with H₂O (100 mL × 3) and brine (100 mL). The organic layer was dried over Na₂SO₄ and the solvent was evaporated, to afford 6 g of beige solid. This solid was purified by silica gel column chromatography, eluting with cyclohexane-AcOEt (95:5, v/v), to furnish **81a** as a pale yellow solid (4.41 g, 96% yield).

mp: 89-90°C.

TLC (Cyclohexane-AcOEt, 9:1, v/v): R_f = 0.4.

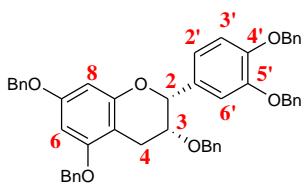
[α]_D = + 39.0°, 1.24 M, CH₂Cl₂.

¹H NMR (300MHz, CDCl₃): δ 7.21-7.47 (m, OBn), 7.00-7.05 (m, H-2'), 6.94 (bs, H-3', H-6'), 6.26 (d, *J* = 2.1, H-8), 6.21 (d, *J* = 2.1, H-6), 6.21 (d, *J* = 2.1, H-6), 5.20 (bs, CH₂, OBn), 5.11 (d, *J* = 6.2, CH₂, OBn), 5.03 (bs, CH₂, OBn), 4.99 (bs, CH₂, OBn), 4.78 (d, *J* = 8.1, H-2), 4.13 (d, *J* = 11.7, CH₂, OBn), 3.69-3.76 (m, H-3), 3.05 (dd, *J* = 5.5, 16.4, H-4a), 2.69 (dd, *J* = 8.7, 16.4, H-4b).

¹³C NMR (75MHz, CDCl₃): δ 158.7 (C-7), 157.6 (C-5), 155.3 (C-9), 148.8 (C-5'), 148.7 (C-4'), 137.9 (Cq), 137.2 (Cq), 137.1 (Cq), 136.9 (Cq), 136.8 (Cq), 132.3 (C-1'), 128.8 (CH), 128.5 (CH), 128.4 (2CH), 128.3 (CH), 128.1 (CH), 127.8 (3CH), 127.7 (CH), 127.4 (2CH), 127.3 (CH), 127.2 (CH), 127.1 (CH), 120.5 (C-2'), 114.8 (C-3'), 113.7 (C-6'), 102.3 (C-10), 94.3 (C-8), 93.7 (C-6), 80.0 (C-2), 74.5 (C-3), 71.5 (CH₂, OBn), 71.2 (CH₂, OBn), 71.0 (CH₂, OBn), 70.0 (CH₂, OBn), 69.8 (CH₂, OBn), 26.0 (C-4).

IR (Zn/Se): 3646, 2924, 1685, 1592, 1496, 1454, 1376, 1261, 1215, 1120, 1027 cm⁻¹.

MS (ESI) *m/z* (rel. intensity): 763 [M+Na]⁺, (77).

81b**per-O-benzyl epicatechin**

- CAS: 301539-02-6
- MM: 740.9
- EM: 740.3138
- MF: C₅₀H₄₄O₆

Under Ar atmosphere **68b** (2.77 g, 4.26 mmol) was dissolved with DMF (9 mL, dry, distilled). In a separate flask NaH (60% suspended in oil, 341 mg, 8.53 mmol) was washed with n-pentane (3 × 4 mL), dried under vacuum and suspended with DMF (3 mL). Both solutions were allowed to cool in an ice bath (0°C) and the **68b** solution was added dropwise to the NaH solution. Then, Bn-Br (0.6 mL, 5.01 mmol) was added to the mixture, which was allowed to stir at 0°C for 3 ½ h; after which time TLC analysis indicated completion of the reaction. At 0°C, H₂O (4 mL) was added slowly until no more H₂(g)↑ was observed. The reaction mixture was diluted with AcOEt (100 mL) and extracted with H₂O (100 mL × 3) and brine (100 mL). The organic layer was dried over Na₂SO₄ and the solvent was evaporated, to afford 6 g of beige solid. This solid was purified by silica gel column chromatography, eluting with cyclohexane-AcOEt (95:5, v/v), to furnish **81b** as a white solid (2.94 g, 93% yield).

mp: 43-44°C.

TLC (Cyclohexane-AcOEt, 9:1, v/v): R_f = 0.4.

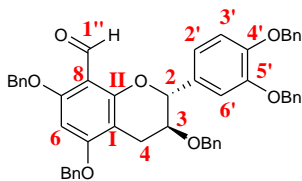
[α]_D = -23.3°, 1.35 M, CH₂Cl₂.

¹H NMR (300 MHz, CDCl₃): δ 7.24-7.56 (m, OBn), 7.10-7.11 (m, H-2'), 7.01 (bs, H-3', H-6'), 6.38 (bs, H-8), 6.36 (bs, H-6), 5.26 (bs, CH₂, OBn), 5.15 (bs, CH₂, OBn), 5.10 (bs, CH₂, OBn), 5.08 (bs, CH₂, OBn), 5.03 (bs, H-2), 4.47 (dd, *J* = 12.5, CH₂, OBn), 4.01 (bs, H-3), 3.09 (dd, *J* = 2.1, 17.0, H-4), 2.87 (dd, *J* = 4.1, 17.0, H-4).

¹³C NMR (75MHz, CDCl₃): δ 158.6 (C-7), 157.9 (C-5), 155.6 (C-9), 148.7 (C-5'), 148.3 (C-4'), 138.1 (Cq), 137.4 (Cq), 137.3 (Cq), 137.1 (Cq), 136.9 (Cq), 132.2 (C-1'), 128.5 (CH), 128.4 (2CH), 128.3 (CH), 128.0 (CH), 127.8 (2CH), 127.7 (CH), 127.6 (3CH), 127.5 (CH), 127.3 (CH), 127.2 (2CH), 119.8 (C-2'), 114.7 (C-3'), 113.8 (C-6'), 101.4 (C-10), 94.7 (C-8), 93.7 (C-6), 76.6 (C-2), 72.6 (C-3), 71.3 (CH₂, OBn), 71.1 (CH₂, OBn), 71.0 (CH₂, OBn), 70.0 (CH₂, OBn), 69.8 (CH₂, OBn), 24.4 (C-4).

IR (Zn/Se): 2922, 2852, 1652, 1646, 1635, 1575, 1558, 1540, 1521, 1457, 696, 668 cm⁻¹.

MS (ESI) *m/z*: 741 [M+H]⁺, (100) and 763 [M+Na]⁺, (75).

82a**per-O-benzyl-8-carbaldehyde catechin**

- CAS: 89385-18-2
- MM: 768.9
- EM: 768.3087
- MF: C₅₁H₄₄O₇

According to the procedure described in the literature,¹⁰⁴ in a 100 mL flask, POCl₃ (2.3 mL, 24.7 mmol) was added dropwise to 4 mL of anhydrous DMF and the reaction mixture was stirred at room temperature under argon atmosphere for 1 h. A solution of compound **81a** (4.19 g, 5.66 mmol) in dry DMF (17 mL) was then added under argon atmosphere. The resulting brown mixture was first stirred at 75°C for 4 h and then at room temperature for 18 h, after which time the reaction mixture was cooled down to 0°C. After the addition of water (20 mL) to quench the reaction (a beige sticky precipitate was formed), the pH was adjusted to 8 with a 2 N solution of NaOH. AcOEt (100 mL) was then added and the reaction mixture was stirred vigorously for 2 h. After separation, the aqueous layer was extracted with AcOEt (3 × 50 mL) and the combined organic extracts were washed with water (3 × 100 mL) and brine (200 mL), dried over Na₂SO₄, filtered and evaporated. The residue was then subjected to chromatography purification, eluting with cyclohexane-AcOEt 9:1, v/v) to (8:2, v/v), to afford the expected product **82a** as a white solid (2.96 g, 68% yield).

mp: 66-67°C.

TLC (Cyclohexane-AcOEt, 8:2, v/v): R_f = 0.3.

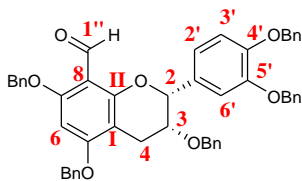
[α]_D = −26.0°, 1.90 M, CH₂Cl₂, (lit.¹⁰⁴ −35.3, 4.9 M, CHCl₃).

¹H NMR (300MHz, CDCl₃): δ 10.47 (s, CHO), 7.13-7.51 (m, HAr), 7.03 (bs, H-2'), 6.95 (bs, H-3', H-6'), 6.20 (s, H-6), 5.21 (bs, CH₂, OBn), 5.17 (bs, CH₂, OBn), 5.13 (bs, CH₂, OBn), 5.07 (bs, CH₂, OBn), 5.03 (d, *J* = 7.0, H-2), 4.33 (d, *J* = 11.9, CH₂, OBn), 3.78 (dd, *J* = 7.1, 12.6, H-3), 2.89 (dd, *J* = 5.2, 16.7, H-4a), 2.73 (dd, *J* = 7.6, 16.6, H-4b).

¹³C NMR (75MHz, CDCl₃): δ 187.3 (CHO), 161.8 (C-7), 160.7 (C-5), 157.7 (C_{II}), 148.6 (C-5'), 148.6 (C-4'), 137.7 (Cq), 137.1 (Cq), 137.0 (Cq), 136.3 (Cq), 135.8 (Cq), 131.5 (C-1'), 128.5 (2CH), 128.3 (2CH), 128.1 (2CH), 127.7 (CH), 127.6 (2CH), 127.5 (CH), 127.2 (CH), 127.1 (2CH), 127.0 (CH), 126.7 (CH), 119.7 (C-2'), 114.7 (C-3'), 113.4 (C-6'), 108.6 (C-8), 102.3 (C_I), 90.7 (C-6), 79.4 (C-2), 73.4 (C-3), 71.3 (CH₂, OBn), 71.1 (CH₂, OBn), 71.0 (CH₂, OBn), 70.5 (CH₂, OBn), 70.0 (CH₂, OBn), 24.8 (C-4).

IR (Zn/Se): 3687, 3064, 3031, 2872, 1674, 1599, 1514, 1454, 1402, 1334, 1261, 1220, 1126, 1026, 738 cm^{−1}.

MS (ESI) *m/z* (rel. intensity): 769 [M+H]⁺, (100).

82b**per-O-benzyl-8-carbaldehyde epicatechin**

- CAS: 1312298-11-5
- MM: 768.9
- EM: 768.3087
- MF: C₅₁H₄₄O₇

According to the procedure described in the literature,¹⁰⁴ POCl₃ (2.1 mL, 22.5 mmol) was added dropwise to 4 mL of anhydrous DMF and the mixture was stirred at room temperature under argon atmosphere for 1 h. A solution of compound **81b** (3.83 g, 5.17 mmol) in dry DMF (15 mL) was then added under argon atmosphere and the resulting brown mixture was first stirred at 75°C for 4 h and then at room temperature for 18 h, after which time the reaction mixture was cooled at 0°C. After the addition of water (20 mL) to quench the reaction (a beige sticky precipitate was formed), the pH was adjusted to 8 with a 2 N solution of NaOH. AcOEt (100 mL) was then added and the reaction mixture was stirred vigorously for 2h. After separation, the aqueous layer was extracted with AcOEt (3 × 50 mL). The combined organic extracts were washed with H₂O (3 × 100 mL) and brine (200 mL), dried over Na₂SO₄, filtered and evaporated. The residue was then subjected to chromatography purification, eluting with cyclohexane-AcOEt (9:1, v/v) to (8:2, v/v), to afford the expected product **82b** as a white solid (2.89 g, 73%).

mp: 55-56°C.

TLC (Cyclohexane-AcOEt, 8:2, v/v): R_f = 0.4.

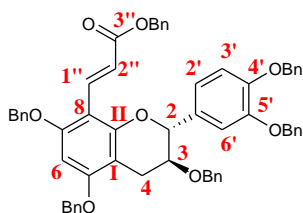
[α]_D = − 81.0°, 1.30 M, CH₂Cl₂.

¹H NMR (300MHz, CDCl₃): δ 10.63 (s, CHO), 7.23-7.55 (m, OBn), 7.03-7.08 (m, H-3', H-6'), 6.96-7.01 (m, H-2'), 6.22 (s, H-6), 5.24 (bs, CH₂, OBn), 5.19 (bs, CH₂, OBn), 5.18 (bs, CH₂, OBn), 5.09 (d, *J* = 17.1, CH₂, OBn), 5.12 (bs, H-2), 4.39 (d, *J* = 12.5, CH₂, OBn), 4.04 (bs, H-3), 3.03 (dd, *J* = 2.8, 17.0, H-4a), 2.81 (dd, *J* = 4.3, 17.0, H-4b).

¹³C NMR (75MHz, CDCl₃): δ 187.1 (CHO), 162.1 (C-7), 160.9 (C-5), 157.8 (C_{II}), 148.6 (C-5'), 148.0 (C-4'), 137.7 (Cq), 137.2 (Cq), 137.1 (Cq), 136.3 (Cq), 135.9 (Cq), 131.4 (C-1'), 128.5 (CH), 128.4 (CH), 128.3 (CH), 128.2 (CH), 128.0 (2 CH), 127.7 (CH), 127.5 (2CH), 127.4 (CH), 127.3 (CH), 127.2 (CH), 127.1 (CH), 127.0 (CH), 126.7 (CH), 119.0 (C-2'), 114.6 (C-3'), 113.1 (C-6'), 108.7 (C-8), 101.6 (C-10), 90.5 (C-6), 77.8 (C-2), 71.4 (C-3), 71.1 (2 CH₂, OBn), 70.7 (CH₂, OBn), 70.5 (CH₂, OBn), 70.0 (CH₂, OBn), 24.4 (C-4).

IR (Zn/Se): 3673, 3654, 3646, 3350, 2924, 2359, 1670, 1599, 1514, 1455, 1418, 1341, 1266, 1226, 1129 cm⁻¹.

MS (ESI) *m/z* (rel. intensity): 769 [M+H]⁺, (65).

83a**per-O-benzyl-8-benzyloxy acrylate catechin**

- CAS: 1312298-13-7
- MM: 901.1
- EM: 900.3662
- MF: C₆₀H₅₂O₈

A 60% dispersion of sodium hydride in mineral oil (115.6 mg, 4.82 mmol) was placed in a 100 mL flask and mineral oil was removed by washing with pentane (3 × 5 mL). Anhydrous DMF (27 mL) was added to the flask containing the sodium hydride under argon atmosphere. To the resulting suspension of NaH, cooled at 0°C, was added dropwise benzyl phosphonoacetate (**87**, 1.26 g, 4.40 mmol) under argon atmosphere. After stirring at room temperature for 20 min, a solution of **82a** (1.81 g, 2.35 mmol) in dry DMF (20 mL) was added dropwise at 0°C. The reaction mixture was stirred at room temperature under argon atmosphere for 19 h, after which time it was diluted with AcOEt (200 mL), extracted with H₂O (3 × 200 mL) and brine (100 mL). The organic extract was dried over anhydrous Na₂SO₄, filtered and evaporated. The resulting residue was purified by column chromatography, eluting with cyclohexane-AcOEt (9:1, v/v) to remove impurities, and then with cyclohexane-AcOEt (8:2, v/v), to give the expected product **83a** as a pale yellow solid (1.67 g, 79%).

mp: 59-60°C.

TLC (Cyclohexane-AcOEt, 8:2, v/v): R_f = 0.5.

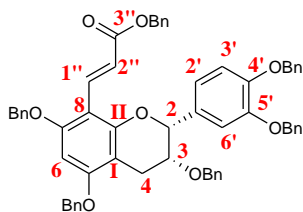
[α]_D = −21.0°, 1.11 M, CH₂Cl₂.

¹H NMR (300MHz, CDCl₃): δ 8.42 (d, *J* = 16.2, H-11), 7.31-7.57 (m, OBn), 7.19-7.22 (m, OBn), 7.10 (bs, H-2'), 7.06 (d, *J* = 16.2, H-12), 7.01 (bs, H-3', H-6'), 6.29 (s, H-6), 5.28 (bs, CH₂, OBn), 5.25 (bs, CH₂, OBn), 5.19 (bs, CH₂, OBn), 5.16 (bs, CH₂, OBn), 5.08 (bs, CH₂, OBn), 5.06 (bs, H-2), 4.38 (d, *J* = 11.9, CH₂, OBn), 3.83 (dd, *J* = 7.2, 12.6, H-3), 2.98 (dd, *J* = 5.3, 16.6, H-4a), 2.83 (dd, *J* = 7.6, 16.4, H-4b).

¹³C NMR (75MHz, CDCl₃): δ 168.5 (C=O), 158.5 (C-7), 158.3 (C-5), 155.1 (C_{II}), 148.8 (C-5'), 148.6 (C-4'), 137.8 (Cq), 137.2 (Cq), 137.1 (Cq), 136.6 (Cq), 136.5 (Cq), 136.3 (Cq), 135.9 (C-11), 131.8 (C-1'), 128.5 (2CH), 128.3 (3CH), 128.1 (CH), 127.9 (CH), 127.8 (CH), 127.7 (CH), 127.6 (4CH), 127.5 (CH), 127.2 (2CH), 127.0 (2CH), 119.8 (C-3'), 117.8 (C-12), 114.8 (C-6'), 113.8 (C-2'), 105.7 (C-8), 102.5 (C_I), 90.9 (C-6), 79.5 (C-2), 73.7 (C-3), 71.3 (CH₂, OBn), 71.2 (CH₂, OBn), 70.1 (CH₂, OBn), 70.7 (CH₂, OBn), 69.9 (CH₂, OBn), 65.4 (CH₂, OBn), 25.1 (C-4).

IR (Zn/Se): 3718, 3063, 3031, 2867, 2364, 1702, 1599, 1513, 1454, 1420, 1378, 1251, 1215, 1126, 1027 cm^{−1}.

HRMS (ESI-TOF) *m/z*: [M+Na]⁺ calcd. for C₆₀H₅₂O₈Na 923.3554, found 923.3566.

83b**per-O-benzyl-8-benzyloxy acrylate epicatechin**

- CAS: 1312298-14-8
- MM: 901.1
- EM: 900.3662
- MF: C₆₀H₅₂O₈

A 60% dispersion of sodium hydride in mineral oil (179.9 mg, 7.50 mmol) was placed in a 100 mL flask and mineral oil was removed by washing with pentane (3 × 5 mL). Anhydrous DMF (20 mL) was added to the flask containing the sodium hydride under argon atmosphere. To the resulting suspension of NaH, cooled at 0°C, was added dropwise benzyl phosphonoacetate (**87**, 1.59 g, 5.55 mmol) under argon atmosphere. After stirring at room temperature for 20 min, a solution of **82b** (2.80 g, 3.64 mmol) in dry DMF (35 mL) was added dropwise at 0°C. The reaction mixture was stirred at room temperature under argon atmosphere for 19 h, after which time it was diluted with AcOEt (200 mL), extracted with H₂O (3 × 200 mL) and brine (100 mL). The organic extract was dried over anhydrous Na₂SO₄, filtered and evaporated. The resulting residue was purified by column chromatography, eluting with cyclohexane-AcOEt (9:1, v/v) to remove impurities, and then with cyclohexane-AcOEt (8:2, v/v), to give the expected product **83b** as a white solid (2.64 g, 80%).

mp: 95-96°C.

TLC (Cyclohexane-AcOEt, 8:2, v/v): R_f = 0.5.

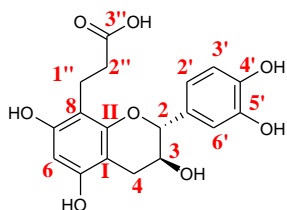
[α]_D = − 27.9°, 0.6 M, CH₂Cl₂.

¹H NMR (300MHz, CDCl₃): δ 8.38 (d, *J* = 16.2, H-11), 7.20-7.53 (m, OBn), 7.04 (d, *J* = 16.3, H-12), 7.02-7.05 (m, H-2'), 6.94 (bs, H-3', H6'), 6.22 (s, H-6), 5.21 (bs, CH₂, OBn), 5.21 (s, CH₂, OBn), 5.13 (d, *J* = 12.5, H-2), 5.03 (bs, 2CH₂, OBn), 4.38 (d, *J* = 12.5, CH₂, OBn), 3.98 (bs, H-3), 2.97 (dd, *J* = 3.5, 17.1, H-4a), 2.82 (dd, *J* = 4.3, 17.0, H-4b).

¹³C NMR (300MHz, CDCl₃): δ 168.6 (C=O), 158.9 (C-7), 158.3 (C-5), 155.4 (C_{II}), 148.9 (C-5'), 148.2 (C-4'), 137.9 (Cq), 137.4, (Cq), 137.3 (Cq), 136.7 (Cq), 136.6 (Cq), 136.5 (Cq), 136.1 (C-11), 131.7 (C-1'), 128.6 (2CH), 128.4 (CH), 128.3 (2CH), 128.1 (CH), 128.0 (CH), 127.9 (CH), 127.8 (CH), 127.7 (2CH), 127.6 (CH), 127.5 (CH), 127.4 (CH), 127.3 (2CH), 127.1 (CH), 127.0 (CH), 119.2 (C-3'), 117.8 (C-12), 114.8 (C-6'), 113.3 (C-2'), 106.1 (C-8), 101.9 (C_I), 91.0 (C-6), 78.1 (C-2), 72.0 (C-3), 71.4 (CH₂, OBn), 71.2 (CH₂, OBn), 70.9 (CH₂, OBn), 70.7 (CH₂, OBn), 70.0 (CH₂, OBn), 65.5 (CH₂, OBn), 24.6 (C-4).

IR (Zn/Se): 3700, 3061, 3029, 2363, 2341, 1700, 1599, 1508, 1498, 1452, 1418, 1289, 1269, 1215, 1121, 1014, 732 cm⁻¹.

HRMS (ESI-TOF) *m/z*: [M+Na]⁺ calcd. for C₆₀H₅₂O₈Na 923.3554, found 923.3604.

84a**Catechin-8-propanoic acid**

- CAS: 89385-46-6
- MM: 362.3
- EM: 362.1002
- MF: C₁₈H₁₈O₈

Debenzylation and reduction of compound **83a** (1.06 g, 1.18 mmol) in a mixture of THF (4 mL), MeOH (4 mL) and CH₂Cl₂ (1.4 mL) was carried out under H₂ (balloon) at room temperature for 72 h in the presence of 10 wt % Pd/C (279 mg Pd/C, 0.26 mmol Pd). After evaporation of the solvents, the crude residue was dissolved in EtOAc, filtered through Celite® and the solid was washed with AcOEt (100 mL). Evaporation of the solvent furnished the expected product **84a** as a white solid (428 mg, quantitative yield).

mp: 198-199°C (decomp.).

TLC (CH₂Cl₂-MeOH, 8:2, v/v): R_f = 0.2.

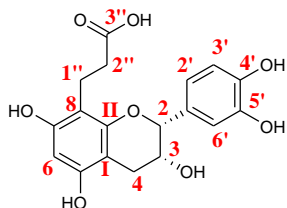
[α]_D = + 61.0°, 2.8 M, acetone.

¹H NMR (300MHz, Acetone-*d*₆): δ 6.92-6.92 (m, H-2'), 6.75-6.81 (m, H-3', H-6'), 6.08 (s, H-6), 4.64 (d, *J* = 7.6, H-2), 3.97 (dd, *J* = 7.6, 13.4, H-3), 3.57 (s, C₃-OH), 2.90 (dd, *J* = 5.3, 16.2, H-4a), 2.79-2.83 (m, H-1''), 2.55-2.60 (m, H-4b), 2.52-2.55 (m, H-2'').

¹³C NMR (75MHz, Acetone-*d*₆): δ 176.2 (C=O), 154.8 (C-7), 154.8 (C-5), 154.2 (C_{II}), 145.5 (C-5'), 145.4 (C-4'), 132.2 (C-1'), 119.5 (C-3'), 115.6 (C-6'), 114.7 (C-2'), 106.5 (C-8), 100.7 (C_I), 96.4 (C-6), 82.4 (C-2), 68.2 (C-3), 34.1 (C-2''), 28.5 (C-4), 18.9 (C-1'').

IR (Zn/Se): 3362, 1694, 1619, 1523, 1454, 1378, 1283, 1209, 1174, 1060 cm⁻¹.

HRMS (ESI-TOF) *m/z*: [M+Na]⁺ calcd. for C₁₈H₁₈O₈Na 385.0893, found 385.0891.

84b**Epicatechin-8-propanoic acid**

- CAS: 1312298-17-1
- MM: 362.3
- EM: 362.1002
- MF: C₁₈H₁₈O₈

Debenzylation and reduction of compound **83b** (668.6 mg, 0.74 mmol) in a mixture of THF (2.7 mL), MeOH (2.7 mL) and CH₂Cl₂ (0.9 mL) was carried out under H₂ (balloon) at room temperature for 72 h in the presence of 10 wt % Pd/C (185 mg Pd/C, 0.17 mmol Pd). After evaporation of the solvents, the crude residue was dissolved in EtOAc, filtered through Celite® and the solid was washed with AcOEt (100 mL). Evaporation of the solvent furnished the expected product **84b** as a white solid (267 mg, quantitative yield).

mp: 66-67°C.

TLC (CH₂Cl₂-MeOH, 8:2, v/v): R_f = 0.2.

[α]_D = − 28.6°, 1.0 M, acetone.

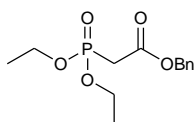
¹H NMR (300MHz, Acetone-*d*₆): δ 7.10 (d, *J* = 1.7, H-2'), 6.78-6.88 (m, H-3', H-6'), 6.07 (s, H-6), 4.93 (bs, H-2), 4.23 (bs, H-3), 2.87-2.92 (m, H-4a), 2.83-2.85 (m, H-2''), 2.77 (dd, *J* = 2.9, 16.8 H-4b), 2.59 (m, H-1'').

¹³C NMR (300MHz Acetone-*d*₆): δ 177.4 (C=O), 155.2 (C-7), 154.8 (C-5), 154.4 (C_{II}), 145.3 (C-5'), 145.1 (C-4'), 132.2 (C-1'), 118.8 (C-3'), 115.4 (C-6'), 114.8 (C-2'), 107.1 (C-8), 99.8 (C-10), 96.6 (C-6), 79.1 (C-2), 66.5 (C-3), 34.7 (C-2''), 28.9 (C-4), 18.9 (C-1'').

IR (Zn/Se): 3356, 2930, 2349, 1697, 1620, 1520, 1455, 1368, 1285, 1240, 1203, 1171, 1105, 1068, 1045 cm^{−1}.

HRMS (ESI-TOF) *m/z*: [M+Na]⁺ calcd. for C₁₈H₁₈O₈Na 385.0893, found 385.0897.

87

Benzyl *O*, *O*-diethylphosphonoacetate

- CAS: 7396-44-3
- MM: 286.3
- EM: 286.0970
- MF: C₁₃H₁₉O₅P

According to the procedure described in the literature,¹⁴⁶ a mixture of benzyl-2-bromoacetate (5.5 mL, 35 mmol) and triethyl phosphite (6.6 mL, 39 mmol) was stirred and gradually heated to distil ethyl bromide (bp = 39°C). After completion of the distillation, the reaction mixture was heated to 200°C for 1 h and then cooled gently to room temperature. The fractionated distillation under vacuum provided **87** [bp = 165°C, 0.9 mm Hg, (lit.¹⁴⁶ bp = 130°C, 0.1 mm Hg)], as a colorless oil (7.23 g, 72%).

TLC (Cyclohexane-CH₂Cl₂): R_f = 0.1.

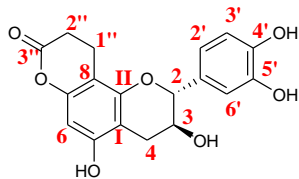
¹H NMR (300 MHz, CDCl₃): δ 7.32-7.39 (m, OBn), 5.18 (s, CH₂, OBn), 4.08-4.18 (m, CH₂), 3.01 (d, *J* = 21.5, CH₂), 1.29 (t, *J* = 7.0, 2CH₃).

¹³C NMR (75.5 MHz, CDCl₃): δ 165.6 (d, *J*_{C-P} = 6.3, C=O), 135.3 (Cq), 128.5 (CH), 128.4 (CH), 128.3 (CH), 67.3 (CH₂, OBn), 62.7 (CH₂), 62.6 (CH₂), 34.4 (d, *J*_{C-P} = 134.2, CH₂), 16.3 (CH₃), 16.2 (CH₃).

³¹P NMR (75.5 MHz, CDCl₃): δ 19.42 (bs).

IR (Zn/Se): 3477, 2985, 2335, 1737, 1456, 1394, 1270, 1213, 1163, 1116, 1051, 1024, 973, 838, 782, 752, 700, 615 cm⁻¹.

HRMS (ESI-TOF) *m/z*: [M+Na]⁺ calcd. for C₁₃H₁₉O₅NaP 309.0862, found 309.0869.



- CAS: 1312298-20-6
- MM: 344.3
- EM: 344.0896
- MF: C₁₈H₁₆O₇

84a (61.4 mg, 0.17 mmol) was dissolved with DMF (1.5 mL, distilled), under Ar atmosphere, to give a colorless solution. To this solution was added HOBT (22.9 mg, 0.17 mmol) and EDCI (33.1 mg, 0.17 mmol) and the mixture was allowed to stir at room temperature for 21 h. After which time TLC analysis indicated complete consumption of **84a**, and apparition of a new compound with the same R_f of compound **88**. Then, octanedithiol (47 μ L, 0.25 mmol, 1.5 equiv.) was added and the mixture was heated to 50°C, for 7 days without evolution of the reaction mixture. More octanedithiol (47 μ L, 0.25 mmol, 1.5 equiv.) was added and the reaction mixture was submitted to microwave irradiation (50 watts, 50°C) for 15 min (\times 3). TLC monitoring indicated still no evolution of the reaction. The reaction mixture was diluted with AcOEt (30 mL) and extracted with H₂O (20 mL \times 2) and brine (20 mL). The organic layer was dried over Na₂SO₄ and the solvent was evaporated to afford 137 mg of a white solid. This solid was purified by silica gel column chromatography, eluting with CH₂Cl₂-MeOH (9:1, v/v) to furnish 31.6 mg, 54% yield of **88** as a white solid.

mp: 222-223°C.

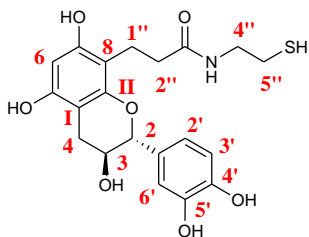
TLC (CH₂Cl₂-MeOH, 9:1 v/v): R_f = 0.5

¹H NMR (300MHz, Acetone-*d*₆): δ 8.60 (bs, OH), 7.92 (bs, OH), 6.90 (d, *J* = 1.7, H-2'), 6.75-6.82 (m, H-3', H-6'), 6.16 (s, H-6), 4.72 (d, *J* = 7.4, H-2), 4.02-4.12 (m, H-3), 3.02 (bs, C₃-OH), 2.91-2.98 (m, H-4a), 2.79-2.86 (m, H-1''), 2.66-2.71 (m, H-2''), 2.58-2.63 (m, H-4b).

¹³C NMR (75MHz, Acetone-*d*₆): δ 168.8 (C=O), 155.7 (C-7), 152.8 (C-5), 152.1 (C_{II}), 145.9 (C-5'), 145.8 (C-4'), 131.8 (C-1'), 119.8 (C-3'), 115.9 (C-6'), 115.1 (C-2'), 105.4 (C-8), 102.3 (C_I), 96.2 (C-6), 82.9 (C-2), 67.8 (C-3), 32.0 (C-2''), 28.6 (C-4), 18.1 (C-1'').

IR (Zn/Se): 3395, 2263, 1739, 1618, 1521, 1454, 1418, 1372, 1337, 1286, 1114 cm⁻¹.

MS (ESI) *m/z* (rel. intensity): 343 [M-H]⁻, (51).

89a**Catechin-8-propanamide -N-(5''-mercaptoethyl)**

- CAS: New product
- MM: 421,5
- EM: 421,1195
- MF: C₂₀H₂₃NO₇S

To a solution of **84a** (105.9 mg, 0.29 mmol) in MeCN (8 mL), under Ar atmosphere, was added EDCI (62.9 mg, 0.33 mmol). The mixture was stirred at 50°C for 2 h, after which time TLC analysis indicated complete consumption of **84a** to give the corresponding lactone **88a** (TLC (CH₂Cl₂-MeOH, 9:1, v/v: R_f _{lactone} = 0.5). The mixture was allowed to reach room temperature and cysteamine (71 mg, 0.92 mmol) was added. The mixture was heated to 40°C for 1 h, after which time TLC analysis indicated completion of the reaction. The solvent was evaporated under reduced pressure to give 205 mg of a sticky pale yellow residue. This residue was purified by silica gel column chromatography eluting with a CH₂Cl₂-MeOH (9:1, v/v) to furnish pure **89a** (76 mg, 62%) as white sticky solid.

TLC (CH₂Cl₂-MeOH, 9:1 v/v): R_f = 0.2.

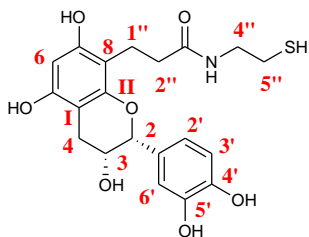
¹H NMR (300MHz, Acetone-*d*₆): δ 8.92 (bs, O-H), 8.01 (bs, O-H), 7.58 (t, J = 5.4, NH), 6.92 (d, J = 1.8, H-6'), 6.80 (d, J = 7.9, H-3'), 6.76 (dd, J = 1.8, 8.3, H-2'), 6.04 (s, H-6), 4.62 (d, J = 7.6, H-2), 3.99-3.92 (m, H-3), 3.35-3.26 (m, H-4''), 2.89 (dd, J = 5.4 (cis), 16.1 (gem), H-4), 2.77-2.72 (m, H-1''), 2.60-2.50 (m, H-2'', H-5'', H-4 (trans)), 1.75 (t, J = 8.4, S-H).

¹³C NMR (100 MHz, Acetone-*d*₆): δ 175.9 (C₃'=O), 155.5, 155.1 (C-5, C-7), 154.3 (C_{II}), 145.7, 145.6 (C-4', C-5'), 132.4 (C-1'), 119.7 (C-2'), 115.7 (C-3'), 115.0 (C-6'), 107.6 (C-8), 100.8 (C_I), 97.4 (C-6), 82.6 (C-2), 68.3 (C-3), 43.7 (C-4''), 35.9 (C-2''), 28.8 (C-4), 24.3 (C-5''), 18.6 (C-1'').

IR (Zn/Se): 3331, 2936, 1698, 1617, 1528, 1453, 1106 cm⁻¹.

UV/Vis: λ_{max1} 235 nm, λ_{max2} 270 nm.

HRMS (ESI-TOF) *m/z*: [M+Na]⁺ calcd. for C₂₀H₂₃NO₇NaS 444.1087, found 444.1103.

89b**Epicatechin-8-propanamide-N-(5''-mercaptoethyl)**

- CAS: New product
- MM: 421,5
- EM: 421,1195
- MF: C₂₀H₂₃NO₇S

To a solution of **84b** (118.1 mg, 0.33 mmol) in MeCN (9 mL), under Ar atmosphere, was added EDCI (71.5 mg, 0.37 mmol). The mixture was stirred at 50°C for 2 h, after which time TLC analysis indicated complete consumption of **84b** to give the corresponding lactone **88b** (TLC (CH₂Cl₂-MeOH, 9:1 v/v): R_f _{lactone} = 0.5). The mixture was allowed to reach room temperature and cysteamine (79 mg, 1.02 mmol) was added. The mixture was heated to 40°C for 1 h, after which time TLC analysis indicated completion of the reaction. The solvent was evaporated under reduced pressure to give 233 mg of a sticky white residue. This residue was purified by silica gel column chromatography eluting with a CH₂Cl₂-MeOH (9:1, v/v) to furnish **89b** (49.4 mg, 36%) as white sticky solid.

TLC (CH₂Cl₂-MeOH, 9:1 v/v): R_f = 0.2.

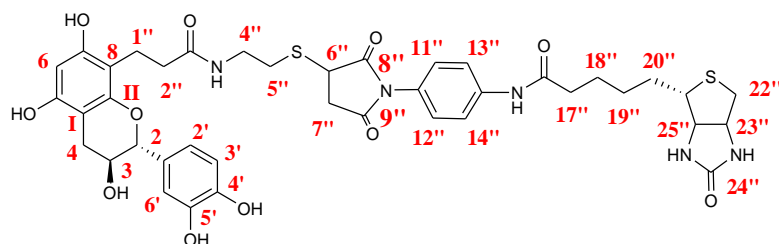
¹H NMR (300MHz, MeOD-*d*₄): δ 7.02 (d, *J* = 1.9, H-6'), 6.83 (dd, *J* = 1.9, 8.6, H-2'), 6.78 (d, *J* = 8.1, H-3'), 6.00 (s, H-6), 4.84 (s, H-2), 4.23-4.21 (m, H-3), 3.24 (dd, *J* = 7.0, 15.0, H-4''), 2.97-2.74 (m, H-4, H-5''), 2.54-2.46 (m, H-2'', H-1'').

¹³C NMR (75 MHz, MeOD-*d*₄): δ 177.0 (C₃'=O), 155.8 (C-5 or C-7), 155.1 (C_{II}), 154.9 (C-5 or C-7), 146.0, 145.7 (C-4', C-5'), 132.4 (C-1'), 119.1 (C-2'), 116.0 (C-3'), 115.0 (C-6'), 107.3 (C-8), 100.1 (C_I), 96.5 (C-6), 79.6 (C-2), 67.1 (C-3), 44.0 (C-4''), 36.9 (C-2''), 29.6 (C-4), 24.3 (C-5''), 20.0 (C-1'').

IR (Zn/Se): 3356, 2978, 1620, 1530, 1454, 1106 cm⁻¹.

UV/Vis: λ_{max1} 288 nm, λ_{max2} 277 nm.

HRMS (ESI-TOF) *m/z*: [M+Na]⁺ calcd. for C₂₀H₂₃NO₇NaS 444.1087, found 444.1083.

90a**Catechin-8-biotin adduct**

- CAS: New product
- MM: 835,9
- ME: 835,2557
- MF: C₄₀H₄₅N₅O₁₁S₂

To a solution of **89a** (10.6 mg, 0.025 mmol) in DMSO-*d*₆ (0.6 mL), under Ar atmosphere, was added **59** (9.4 mg, 0.023 mmol). The mixture was shaken for 10 min after which time ¹H NMR analysis indicated completion of the reaction. The desired reaction product was conveniently precipitated out of the reaction mixture using Et₂O-CHCl₃ (40 mL, 35:4, v/v) to directly furnish **90a** (19 mg, quantitative yield) as pale pink sticky solid.

Retention time: 17.7 min.

Method: 0-25 min: 0 to 50% MeCN-TFA 0.1%.

Column: Varian Microsorb C-18 (10 × 250 mm, 5 μm).

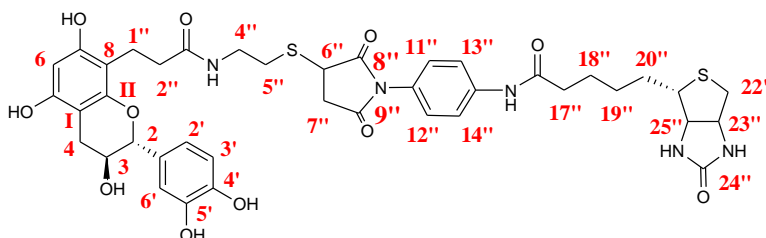
Flow rate: 1 mL/min.

¹H NMR (300 MHz, DMSO-*d*₆): δ 10.07 (s, 16''-NH), 8.99 (s, OH-Ar), 8.95 (s, OH-Ar), 8.85 (s, OH-Ar), 7.94 (t, J = 5.6, 3''-NH), 7.68 (d, J = 8.9, H-13'', H-14''), 7.18 (d, J = 8.8, H-11'', H-12''), 6.71 (d, J = 1.7, H-6'), 6.68 (d, J = 8.1, H-3'), 6.59 (dd, J = 1.7, 8.2, H-2''), 6.45 (s, NH), 6.37 (s, NH), 5.97 (s, H-6), 4.88 (d, J = 5.0, C3-OH), 4.56 (d, J = 7.0, H-2), 4.33-4.27 (m, H-23''), 4.16-4.09 (m, H-6'', H-25''), 3.82-3.74 (m, H-3), 3.32-3.26 (m, H-4''), 3.19-3.11 (m, H-21''), 2.92-2.56 (m, H-4, H-1'', H-2'', H-7'', H-22''), 2.33 (t, J = 7.3, H-17''), 2.07-2.18 (m, H-5''), 1.64 - 1.36 (m, H-18''- H-20'').

¹³C NMR (100 MHz, DMSO-*d*₆): δ 176.1, 174.4 (C₈''=O, C₉''=O), 172.9 (C₃''=O), 171.5 (C₁₆''=O), 162.8 (C₂₄''=O), 153.8, 153.7 (C-5, C-7), 153.0 (C_{II}), 144.8, 144.7 (C-4', C-5'), 139.3 (C-10''), 131.0 (C-1'), 127.4 (C-11'', C-12''), 126.9 (C-15''), 119.3 (C-13'', C-14''), 117.9 (C-2'), 115.1 (C-3'), 114.3 (C-6'), 105.1 (C-8), 99.1 (C_I), 95.2 (C-6), 80.9 (C-2), 66.4 (C-3), 61.1 (C-25''), 59.3 (C-23''), 55.4 (C-21''), 39.8 (C-6''), 39.4 (C-22''), 38.2 (C-4''), 36.3, 36.2 (C-7'', C-17''), 35.2 (C-5''), 30.6 (C-2''), 27.7 (C-4), 28.3, 28.1, 25.1 (C₁₈'', C-19'', C-20''), 18.5 (C-1').

UV/Vis: λ_{max1} 202 nm, λ_{max2} 225 nm, λ_{max} 250 nm.

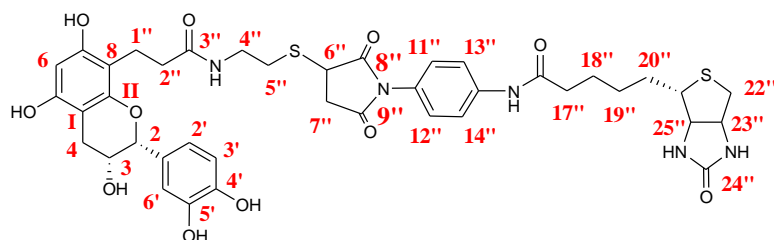
MS (ESI) *m/z* (rel. intensity): 836 [M+H]⁺, (40).



position	δ_H (mult., J in Hz)	δ_C (mult.)	HSQC ^a	HMBC ^b
Catechin Moiety				
2	4.56 (d, 7.0)	80.9	C-2	C-4, C-3, C-1', C-2', C-3', C-6', C _{II} 3-OH, H-4, H-2', H-6'
3	3.82-3.74 (m)	66.4	C-3	H-2, 3-OH
4	2.92-2.31 (m)	27.7	C-4	C-3, C-2, C _I , C _{II} H-2, 3-OH
5, 7	-	153.8, 153.7	-	H-6, OH(Ar)
6	5.97 (s)	95.2	C-6	C-8, C _I , C-5, C-7
8	-	105.1	-	H-6, OH(Ar)
1'	-	131.0	-	H-2, H-3'
2'	6.59 (dd, 1.7, 8.2)	117.9	C-2'	C-4', C-5', C-6' H-2, H-3', H-6'
3'	6.68 (d, 8.1)	115.2	C-3'	C-1', C-2', C-4', C-5', C-6' H-2, H-6'
4', 5'	-	144.7, 144.8	-	H-2', H-3', H-6'
6'	6.71 (d, 1.7)	114.3	C-6'	C-1', C-2', C-4', C-5' H-2, H-2'
C _I	-	99.1	-	H-6, H-4
C _{II}	-	153.0	-	H-6
Biotin maleimide moiety				
6''	4.16-4.09 (m)	39.4	C-6''	C-7'', C-8'', C-9'' H-7'', H-5''
7a,b''	2.92-2.31 (m) 3.32-3.26 (m)	36.3 or 36.2	C-7''	C-8'', C-9'' H-6''
8''- 9''	-	176.1, 174.4	-	H-6'', H-7''
10''	-	126.9	-	H-11'' - H-14''
11''-12''	7.18 (d, 8.8)	127.4	C-11'', 12''	C-10'' - C-15'' H-11'' - H-14''
13''- 14''	7.68 (d, 8.9)	119.3	C-13'', 14''	C-10'' - C-15'' N-H (16''), H-13'', H-14''
15''	-	139.3	-	H-11'' - H-14''
16''	-	171.5	-	N-H, H-17''

17''	2.33 (t, 7.3)	36.3 or 36.2	C-17''	C ₁₆ '=O H-18''
18''-20''	1.64 - 1.36 (m)	25.1 28.3, 28.1	C-18'' C19''-20''	C-17'' - C-21'' H-17'' - H-21''
21''	3.19-3.11 (m)	55.4	C-21''	C-20'' H-20'', H-22'', H-23'', H-25''
22''	2.92-2.56 (m)	39.8	C-22''	C-21'', C-23'', C-25'' H-22'', H-25''
23''	4.33-4.27 (m)	59.3	C-23''	C-21'', C-22'' NH (24''), H-22''
24''	-	162.8	-	NH, H-23'', H-25''
25''	4.16-4.09 (m)	61.1	C-25''	C-21'', C-22'', C-24'' NH (24''), H-22''
Carbonyls				
C ₃ '=O	-	172.9	-	N-H, H-4''
C ₈ '=O	-	176.1, 174.4	-	H-6'', H-7''
C ₉ '=O	-	171.5	-	N-H
C ₁₆ '=O	-	162.8	-	N-H, H-23''
C ₂₄ '=O	-			
Hydroxyls (OH)				
5, 7, 4', 5'	8.99 (bs), 8.95 (bs), 8.85 (bs)	-	-	C-5 - C-8, C ₁
3''	4.88 (d, 5.0)	-	-	C-3, C-2
Amides (NH)				
3''-NH	7.95 (t, 5.6)	-	-	C ₃ '=O
16''-NH	10.07 (s)	-	-	C ₁₆ '=O
24''-NH	6.45 (bs) 6.47 (bs)	-	-	C ₂₄ '=O, C-25'', C23''
Linker				
1''	2.92-2.31 (m)	18.5	C-1''	
2''	2.07-2.18 (m)	35.2	C-2''	
3''	-	172.9	-	N-H, H-4''
4''	3.32-3.26 (m)	38.2	C-4''	C ₃ '=O, C ₈ '=O, C ₉ '=O H-5''
5''	2.92-2.31 (m)	30.6	C-5''	C-6'', C ₈ '=O, C ₉ '=O H-6''

^aCarbons correlate with the protons resonating at the ppm value indicated in the δ_{H} column. ^bIndicated carbons and protons correlated with the protons or carbons at the position indicated in the left column.

90b**Epicatechin-8-biotin adduct**

- CAS: New product
- MM: 835,9
- EM: 835,2557
- MF: C₄₀H₄₅N₅O₁₁S₂

To a solution of **89b** (11.7 mg, 0.028 mmol) in DMSO-*d*₆ (0.5 mL), under Ar atmosphere, was added **59** (10.4 mg, 0.025 mmol). The mixture was shaken for 30 min, after which time ¹H NMR analysis indicated completion of the reaction. The desired reaction product was conveniently precipitated out of the reaction mixture using Et₂O-CHCl₃ (40 mL, 9:1, v/v) to directly furnish **90b** (21 mg, quantitative yield) as pale pink sticky solid.

Retention time: 18.6 min.

Method: 0-25 min: 0 to 50% MeCN-TFA 0.1%.

Column: Varian Microsorb C-18 (10 × 250 mm, 5μm).

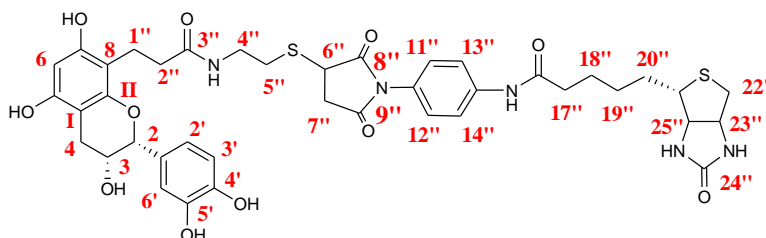
Flow rate: 1mL/min.

¹H NMR (300MHz, DMSO-*d*₆): δ 10.01 (s, N-H), 8.93 (s, O-H), 8.92 (s, O-H), 8.77 (bs, O-H), 7.96 (t, *J* = 5.6, N-H), 7.68 (d, *J* = 8.8, H-13", H-14"), 7.18 (d, *J* = 8.8, H-11", H-12"), 6.87 (s, H-6'), 6.67 (bs, H-2', H-3'), 6.45 (s, N-H), 6.37 (s, N-H), 5.97 (s, H-6), 4.78 (s, H-2), 4.62 (d, *J* = 4.7, O-H), 4.32- 4.29 (m, H-23"), 4.16-4.09 (m, H-6", H-25"), 4.02 (m, H-3), 3.32-3.26 (m, H-4", H-7"), 3.14-3.09 (m, H-21"), 2.92-2.31 (m, H-4, H-1", H-5", H-7", H-22"), 2.35-2.18 (m, H-2"), 2.33 (t, *J* = 7.4, H-17"), 1.64-1.36 (m, H-18" - H-20").

¹³C NMR (100 MHz, DMSO-*d*₆): δ 176.1, 174.4 (C₈=O, C₉=O), 173.0 (C₃=O), 171.5 (C₁₆=O), 162.8 (C₂₄=O), 154.0, 153.7, 153.3 (C-5, C-7, C₁₁), 144.6, 144.3 (C-4', C-5'), 139.3 (C-15"), 130.9 (C-1'), 127.4 (C-11", C-12"), 126.8 (C-10"), 119.3 (C-13", C-14"), 117.6 (C-3'), 114.8, 114.5 (C-2', C-6'), 105.3 (C-8), 98.5 (C₁), 95.2 (C-6), 78.0 (C-2), 64.8 (C-3), 61.1 (C-25"), 59.2 (C-23"), 55.4 (C-21"), 39.9 (C-22"), 39.5 (C-6"), 38.2 (C-4"), 36.2 (C-7", C-17"), 35.2 (C-2"), 30.6 (C-5"), 28.2, 28.1 (C-4, C-19", C-20"), 25.1 (C-18"), 18.4 (C-1").

UV/Vis: λ_{max1} 240 nm, λ_{max2} 280 nm.

HRMS (ESI-TOF) *m/z*: [M+Na]⁺ calcd. for C₄₀H₄₅N₅O₁₁NaS₂ 858.2449, found 858.2435.



NMR signal assignments of epicatechin-biotin conjugate (A-Ring)

position	δ_H (mult., J in Hz)	δ_C (mult.)	HSQC ^a	HMBC ^b
Catechin Moiety				
2	4.78 (s)	78.0	C-2	C-4, C-1', C-2', C-3', C-6', C _{II} H-4, H-2', H-3', H-6'
3	4.02 (m)	64.8	C-3	3-OH, H-4
4	2.94-2.45 (m)	28.2	C-4	C-3, C-2, C _I H-2, 3-OH
5, 7, II	-	154.0, 153.7, 153.3	-	H-6, OH(Ar)
6	5.97 (s)	95.2	C-6	C-8, C _I , C-5, C-7
8	-	105.3	-	H-6, OH(Ar)
1'	-	130.9	-	H-2, H-6', H-3'
2', 3'	6.67 (bs)	114.8 or 114.5	C-2'	C-4', C-5', C-1', C-6' H-2, H-3', H-6'
		117.6	C-3'	
4', 5'	-	144.6, 144.3	-	H-2', H-3', H-6', O-H(Ar)
6'	6.87 (s)	114.8 or 114.5	C-6'	C-4', C-5', C-1', C-2' H-2, H-2', O-H (Ar)
C _I	-	98.5	-	H-6, H-4, O-H (Ar)
C _{II}	-	154.0 or 153.7 or 153.3	-	H-6
Biotin maleimide moiety				
6''	4.16-4.09 (m)	39.5	C-6''	C-5'', C-7'', C-8'', C-9'' H-5'', H-7''
7a,b''	2.94-2.45 (m) 3.32-3.26 (m)	36.2	C-7''	C-5'', C-6'', C-8'', C-9'' H-6''
8''- 9''	-	176.1, 174.4	-	H-6'', H-7''
10''	-	126.8	-	H-11'', H-12'', H-13'', H-14''
11''-12''	7.18 (d, 8.8)	127.4	C-11'', 12''	C-10'', C-11'', C-12'', C-15'' H-13'', H-14'', H-11'', H-12''
13''- 14''	7.68 (d, 8.8)	119.3	C-13'', 14''	C-10'', C-11'', C-12'', C-13'', C-14'' C-15'', N-H (16''), H-13'', H-14''
15''	-	139.3	-	N-H (16''), H-11'', H-12'', H-13'', H-14''

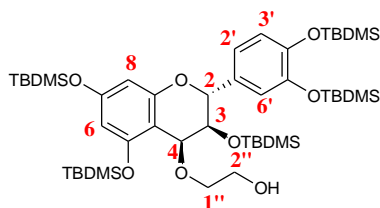
16''	-	171.5	-	N-H (16''), H-17''
17''	2.33 (t, 7.4)	36.2	C-17''	C ₁₆ =O H-18''
18''-20''	1.64-1.36 (m)	28.2, 28.1	C-19''-20''	C-17'' - C-21'' H-17'' - H-21
21''	3.14-3.09 (m)	55.4	C-21''	C-20'' H-20'', H-22'', H-23'', H-25''
22''	2.94-2.45 (m)	39.9	C-22''	C-21'', C-23'', C-25'' H-22'', H-25''
23''	4.32- 4.29 (m)	59.2	C-23''	C-21'', C-22'', C-25'' N-H (24''), H-22''
24''	-	162.8	-	N-H (24''), H-23'', H-25''
25''	4.16-4.09 (m)	61.1	C-25''	C-21'', C-22'', C-24'' N-H (24''), H-22'', H-23''
Carbonyls				
C ₃ =O	-	173.0	-	N-H (3''), H-4'', H-2''
C ₈ =O	-	176.1, 174.4	-	H-6'', H-7''
C ₉ =O	-		-	
C ₁₆ =O	-	171.5	-	N-H (16'')
C ₂₄ =O	-	162.8	-	N-H (24''), H-23''
Hydroxyls (OH)				
5, 7,	8.93 (s), 8.92 (s),	-	-	C ₁ , C-6, C-8, C-5, C-7
4', 5'	8.77 (bs)			C-4', C-5'
3''	4.62 (d, 4.7)	-	-	C-3, C-4
Amides (NH)				
3''-NH	7.96 (t, 5.6)	-	-	C ₃ =O
16''-NH	10.01 (s)	-	-	C-13'', C-14'', C-15'', C ₁₆ =O
24''-NH	6.45 (s), 6.37 (s)	-	-	C ₂₄ =O, C-25'', C23''
Linker				
1''	2.94-2.45 (m)	18.4	C-1''	C-2'' H-2''
2''	2.35-2.18 (m)	35.2	C-2''	H-1''
3''	-	173.0	-	N-H (3''), H-4'', H-2''
4''	3.32-3.26 (m)	38.2	C-4''	C ₃ =O, C ₈ =O, C ₉ =O H-5''
5''	2.94-2.45 (m)	30.6	C-5''	C ₈ =O, C ₉ =O H-6'', H-7''

^aCarbons correlate with the protons resonating at the ppm value indicated in the δ_{H} column.

^bIndicated carbons and protons correlated with the protons or carbons at the position indicated in the left column.

91

per-O-TBDMS-4-(2-hydroxyethoxy)-catechin



- CAS: New product
- MM: 921,6
- EM: 920,5326
- MF: C₄₇H₈₈O₈Si₅

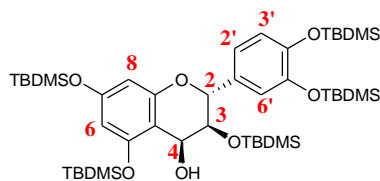
66a (1.02 g, 1.18 mmol) was dissolved with 30 mL of CH₂Cl₂ (dry, distilled), under Ar atmosphere. To this solution was added ethylene glycol (2.6 mL, 47 mmol) and DDQ (539.8 mg, 2.38 mmol), with vigorous stirring. The reaction mixture was stirred for 14 h, after which time TLC monitoring indicated quasi completion of the reaction. The solvent was evaporated under reduced pressure to give a violet oily residue. This residue was purified by silica gel column chromatography eluting with CH₂Cl₂-cyclohexane (1:1, v/v), to afford **91** as a pale yellow (842 mg, 77%).

TLC (CH₂Cl₂-cyclohexane, 1:1 v/v): R_f = 0.3.

¹H NMR (300MHz, Acetone-*d*₆): δ 6.99 (d, J = 1.7, H-6'), 6.93 (dd, J = 1.9, 8.2, H-2'), 6.89 (d, J = 8.2, H-3'), 6.03 (d, J = 2.2, H-6 or H-8), 6.01 (d J = 2.2, H-6 or H-8), 5.17 (d, J = 9.9, H-2), 4.73 (d, J = 2.6, H-4), 4.03-3.93 (m, H-1'', H-2'' or OH), 3.84-3.78 (m, H-1'', H-2'' or OH), 3.68-3.62 (m, H-3), 3.41 (H-1'' or H-2''), 1.06 (bs, OTBDMS), 1.03 (bs, OTBDMS), 1.02 (bs, OTBDMS), 0.99 (bs, OTBDMS), 0.82 (bs, C3-OTBDMS), 0.34 (bs, OTBDMS), 0.31 (bs, OTBDMS), 0.24-0.23 (m, OTBDMS), -0.003 (bs, C3-OTBDMS), -0.04 (bs, C3-OTBDMS).

¹³C NMR (100 MHz, Acetone-*d*₆): δ 157.9, 157.0, 155.9 (C-5, C-7, C_{II}), 147.4, 147.3 (C-4', C-5'), 134.2 (C-1'), 122.5, 121.6, 121.5 (C-2', C-3', C-6'), 108.4, 103.8, 101.8 (C_I, C-6, C-8), 77.0, 74.5, 73.2, 71.5, 62.5 (C-2, C-3, C-4, C-1'', C-2''), 26.4, 26.4, 26.4, 26.4, 26.0, 19.1, 19.1, 19.0, 18.8, 18.6, -3.7, -3.7, -3.7, -3.8, -3.9, -4.2, -4.2, -5.1 (OTBDMS).

MS (ESI) *m/z* (rel. intensity): 943 [M+Na]⁺, (10) and 1863 [2M+Na]⁺.



- CAS: New product
- MM: 877.6
- EM: 876.5063
- MF: C₄₅H₈₄O₇Si₅

In a 5 mL, flame dried conical flask, under Ar atmosphere, were added **91** (70.5 mg, 0.08 mmol) and **66a** (339.5 mg, 0.39 mmol) and dissolved with CH₂Cl₂ (dry, distilled, 1 mL) and THF (dry, 1 mL) to give a colorless solution. This solution was allowed to cool to 0°C and TiCl₄ 1M in CH₂Cl₂ (160 µL, 0.16 mmol) was added dropwise. The bright orange mixture was allowed to stir at room temperature for 3 h, after which time TLC monitoring indicated quasi completion of the reaction. NaHCO₃(sat) (1 mL) was added to the reaction mixture, which was then diluted with CH₂Cl₂, extracted with H₂O (2 mL) and brine (2 mL). The organic layer was dried over Na₂SO₄ and the solvent was evaporated to afford a pink oily residue. This residue was purified by silica gel column chromatography, eluting with cyclohexane-CH₂Cl₂ (8:2, v/v) to (7:3, v/v), to furnish 45 mg, 64% yield of compound **92**.

mp: 143-144°C.

TLC (Cyclohexane-CH₂Cl₂, 6:4 v/v): R_f = 0.6.

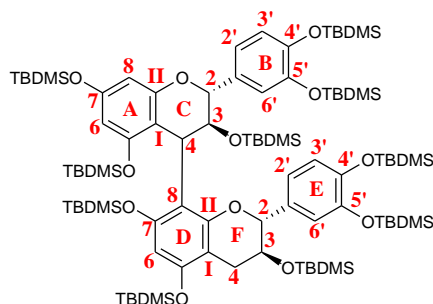
[α]_D = + 34.0°, 0.57 M, CH₂Cl₂.

¹H NMR (300MHz, CDCl₃): δ 6.80-6.88 (m, H-2', H-3', H-6'), 6.05 (d, *J* = 2.3, H-8), 5.97 (d, *J* = 2.1, H-6), 4.91 (d, *J* = 10.0, H-2), 4.83 (d, *J* = 3.4, H-4), 3.82 (dd, *J* = 3.4, 9.8, H-3), 2.79 (s, C₄-OH), 1.03 (bs, OTBDMS), 0.99 (2bs, OTBDMS), 0.95 (bs, OTBDMS), 0.80 (bs, OTBDMS), 0.29 (bs, OTBDMS), 0.25 (bs, OTBDMS), 0.19 (bs, OTBDMS), 0.18 (bs, OTBDMS), 0.17 (bs, OTBDMS).

¹³C NMR (75MHz, CDCl₃): δ 157.3 (C-7), 156.2 (C_{II}), 155.9 (C-5), 146.8 (C-5'), 146.6 (C-4'), 132.0 (C-1'), 121.0 (C-1'), 120.9 (C-3'), 120.8 (C-6'), 107.3 (C_I), 103.7 (C-6), 101.2 (C-8), 75.4 (C-2), 73.1 (C-3), 62.5 (C-4), 26.0, 25.7, 18.5, 18.4, 18.2, 18.0, -4.1 (2C), -4.2, -4.4, -5.0, -5.2, -5.3 (OTBDMS).

IR (Zn/Se): 2956, 2930, 2858, 2348, 1612, 1583, 1254, 1160, 1120, 1075 cm⁻¹.

HRMS (ESI-TOF) *m/z*: [M+Na]⁺ calcd. for C₄₅H₈₄O₇NaSi₅, 899.4961, found 899.4985.

93a**per-O-TBDMS catechin-4→8-catechin**

- CAS: New product
- MM: 1721,1
- EM: 1719,0072
- MF: C₉₀H₁₆₆O₁₂Si₁₀

74a (186.5 mg, 0.20 mmol) and **66a** (533.6 mg, 0.62 mmol) were dried under vacuum overnight and then dissolved with 3.7 mL of CH₂Cl₂ (dry, freshly distilled), under Ar atmosphere. The colorless mixture was allowed to cool at – 78°C and BF₃·OEt₂ (38 µL, 0.30 mmol) was added dropwise. The orange mixture was stirred at this temperature for 40 min, after which time TLC monitoring indicated completion of the reaction. Then, NaHCO_{3(sat)} (1 mL) was added to the mixture at – 78°C and the temperature was slowly allowed to reach room temperature. The mixture was diluted with CHCl₃ (20 mL), and extracted with H₂O (10 mL) and brine (10 mL). The organic layer was dried over Na₂SO₄ and the solvent was evaporated to give yellow oily residue. This residue was purified by silica gel column chromatography, eluting with petroleum ether-CH₂Cl₂ (8:2, v/v) to furnish **93a** as a white foamy solid (119 mg, 35%), a mixture containing two compounds in 1:0.5 ratio (calculated by ¹H NMR, based on the literature, the ratio should correspond to α:β stereoisomers).

TLC (Petroleum ether-CH₂Cl₂, 8:2 v/v): R_f = 0.5.

¹H NMR (300MHz, Acetone-*d*₆): **δ Major compound (α-isomer):** 6.81 (d, J = 8.3, H-3'), 6.78 (bs, H-6'), 6.71 (dd, J = 2.0, 8.4, H-2'), 6.64 (d, J = 8.2, H-3'), 6.61 (d, J = 1.9, H-6'), 6.57 (dd, J = 1.9, 8.3, H-2'), 6.02 (s, H-6D), 5.97-5.96 (m, H-6A or H-8A), 5.41 (d, J = 2.4, H-6A or H-8A), 5.23 (d, J = 1.7, H-2F), 4.39 (dd, J = 2.1, 4.5, H-3C), 4.36 (d, J = 4.5, H-4C), 4.15 (d, J = 9.0, H-2C), 3.69 (dt, J = 6.2, 9.3, H-3F), 3.06 (dd, J = 6.3, 16.3, H-4F), 2.57 (dd, J = 9.8, 16.3, H-4F), 1.06-0.71 (14 bs, OTBDMS), 0.30-(-0.09) (22bs, OTBDMS), 0.26-0.04 (5s, OTBDMS).

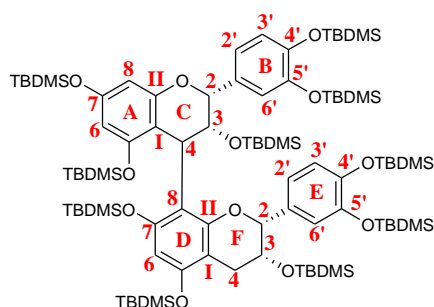
Minor compound (β-isomer): 7.11 (dd, J = 2.0, 8.2, H-2'), 7.03 (d, J = 1.9, H-6'), 6.98 (d, J = 8.2, H-3'), 6.89 (bs, H-2', 3' or 6'), 6.47 (bs, H-2', 3' or 6'), 6.10 (d, J = 2.4, H-6A or H-8A), 5.97-5.96 (m, H-6D), 5.86 (d, J = 2.4, H-6A or H-8A), 5.19 (d, J = 5.3, H-2F), 4.69-4.65 (m, H-4C, H-2C), 4.48 (m, H-3C), 4.00 (dt, J = 5.8, 9.5, H-3F), 3.19 (dd, J = 6.0, 16.6, H-4F), 2.63 (dd, J = 10.0, 16.0, H-4F).

¹³C NMR (75 MHz, Acetone-*d*₆): **δ** 158.0, 156.1 (2C), 156.0, 155.2, 155.0, 154.8, 154.5, 152.3, 152.2, 152.1, 147.4 (2C), 147.3, 147.2, 146.8, 146.6, 146.4, 145.6, 134.5, 134.1, 133.9, 132.8, 123.0, 122.4, 121.9, 121.8, 121.7, 121.5, 121.3, 120.2, 119.5, 112.7, 112.3, 110.8, 109.1, 107.1, 105.7, 104.6, 104.1, 103.9, 102.9, 102.4, 101.5, 83.1, 82.0, 81.7, 79.3, 71.9, 71.0, 70.5, 34.0, 33.3 (2C), 32.0, 30.9, 30.6, 30.3, 30.1, 29.8, 29.6, 29.3, 29.1, 27.5, 27.3, 27.0, 26.6 (2C), 26.5, 26.4 (2C), 26.3, 26.2 (2C), 26.1, 19.9, 19.2 (2C), 19.1, 19.0 (2C), 18.9 (2C), 18.8 (3C), 18.7 (3C), 18.6, 1.4 (2C), -2.7, -2.9, -3.1, -3.2 (2C), -3.3, -3.4, -3.5 (2C), -3.6, -3.7 (2C), -3.8 (3C), -3.9, -4.0, -4.5, -4.6 (3C), -4.7, -4.8, -5.2;

IR (Zn/Se): 3063, 3031, 2925, 2870, 1614, 1265, 1119 cm⁻¹.

UV/Vis: λ_{max1} 252 nm, λ_{max2} 267 nm, λ_{max3} 284 nm.

HRMS (ESI-TOF) *m/z*: [M+Na]⁺ calcd. for C₉₀H₁₆₆O₁₂NaSi₁₀, 1741.9964; found, 1741.9910.

93b**per-O-TBDMS epicatechin-4→8-epicatechin**

- CAS: New product
- MM: 1721,1
- EM: 1719,0072
- MF: C₉₀H₁₆₆O₁₂Si₁₀

74d (211 mg, 0.23 mmol) and **66d** (597 mg, 0.69 mmol) were dried under vacuum overnight and then dissolved with 3.3 mL of CH₂Cl₂ (dry, freshly distilled), under Ar atmosphere. The mixture was allowed to cool at – 78°C and BF₃·OEt₂ (44 µL, 0.35 mmol) was added dropwise to give an orange mixture. The mixture was stirred at this temperature for 1 h, after which time TLC monitoring indicated completion of the reaction. Then, NaHCO₃(sat) (1 mL) was added at – 78°C and the temperature was slowly allowed to reach room temperature. The mixture was diluted with CHCl₃ (15 mL), extracted with H₂O (10 mL) and brine (10 mL). The organic layer was dried over Na₂SO₄ and the solvent was evaporated to give an off white foamy solid. This solid was purified by silica gel column chromatography, eluting with petroleum ether-CH₂Cl₂ (8:2, v/v) to furnish **93b** as a white foamy solid (118 mg, 30%), a mixture containing two compounds in 0.3:1 ratio (calculated by ¹H NMR, based on the literature, the ratio should correspond to α:β stereoisomers).

TLC (Petroleum ether-CH₂Cl₂, 8:2 v/v): R_f = 0.5.

¹H NMR (300MHz, Acetone-*d*₆): δ **Major compound (β-isomer)**: 7.31 (dd, *J* = 2.0, 6.4, 1H), 6.90 (d, *J* = 2.0, 1H), 6.86 (bs, 2H), 6.83-6.74 (m, 5H), 6.08 (d, *J* = 2.3, H-6A or H-8A), 6.01 (s, H-6D), 5.92 (d, *J* = 2.3, H-6A or H-8A), 5.08 (s, H-2C or H-2F), 5.07 (s, H-2C or H-2F), 4.69 (d, *J* = 2.2, H-4C), 4.29 (bs, H-3F), 3.95 (d, *J* = 2.5, H-3C), 3.06 (dd, *J* = 4.1, 17.1, H-4F), 2.97 (dd, *J* = 2.4, 17.1, H-4F). OTBDMS: 1.06-0.84 (m, 126H), 0.67 (s, 3H), 0.65 (s, 3H), 0.51 (s, 9H), 0.30 (s, 4H), 0.27-0.10 (m, 60H), 0.06 (s, 3H), 0.008 (s, 3H), -0.05 (s, 3H), -0.07 (s, 0.7H), -0.11 (s, 3H), -0.19 (s, 2H), -0.21 (s, 3H), -0.36 (s, 3H), -0.39 (s, 1H), -0.66 (s, 3H).

Minor compound (α-isomer): 7.06 (bs, 0.4H), 6.61 (d, *J* = 1.8, 0.4H), 6.13 (s, H-6D), 5.78 (d, *J* = 2.3, H-6A or H-8A), 5.76 (d, *J* = 2.3, H-6A or H-8A), 5.36 (s, H-2), 4.58 (d, *J* = 3.7, H-4C), 4.52 (bs, H-3), 4.45 (s, H-2), 4.00 (bs, H-3), 2.84 (dd, *J* = 4.2, 16.7, H-4F), 2.68 (dd, *J* = 3.0, 16.8, H-4F).

¹³C NMR (75 MHz, Acetone-*d*₆): δ 157.7, 157.2, 156.2, 155.6, 155.0 (2C), 154.9, 154.5 (2C), 153.7, 153.3, 153.2, 147.0 (2C), 146.9 (2C), 146.5, 146.3, 146.1, 146.0, 135.0, 134.6, 133.9, 132.8, 123.6, 121.4, 121.3, 121.0, 120.8, 120.4, 120.2, 120.1, 119.9, 113.8, 113.6, 109.5, 105.8, 105.2, 103.5, 103.1, 103.0, 102.7, 102.5, 101.8, 80.9, 80.1, 75.8, 74.4, 74.1, 68.5, 68.1, 44.3, 37.3, 32.6, 30.9, 30.8, 30.4, 27.5, 27.1 (2C), 26.7, 26.6 (3C), 26.5 (3C), 26.4, 26.3 (2C), 26.2, 26.1, 19.9, 19.2, 19.1 (3C), 19.0 (2C), 18.9 (2C), 18.8, 18.7, 18.6, 18.5.

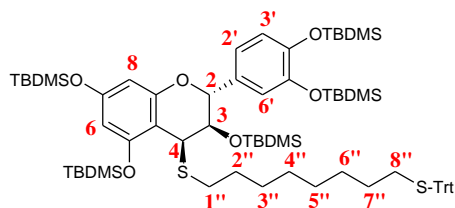
IR (Zn/Se): 2956, 2930, 2894, 2858, 1255, 837 cm⁻¹.

UV/Vis: λ_{max1} 250 nm, λ_{max2} 276 nm.

HRMS (ESI-TOF) *m/z*: [M+Na]⁺ calcd. for C₉₀H₁₆₆O₁₂NaSi₁₀, 1741.9964; found, 1741.9932.

94

per-O-TBDMS-4-(1''-thioetheroctane-8''-tritylthioether) catechin



- CAS: New product
- MM: 1280,2
- EM: 1278,6903
- MF: C₇₂H₁₁₄O₆S₂Si₅

75a (145 mg, 0.14 mmol) was dissolved with CH₂Cl₂ (2.6 mL, distilled), under Ar atmosphere. To this solution was added dropwise, a solution of Trt-Cl (108 mg, 0.39 mmol) and Et₃N (52 µL, 0.39 mmol) in 2.6 mL of CH₂Cl₂ (distilled). The reaction mixture was stirred at room temperature for 5 h ½. The solvent was evaporated under reduced pressure to give a yellow solid. This solid was purified by silica gel column chromatography eluting from cyclohexane-CHCl₃ (7:3, v/v) to (1:1, v/v), to afford **94** as a sticky solid (159.6 mg, 89%).

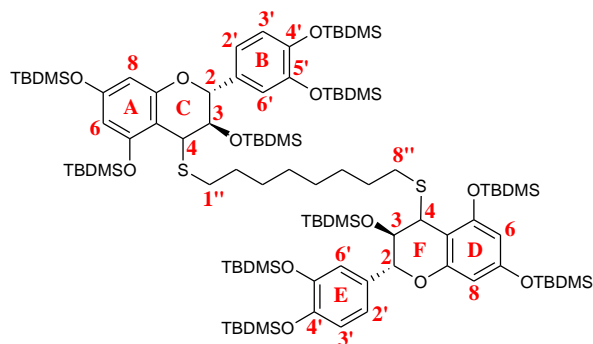
TLC (Petroleum ether-CH₂Cl₂, 7:3 v/v): R_f = 0.5.

¹H NMR (300MHz, Acetone-*d*₆): δ 7.31-7.20 (m, Trt), 6.98-6.88 (m, H-2', H-3', H-6'), 6.02 (bs, H-6, H-8), 5.34 (d, *J* = 9.3, H-2), 4.55 (d, *J* = 3.9, H-4), 4.10 (dd, *J* = 3.9, 9.3, H-3), 2.67 (dt, *J* = 7.5, 11.9, H-1''a), 2.45 (dt, *J* = 7.5, 11.9, H-1''b), 2.14 (t, *J* = 7.2, H-8''), 1.44-1.15 (m, H-2''-H-7''), 1.07 (OTBDMS), 1.02 (OTBDMS), 1.01 (OTBDMS), 0.98 (OTBDMS), 0.82 (C₃-OTBDMS), 0.35 (OTBDMS), 0.30 (OTBDMS), 0.24-0.23 (m, OTBDMS), -0.04 (C₃-OTBDMS), -0.40 (C₃-OTBDMS).

HRMS (ESI-TOF) *m/z*: [M+Na]⁺ calcd. for C₇₂H₁₁₄O₆NaSi₅S₂, 1301.6795; found, 1301.6738.

95

per-O-TBDMS catechin-4-(1''-thioetheroctane-8''-thioether)→4-catechin



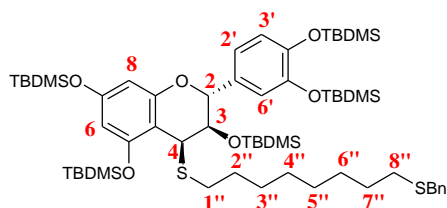
- CAS: New product
- MM: 1897,5
- EM: 1895,0765
- MF: C₉₈H₁₈₂O₁₂S₂Si₁₀

In a conical flask, **74a** (20.1 mg, 0.022 mmol) and **94** (80.1 mg, 0.063 mmol) were dried under vacuum overnight and dissolved with 1 mL of CH₂Cl₂ (dry, freshly distilled), under Ar atmosphere. The colorless mixture was allowed to cool at – 78°C and BF₃·OEt₂ (3.3 μL, 0.023 mmol) was added. The yellow mixture was stirred at this temperature for 19 h, after which time TLC monitoring indicated completion of the reaction. Then, NaHCO₃(sat) (0.5 mL) was added to the mixture at – 78°C and the temperature was slowly allowed to reach room temperature. The mixture was diluted with Et₂O (15 mL), and extracted with H₂O (5 mL) and brine (5 mL). The organic layer was dried over Na₂SO₄ and the solvent was evaporated to give a colorless oily residue. This residue was purified by silica gel column chromatography, eluting with petroleum ether-CH₂Cl₂ (8:2, v/v) to furnish **95** as a white solid (12.5 mg, 30% yield).

TLC (petroleum ether-CH₂Cl₂, 7:3 v/v): R_f = 0.3.

¹H NMR (300MHz, Acetone-*d*₆): δ 6.98-6.91 (m, H-2', H-3', H-6'), 6.02 (bs, H-6, H-8), 5.34 (d, *J* = 9.3, H-2), 4.55 (d, *J* = 3.8, H-4), 4.10 (dd, *J* = 3.8, 9.2, H-3), 2.70 (dt, *J* = 7.5, 11.9, H-1''a), 4.47 (td, *J* = 7.5, 11.9, H-1''b), 1.47-1.25 (m, H-2''-H-8''), 1.08 (OTBDMS), 1.02 (2OTBDMS), 0.99 (OTBDMS), 0.83 (C₃-OTBDMS), 0.36 (OTBDMS), 0.31 (OTBDMS), 0.24 (OTBDMS), 0.24-0.23 (m, OTBDMS), -0.04 (C₃-OTBDMS), -0.40 (C₃-OTBDMS).

MS (ESI) *m/z*: 1896 [M+H]⁺, 1913 [M+H₂O]⁺, 1918 [M+Na]⁺.



- CAS: New product
- MM: 1128,0
- EM: 1126,6277
- MF: C₆₀H₁₀₆O₆S₂Si₅

74a (141.3 mg, 0.15 mmol) was dissolved with 2.8 mL of CH₂Cl₂ (distilled), under Ar atmosphere. To this solution was added 8-(benzylthio)octane-1-thiol (96.4 mg, 0.36 mmol). After cooling to -78°C, BF₃Et₂O (19 µL, 0.15 mmol) was added. The mixture was allowed to stir at -78°C for 30 min, after which time TLC monitoring indicated completion of the reaction. At this temperature NaHCO_{3(sat)} (1 mL) was added and the mixture was allowed to reach room temperature. The mixture was diluted with Et₂O (30 mL) and extracted with H₂O (10 mL) and brine (10 mL). The organic layer was dried over Na₂SO₄ and the solvent was evaporated under reduced pressure to give yellow oily residue. This oil was purified by silica gel column chromatography, eluting with petroleum ether-CH₂Cl₂ (9:1, v/v), to afford **96** as a sticky solid (135.8 mg, 80% yield).

TLC (Cyclohexane-CH₂Cl₂, 7:3, v/v): R_f = 0.3.

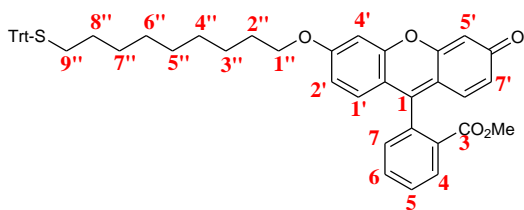
¹H NMR (300MHz, Acetone-*d*₆): δ 7.35-7.20 (m, OBn), 6.98 (d, *J* = 1.6, H-6'), 6.93 (dd, *J* = 1.8, 8.2, H-2'), 6.89 (d, *J* = 8.1, H-3'), 6.02 (s, H-6, H-8), 5.35 (d, *J* = 9.3, H-2), 4.56 (d, *J* = 3.8, H-4), 4.10 (dd, *J* = 3.9, 9.3, H-3), 3.71 (s, CH₂ OBn), 2.77-2.65 (m, H-1''), 2.67 (t, *J* = 7.5, H-8''), 1.59-1.20 (m, H-2'' - H-7''), 1.09 (s, O-TBDMS), 1.03 (s, O-TBDMS), 1.02 (s, O-TBDMS), 1.00 (s, O-TBDMS), 0.84 (s, C3-O-TBDMS), 0.36 (s, O-TBDMS), 0.31 (s, O-TBDMS), 0.24 (bs, O-TBDMS), 0.23 (s, O-TBDMS), -0.03 (s, C3-O-TBDMS), -0.39 (s, C3-O-TBDMS).

¹³C NMR (75 MHz, Acetone-*d*₆): δ 157.2 (Cq), 156.5 (Cq), 154.8 (Cq), 147.5 (Cq), 147.4 (Cq), 139.9 (Cq, OBn), 134.1 (Cq), 129.7 (CH, OBn), 129.1 (CH, OBn), 127.5 (CH, OBn), 122.6, 121.6, 121.5 (C-2', C-3', C-6'), 107.2 (Cq), 103.5, 101.7 (C-6, C-8), 78.2 (C-2), 74.0 (C-3), 43.6 (C-4), 36.5 (CH₂, OBn), 31.8 (C-1'', C-8''), 30.8, 29.9, 29.8, 29.4 (C-2'' - C-6''), 26.5, 26.4, 26.2, 26.1, 19.1, 19.0, 18.9 (2C), 18.7, -3.7 (2C), -3.8 (2C), -3.9 (2C), -4.1, -4.2 (2C), -5.0 (O-TBDMS).

IR (Zn/Se): 2954, 2929, 2896, 2857, 1254, 1195, 838, 780 cm⁻¹.

HRMS (ESI-TOF) *m/z*: [M+Na]⁺ calcd. for C₆₀H₁₀₆O₆NaSi₅S₂, 1149.6169; found, 1149.6165.

(3'-(9''-(tritylthio)nonyl-1''-oxy) fluorescein methyl ester



- CAS: New product
- MM: 747.0
- EM: 746.3066
- MF: C₄₉H₄₆O₅S

A solution of **63** (50 mg, 0.12 mmol), PPh₃ (41 mg, 0.15 mmol) and fluorescein **108** (30.1 mg, 0.09 mmol) in anhydrous THF (6 mL), under N₂ atmosphere, was heated to 50°C, and DIAD (32 µL, 0.15 mmol) was added. After 1h, more PPh₃ (21 mg, 0.08 mmol) and DIAD (17 µL, 0.08 mmol) were added, and stirring was continued overnight. The solvent was removed under reduced pressure to afford an orange oil. This oil was purified by silica gel chromatography eluting first with CH₂Cl₂-AcOEt (7:3, v/v) and then with pure AcOEt, to afford **114** (29 mg, 43%) as an orange solid.

m.p: 72-73°C.

TLC (AcOEt): R_f = 0.5

¹H NMR (300MHz, CDCl₃): δ 8.24 (dd, *J* = 1.3, 7.7, 1H), 7.73 (td, *J* = 1.5, 7.5, 1H), 7.66 (td, *J* = 1.5, 7.5, 1H), 7.42-7.38 (m, 6H), 7.32-7.17 (m, 15H), 6.93 (d, *J* = 2.4, 1H), 6.87 (d, *J* = 6.9, 1H), 6.84 (d, *J* = 7.7, 1H), 6.71 (dd, *J* = 2.4, 8.9, 1H), 6.54 (dd, *J* = 1.9, 9.7, 1H), 6.45 (d, *J* = 1.9, 1H), 4.04 (t, *J* = 6.5, H-1''), 3.63 (s, C₃-O-CH₃), 2.13 (t, *J* = 7.2, H-9''), 1.80 (q, *J* = 7.3, H-8''), 1.43-1.20 (m, H-2''-H-7'').

¹³C NMR (75MHz, CDCl₃): δ 185.7 (C=O), 165.7, 163.8, 159.1, 154.4, 150.3, 145.2, 134.8, 132.8, 131.2, 130.7, 130.4, 130.3, 129.9, 129.7, 128.9, 127.9, 126.6, 117.6, 114.7, 113.9, 105.8, 100.8, 69.0, 66.5, 52.5, 32.1, 29.4, 29.3, 29.2, 29.0, 29.0, 28.7, 26.0.

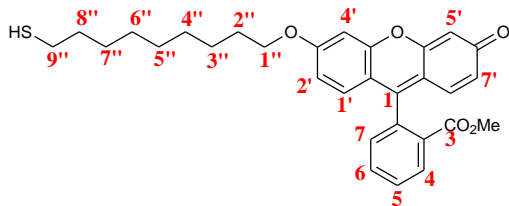
IR (Zn/Se): 1726, 1643, 1274, 1209 cm⁻¹.

UV/Vis: λ_{max1} 231 nm, λ_{max2} 442 nm.

HRMS (ESI-TOF) *m/z*: [M+H]⁺ calcd. for C₄₉H₄₇O₅S, 747.3144; found, 747.3132.

115

3'-(9"-mercaptononyl-1"-oxy) fluorescein methyl ester



- CAS: New product
- MM: 504.6
- EM: 504.1970
- MF: C₃₀H₃₂O₅S

114 (17 mg, 0.023 mmol) was dissolved in triisopropylsilyl (TIS)-TFA (95:5, v/v) solution (1mL). The reaction mixture was stirred for 1h, after which time the solvent was evaporated under reduced pressure to give an orange oil. This oil was purified by silica gel chromatography, eluting from chloroform-acetone (9:1, v/v) to acetone-methanol (9:1, v/v) to furnish **115** (6 mg, 52% yield) as an orange solid.

m.p: 79-80°C.

TLC (AcOEt-MeOH, 96:4 v/v): R_f = 0.5.

¹H NMR (300MHz, CDCl₃/MeOD-*d*₄, 7:3, v/v): δ 8.25 (dd, *J* = 1.3, 7.7, 1H), 7.74 (td, *J* = 1.5, 7.5, 1H), 7.67 (td, *J* = 1.5, 7.5, 1H), 7.31 (dd, *J* = 1.2, 7.4, 1H), 6.96 (d, *J* = 2.3, 1H), 6.90 (d, *J* = 8.8, 1H), 6.87 (d, *J* = 9.3, 1H), 6.74 (dd, *J* = 2.4, 8.9, 1H), 6.60 (dd, *J* = 1.6, 9.7, 1H), 6.54 (bs, 1H), 4.07 (t, *J* = 6.5, 2H), 3.63 (s, 3H), 2.52 (q, *J* = 7.3, 2H), 1.83 (q, *J* = 6.9, 2H), , 1.61 (q, *J* = 7.2, 2H), 1.47-1.21 (m, 12H).

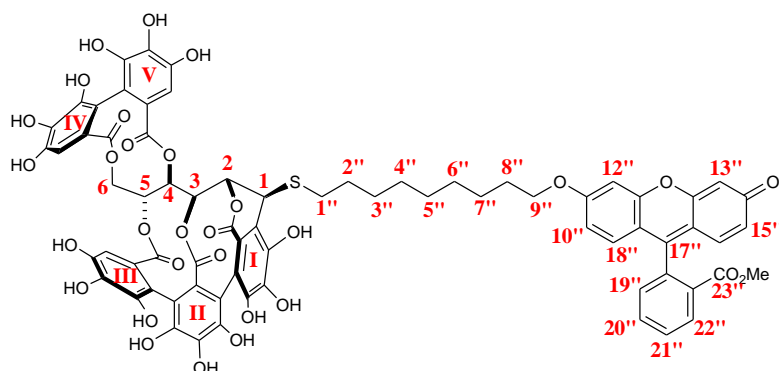
¹³C NMR (75MHz, CDCl₃/MeOD-*d*₄, 7:3, v/v): δ 185.5, 166.7, 166.6, 161.1, 157.3, 156.5, 135.1, 133.9, 132.3, 132.1, 131.4, 131.2, 131.0, 130.6, 128.4, 117.8, 116.4, 116.0, 105.2, 101.6, 70.2, 52.9, 39.7, 34.9, 30.2, 30.2, 30.0, 29.9, 29.8, 29.7, 29.1, 26.7, 24.9.

IR (Zn/Se): 3061, 1725, 1643, 1274, 1207, 1106 cm⁻¹.

UV-Vis: λ_{max1} 231 nm, , λ_{max2} 251 nm, λ_{max3} 442 nm.

HRMS (ESI-TOF) *m/z*: [M+H]⁺ calcd. for C₃₀H₃₃O₅S, 505.2049; found, 505.2056.

Vescalagin-fluorescein conjugate I



- CAS: New product
- MM: 1421.3
- EM: 1420.2577
- MF: C₇₁H₅₆O₃₀S

(–)-Vescalagin (11 mg, 0.012 mmol) was dissolved in 4 mL of THF-TFA (1.5% v/v), under Ar atmosphere. To this solution was added Tris(2-carboxyethyl)phosphine hydrochloride (TCEP, 3.2 mg, 0.012 mmol) and the mixture was stirred at 50°C for 15 min, after which time **115** (6 mg, 0.01 mmol) was added. The yellow reaction mixture was stirred at 50°C for 6 h, after which time HPLC monitoring indicated quasi completion of the reaction. The solvent was evaporated under reduced pressure to furnish a yellow powder. This powder was purified by semi-preparative RP-HPLC to furnish, after freeze-drying, **116** as a yellow powder (4 mg, 23%).

mp: 193°C (dec.).

Retention time: 29.7 min.

Method: 0-50 min: 20% to 70% MeCN-TFA 0.1%.

Column: Varian Microsorb C-18 (10 × 250 mm, 5μm).

Flow rate: 17 mL/min.

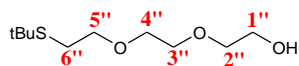
Detection: 237 nm, 443 nm.

¹H NMR (300MHz, MeOD-*d*₄): δ 8.35-8.32 (m, 1H), 7.89-7.81 (m, 2H), 7.54 (dd, *J* = 1.8, 6.6, 1H), 7.47 (d, *J* = 1.9, 1H), 7.43 (bs, 1H), 7.40 (bs, 1H), 7.28 (bs, 1H), 7.19 (dd, *J* = 1.8, 7.2, 1H), 7.12 (d, *J* = 8.7, 1H), 6.75 (s, 1H), 6.62 (s, 1H), 6.53 (d, *J* = 3.3, 1H), 5.57 (dd, *J* = 6.9, 1H), 5.23 (s, 1H), 5.14 (t, *J* = 7.0, 1H), 4.95 (dd, *J* = 2.0, 12.5, 1H), 4.57 (t, *J* = 5.5, 1H), 4.31 (q, *J* = 7.0, 1H), 4.25 (d, *J* = 1.5, 1H), 3.96 (d, *J* = 12.6, 1H), 3.60 (s, 3H), 2.87 (m, 2H), 1.86 (t, *J* = 6.3, 2H), 1.74 (m, 2H), 1.50 (bs, 4H), 1.36 (bs, 6H), 1.29 (2H).

IR (Ge): 3355, 1682, 1639, 1206, 1141 cm⁻¹.

UV/Vis: λ_{max1} 237 nm, λ_{max2} 443 nm.

HRMS (ESI-TOF) *m/z*: [M+H]⁺ calcd. for C₇₁H₅₇O₃₀S, 1421.2655; found, 1421.2650.

118**2-(2-(2-(tert-butylthio)ethoxy)ethoxy)ethanol**

- CAS: 178212-23-2
- MM: 222.3
- EM: 222.1290
- MF: C₁₀H₂₂O₃S

To a solution of t-buthanethiol (307 μ L, 2.70 mmol) in THF (8 mL) at 0°C, under Ar atmosphere, was added NaH (60% suspension in oil, 108 mg, 2.70 mmol). When H_{2(g)} release had stopped, 2-(2-(2-chlorethoxy)-ethoxy)-ethanol (**117**, 449 μ L, 2.97 mmol) was added and the milky white mixture was stirred overnight. To the mixture was added, isopropanol (2 mL), MeOH (2 mL) and the solvent was evaporated under reduced pressure to furnish a white oily residue. This residue was dissolved with CH₂Cl₂ (20 mL) and washed with brine (3×10mL). The organic layer was dried over Na₂SO₄ and the solvent was evaporated to give a pale yellow oil. This oil was purified by silica gel column chromatography from pure cyclohexane to cyclohexane-acetone (1:1, v/v) to afford **118** as a clear liquid (514 mg, 86%).

bp: 100 – 105 lit.¹³³

TLC (CH₂Cl₂-AcOEt, 2:8 v/v): R.f = 0.6.

¹H NMR (300MHz, CDCl₃): δ 3.75-3.60 (m, H-1''-H-5''), 2.75 (t, J = 7.2, H-6''), 1.32 (s, CH₃, tBu).

¹³C NMR (75MHz, CDCl₃): δ 72.6 (CH₂), 71.2 (CH₂), 70.4 (2CH₂), 61.8 (C-1''), 42.2 (CQ), 31.1 (CH₃, tBu), 28.0 (C-6'').

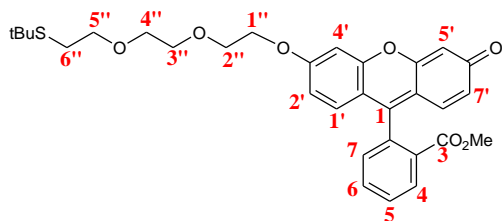
IR (Zn/Se): 3446, 1112 cm⁻¹.

UV-Vis: λ_{max} 225 nm.

MS (ESI) m/z (rel. intensity): 245 [M+Na]⁺, (100).

119

3'-(1''-(3''-(5''-(tert-butylthio)ethoxy)ethoxy)ethoxy)ethoxy) fluorescein methyl ester



- CAS: New product
- MM: 550.7
- EM: 550.2025
- MF: C₃₁H₃₄O₇S

A solution of **118** (258 mg, 1.15 mmol), Ph₃P (307 mg, 1.17 mmol) and **108** (303 mg, 0.88 mmol) in anhydrous THF (10 mL), under N₂ atmosphere, was heated to 50°C and DIAD (230 µL, 1.17 mmol) was added. Heating was continued at 50°C for 3h. The solvent was removed under reduced pressure to afford an orange oil. This oil was purified by silica gel chromatography eluting from pure AcOEt to AcOEt-MeOH (98:2, v/v) to give **119** as an orange solid (361 mg, 74%).

mp: 99-100°C.

TLC (AcOEt-MeOH, 95:5 v/v): R_f = 0.5.

¹H NMR (300MHz, CDCl₃): δ 8.24 (dd, *J* = 1.1, 7.6, 1H), 7.73 (td, *J* = 1.3, 7.4, 1H), 7.66 (td, *J* = 1.3, 7.7, 1H), 7.30 (dd, *J* = 1.2, 7.5, 1H), 6.97 (d, *J* = 2.2, 1H), 6.87 (d, *J* = 8.7, 1H), 6.84 (d, *J* = 9.5, 1H), 6.76 (dd, *J* = 2.3, 8.9, 1H), 6.54 (d, *J* = 9.0, 1H), 6.46 (s, 1H), 4.24 (t, *J* = 4.6, 2H), 3.90 (t, *J* = 4.6, 2H), 3.73-3.71 (m, 2H), 3.67-3.60 (m, 4H), 3.63 (s, 3H), 2.74 (t, *J* = 7.2, 2H), 1.31 (s, 9H).

¹³C NMR (75 MHz, CDCl₃): δ 185.6, 165.6, 163.4, 159.0, 154.3, 150.4, 134.6, 132.7, 131.2, 130.6, 130.3, 130.3, 129.8, 129.7, 128.9, 117.6, 115.0, 113.9, 105.8, 101.1, 71.3, 70.9, 70.4, 69.4, 68.3, 52.4, 42.1, 31.0, 28.0, 22.8.

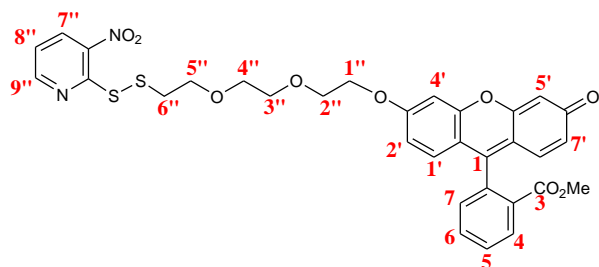
IR (Zn/Se): 1726, 1643, 1276, 1211, 1107 cm⁻¹.

UV/Vis: λ_{max1} 238 nm, λ_{max2} 250 nm, λ_{max3} 429 nm λ_{max4} 443 nm.

HRMS (ESI-TOF) *m/z*: [M+H]⁺ calcd. for C₃₁H₃₅O₇S, 551.2104; found, 551.2216.

120

3'-(1''-(3''-(5''-(6''-(7''-nitropyridin-10''-yl)disulfanyl))ethoxy)ethoxy)ethoxy) fluorescein methyl ester



- CAS: New product
- MM: 648.7
- EM: 648.1236
- MF: C₃₂H₂₈N₂O₉S₂

To a solution of **119** (200 mg, 0.36 mmol) in acetic acid (6 mL), under Ar atmosphere, was added 3-nitro-2-pyridinesulfonyl chloride (77 mg, 0.40 mmol), the formation of a yellow precipitate was observed during the course of the reaction. The reaction mixture was stirred for 3h after which time the acetic acid was removed by co-evaporation under reduced pressure with cyclohexane to furnish an orange sticky solid. This solid was purified by silica gel column chromatography from pure CH₂Cl₂ to acetone-methanol mixture (95:5), to afford **120** as an orange solid (193 mg, 83%).

m.p: 99 °C.

TLC (CH₂Cl₂-Acetone, 3:7 v/v): R_f = 0.5.

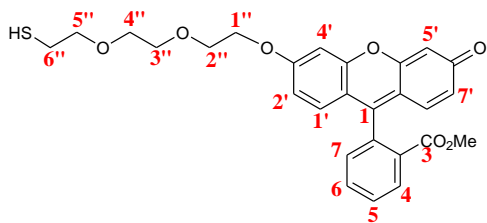
¹H NMR (300MHz, CDCl₃): δ 8.86 (dd, *J* = 1.5, 4.5, 1H), 8.50 (dd, *J* = 1.4, 8.1, 1H), 8.24 (d, *J* = 7.6, 1H), 7.73 (td, *J* = 1.4, 7.4, 1H), 7.66 (td, *J* = 1.4, 7.6, 1H), 7.34 (dd, *J* = 4.2, 7.8, 1H), 7.31 (d, *J* = 7.2, 1H), 6.97 (d, *J* = 2.1, 1H), 6.87 (d, *J* = 9.0, 1H), 6.84 (d, *J* = 9.6, 1H), 6.76 (dd, *J* = 2.1, 8.8, 1H), 6.53 (dd, *J* = 1.7, 9.8, 1H), 6.44 (d, *J* = 1.5, 1H), 4.24 (t, *J* = 4.1, 2H), 3.92 (t, *J* = 4.1, 2H), 3.80 (t, *J* = 6.3, 2H), 3.73-3.72 (m, 2H), 3.69-3.67 (m, 2H), 3.63 (s, 3H), 3.06 (t, *J* = 6.5, 2H).

¹³C NMR (75 MHz, CDCl₃): δ 185.7, 165.7, 163.4, 159.1, 157.4, 154.3, 153.8, 150.3, 142.9, 134.7, 133.9, 132.8, 131.2, 130.7, 130.5, 130.3, 130.0, 129.8, 128.9, 120.9, 117.8, 115.1, 113.9, 105.9, 101.2, 71.0, 70.7, 69.6, 69.5, 68.4, 52.5, 37.6, 29.8.

IR (Zn/Se): 1724, 1643, 1518, 1342, 1276, 1107 cm⁻¹.

UV/Vis: λ_{max1} 250 nm, λ_{max2} 423 nm, λ_{max3} 444 nm.

HRMS (ESI-TOF) *m/z*: [M+H]⁺ calcd. for C₃₂H₂₉N₂O₉S₂, 649.1314; found, 649.1314.

121**3'-(1''-(3''-(6''-mercaptoethoxy)ethoxy)ethoxy)ethoxy) fluorescein methyl ester**

- CAS: New product
- MM: 494.6
- EM: 494.1399
- MF: C₂₇H₂₆O₇S

To a solution of **120** (150 mg, 0.23 mmol), in a mixture of acetone (6 mL) and H₂O (1.2 mL), was added tri-*n*-butylphosphine (59 μ L, 0.23 mmol). The reaction mixture was stirred for 4h and acetone was removed by evaporation under reduced pressure. The residual aqueous phase was extracted with CHCl₃ (3 \times 10mL). The organic layers were combined, dried over Na₂SO₄ and evaporated under reduced pressure to furnish a sticky orange oily residue. This residue was first purified by silica gel column chromatography eluting with AcOEt-MeOH mixture (9:1, v/v) to afford a dark orange solid that was again dissolved in CHCl₃, and precipitated with *ter*-butylmethylether, to give **121** as an orange solid (84 mg, 74%).

mp: 80°C.

TLC (AcOEt-MeOH, 96:4 v/v): R_f = 0.4.

¹H NMR (300MHz, CDCl₃): δ 8.31 (dd, *J* = 1.4, 7.6, 1H), 7.81 (td, *J* = 1.5, 7.3, 1H), 7.76 (td, *J* = 1.6, 7.5, 1H), 7.33 (dd, *J* = 1.4, 7.3, 1H), 7.25 (d, *J* = 1.3, 1H), 7.24 (s, 1H), 7.18 (d, *J* = 7.3, 1H), 7.15 (d, *J* = 7.7, 1H), 7.08 (dd, *J* = 2.0, 9.5, 1H), 7.03 (dd, *J* = 2.4, 9.1, 1H), 4.36 (t, *J* = 4.5, 2H), 3.96 (t, *J* = 4.5, 2H), 3.76-3.72 (m, 3H), 3.68-3.60 (m, 5H), 3.63 (s, 3H), 2.69 (t, *J* = 6.5, 2H), 1.57 (t, *J* = 8.2, 1H).

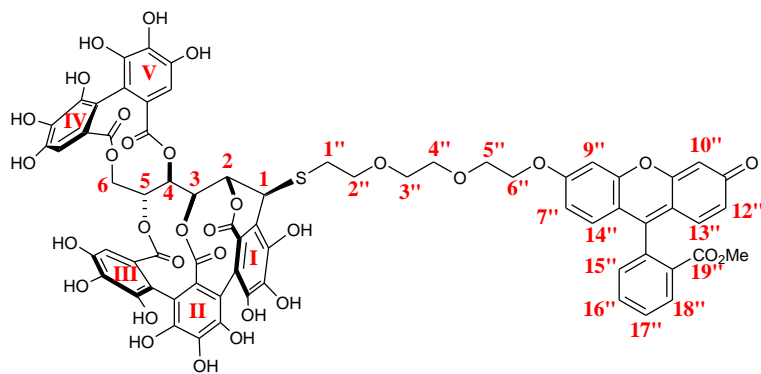
¹³C NMR (75MHz, CDCl₃): δ 180.5, 166.7, 165.3, 161.0, 160.2, 156.7, 133.8, 133.1, 131.7, 131.5, 130.7, 130.3, 130.2, 130.1, 126.0, 117.6, 117.2, 115.9, 104.3, 100.9, 73.0, 71.0, 70.4, 69.3, 69.2, 52.8, 24.4.

IR (Zn/Se): 2954, 1717, 1637, 1281, 1202, 1115 cm⁻¹.

UV/Vis: $\lambda_{\text{max}1}$ 251 nm, $\lambda_{\text{max}2}$ 421 nm, $\lambda_{\text{max}3}$ 444 nm.

HRMS (ESI-TOF) *m/z*: [M+H]⁺ calcd. for C₂₇H₂₇O₇S, 495.1478; found, 495.1462.

Vescalagin-fluorescein conjugate II



- CAS: New product
- MM: 1411.2
- EM: 1410.2006
- MF: C₆₈H₅₀O₃₂S

(–)-Vescalagin (28 mg, 0.029 mmol) was dissolved with 5 mL of THF-TFA (1.5%, v/v), under Ar atmosphere, and stirred at 50°C for 15 min after which time **121** (7.75 mg, 0.02 mmol) was added. The reaction mixture was stirred at 50°C for 19 h, after which time HPLC monitoring indicated quasi completion of the reaction. The reaction mixture was concentrated under reduced pressure to furnish of orange solid. This solid was purified by semi-preparative HPLC to furnish, after freeze-drying, **122** as dark orange crystals (8.6 mg, 21%).

Retention time: 23 min.

Method: 0-30 min: 0% to 60% MeCN-TFA 0.1%.

Column: Varian Microsorb C-18 (10 × 250 mm, 5μm).

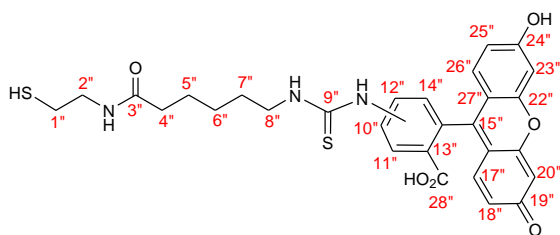
Flow rate: 17 mL/min.

Detection: 230 nm, 442 nm.

¹H NMR (300MHz, MeOD-*d*₄): δ 8.26 (d, *J* = 8.8, 2H), 7.78 (m, 4), 7.37 (d, *J* = 3.4, 1H), 7.34 (d, *J* = 6.2, 1H), 7.26 (dd, *J* = 2.1, 7.5, 2H), 7.09 (d, *J* = 9.4, 4H), 6.94 (dt, *J* = 2.8, 2H), 6.77 (t, *J* = 4.4, 3H), 6.17 (d, *J* = 9.2, 3H), 6.57 (s, 1H), 5.39 (d, *J* = 7.1, 2H), 5.34 (s, 2H), 5.16 (t, *J* = 6.5, 2H), 4.83 (d, *J* = 12.7, 2H), 4.57 (d, *J* = 6.7, 2H), 4.54 (dd, *J* = 7.4, 10.2, 2H), 4.17 (m, 4H), 3.96 (bs, 6H), 3.77 (m, 4H), 3.68 (m, 7H).

UV/Vis: λ_{max1} 230 nm, λ_{max2} 442 nm.

MS (ESI) *m/z* (rel. intensity): 1411 [M+H]⁺, (70).



- CAS: New product
- MM: 579.7
- EM: 579.1498
- MF: C₂₉H₂₉N₃O₆S₂

Amino PEGA resin (350 mg, 0.14 mmol) was pre-swelled in 5 mL of DMF for 15 min, after which time succinic anhydride (148 mg, 1.48 mmol, *ca.* 11 equiv. relative to the resin loading) and di-*iso*-propylethyl amine (DIEA, 255 mL, 1.46 mmol, 10 equiv.) were added. The resin was shaken for 2 h and was successively washed (2 × 5 mL each) with DMF, MeOH, CH₂Cl₂ and again with DMF. After these washings, the TNBS test¹³⁸ was uncoloured, thus revealing completion of the coupling reaction. To the resulting resin (**123**) swelled in DMF (5 mL) were added PyBOP (370 mg, 0.71 mmol, 5 equiv.) and DIEA (122 mL, 0.70 mmol, 5 equiv.). Shaking was maintained for 20 min, after which time a solution of cystamine dihydrochloride (319 mg, 1.42 mmol, 10 equiv.) and DIEA (487 mL, 2.80 mmol, 20 equiv.) in DMSO (5 mL) was added. The resin was shaken overnight, the reaction mixture was filtered off and the resin was washed as described above. The resulting resin **124** pre-swelled in DMF (5 mL) was then acylated with Fmoc-Ahx-OH (149 mg, 0.42 mmol, 3 equiv.) in the presence of DIEA (120 mL, 0.69 mmol, 5 equiv.) and HBTU (160 mg, 0.42 mmol, 3 equiv.) for 45 min. Excess of the reaction mixture was then filtered off and the resulting disulfide resin **125** was then filtered off and washed as described above. The Fmoc protecting group was next removed by using twice a solution of piperidine in DMF (1:4, v/v) for 3 min, then for 7 min. After filtration, the resin was successively washed as described before. Finally, FITC (**107**, 57 mg 0.15 mmol, 1.1 equiv., mixture of 5- and 6-fluorescein isothiocyanates) was added to the resin swollen in DMF (5 mL) in the presence of DIEA (127 mL, 0.73 mmol, 5.2 equiv.) and shaking was maintained overnight. After the resin was washed several times with DMF and dried, the desired thiol **127** was released from the resin by adding 5 mL of a 50 mM dithiothreitol (DTT) solution in MeOH-Et₃N (11:1, v/v). The resin was washed several times with MeOH and the combined MeOH washings were concentrated under reduced pressure. The crude mixture was purified by RP-HPLC chromatography to give, after freeze-drying, pure **127** as an orange solid (20 mg, 25%).

mp: 162-166 °C.

Retention time: 20.7 min.

Method: 0-30 min: 20% to 50% MeCN-TFA 0.1%.

Column: Varian Microsorb C-18 (10 × 250 mm, 5μm). Flow rate: 17 mL/min. Detection: 232 nm, 442 nm.

¹H NMR (300 MHz, MeOD-*d*₄): δ 8.19 (d, *J* = 1.8, 1H), 7.96 (d, *J* = 8.4, 1H), 7.81 (dd, *J* = 1.7, 8.3, 2H), 7.47 (s, 1H), 7.20 (d, *J* = 8.3, 1H), 6.88-6.78 (m, 7H), 6.66 (td, *J* = 2.2; 8.2, 4H), 3.62 (bs, 2H), 3.54 (bs, 2H), 2.58 (q, *J* = 7.7, 4H), 2.24 (t, *J* = 7.4 2H), 2.18 (t, *J* = 7.4, 2H), 1.73-1.54 (m, 9H), 1.48-1.29 (m, 6H).

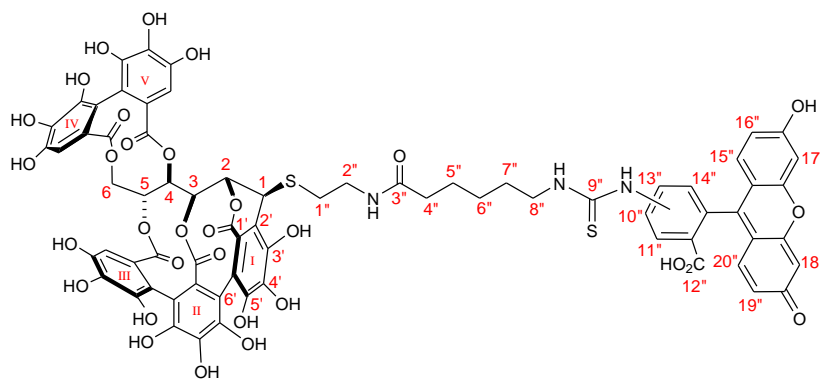
¹³C NMR (100 MHz, MeOD-*d*₄): δ 182.8 (C=O or C=S), 182.3 (C=O or C=S), 176.3 (QC), 176.2 (QC), 170.7 (QC), 170.4 (QC), 163.6 (QC), 163.1 (QC), 155.5 (2QC), 147.6 (QC), 142.7 (QC), 131.1 (CH), 130.9 (CH), 129.7 (QC), 127.5 (CH), 126.8 (CH), 126.1 (CH), 124.5 (CH), 123.3 (CH), 121.3 (CH), 118.3 (CH), 115.1 (CH), 114.8 (CH), 112.9 (QC), 112.5 (QC), 103.5 (CH), 45.4 (CH₂), 45.3 (CH₂), 43.9 (CH₂), 43.8 (CH₂), 36.9 (CH₂), 36.8 (CH₂), 30.9 (CH₂), 29.7 (CH₂), 29.4 (CH₂), 27.5 (CH₂), 27.4 (CH₂), 26.7(CH₂), 26.6 (CH₂), 24.5 (CH₂).

IR (Ge): 3316, 1734, 1684, 1609, 1320 cm⁻¹.

UV/Vis: λ_{max} 232 nm, λ_{max2} 442 nm.

HRMS (ESI-TOF) *m/z*: [M+H]⁺ calcd. for C₂₉H₃₀N₃O₆S₂, 580.1576; found, 580.1567.

Vescalagin-fluorescein conjugated III



- CAS: New product
- MM: 1496.3
- EM: 1495.2104
- MF: C₇₀H₅₃N₃O₃₁S₂

(–)-Vescalagin (**10**) (26 mg, 0.03 mmol) was dissolved in 22 mL of anhydrous THF-TFA (1.5% v/v), under Ar atmosphere and stirred at 50 °C for 15 min, after which time **127** (15 mg, 0.03 mmol) was added. The reaction mixture was stirred at 50 °C for 7 h, after which time HPLC monitoring indicated quasi completion of the reaction. The solvent was evaporated under reduced pressure to furnish a yellow powder. This powder was purified by semi-preparative RP-HPLC to furnish, after freeze-drying, pure **129** (13.6 mg, 30%) as a yellow powder.

mp: 253 °C (decomp.).

Retention time: 20 min.

Method: 0-40 min: 10% to 70% MeCN-TFA 0.1%.

Column: Varian Microsorb C-18 (10 × 250 mm, 5μm).

Flow rate: 17 mL/min.

Detection: 236 nm, 442 nm.

[α]_D = –82.7°, 0.6 mM, MeOH.

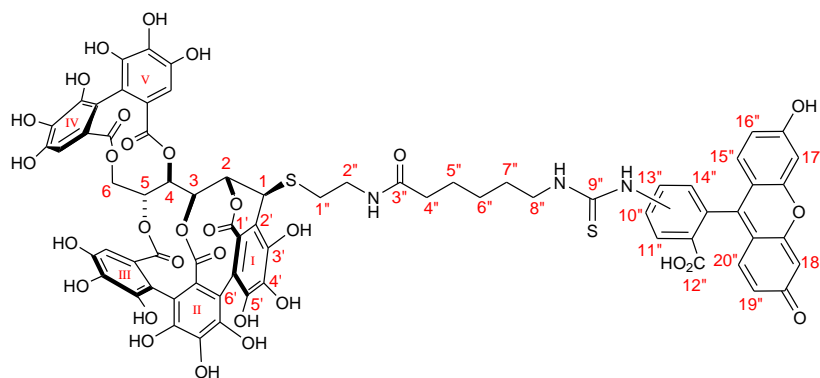
¹H NMR (400 MHz, MeOD-*d*₄): δ 8.24 (s, 1H), 7.96 (d, *J* = 8.2, 1H), 7.76 (dd, *J* = 2.0, 8.2, 1H), 7.71 (d, *J* = 7.6, 1H), 7.59 (s, 1H), 7.18 (d, *J* = 8.2, 1H), 6.86 (bs, 3H), 6.81 (bs, 4H), 6.76 (s, 1H), 6.75 (s, 1H), 6.69 (bs, 3H), 6.67 (bs, 3H), 6.56 (s, 1H), 6.55 (s, 1H), 5.58 (t, *J* = 6.5, 2H), 5.23-5.16 (m, 4H), 4.99 (d, *J* = 2.7, 1H), 4.97 (d, *J* = 2.2, 1H), 4.63-4.61 (m, 2H), 4.42 (d, *J* = 1.7, 1H), 4.40 (d, *J* = 1.6, 1H), 3.99 (d, *J* = 8.9, 1H), 3.96 (d, *J* = 8.8, 1H), 3.78-3.66 (m, 2H), 3.61 (bs, 2H), 3.53 (bs, 2H), 3.46-3.35 (m, 3H), 3.11-3.01 (m, 2H), 2.98-2.87 (m, 2H), 2.30 (t, *J* = 7.1, 2H), 2.24 (t, *J* = 7.2, 2H), 1.73-1.55 (m, 9H), 1.47 (m, 2H), 1.41-1.29 (m, 4H).

¹³C NMR (100 MHz, MeOD-*d*₄): δ 182.6, 182.1, 176.9 (2C), 170.7, 170.5, 168.1, 167.5, 166.5, 165.9, 163.6, 163.1, 155.5, 148.0, 147.5, 146.2 (2C), 146.1, 145.3, 145.1, 145.0, 144.9, 144.7, 144.3, 142.8, 139.2, 138.2, 137.7 (2C), 137.1, 136.1, 132.4, 131.3, 131.1, 129.9, 128.0, 126.9, 126.8, 125.2 (2C), 124.9, 124.7, 124.3 (2C), 118.0, 117.0, 115.9, 115.6, 115.2, 115.1, 115.0, 114.0, 112.9, 109.4, 109.0, 108.0, 103.5, 103.4, 77.4, 72.9, 71.9, 71.4, 70.6, 66.0, 45.5, 45.3, 43.6, 40.1, 40.0, 37.0, 36.9, 32.4, 29.6, 29.4, 27.4, 27.3, 26.9, 26.8.

IR (Ge): 3650-1800, 1731, 1675, 1602, 1455, 1308, 1177 cm^{–1}.

UV/Vis: λ_{max1} 236 nm, λ_{max2} 442 nm.

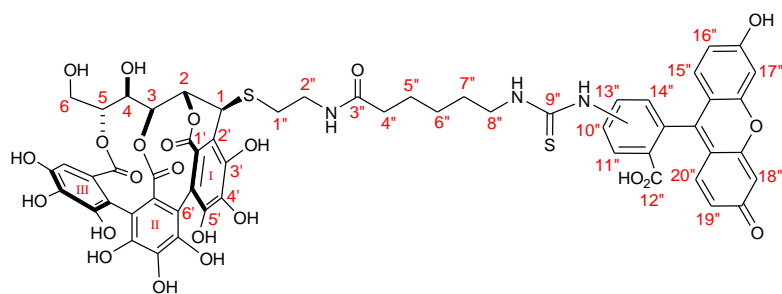
HRMS (ESI-TOF) *m/z*: [M+H]⁺ calcd. for C₇₀H₅₄N₃O₃₁S₂, 1496.2183; found, 1496. 2123.

NMR signal assignments of vescalagin-FITC conjugate in MeOD-*d*₆ 400MHz

<i>position</i>	δ_{H} (mult., <i>J</i> in Hz)	δ_{C} (mult.)	HMQC ^a	HMBC ^b
Glucose ^[7,8]				
1	4.42 (d, 1.7) 4.40 (d, 1.6)	43.6	C-1	C-1', C-2', C-3', C-1'' H-2, H-3, H-1''
2	5.23-5.16 (m)	77.4	C-2	C-1, C-4, C-2', C _I =O H-4
3	4.63-4.61 (m)	71.4	C-3	C-1, C-4, C-5, C _{II} =O H-5
4	5.23-5.16 (m)	70.6	C-4	C-2, C-5, C _V =O H-2, H-3, H-6
5	5.58 (t, 6.5)	71.9	C-5	C-3, C _{III} =O H-3, H-4, H-6
6	4.99 (d, 2.7), 4.97 (d, 2.2) 3.99 (d, 8.9), 3.96 (d, 8.8)	66.0	C-6	C-4, C-5
Aromatics ^[7,8]				
1' _I		124.3 (2C)		H-1
1' _[II-V]		128.0, 126.9, 126.8, 125.2 (2C), 124.9, 124.7		
2' _I		118.0		H-1, H-2
2' _{III}	6.76 (s), 6.75 (s)	109.4	C-2' _{III}	C-3' _{III} , C-4' _{III} , C-6' _{III} , C _{III} =O
2' _{IV}	6.69 (bs), 6.67 (bs)	109.0	C-2' _{IV}	C-3' _{IV} , C-4' _{IV} , C-6' _{IV} , C _{IV} =O
2' _V	6.56 (s), 6.55 (s)	108.0	C-2' _V	C-3' _V , C-4' _V , C-6' _V , C _V =O
2' _{II} and 6' _[I-II]		114.0, 115.9, 115.2		
3' _I		144.3		H-1
3' _[III-V]		146.2 (2C), 146.1		H-2' _{III} , H-2' _{IV} , H-2' _V
3' _{II} and 5' _[I-V]		145.3, 145.1, 145.0, 144.9, 144.7		
4' _I		139.2		
4' _{II}		136.1		
4' _{III}		137.7 (2C)		H-2' _{III}

4' _{IV}		138.2		H-2' _{IV}
4' _V		137.1		H-2' _V
6' _{III}		115.2		H-2' _{III}
6' _{IV}		117.0		H-2' _{IV}
6' _V		115.6		H-2' _V
Carbonyls ^[7,8]				
C _I =O		166.5		H-2
C _{II} =O		165.9		H-3
C _{III} =O		168.1		H-2' _{III} , H-5
C _{IV} =O		167.5		H-2' _{IV} , H-4
C _V =O		170.5		H-2' _V , H-6
Linker				
1''	3.11-3.01 (m), 2.98-2.87 (m)	32.4	C-1''	C-1 H-1, H-2''
2''	3.78-3.66 (m), 3.46-3.35 (m)	40.1, 40.0	C-2''	C-1'', C-3'' H-1''
3''		176.9 (2C)	C-3''	H-2'', H-4''
4''	2.30 (t, 7.1), 2.24 (t, 7.2)	37.0, 36.9	C-4''	C-3'' H-2''
5''- 7''	1.73-1.55 (m), 1.47 (m.), 1.41-1.29 (m)	29.6, 29.4, 27.4, 27.3, 26.9, 26.8		
8''	3.61 (bs), 3.53 (bs)	45.3		
FITC moiety				
10'' – 20''	8.24 (s), 7.80 (d, 8.2), 7.76 (dd, 8.2), 7.71 (d, 7.6), 7.59 (s), 7.18 (d, 8.2), 6.86 (bs), 6.81 (bs), 6.67 (bs)	182.6, 182.1, 170.7, 163.6, 163.1, 155.5, 148.0, 147.5, 132.4, 131.3, 131.1, 129.9, 128.0, 126.8, 124.7, 118.0, 115.0, 112.9, 103.5, 103.4		

^aCarbons directly bonded with the protons resonating at the ppm value indicated in the δ_H column. ^bCarbons are two, three, or even four bonds away from the protons indicated in the left column.



- CAS: New product
- MM: 1194.1
- EM: 1193.2042
- MF: C₅₆H₄₇N₃O₂₃S₂

(–)-Vescalin (**29a**, 11.7 mg, 0.019 mmol) was dissolved in 12.5 mL of anhydrous THF-TFA (1.5% v/v), under Ar atmosphere and stirred at 50 °C for 10 min, after which time **127** (13.3 mg, 23 μmol) was added. The reaction mixture was stirred at 50 °C for 7 h 30 min, after which time HPLC monitoring indicated quasi completion of the reaction. The solvent was evaporated under reduced pressure to furnish a yellow powder. This powder was purified by semi-preparative RP-HPLC to furnish, after freeze-drying, **130** (8.9 mg, 39%) as a yellow amorphous powder.

Retention time: 9.7 min.

Method: 0-20 min: 0% to 100% MeCN-TFA 0.1%.

Column: Varian Microsorb C-18 (10 × 250 mm, 5 μm).

Flow rate: 1 mL/min.

Detection: 235 nm, 440 nm.

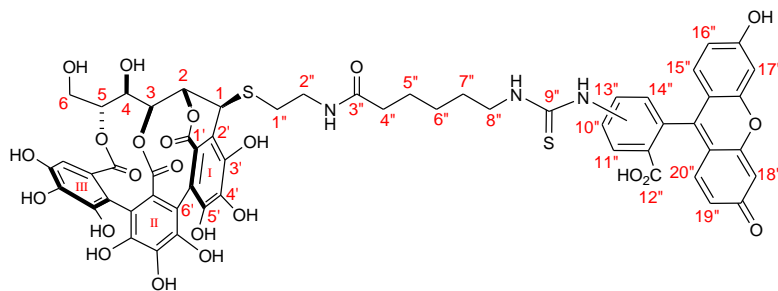
¹H NMR (400 MHz, MeOD-*d*₄): δ 8.28 (s, FITC), 7.98 (d, *J* = 8.3, FITC), 7.79 (dd, *J* = 1.9, 8.3, FITC), 7.76-7.72 (m, FITC), 7.62 (dd, *J* = 3.3, 5.7, FITC), 7.60 (bs, FITC), 7.20 (d, *J* = 8.2, FITC), 6.90-6.84 (2bs, FITC), 6.73, 6.71 (2d, *J* = 1.5, H-2'III), 6.70 (bs, FITC), 5.45 (s, OH), 5.39, 5.37 (2bs, H-2), 5.18-5.12 (m, H-5), 4.47-4.45 (m, H-3), 4.22 (2d, *J* = 1.5, H-1), 4.07 (d, *J* = 6.6, O-H), 3.94-3.90 (m, H-4, H-6a), 3.79 (2dd, *J* = 6.8, 12.3, H-6), 3.64, 3.54 (2bs, N-H, H-8''), 3.50-3.344 (m, H-2''), 2.86 (2t, *J* = 6.5, 13.0, H-1''), 2.25, 2.18 (2t, *J* = 7.2, H-4''), 1.71-1.29 (m, H-5''-H-7'').

¹³C NMR (100 MHz, MeOD-*d*₄): δ 176.4 (C_{3''}=O, C_{9''}=O), 169.0 (C_{III}=O), 167.2 (C_I=O), 166.9 (C_{II}=O), 147.9, 146.2, 145.1, 144.9, 144.6, 144.4 (C-3'I-III, C-5'I-III), 138.9 (C-4'I or C-4'II), 137.1 (C-4'III), 136.0 (C-4'I or C-4'II), 132.4 (CH, FITC), 131.4 (CH, FITC), 131.2 (CH, FITC), 129.9 (C_q, FITC), 128.5 (CH, FITC, C-1'II or C1'II), 126.3, 126.2 (CH, FITC, C-1'II or C1'II), 124.8 (2CH, FITC and C-1'I), 117.7 (C-2'I), 115.9 (C6'I-II or C-2'II), 115.4 (C_q, FITC), 114.7 (C-6'III and C6'I-II or C-2'II), 114.0 (C6'I-II or C-2'II), 109.1 (C-2'III), 103.5 (CH, FITC), 103.4 (CH, FITC), 76.0 (C-2), 75.0 (C-5), 74.1 (C-3), 70.1 (C-4), 62.8 (C-6), 45.3 (C-8''), 44.1 (C-1), 40.0 (2C-2''), 36.9, 36.8 (C-4''), 32.1 (2C-1''), 29.6, 29.4, 27.4, 27.3 (C-6''-C-8''), 26.6 (2C-5'').

IR (Zn/Se): 3331-2200, 1731, 1602, 1542, 1456, 1312, 1206 cm⁻¹.

UV/Vis: λ_{max1} 235 nm, λ_{max2} 440 nm.

MS (ESI) *m/z* (rel. intensity): 1194 [M+H]⁺, (55); 1216 [M+Na]⁺, (10).

NMR signal assignments of vescaline-fluorescein conjugate in MeOD-*d*₆ (400 MHz)

<i>position</i>	δ_{H} (mult., <i>J</i> in Hz)	δ_{C} (mult.)	HSQC ^a	HMBC ^b
Glucose ^[7,8]				
1	4.21 (d, 1.5) 4.21 (d, 1.5)	44.1	C-1	C-1', C-2', C-3', C-1'' H-2, H-3, H-1''
2	5.39 (bs) 5.37 (bs)	76.0	C-2	C-1, C-4, C-2', C _I =O
3	4.47-4.45 (m)	74.1	C-3	-
4	3.94-3.90 (m)	70.1	C-4	H-2, H-3
5	5.18-5.12 (m)	75.0	C-5	H-3, H-6
6	3.79 (2dd, 6.8, 12.3) 3.94-3.90 (m)	62.8	C-6	C-5
Aromatics ^[7,8]				
1' _I	-	124.8	-	H-1
1' _[II-V]	-	128.5, 126.3 or 126.2	-	-
2' _I	-	117.7	-	H-1, H-2
2' _{III}	6.73 (d, 1.5) 6.71 (d, 1.5)	109.1	C-2' _{III}	C-3' _{III} , C-4' _{III} , C-6' _{III} , C _{III} =O
2' _{II} and 6' _[I-II]	-	115.9, 114.7, 114.0	-	-
3' _[I-III] , 5' _[I-III]	-	147.9, , 145.1, 144.9, 144.6, 144.4	-	-
3' _{III}	-	146.2	-	H-2' _{III}
4' _[I-II]	-	138.9, 136.0	-	-
4' _{III}	-	137.1	-	H-2' _{III}
6' _{III}	-	114.7	-	H-2' _{III}
Carbonyls ^[7,8]				
C _I =O	-	167.2	-	H-2
C _{II} =O	-	166.9	-	H-3
C _{III} =O	-	169.0	-	H-2' _{III}
Linker				
1''	2.88 (t, 6.5, 13.0) 2.84 (t, 6.5, 13.0)	32.1	C-1''	C-1, C-2'' H-1
2''	3.50-3.344 (m)	40.0 (2C)	C-2''	H-1''
3'', 9''	-	176.4 (2C)	-	H-2'', H-4''
4''	2.25 (t, 7.2) 2.18 (t, 7.2)	36.9, 36.8	C-4''	-
5''	1.45-1.29 (m)	26.6 (2C)	C-5''	H-4''
6''- 7''	1.71-1.58 (m)	29.6, 29.4, 27.4, 27.3	C-6''- C-7''	-
8'', N-H	3.64, (bs) 3.54 (bs)	45.3	C-8''	-
FITC moiety				
10'' – 20''	8.28 (s), 7.98 (d, 8.3), 7.79 (dd, 1.9, 8.3), 7.76-7.72 (m), 7.62 (dd, 3.3, 5.7), 7.60 (bs), 7.20 (d, 8.2), 6.90-6.84 (2bs), 6.70 (bs)	132.4 (CH), 131.4 (CH), 131.2 (CH), 129.9 (QC), 128.5 (CH), 124.8 (CH), 115.4 (QC), 103.5 (CH), 103.4 (CH).	-	-

^aCarbons directly bonded to the protons resonating at the ppm value indicated in the δ_{H} column. ^bCarbons are two, three, or even four bonds away from the protons indicated in the left column.

Vd. Surface plasmon resonance procedures

V.d.1 Generalities

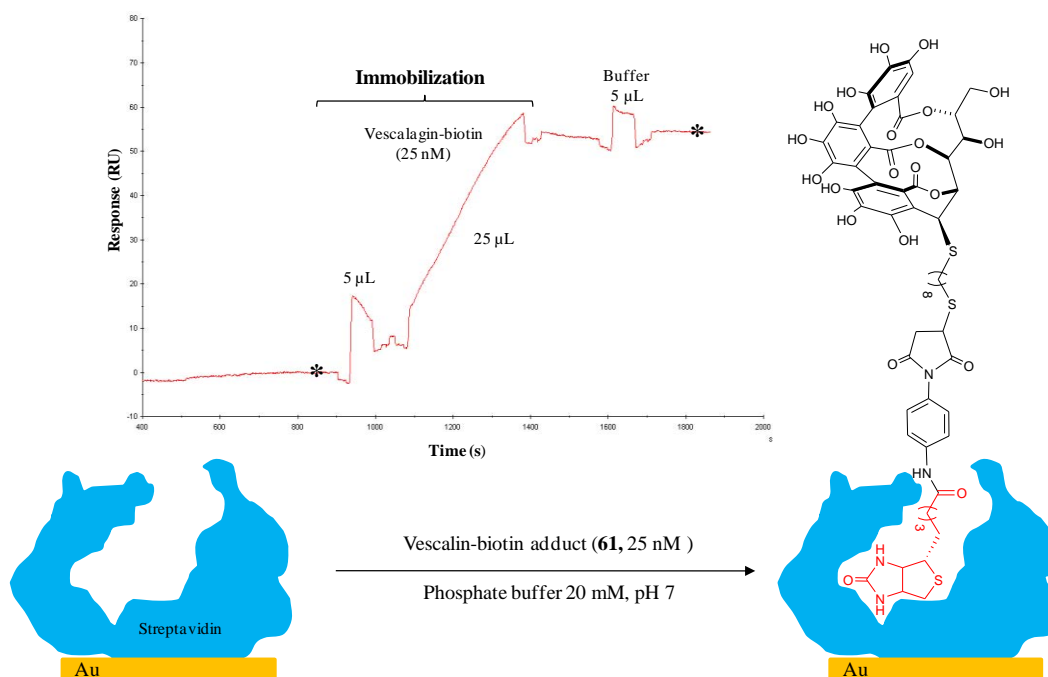
SPR experiments were performed at 25 °C on a BIAcore™ 3000 apparatus (Biacore, GE Healthcare, Uppsala, Sweden) using streptavidin sensor chips SAD200m, SAHC 80m (XanTec Bioanalytics, Duesseldorf, Germany) and SA (BIAcore). Buffer solutions were prepared to have the compositions specified in the previous and following sections. Bovin serum albumin (Sigma), streptavidin (Roche Diagnostics), myoglobin (Aldrich), collagen type I (rat tail, BD biosciences), G-actin (Tebu) and F-actin (polymerized from G-actin, see below), were used without further purification and were prepared at the specified concentration in the running buffer. N-terminal His₆-tagged recombinant ANS from *Vitis vinifera*, was used partially purified by using Ni-chelating affinity chromatography and dialyzed against the running buffer. Phalloidin, Alexa546-phalloidin, Alexa633-phalloidin were purchased from Invitrogen. Each SPR experiment was performed in triplicate.

Vd.2. Immobilization of polyphenol-biotin adducts on to SPR sensor chips

Biotinylated-polyphenol adducts were respectively immobilized on to streptavidin coated SPR surfaces thanks to the strong non-covalent interaction between streptavidin and biotin ($K_d = 10^{-14}$).⁷⁰ In comparison to the disulfide mode of immobilization used previously,⁶¹ this mode of immobilization has the advantage of being performed in one step and has better stability over time. Before immobilization of the biotinylated polyphenol adduct, the commercially available streptavidin coated sensor chip was rinsed by passing the immobilization running buffer (phosphate 50 mM, pH 7, NaCl 150 mM, P20 0.005%) at a flow rate of 100 µL/min. Then, to remove the surface's protective coating as well as any unbound streptavidin, 20 µL of NaOH (20 mM in H₂O) was injected on to the surface, followed by an injection of 20 µL of running buffer, the procedure was repeated twice. Afterwards, the flow rate was changed to 5 µL/min and buffer was allowed to run over the surface until a stable baseline was observed. Polyphenol-biotin adduct solutions were prepared by dissolving the compound in pure DMSO to give a 500 µM solution, which was diluted to 25-50 nM with running buffer. All solutions were prepared fresh before immobilization. However, the DMSO 500 µM solution is stable over time (at least 3 months) when prepared with degassed (Ar) DMSO and frozen right after preparation at -20°C. To immobilize the polyphenol-biotin adduct, a flow cell was selected and the aqueous 25-50 nM solution was injected on to the surface until the desired level of immobilization (in RU) was

obtained. Finally, the flow cell was rinsed by injecting 5 μL of running buffer with DMSO (same concentration of DMSO as used for the polyphenol-biotin adduct solution) and 5 μL of running buffer. An example of a sensorgram obtained for the immobilization of vescalagin-biotin adduct (**61**) is shown in the figure below.

Figure 73. Immobilization of **61** on to a SPR surface by biotin-streptavidin interaction



Vd.3. Protein solutions

TopII α (175 KDa): Human TopII α (from *E. coli* containing a clone of the human Topoisomerase II gene) solutions were prepared from a commercial solution (4.08 μM TopII α , in sodium phosphate 15 mM, pH 7.1, NaCl 700 mM, EDTA 0.1mM, DTT 0.5mM, glycerol 50%) diluted with running buffer (sodium phosphate 50 mM, pH 7, NaCl 150 mM, P20 0.005%)⁶¹ to obtain the desired concentrations of 6.25, 12.5 and 25 nM.

Streptavidin (54308 Da): A streptavidin stock solution 2.5 mg/mL or 46 μM (in Tris-HCl 10 mM, pH 7, glycerol 1%) was diluted with running buffer successively to obtain the desired concentrations (6. 25 nM, 12.5 nM, 25 nM and 1, 2, 4 μM).

Collagen Type I (aprox. 300 KDa): 3.3 mg/mL stock solution in (in 0.02 N acetic acid) diluted with running buffer successively to obtain the desired concentrations (6. 25 nM, 12.5 nM, 25, 125, 250, 500 nM and 1, 2, 4 μM).

BSA (66430 Da): 19.1 mg of lyophilized BSA (Aldrich) was allowed to dissolve slowly in 575 μL of running buffer, then this solution was diluted with running buffer successively to obtain the desired concentrations (6.25 nM, 12.5 nM, 25, 125, 250, 500 nM and 1, 2, 4 μM).

Myoglobin (17120 Da): 9.1 mg of lyophilized myoglobin (from whale skeletal muscle, Aldrich) was allowed to dissolve slowly in 10 mL of running buffer, then this solution was diluted with running buffer successively to obtain the desired concentrations (6.25 nM, 12.5 nM, 25, 125, 250, 500 nM and 1, 2, 4 μM).

G-Actin (238 μM , MM. 42 051 Da): From powder α -Actin (from rabbit skeletal muscle) 1 mg dissolved with 100 μL of G-buffer (Tris-HCl 5 mM, pH = 8.0, and CaCl_2 0.2 mM). The solution was prepared in an ice bath to delay natural polymerization, allowing the powder to dissolve without agitation for at least 1 h. The mixture turned into a colorless gel and was homogenized with pipette, then centrifuged to remove air bubbles (45 sec, 10 rpm). The mixture became clear, leading to a 238 μM stock solution.

G-Actin 2 μM / 4 μM / 8 μM solution (400 μL final volume): In 1.5 mL eppendorf tubes were added the following solutions (in that order) at 0°C.

396 μL / 392 μL / 386 μL G-Buffer BIAcore (Phosphate 10mM Buffer, pH = 7, NaCl 150 mM, CaCl_2 0.2 mM, ATP 0.2 mM, P20 0.005%).

0.8 μL ATP 100 mM (in Tris-HCl 100 mM, pH 7.5).

3.36 μL / 6.72 μL / 13.4 μL G-actin 238 μM solution.

F-Actin 2 μM solution (400 μL final volume): In 1.5 mL eppendorf tubes were added the following solutions (in that order):

356 μL G-Buffer BIAcore (Phosphate 10mM Buffer, pH = 7, NaCl 150 mM, CaCl_2 0.2 mM, ATP 0.2 mM, P20 0.005%).

0.8 μL ATP 100 mM (in Tris-HCl 100 mM, pH 7.5).

3.36 μL of G-actin 238 μM solution.

40 μL F-buffer (Tris-HCl 5 mM, pH = 7.5, KCl 500 mM, MgCl_2 20 mM, 10 mM ATP).

G-actin was allowed to polymerize at room temperature for 40 min, after which time was added 24 μL of phalloidin 6.6 μM in MeOH (20% of G-actin moles). The mixture was allowed to remain still at room temperature for 40 min before use.

F-Actin 4 μM solution (400 μL final volume): In 1.5 mL eppendorf tubes were added the following solutions (in that order):

352 μL G-Buffer BIAcore (Phosphate 10mM Buffer, pH = 7, NaCl 150 mM, CaCl_2 0.2 mM, ATP 0.2 mM, P20 0.005%).

0.8 μ L ATP 100 mM (in Tris-HCl 100 mM, pH 7.5).

6.72 μ L of G-actin 238 μ M solution.

40 μ L F-buffer (Tris-HCl 5 mM, pH = 7.5, KCl 500 mM, MgCl₂ 20 mM, 10 mM ATP).

G-actin was allowed to polymerize at room temperature for 40 min, after which time was added 24 μ L of phalloidin 6.6 μ M in MeOH (**10%** of G-actin moles). The mixture was allowed to remain still at room temperature for 40 min before use.

F-Actin 4 μ M solution (400 μ L final volume): In 1.5 mL eppendorf tubes were added the following solutions (in that order):

346 μ L G-Buffer BIAcore (Phosphate 10mM Buffer, pH = 7, NaCl 150 mM, CaCl₂ 0.2 mM, ATP 0.2 mM, P20 0.005%).

0.8 μ L ATP 100 mM (in Tris-HCl 100 mM, pH 7.5).

13.4 μ L of G-actin 238 μ M solution.

40 μ L F-buffer (Tris-HCl 5 mM, pH = 7.5, KCl 500 mM, MgCl₂ 20 mM, 10 mM ATP).

G-actin was allowed to polymerize at room temperature for 40 min, after which time was added 24 μ L of phalloidin 6.6 μ M in MeOH (5% of G-actin moles). The mixture was allowed to remain still at room temperature for 40 min before use.

Mock Buffer: same composition as each F-actin solution, but without G-actin.

ANS-histidine tagged (41 KDa): The LDOX stock solution (1.2 mg/mL = 26 μ M) was freshly dialyzed against the running buffer and kept in an ice bath at all times. In 1.5 mL eppendorf tubes, the LDOX stock solution was successively diluted with running buffer (cold) to obtain 200, 400 and 800 nM LDOX solutions. These solutions were injected using the method below, right after preparation. For the first experience the running buffer was cold (right out of the fridge).

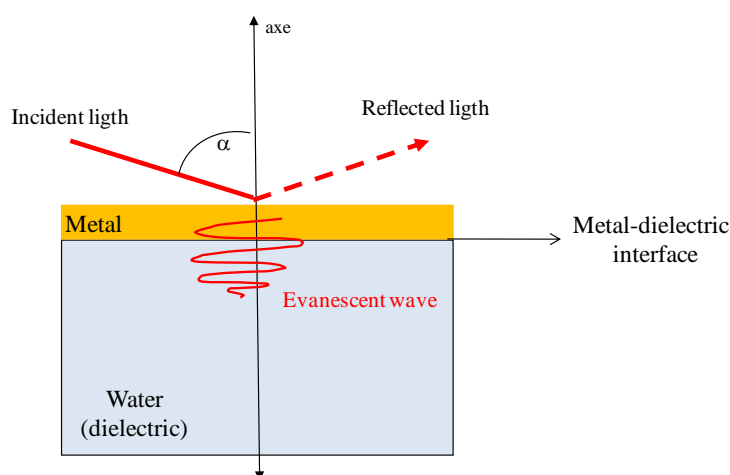
Appendix

Generalities about SPR detection system for intermolecular interaction studies

SPR the physical phenomenon⁵⁹

Surface plasmons are **surface electromagnetic waves** or electron charge density waves that propagate parallel to the metal-dielectric interface. In order for this phenomenon to occur the real part of the dielectric constant of the metal must be negative and its magnitude greater than that of the dielectric. These conditions are met between metal and water or metal and vacuum on the IR-visible range. At a certain combination of wavelength and angle of incidence (**conditions of total internal reflection**, Figure 74) the incident light excites plasmons in the metal film, which causes a characteristic absorption of energy by the system. This absorption of energy is a consequence of the generation of the evanescent electromagnetic wave. It is called surface Plasmon *Resonance* because this phenomenon will occur for a specific angle of incidence and of a specific wavelength of light.

Figure 74. Conditions of total internal reflection.

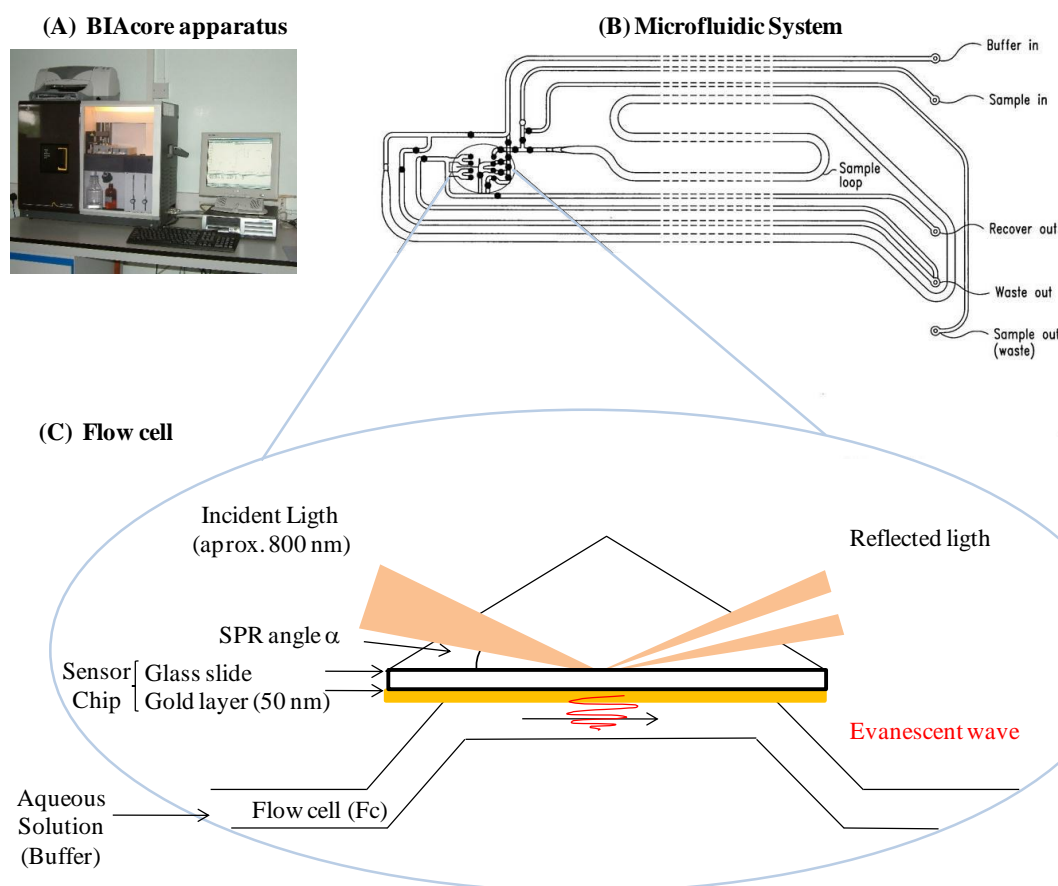


The oscillations of these waves are very sensitive to the changes produced on the proximity of this interface and they will fade exponentially as a function of distance. As a consequence, any modification at the interface will produce a change in the SPR angle. There are several SPR detection systems available in the market, the one available to us was the one developed by BIAcore (GE Healthcare). For this reason, this is the detection system that will be described herein. In the BIAcore systems the metal used is gold and the dielectric is an aqueous solution (buffer).

BIAcore Detection System^{59,118}

In the following figure is shown: a picture of the BIAcore 3000 apparatus (A) used to perform the assays described in this work, a drawing of the internal fluidic cartridge (IFC) or microfluidic system (B) and a zoom of the region within the IFC (B) that forms part of the flow cell (C) in which the intermolecular interaction takes place. One of the walls of the flow cell is composed by the removable sensor chip surface. The system allows 4 flow cells by sensor chip. The sensor chip is basically a thin glass slide coated on one of its sides with a thin gold layer (50 nm). The gold layer is chemically modified into a versatile functionalized surface, in our case the surface is modified to bear a streptavidin layer. These surfaces are commercially available, even though it is possible to have “homemade” ones.

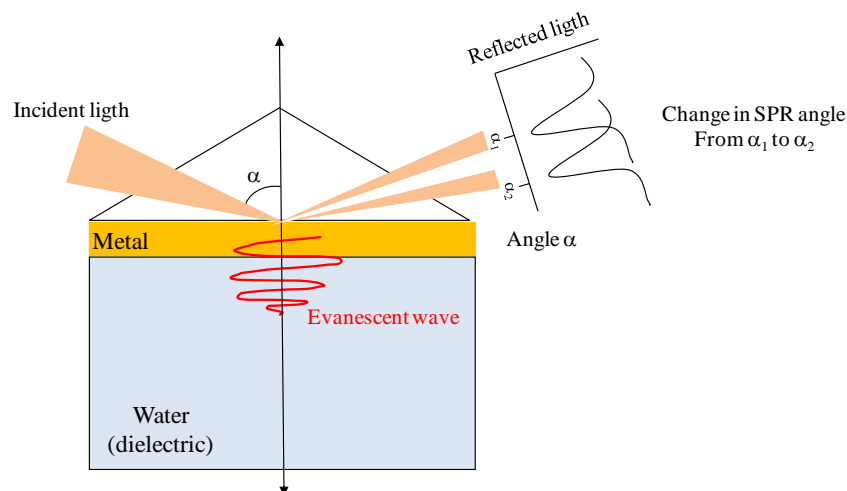
Figure 75. BIAcore apparatus and microfluidic system.



The chemically modified gold surface (or flow cell, Fc) is put in contact with an aqueous solution. Light from a light emitting diode (about 800 nm) is sent through a glass prism (to magnify the signal) and through the glass slide into the gold surface. Most of this light is reflected by the metal surface, but a small part of this light is transformed into the non propagating wave (evanescent wave or surface plasmons) that extends from the metal surface into the aqueous solution. The SPR response is then measured by a diode array detector. This

is, by measuring the decrease in intensity of the incident light as a function of the SPR angle (dips in the following figure).

Figure 76. **SPR angle.**



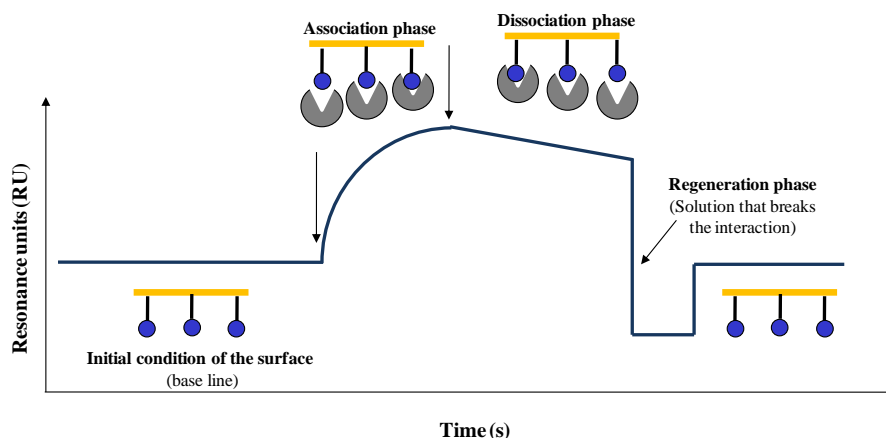
The SPR angle will change when the gold-aqueous solution interface changes, which is how SPR allows to study intermolecular interactions. One of the molecular partners is immobilized on the metal surface (ligand) and a solution of the other molecular partner is injected on to the surface. When a macromolecular complex is formed at the interface, the refractive index of the solution at the interface is modified and consequently the SPR angle. The changes at the interface are followed in real time and are observed as a graph of relative response (measured in relative units or RU; which is proportional to the change in SPR angle) as a function of time. This graph is called a sensorgram (Chapter III, section IIIa).

Phases of a Sensorgram (Figure 77)

As mentioned in Chapter III, Section IIIa, the resonance units are units relative to the initial state of the surface, meaning the SPR angle caused by the initial conditions (base line). The initial condition is a surface containing the immobilized ligand and the passing buffer solution called **running buffer**. The passing of the second molecular partner (analyte) gives a SPR response (**association phase**). The change in SPR response is positive due to a proportional relation between the mass of the analyte and the SPR response. Once the injection of analyte is over, the association phase is over and the **dissociation phase** begins. During the dissociation phase, the system allows the passing of a constant flow of running buffer. The expected SPR response is thus equal or lower than the SPR response at the end of the association phase. A rapid descent of the SPR response during this phase is interpreted as rapid dissociation of the intermolecular complex. On the other hand if the SPR response is equal to the SPR response of the association phase, this is interpreted as a stable

intermolecular complex. This is because all of the analyte associated to the ligand remains bound to the surface, sometimes irreversibly (as is the case for the biotin-streptavidin interaction).

Figure 77. Phases of a sensorgram



To test the reproducibility of the interaction, at least three cycles are performed, for the same ligand-analyte partners. For this, after the dissociation phase is over, a solution of a substance capable of breaking the intermolecular interactions is allowed to pass over the surface, this is called the **regeneration phase**. The regeneration phase is efficient when the surface regains its initial state. This is verified by the repetition of the experiment and the obtention of superposable sensorgrams. When regeneration of the surface is not efficient, a new surface should be used to repeat the assay under the same conditions. Unfortunately, in this way it is more difficult to obtain superposable sensorgrams due to the high sensitivity of the SPR detection.

When measuring intermolecular interactions by SPR, it is important to stress, that the analyte should be dissolved in the running buffer used to conduct the assays, because to conclude that the change in SPR response observed during the injection of the analyte is due the analyte-ligand interaction, the analyte should be the only component injected in the system. While other components present in the solution will most probably not interact with the ligand, they may cause a change in the SPR response leading to misinterpretation of the results. Since, dissolving the pure analyte in running buffer is not always possible, the differences between the running buffer and analyte solution should be minimized so the other components do not interfere with the analysis (example, glycerol in the protein's stock solution). This may be achieved by using dilute solutions of analyte, or by purifying the analyte with dialysis of the analyte solution against the running buffer.

SPR response and molar mass^{59,144,155}

The change in SPR response (RU) as a consequence of the proximity of the analyte to the immobilized ligand is related to their respective molar mass and the refractive index increment ($\delta n/\delta C$) by equation 1 (Eq. 1).

$$\frac{\text{RU analyte}}{\text{RU ligand}} = \frac{\text{MW analyte}}{\text{MW ligand}} \times \frac{(\delta n/\delta C)_{\text{analyte}}}{(\delta n/\delta C)_{\text{ligand}}} \times S \text{ (Eq. 1)}$$

Where: n = refractive index at the surface, C = the concentration of one partner and S = stoichiometry.

For interaction between similar molecules, for example protein-protein, the refractive index increment ($\delta n/\delta C$) term of Eq. 1 is equal to one. If the interaction has a 1:1 stoichiometry, Eq.1 simplifies to Eq. 2. In general for BIAcore instruments, the relation between the SPR response (RU), mass and surface is given by (Eq.3).

$$\frac{\text{RU analyte}}{\text{RU ligand}} = \frac{\text{MW analyte}}{\text{MW ligand}} \quad (\text{Eq. 2})$$

$$1000 \text{ Resonance Units (RU)} = 1 \text{ ng/mm}^2 \quad (\text{Eq. 3})$$

However, studies have shown that in some cases the refractive index increment ($\delta n/\delta C$) can differ significantly from one molecule to another^{144,155} and therefore, the refractive index increment values should be determined for correct data interpretation. Since the polyphenols used in this study are diverse in structure, for example vescalagin is very different in structure than catechin, and were modified to give new unreported compounds, the ($\delta n/\delta C$) factor of the modified polyphenols used in this study is not known, but it could be determined by differential refractometry for example. For our preliminary qualitative study of polyphenol-protein interaction, this factor was considered as equal to 1 (Eq. 2). Nonetheless, the importance of this factor should be kept in mind for quantitative studies in the future.

Sensorgrams: Proteins injected on to the reference streptavidin surface

The following sensorgrams show the SPR response observed for the injection of the proteins mentioned in chapter II, over the reference streptavidin surface.

Figure 78. Sensorgram of topoisomerase II α injected on to reference surface.

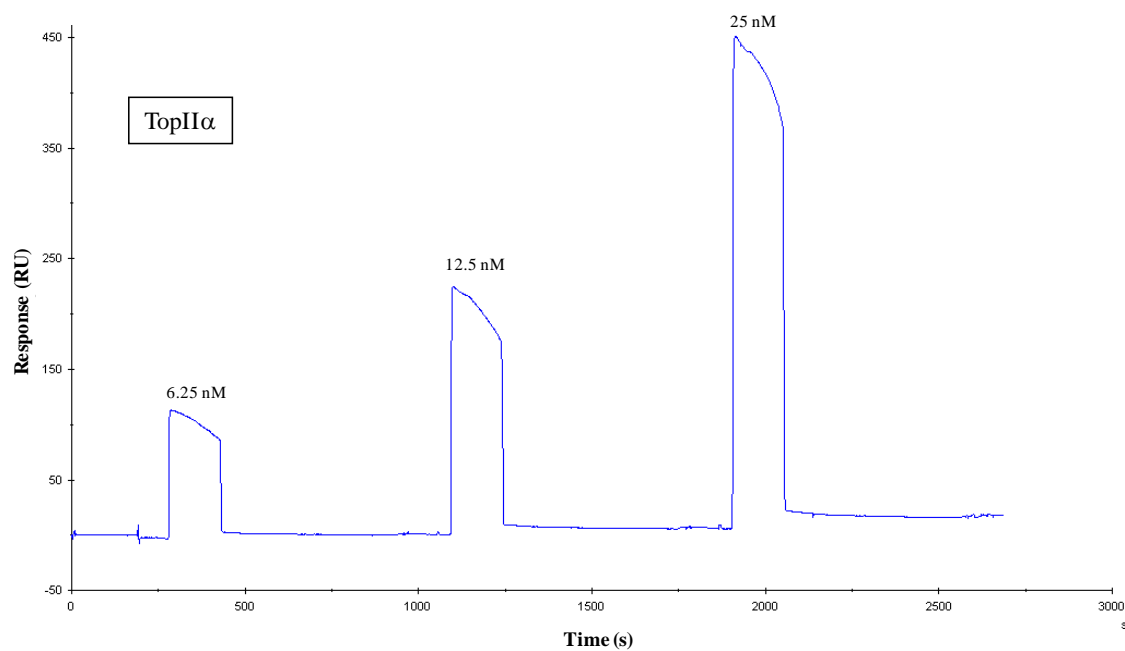


Figure 79. Sensorgram of BSA injected on to reference surface.

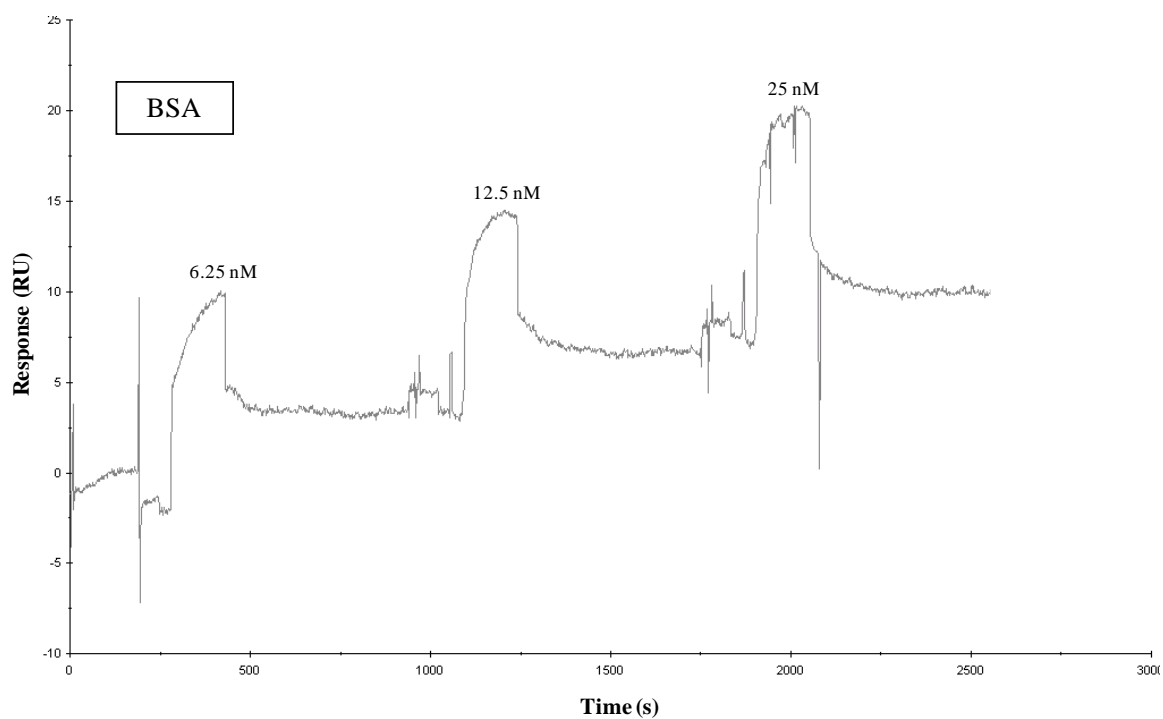
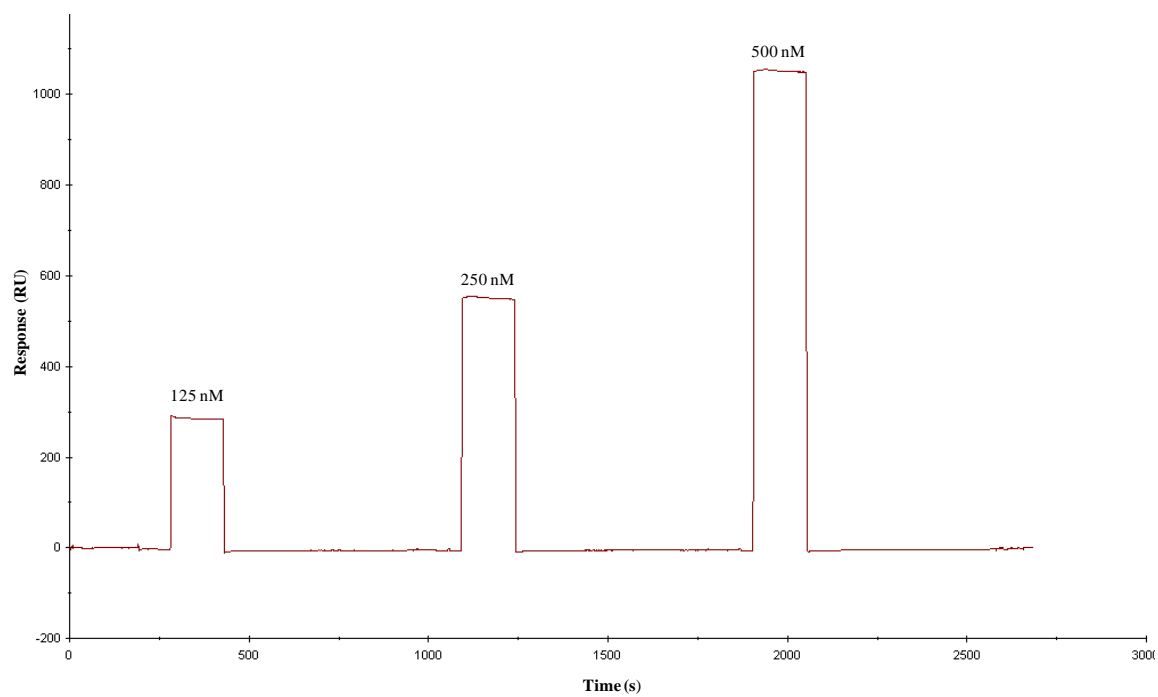
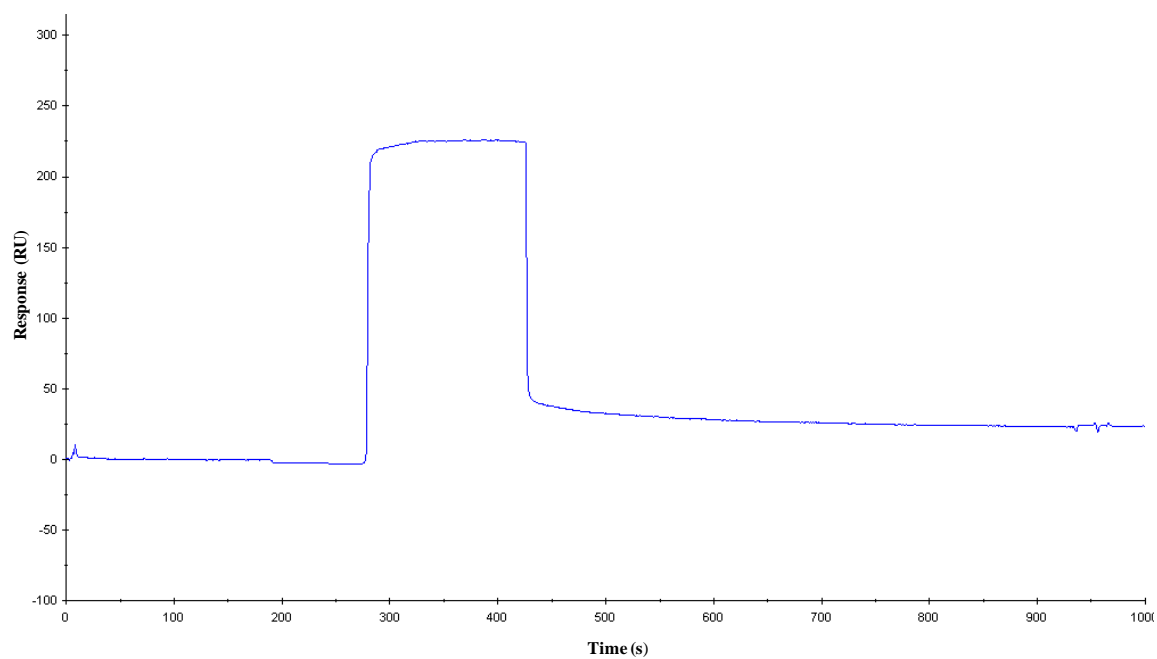
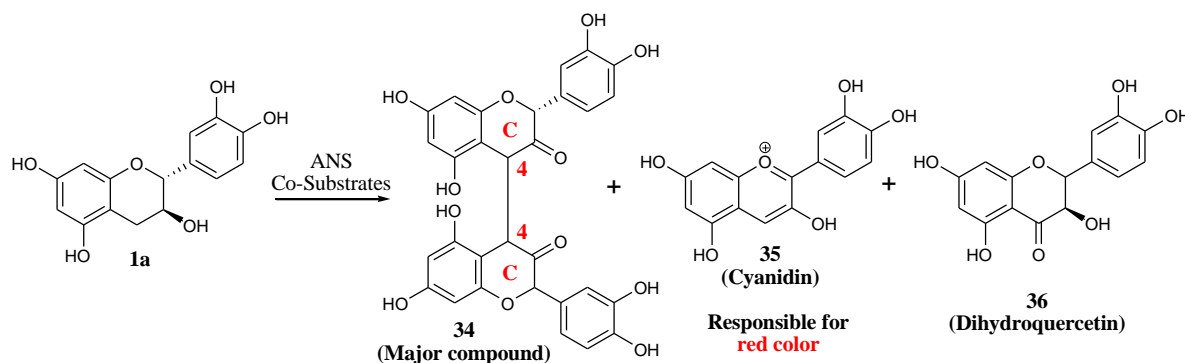


Figure 80. Streptavidin vs. reference surface (streptavidin)**Figure 81.** G-actin (2 μ M) vs. Streptavidin reference surface

ANS activity assays performed

In the figure below is shown the reaction scheme of the reaction between ANS and catechin (**1a**), which is transformed by the enzyme to afford: C4-C4 dimer (**34**), cyanidin (**35**) which gives a red coloration to final concentrated reaction mixture and dihydroquercetin (**36**). All of these compounds are detectable by LC/MS analysis.^{34,76} In table 16, is given the composition of the buffers used to perform the activity assays.

Scheme 43. Reaction between ANS protein and catechin (**1a**)**Table 16.** Composition of buffers used to perform ANS activity assays

Buffer I (Control, classic conditions)^{34,76}
Phosphate 200 mM Buffer, pH = 6, Glycerol 10%, 2-oxoglutarate 100 μ M, $[\text{NH}_4]_2[\text{Fe}][\text{SO}_4]$ 50 μ M, Sodium ascorbate 2.5 mM.
Buffer II (BIAcore + DMSO 9%)
Phosphate 20 mM, pH=6, NaCl 100 mM, 2-oxoglutarate 100 μ M, $[\text{NH}_4]_2[\text{Fe}][\text{SO}_4]$ 50 μ M, Sodium ascorbate 2.5 mM, Twin 0.005%, DMSO 9%.
Buffer III (BIAcore + DMSO 5%)
Phosphate 20 mM, pH=6, NaCl 100 mM, 2-oxoglutarate 100 μ M, $[\text{NH}_4]_2[\text{Fe}][\text{SO}_4]$ 50 μ M, Sodium ascorbate 2.5 mM, Twin 0.005%, DMSO 5%.
Buffer IV (BIAcore similar to the one used for TopIIα and actins)
Phosphate buffer 50mM, pH = 7, NaCl 150 mM, 2-oxoglutarate 100 μ M, $[\text{NH}_4]_2[\text{Fe}][\text{SO}_4]$ 50 μ M, Sodium ascorbate 2.5 mM, Twin 0.005%

The ANS activity assays were performed using a batch of ANS kept at room temperature and a batch of ANS kept at 4 °C. The results obtained are presented in the following tables (Table 17, 18 and 19). The time 0 h, corresponds to the end of the dialysis against the BIAcore buffers (buffer II, III and IV) or to the end of purification for the “classic conditions” (buffer I). The area presented in the following tables corresponds to the area below the peak with a retention time $R_t = 8.7$ min in the chromatogram, which corresponds to the catechin dimer (**34**) formed during the reaction of catechin with ANS. This measure is used to evaluate the

efficiency of the activity of the enzyme to transform the substrate (**1a**) and consequently the stability of the enzyme in the given buffer.

Table 17. ANS activity assays at room temperature

Time (h)	Buffer I (Control)		Buffer II	
	Area (Rt 8.7 min)	% Area Rel. to control	Area (Rt 8.7 min)	% Area Rel. to control
1/2	113404476	100%	28590915	25%
Red spot present?	yes		No	

Table 18. ANS activity assays at room temperature

Time (h)	Buffer I (Control)		Buffer III		Buffer IV	
	Area (Rt 8.7 min)	% Area Rel. ½ h	Area (Rt 8.7 min)	% Area Rel. ½ h	Area (Rt 8.7 min)	% Area Rel. ½ h
1/2	81 998 220	100%	37 915 541	100%	5 928 805	100%
1	92 475 031	113%	18 893 624	50%	2 005 406	34%
4	100 584 411	123%	11 426 794	30%	871 088	15%
14	114 487 216	140%	3 303791	9%	-	-
Red spot present?	yes		No		No	

Qualitatively, the presence of the red spot due to the presence of cyanidin (**35**) in the concentrated reaction mixture indicates a good yield of the reaction. From Table 17 we observe the ANS activity decreases rapidly with time relative to $t = \frac{1}{2}$ h for buffers III and IV (used for the BIAcore experiments). Comparing these results to the ones obtained for ANS under classical conditions (buffer I), we observe that ANS in buffer III (containing 5% DMSO) remains active to about 46%.

Table 19. ANS activity assays at room 4°C

Time (h)	Buffer I		Buffer II		Buffer III	
	Area (Rt 8.7 min)	% Area Rel. ½ h	Area (Rt 8.7 min)	% Area Rel. ½ h	Area (Rt 8.7 min)	% Area Rel. ½ h
1/2	75 926 287	100%	37 997 447	100%	5 856 886	100%
1	96 102 550	127%	32 448 666	85%	4 610 740	79%
4	95 444 681	126%	24 555 984	65%	3 222 743	55%
14	115 412 151	152%	7 346 125	19%	-	-
Red spot present?	yes		No		No	

At 4°C the results are similar to those obtained at room temperature, but with less rapid loss of activity through time. When the ANS activity assay was performed using compound **76a** as substrate no reaction occurred.

Scheme 44. ANS activity assay with catechin-4-thioetheroctanethiol (**76a**) as substrate

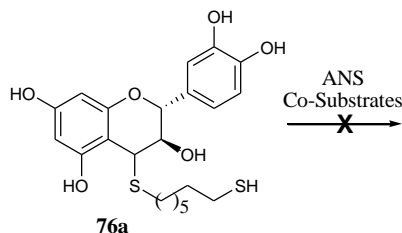
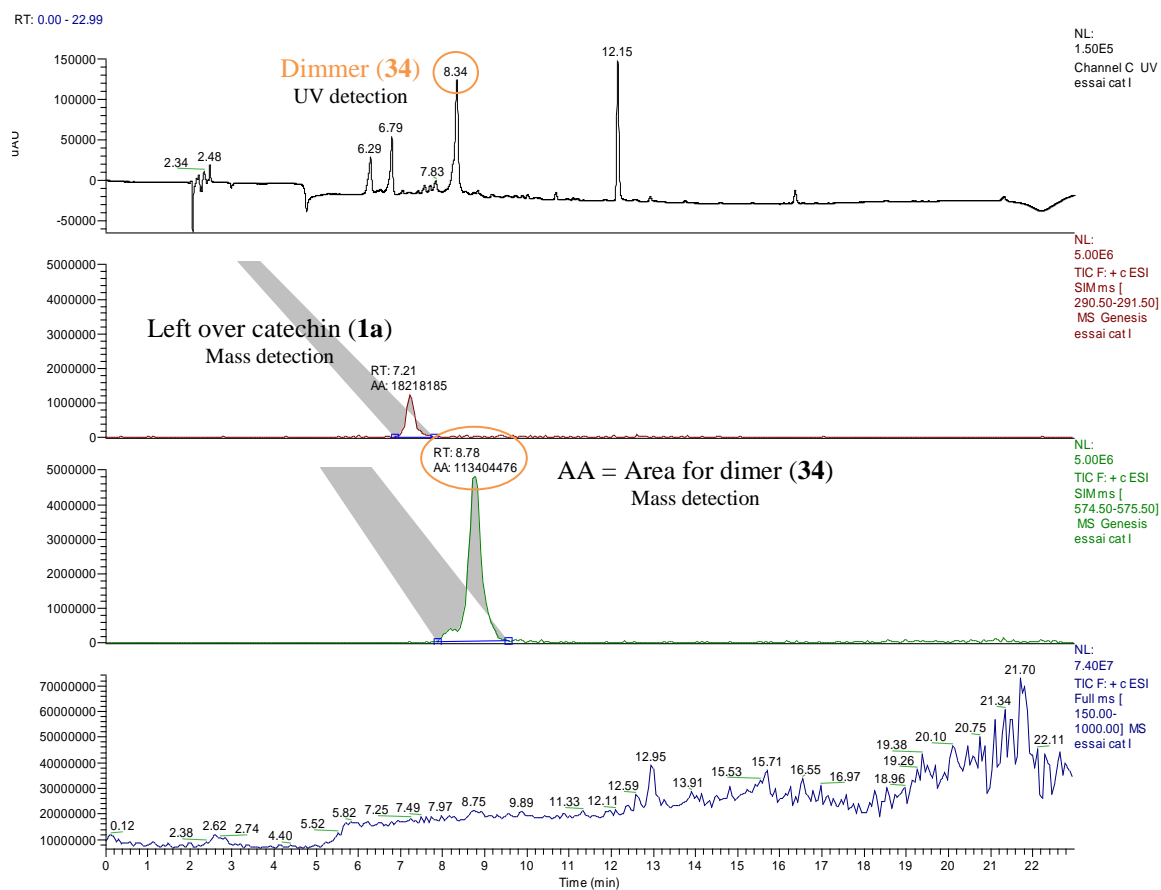
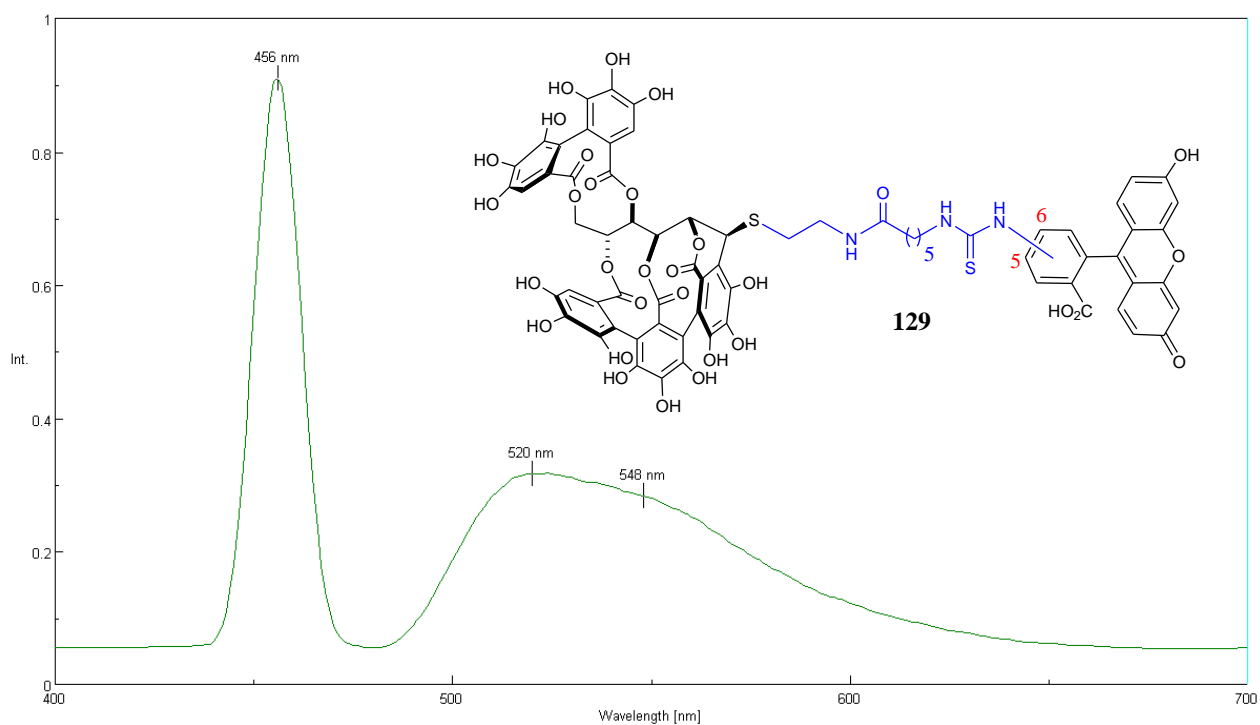


Figure 82. General example: Chromatograms obtained from ANS activity assays (mass and UV detection) in buffer I (control)



Fluorescence emission spectra

Figure 83. Fluorescence emission spectra of compound **129** excited at 456 nm; 25 μ M in AcN 34% / TFA 0.1% solution



References

- (1) Nicolaou, K. C.; Montagnon, T. *Molecules that changed the world*, WILEY-VCH, 2008, Chapter 4 and Chapter 10.
- (2) Quideau, S.; Deffieux, D.; Douat-Casassus, C.; Pouységu, L. Plant polyphenols: chemical properties, biological activities, and synthesis. *Angew. Chem. Int. Ed.* **2011**, *50*, 586.
- (2a) Freitas, V.; Mateus, N.; Protein/polyphenol interactions: past and present contributions. Mechanisms of astringency perception. *Curr. Org. Chem.* **2012**, *16*, 724.
- (3) Haslam, E. Natural polyphenols (vegetable tannins) as drugs: possible modes of action. *J. Nat. Prod.* **1996**, *59*, 205.
- (4) Crozier, A.; Jaganath, I. B.; Clifford, M. N. Dietary phenolics: chemistry, bioavailability and effects on health. *Nat. Prod. Rep.* **2009**, *26*, 965.
- (5) Marcano, D.; Hasegawa, M. *Fitoquímica orgánica*, 2002, Chapter 3.
- (6) Torres, J. L.; Bobet, R. New Flavanol derivatives from grape (*Vitis vinifera*) byproducts. Antioxidant aminoethylthio-flavan-3-ol conjugates from a Polymeric waste fraction used as a source of flavanols. *J. Agric. Food Chem.* 2001, *49*, 4627.
- (7) Oyama, K.; Kuwano, M.; Ito, M.; Yoshida, K.; Kondo, T. Synthesis of procyanidins by stepwise- and self-condensation using 3,4-cis-4-acetoxy-3-O-acetyl-4-dehydro-5,7,3',4'-tetra-O-benzyl-(+)-catechin and (–)-epicatechin as a key building monomer. *Tetrahedron* **2008**, *49*, 3176.
- (8) USDA Food Composition Data: USDA database for the proanthocyanidin content of selected foods-2004. Nutrient data Laboratory and Food Composition Laboratory, U.-A. T. A. C. s. N. C., USDA-ARS; Mars, Inc.; and Ocean Spray Cranberries, Inc. <http://www.nal.usda.gov/fnic/foodcomp/Data/PA/PA.html>.
- (9) Ferreira, D.; Slade, D. Oligomeric proanthocyanidins: naturally occurring O-heterocycles. *Nat. Prod. Rep.* **2002**, *19*, 517.
- (10) Haslam, E. Symmetry and promiscuity in procyanidin biochemistry. *Phytochemistry* **1977**, *16*, 1625.
- (11) Krohn, K.; Ahmed, I.; John, M.; Letzel, M. C.; Kuck, D. Stereoselective synthesis of benzylated prodelfphinidins and their diastereomers with use of the Mitsunobu reaction in the preparation of their gallocatechins precursors. *Eur. J. Org. Chem.* **2010**, 2544.
- (12) Steenkamp, J. A.; Malan, J. C. S.; Roux, D. G.; Ferreira, D. Oligomeric flavanoids. Part 1. Novel dimeric profisetinidins from *Colophospermum mopane*. *J. Chem. Soc., Perkin Trans. I* **1988**, 1325.
- (13) Quideau, S. Chemistry and biology of ellagitannins: an underestimated class of bioactive plant polyphenols, World Scientific, 2009, Chapter 1.
- (14) Gross, G. G. Plant polyphenols 2. Chemistry, biology, pharmacology, ecology. Kluwer Academic/Plenum publishers, 1999. Page 83.
- (15) Niemetz, R.; Gross, G. G. Enzymology of gallotannin and ellagitannin biosynthesis. *Phytochemistry* **2005**, *66*, 2001.
- (16) Sailer, B.; Glombitza, K.-W. Phlorethols and fucophlorethols from the brown alga *Cystophora retroflexa*. *Phytochemistry* **1999**, *50*, 869.
- (17) Glombitza, K.-W.; Hauperich, S. Phlorotannins from the brown alga *Cystophora torulosa*. *Phytochemistry* **1977**, *46*, 735.

- (18) Harborne, J. B.; Williams, C. A. Advances in favonoid research since 1992. *Phytochemistry* **2000**, *55*, 481.
- (19) Tang, H. R.; Covington, A. D.; Hancock, R. A. Structure-activity relationships in the hydrophobic interactions of polyphenols with cellulose and collagen. *Biopolymers* **2003**, *70*, 403.
- (20) Whitford, D. Proteins structure and function, Wiley, 2005.
- (21) Haslam, E. Polyphenol-protein interactions. *Biochem. J.* **1974**, *139*, 285.
- (22) Charlton, A. J.; Baxter, N. J.; Khan, M. L.; Moir, A. J. G.; Haslam, E.; Davies, A. P.; Williamson, M. P. Polyphenol/peptide binding and precipitation. *J. Agric. Food Chem.* **2002**, *50*, 1593.
- (23) Baxter, N. J.; Lilley, T. H.; Haslam, E.; Williamson, M. P. Multiple interactions between polyphenols and a salivary proline-rich protein repeat result in complexation and precipitation. *Biochemistry* **1997**, *36*, 5566.
- (24) Hatano, T.; Hemingway, R. W. Association of (+)-catechin and catechin-(4 α →8)catechin with oligopeptides. *Chem. Commun.* **1996**, 2537.
- (25) MacManus, J. P.; Davis, K. G.; Gaffney, S. H.; Lilley, T. H.; Haslam, E. Polyphenol interactions. Part 1. Introduction: some observations on the reversible complexation of polyphenols with proteins and polysaccharides. *J. Chem. Soc., Perkin Trans. 2* **1985**, 1429.
- (26) Hagerman, A., E; Rice, M. E.; Ritchard, N. T. Mechanism of protein precipitation of for two tannins, pentagalloyl glucose and epicatechin₁₆(4→8) catechin (procyanidin). *J. Agric. Food Chem.* **1998**, *46*, 2590.
- (27) Hofmann, T.; Glabasnia, A.; Schwarz, B.; Wisman, K. N.; Gangwer, K. A.; Hagerman, A. E. Protein binding and astringent taste of a polymeric procyanidin, 1,2,3,4,6-penta-O-galloyl- β -D-glucopyranose, castalagin and grandinin. *J. Agric. Food Chem.* **2006**, *54*, 9503.
- (28) Zheng, J.; Ramirez, V. D. Inhibition of mitochondrial proton F₀F₁-ATPase/ATP synthase by polyphenolic phytochemicals. *Br. J. of Pharmacol.* **2000**, *130*, 1115.
- (29) Gledhill, J. R.; Montgomery, M. G.; Leslie, A. G. W.; Walker, J. E. Mechanism of inhibition of bovine F₁-ATPase by resveratrol and related polyphenols. *PNAS* **2007**, *104*, 13632.
- (30) Goodsell, D. In Molecule of the Month (December, 2005): ATP Synthase. RCSB Protein Data Bank: <http://www.rcsb.org/pdb/101/motm.do?momID=72>.
- (31) Wilmouth, R. C.; Turnbull, J. J.; Welford, R. W. D.; Clifton, I. J.; Prescott, A. G.; Schofield, C. J. Structure and Mechanism of Anthocyanidin Synthase from *Arabidopsis thaliana*. *Structure* **2002**, *10*, 93.
- (32) Wellmann, F.; Griesser, M.; Schwab, W.; Martens, S.; Eisenreich, W.; Matern, U.; Lukacin, R. Anthocyanidin synthase from *Gerbera hybrida* catalyzes the conversion of (+)-catechin to cyanidin and a novel procyanidin. *FEBS Letters* **2006**, *580*, 1642.
- (33) Welford, R. W. D.; Clifton, I. J.; Turnbull, J. J.; Wilson, S. C.; Schofield, C. J. Structural and mechanistic studies on anthocyanidin synthase catalysed oxidation of flavanone substrates: the effect of C-2 stereochemistry on product selectivity and mechanism. *Org. Biomol. Chem.* **2005**, *3*, 3117.
- (34) Chalumeau, C.; Deffieux, D.; Chaignepain, S.; Quideau, S. Development of an affinity-based proteomic strategy for the elucidation of proanthocyanidin biosynthesis. *ChemBioChem* **2011** *12*, 1193.
- (35) Goodsell, D. In Molecule of the Month (July, 2006): amyloid-beta precursor protein. RCSB Protein Data Bank: <http://www.rcsb.org/pdb/101/motm.do?momID=79>.

- (36) Porat, Y.; Abramowitz, A.; Gazit, E. Inhibition of amyloid fibril formation by polyphenols: structural similarity and aromatic interactions as a common inhibition mechanism. *Chem. Biol. Drug Des.* **2006**, *67*, 27.
- (37) Ono, K.; Yoshiike, Y.; Takashima, A.; Hasegawa, K.; Naik, H.; Yamada, M. Potent anti-amyloidogenic and fibril-destabilizing effects of polyphenols in vitro: implications for the prevention and therapeutics of Alzheimer's disease. *J. Neurochem.* **2003**, *87*, 172.
- (38) Ehrnhoefer, D. E.; Bieschke, J.; Boeddrich, A.; Herbst, M.; Masino, L.; Lurz, R.; Engemann, S.; Pastore, A.; Wanker, E. E. EGCG redirects amyloidogenic polypeptides into unstructured, off-pathway oligomers. *Nat. Struct. Mol. Biol.* **2008**, *15*, 558.
- (39) Jankun, J.; Selman, S. H.; Swiercz, R.; Skrzypczak-Jankun, E. Why drinking green tea could prevent cancer. *Nature* **1997**, *387*, 561.
- (40) Quideau, S.; Jourdes, M.; Lefeuvre, D.; Montaudon, D.; Saucier, C.; Glories, Y.; Pardon, P.; Pourquier, P. The chemistry of wine polyphenolic C-glycosidic ellagitannins targeting human topoisomerase II. *Chem. Eur. J.* **2005**, *11*, 6503.
- (41) Pommier, Y. DNA topoisomerase I inhibitors: Chemistry, biology and interfacial inhibition. *Chem. Rev.* **2009**, *109*, 2894.
- (42) Goodsell, D. In Protein of the month (January, 2006): Topoisomerases. RSCB Protein Data Bank: <http://www.rcsb.org/pdb/101/motm.do?momID=73>.
- (43) Wan, S. B.; Landis-Piowar, K. R.; Kuhn, D. J.; Chen, D.; Dou, Q. P.; Chan, T. H. Structure–activity study of epi-gallocatechin gallate (EGCG) analogs as proteasome inhibitors. *Bioorg. Med. Chem.* **2005**, *13*, 2177.
- (44) Quideau, S.; Varadinova, T.; Karagiozova, D.; Jourdes, M.; Pardon, P.; Baudry, C.; Genova, P.; Diakov, T.; Petrova, R. Main structural and stereochemical aspects of the antiherpetic activity of nonhydroxyterphenoyl-containing C-glycosidic ellagitannins. *Chem. Biodivers.* **2004**, *1*, 247.
- (45) Goodsell, D. In Protein of the month (July, 2001): Actin. RSCB Protein Data Bank: <http://www.rcsb.org/pdb/101/motm.do?momID=19>.
- (46) Quideau, S.; Douat-Casassus, C.; Delannoy Lopez, D. M.; Di Primo, C.; Chassaing, S.; Jacquet, R.; Saltel, F.; Génot, E. Binding of filamentous actin and winding into fibrillar aggregates by the polyphenolic C-glucosidic ellagitannin vescalagin. *Angew. Chem. Int. Ed.* **2011**, *50*, 5099.
- (47) Pollard, T. D.; Cooper, J. A. Actin, a central player in cell shape and movement. *Science* **2009**, *326*, 1208.
- (48) Oda, T.; Iwasa, M.; Aihara, T.; Maéda, Y.; Narita, A. The nature of the globular- to fibrous-actin transition. *Nature* **2009**, *457*, 441.
- (49) Fujii, T.; Iwane, A. H.; Yanagida, T.; Namba, K. Direct visualization of secondary structures of F-actin by electron cryomicroscopy. *Nature* **2010**, *724*, 467.
- (50) Frazier, R. A.; Papadopoulou, A.; Mueller-Harvey, I.; Kisson, D.; Green, R. J. Probing protein-tannin interactions by isothermal titration microcalorimetry. *J. Agric. Food Chem.* **2003**, *51*, 5189.
- (51) Soares, S.; Mateus, N.; De Freitas, V. Interaction of different polyphenols with bovine serum albumin (BSA) and human salivary α -amylase (HSA) by fluorescence quenching. *J. Agric. Food Chem.* **2007**, *55*, 6726.
- (52) Kelly, S. M.; Price, N. C. The use of circular dichroism in the investigation of protein structure and function. *Curr. Protein Pept. Sci.* **2000**, *1*, 349.

- (53) Pascal, C.; Paté, F.; Cheynier, V.; Delsuc, M.-A. Study of the interactions between a proline-rich protein and a flavan-3-ol by NMR: residual structures in the natively unfolded protein provides anchorage points for the ligands. *Biopolymers* **2009**, *91*, 745.
- (54) Sinz, A. Investigation of protein–ligand interactions by mass spectrometry. *ChemMedChem* **2007**, *2*, 425.
- (55) Fernandez, C.; Wolfgang, J. New approaches for NMR screening in drug discovery. *Drug Discov. Today Tec* **2004**, *1*, 277.
- (56) Harding, S. E.; Chowdhry, B. Z. Protein-ligand interactions: hydrodynamics and calorimetry. Oxford University Press, 2001, Chapter 1.
- (57) Neumann, T.; Junker, H.-D.; Schmidt, K.; Sekul, R. SPR-based Fragment Screening: advantages and applications. *Curr. Top. Med. Chem.* **2007**, *7*, 1630.
- (58) Kobayashi, M.; Retra, K.; Figaroa, F.; Hollander, J. G.; Ab, E.; Heetebrij, R. J.; Irth, H.; Siegal, G. Target immobilization as a strategy for NMR-based fragment screening : comparison of TINS, STD, and SPR for fragment hit identification. *J Biomol Screen* **2010**, *15*, 978.
- (59) Homola, J. Surface plasmon resonance sensors for detection of chemical and biological species. *Chem. Rev.* **2008**, *108*, 462.
- (60) Borisov, S. M.; Wolfbeis, O. S. Optical Biosensors. *Chem. Rev.* **2008**, *108*, 423.
- (61) Douat-Casassus, C.; Chassaing, S.; Di Primo, C.; Quideau, S. Specific or nonspecific protein-polyphenol Interactions? Discrimination in real time by surface plasmon resonance *Chembiochem* **2009**, *10*, 2321.
- (62) T. Gonçalves, M. S. Fluorescent labeling of biomolecules with organic probes. *Chem. Rev.* **2009**, *109*, 190.
- (63) Chen, L.; Li, F.; Hou, B.; Hong, G.; Yao, Z. Site-specific fluorescent labeling approaches for naringenin, an essential flavonone in plant nitrogen-fixation signaling pathways. *J. Org. Chem.* **2008**, *73*, 8279.
- (64) Wakata, A.; Cahill, S. M.; Blumenstein, M.; Gunby, R. H.; Jockusch, S.; Marti, A. A.; Cimbro, B.; Gambacorti-Passerini, C.; Donella-Deana, A.; Pinna, L. A.; Turro, N. J.; Lawrence, D. S. A mechanistic design principle for protein tyrosine kinase sensors: application to a validated cancer target. *Org. Lett.* **2008**, *10*, 301.
- (65) Lakowicz, J. R. Principles of fluorescence spectroscopy, 3rd edition, Springer, 2006. Chapter 8.
- (66) Kobayashi, T.; Urano, Y.; Kamiya, M.; Ueno, T.; Kojima, H.; Nagano, T. Highly activatable and rapidly releasable caged fluorescein derivatives. *J. Am. Chem. Soc.* **2007**, *129*, 6696.
- (67) Sun, W.-C.; Gee, K. R.; Klaubert, D. H.; Haugland, R. P. Synthesis of fluorinated fluoresceins. *J. Org. Chem.* **1997**, *62*, 6469.
- (68) Ueno, T.; Urano, Y.; Setsukinai, K.-i.; Takakusa, H.; Kojima, H.; Kikuchi, K.; Ohkubo, K.; Fukuzumi, S.; Nagano, T. Rational principles for modulating fluorescence properties of fluorescein. *J. Am. Chem. Soc.* **2004**, *126*, 14079.
- (69) Han, D.-W.; Matsumura, K.; Kim, B.; Hyon, S.-H. Time-dependent intracellular trafficking of FITC-conjugated epigallocatechin-3-O-gallate in L-929 cells. *Bioorg. Med. Chem.* **2008**, *16*, 9652.

- (70) Holmberg, A.; Blomstergren, A.; Nord, O.; Lukacs, M.; Lundeberg, J.; Uhlén, M. The biotin-streptavidin interaction can be reversibly broken using water at elevated temperatures. *Electrophoresis* **2005**, *26*, 501.
- (71) Le Gac, S.; Schwartz, E.; Koepf, M.; Cornelissen, J. J. L. M.; Rowan, A. E.; Nolte, R. J. M. Cysteine-containing polyisocyanides as versatile nanoplatfoms for chromophoric and bioscaffolding. *Chem. Eur. J.* **2010**, *16*, 6176.
- (72) Billiet, L.; Gok, O.; Dove, A. P.; Sanyal, A.; Nguyen, L.-T., T ; Du Prez, F. E. Metal-Free Functionalization of Linear Polyurethanes by Thiol-Maleimide Coupling Reactions. *Macromolecules* **2011**, *44*, 7874.
- (73) Viriot, C.; Scalbert, A.; Lapiere, C.; Moutounet, M. Ellagitannins and Lignins in Aging of Spirits in Oak Barrels. *J. Agric. Food Chem.* **1993**, *41*, 1872.
- (74) Peng, S.; Scalbert, A.; Monties, B. Insoluble ellagitannins in *Castanea sativa* and *Quercus petraea* woods. *Phytochemistry* **1991**, *30*, 775.
- (75) Keana, J. F. W.; Ogan, M. D.; Lu, Y.; Beer, M.; Varkey, J. Functionalized Keggin-and Dawson-type cyclopentadienyltitanium heteropolytungstate anions: small, individually distinguishable labels for conventional transmission electron microscopy. 2. Reactions. *J. Am. Chem. Soc.* **1986**, *108*, 7957.
- (76) Chalumeau, C. Développement d'outils chimiques pour l'elucidation de la biosynthèse des flavonoïdes du rasin: Anthocyanes versus proanthocyanidins. Université de Bordeaux 1, 2010.
- (77) Tückmantel, W.; Kozikowski, A. P.; Romanczyk, J. L. J. Studies in polyphenol chemistry and bioactivity. 1. Preparation of building blocks from (+)-catechin. Procyanidin formation. Synthesis of the cancer cell growth inhibitor, 3-O-galloyl-(2R, 3R)-epicatechin-4 , 8-[3-O-galloyl-(2R, 3R)-epicatechin]. *J. Am. Chem. Soc.* **1999**, *121*, 12073.
- (78) Ohmori, K.; Ushimaru, N.; Suzuki, K. Stereoselective substitution of flavan skeletons: synthesis of dryopteris acid. *Tetrahedron Lett.* **2002**, 7753.
- (79) Hayes, C. J.; Whittaker, B. P.; Watson, S. A.; Grabowska, A. M. Synthesis and preliminary anticancer activity studies of C4 and C8-Modified derivatives of catechin gallate (CG) and epicatechin gallate (ECG). *J. Org. Chem.* **2006**, *71*, 9701.
- (80) Saito, A.; Nakajima, N.; Tanaka, A.; Ubukata, M. Synthetic studies of proanthocyanidins. Part 2: Stereoselective gram-scale synthesis of procyanidin-B3. *Tetrahedron* **2002**, *58*, 7829.
- (81) Oyama, K.; Kondo, T. Total synthesis of apigenin 7,4'-di-O- β -glucopyranoside, a component of blue flower pigment of *Salvia patens*, and seven chiral analogues. *Tetrahedron* **2004**, *60*, 2025.
- (82) Axford, L.; Holden, K.; Hasse, K.; Banwell, M.; Steglich, W.; Wagler, J.; Willis, A. Attempts to Mimic Key Bond-Forming Events Associated with the Proposed Biogenesis of the Pentacyclic Lamellarins. *Aust. J. Chem.* **2008**, *61*, 80.
- (83) Alvarez-Manzaneda, E.; Chahboun, R.; Cabrera, E.; Alvarez, E.; Haidour, A.; Ramos, J.; Alvarez-Manzaneda, R.; Hmamouchi, M.; Bouanous, H. Diels–Alder cycloaddition approach to puupehenone-related metabolites: synthesis of the potent Angiogenesis inhibitor 8-epipuupehedione. *J. Org. Chem.* **2007**, *72*, 3332.
- (84) Calderazzo, F.; Forte, C.; Marchetti, F.; Pampaloni, G.; Pieretti, L. Reaction of phenanthrene-9,10-dione with phenanthrene-9,10-diol: synthesis and characterization of the first ortho-quinhydrone derivative. *Helv. Chim. Acta* **2004**, *87*, 781.

- (85) Magdziak, D.; Rodriguez, A.; Van De Water, R.; Pettus, T. Regioselective Oxidation of Phenols to o-Quinones with o-Iodoxybenzoic Acid (IBX). *Org. Lett.* **2002**, *4*, 285.
- (86) Wuts, P. G. M.; Greene, T. W. *Greene's protective groups in organic synthesis*, John Wiley and Sons, 2006.
- (87) Demirtas, I.; Buyukkidan, B.; Elmastas, M. The selective protection and deprotection of ambident nucleophiles with parent and substituted triarylmethyls. *Turk. J. Chem.* **2002**, *26*, 889.
- (88) Walker, D.; Hiebert, J. D. 2,3-Dichloro-5,6-dicyanobenzoquinone and its reactions. *J. Chem. Rev.* **1967**, *67*, 153.
- (89) Raab, T.; Barron, D.; Vera, F. A.; Crespy, V.; Oliveira, M.; Williamson, G. Catechin glucosides: occurrence, synthesis and stability. *J. Agric. Food Chem* **2010**, *58*, 2138.
- (90) Cruz, L.; Borges, E.; Silva, A. M. S.; Mateus, N.; Freitas, V. Synthesis of a new (+)-catechin-derived compound: 8-vinylcatechin. *Lett. Org. Chem.* **2008**, *5*, 530.
- (91) PCT Int. Appl., 2000063201.
- (92) Boyer, F.-D.; Es-Safi, N.-E.; Beauhaire, J.; Le Guerneve, C.; Ducrot, P.-H. Synthesis of modified proanthocyanidins: easy and general introduction of a hydroxy group at C-6 of catechin; efficient synthesis of elephantorrhizol. *Bioorg. Med. Chem. Lett.* **2005**, *15*, 563.
- (93) De Groot, A. H.; Dommise, R. A.; Lemièrre, G. L. Selective cleavage of tert-butyl dimethyl silyl ethers ortho to a carbonyl group. *Tetrahedron* **2000**, *56*, 1541.
- (94) Steenkamp, J. A.; Mouton, C. H. L.; Ferreira, D. Regio and stereo selective oxidation of flavan-3-ol, 4-arylflavan-3-ol, and biflavanoid derivatives with 2,3-dichloro-5,6-dicyano-1,4-benzoquinone (DDQ). *Tetrahedron* **1991**, *47*, 6705.
- (95) Kaburagi, Y.; Kishi, Y. Operationally simple and efficient workup procedure for TBAF-mediated desilylation: application to halichondrin synthesis. *Org. Lett.* **2007**, *9*, 723.
- (96) Kozikowski, A. P.; Tuckmantel, W.; Hu, Y. Studies in polyphenol chemistry and bioactivity. 3.^{1,2} Stereocontrolled synthesis of epicatechin-4 α ,8-epicatechin, an unnatural isomer of the B-type procyanidins. *J. Org. Chem.* **2001**, *66*, 1287.
- (97) Kwit, M.; Rozwadowska, M. D.; Gawronski, J.; Grajewska, A. Density functional theory calculations of the optical rotation and electronic circular dichroism: the absolute configuration of the highly flexible trans-isocytosaxone revised. *J. Org. Chem.* **2009**, *74*, 8051.
- (98) Clayden, J.; Greeves, N.; Warren, S.; Wothers, P. *Organic Chemistry*, Oxford University Press, 2001. Page 1248.
- (99) Coetzee, J.; Malan, E.; Ferreira, D. Oligomeric flavanoids, part 29: Structure and synthesis of novel ether-linked [4-O-4] bis-teracacinidins. *Tetrahedron* **1998**, *54*, 9153.
- (100) Kumar, S.; Hansen, M. H.; Nanna, A.; Steffansen, S. I. Synthesis of functionalized carbocyclic locked nucleic acid analogs by ring-closing diene and metathesis and their influence on nucleic acid stability structure. *J. Org. Chem.* **2009**, *74*, 6756.
- (101) Jung, M. E.; Davidov, P. Efficient synthesis of a tricyclic BCD analogue of ouabain: lewis acid catalyzed diels-alder reactions of sterically hindered systems. *Angew. Chem. Int. Ed.* **2002**, *41*, 4125.
- (102) Trost, B. M.; Cladwell, C. G.; Murayama, E.; Heissler, D. Sulfur-substituted dienes and the silylene protecting group in synthesis. deoxypillaromycinone. *J. Org. Chem.* **1982**, *48*, 3252.

- (103) Debenham, J. S.; Rodebaugh, R.; Frasser-Reid, B. TCP- and phtalamide-protected n-pentenyl glucosaminide precursors for the synthesis of nodulation factors as illustrated by the total synthesis of NodRf-III (C18:1, MeFuc). *J. Org. Chem* **1997**, *62*, 4591.
- (104) Boyer, F.-D.; Beauhaire, J.; Martin, M. T.; Doucrot, P.-H. Hydroxylation of ring A of flavan-3-ols. Influence of the ring A substitution pattern on the oxidative rearrangement of 6-hydroxyflavan-3-ols. *Synthesis* **2006**, 3250.
- (105) O'Leary, B. M.; Szabo, T.; Svenstrup, N.; Schalley, C. A.; Luetzen, A.; Schaefer, M.; Rebek, J. J. "Flexiball" toolkit: a modular approach to self-assembling capsules. *J. Am. Chem. Soc.* **2001**, *123*, 11519.
- (106) Zhang, J.; Li, S.; Zhang, D.; Wang, H.; Whorton, A. R.; Xian, M. Reductive ligation mediated one-step disulfide formation of S-nitrosothiols. *Org. Lett.* **2010**, *12*, 4208.
- (107) Kharash Organic Sulfur Compounds, Pergamon press, 1961, Vol. 1. Chapter 35.
- (108) Mohri, Y.; Sagehashi, M.; Yamada, T.; Hattori, Y.; Morimura, K.; Kamo, T.; Mitsuru, H.; Makabe, H. An efficient synthesis of procyanidins. Rare earth metal Lewis acid catalyzed equimolar condensation of catechin and epicatechin. *Tetrahedron Lett.* **2007**, *48*, 5891.
- (109) Tarascou, I.; Barathieu, K.; Andre, Y.; Pianet, I.; Dufourc, E. J.; Fouquet, E. An improved synthesis of procyanidin dimmers: regio- and stereocontrol of the interflavan bond. *Eur. J. Org. Chem.* **2006**, 5367.
- (110) Ohmori, K.; Shono, T.; Hatakoshi, Y.; Yano, T.; Suzuki, K. Integrated Synthetic Strategy for Higher Catechin Oligomers. *Angew. Chem. Int. Ed.* **2011**, *50*, 4862.
- (111) Saito, A.; Tanaka, A.; Ubukata, M.; Nakajima, N. Efficient stereoselective synthesis of procyanidin trimers with TMSOTf-catalyzed intermolecular condensation. *Synlett.* **2004**, *6*, 1069.
- (112) Achilonu, M. C.; Bonnet, S. L.; van der Westhuizen, J. H. Synthesis of proanthocyanidins. Part 1. The first oxidative formation of the interflavanyl bond in procyanidins. *Org. lett.* **2008**, *10*, 3865.
- (113) Trahanovsky, W. S.; Young, B. L. Controlled oxidation of organic compounds with cerium (IV). II. The oxidations of toluenes. *J. Org. Chem.* **1966**, *31*, 2033.
- (114) Baciocchi, E.; Rol, C.; Sebastiani, G. V.; Serena, B. Photochemical nitrooxidation of methylbenzenes by cerium (IV) ammonium nitrate in acetonitrile. *Tetrahedron Lett.* **1984**, *25*, 1945.
- (115) Saito, A.; Mizushima, Y.; Tanaka, A.; Nakajima, N. Versatile synthesis of epicatechin series procyanidin oligomers, and their antioxidant and DNA polymerase inhibitory activity. *Tetrahedron* **2009**, *65*, 7422.
- (116) Ohmori, K.; Ushimaru, N.; Suzuki, K. Oligomeric catechins: An enabling synthetic strategy by orthogonal activation and C(8) protection. *PNAS* **2004**, *101*, 12002.
- (117) Myszka, D. G. Improving biosensor analysis. *J. Mol. Recognit.* **1999**, *12*, 279.
- (118) BIAcore sensor surface manual, edition 2003, chapters 1, 2, 3, 6.
- (119) Karlsson, R.; Katsamba, P. S.; Nordin, H.; Pol, E.; Myszka, D. G. Analyzing a kinetic titration series using affinity biosensors. *Anal. Biochem.* **2006**, *349*, 136.
- (120) Di Primo, C. Real time analysis of the RNAI–RNAII–Rop complex by surface plasmon resonance: from a decaying surface to a standard kinetic analysis. *J. Mol. Recognit.* **2008**, *21*, 37.

- (121) Auzanneau, C.; Montaudon, D.; Jacquet, R.; Puyo, S.; Pouysegue, L.; Deffieux, D.; Elkaoukabi-Chaibi, A.; De Giorgi, F.; Ichas, F.; Quideau, S.; Pourquier, P. The polyphenolic ellagitannin vescalagin acts as a preferential catalytic inhibitor of the alpha isoform of human dna topoisomerase II. *Mol Pharmacol.* April 23, 2012, doi:10.1124/mol.111.077537.
- (122) Goodsell, D. In Molecule of the Month (January, 2003): Serum Albumin. RCSB Protein Data Bank: <http://www.rcsb.org/pdb/101/motm.do?momID=37>.
- (123) Goodsell, D. In Molecule of the Month (January, 2000): Myoglobin. RCSB Protein Data Bank: <http://www.rcsb.org/pdb/101/motm.do?momID=1>.
- (124) Le Trong, I.; Wang, Z.; Hyre, D.E.; Lybrand, T.P.; Stayton, P.S.; Stenkamp, R.E. Streptavidin and its biotin complex at atomic resolution. *Acta Crystallogr., Sect.D* **2011**, 67, 813.
- (125) Goodsell, D. In Molecule of the Month (April, 2000): Collagen. RCSB Protein Data Bank: <http://www.rcsb.org/pdb/101/motm.do?momID=4>.
- (126) Barfoot, R. J.; Sheikh, K. H.; Johnson, B. R. G.; Colyer, J.; Miles, R. E.; Jeuke, L. J. C.; Bushby, R. J.; Evans, S. D. Minimal F-Actin cytoskeletal system for planar supported phospholipid bilayers. *Langmuir* **2008**, 24, 6827.
- (127) Kumara Swamy, K. C.; Bhuvan Kumar, N. N.; Balaraman, E.; Pavan Kumar, K. V. P. Mitsunobu and related reactions: advances and applications. *Chem. Rev.* **2009**, 109, 2551.
- (128) Sigmund, H.; Pfeleiderer, W. Nucleotides. Part LXXI. A new type of labeling of nucleosides and nucleotides. *Helv. Chim. Acta.* **2003**, 86, 2299.
- (129) Bernardes, G. J. L.; Grayson, E. J.; Thompson, S.; Chalquer, J. M.; Errey, J. C.; El Oualid, F.; Claridge, T. D. W.; Davis, B. G. From disulfide- to thioether-linked glycoproteins. *Angew. Chem. Int. Ed.* **2008**, 47, 2244.
- (130) March, J.; Smith, M. B. March's advance organic chemistry: reactions, mechanism and structure, 6th edition, Wiley, Chapter 19, page 1785.
- (131) Burns, J. A.; Butler, J. C.; Moran, J.; Whitesides, G. M. Selective reduction of disulfides by tris-(2-carboxyethyl)phosphine. *J. Org. Chem.* **1991**, 56, 2648.
- (132) Ruegg, U. T. Reductive cleavage of S-sulfo groups with tributylphosphine. *Methods Enzymol.* **1977**, 47, 123.
- (133) Brown, H. C.; Zaidlewicz, M.; Dalvi, P. V.; Biswas, G. K. Molecular addition compounds. 18. borane adducts with hydroxydialkyl sulfide borates for hydroboration. New, essentially odorless, water-soluble sulfide borane acceptors for hydroboration. *J. Org. Chem.* **2001**, 66, 4795.
- (134) Pastuszak, J. J.; Chimiak, Andrzej. Ter-butyl group as thiol protection in peptide synthesis. *J. Org. Chem.* **1981**, 46, 1868.
- (135) Humphrey, R. E.; Potter, J. L. Reduction of disulfides with tributylphosphine. *Anal. Chem.* **1965**, 37, 164.
- (136) Wender, P. A.; Mitchell, D. J.; Pattabiraman, K.; Pelkey, E. T.; Steinman, L.; Rothbard, J. B. The design, synthesis, and evaluation of molecules that enable or enhance cellular uptake: peptoid molecular transporters. *PNAS* **2000**, 21, 13003.
- (137) Jullian, M.; Hernandez, A.; Maurras, A.; Puget, K.; Amblard, M.; Martinez, J.; Subra, G. N-terminus FITC labeling of peptides on solid support: the truth behind the spacer. *Tetrahedron lett.* **2009**, 50, 260.

- (138) Hermanson, G. T. Bioconjugate techniques, 2nd edition, Elsevier: Academia press, Pages 127-129.
- (139) Medal, M. PEGA: a flow-stable polyethylene glycol-dimethylacryl copolymer for solid-phase synthesis. *Tetrahedron Lett.* **1192**, 33, 3077.
- (140) Li, H.; Hah, J.-M.; Lawrence, D. S. Ligth-mediated liberation of enzymatic activity: “small molecule” caged protein equivalents. *J. Am. Chem. Soc.* **2008**, 130, 10474.
- (141) Hummel, G.; Hindsagaul, O. Solid-phase synthesis of thio-oligosaccharides. *Angew. Chem. Int. Ed.* **1999**, 38, 1782.
- (142) Shapira, E.; Aron, R. Cleavage of one specific disulfide bond in papain. *J. Biol. Chem.* **1969**, 244, 1026.
- (143) El-Faham, A.; Albericio, F. Peptide coupling reagents, more than a letter soup. *Chem. Rev.* **2011**, 111, 6557.
- (144) Davis, T. M.; Wilson, W. D. Determination of the refractive index increments of small molecules for correction of surface plasmon resonance data. *Anal. Biochem.* **2000**, 284, 348.
- (145) Di Primo, C.; Lebars, I. Determination of refractive index increment ratios for protein-nucleic acid complexes by surface plasmon resonance. *Anal. Biochem.* **2007**, 368, 148.
- (146) Ferreira, D.; Nel, R. J. J.; Bekker, R.; Comprehensive natural products chemistry, Vol. (Ed.: B. M. Pinto), Pergamon, Oxford, 1999, pages 747-797.
- (147) Scalbert, A.; Duval, L.; Peng, S.; Monties, B.; Du Penhoat, C. Polyphenols of *Quercus robur* L. II. Preparative isolation by low-pressure and high-pressure liquid chromatography of heartwood ellagitannins. *J. Chromatogr.* **1990**, 502, 107.
- (148) Quideau, S.; Varadinova, T.; Karagiozova, D.; Jourdes, M.; Pardon, P.; Baudry, C.; Genova, P.; Diakov, T.; Petrova, R. Main Structural and Stereochemical Aspects of the Antiherpetic Activity of Nonahydroxyterphenoyl-Containing C-Glycosidic Ellagitannins. *Chem. Biodiv.* **2004**, 1, 247.
- (149) Mayer, W.; Gabler, W.; Riester, A.; Korger, H. Die Isolierung von Castalagin, Vescalagin, Castalin, Vescalin. *Liebigs Ann. Chem.* **1967**, 707, 177.